RADIO COMMUNICATION SERIES

BEVERLY DUDLEY, CONSULTING EDITOR

RADIO DIRECTION FINDERS

RADIO COMMUNICATION SERIES

BEVERLY DUDLEY · *Consulting Editor*

Bond—

RADIO DIRECTION FINDERS

Hund—

FREQUENCY MODULATION

Preisman—

GRAPHICAL CONSTRUCTIONS FOR VACUUM TUBE CIRCUITS

RADIO DIRECTION FINDERS

BY

DONALD S. BOND
Radio Corporation of America

FIRST EDITION
THIRD IMPRESSION

McGRAW-HILL BOOK COMPANY, INC.
NEW YORK AND LONDON
1944

RADIO DIRECTION FINDERS

PRINTED IN THE UNITED STATES OF AMERICA

THE MAPLE PRESS COMPANY, YORK, PA.

PREFACE

Radio direction finding had its origin almost as early as radio communication itself, but the progress made within the last ten years has been so rapid that only a specialist has been able to keep abreast of the literature and of the development on the subject. Despite this long history, extensive technical need, and theoretical interest, the subject matter has been treated extensively by only one other modern reference in English. This is the very excellent work by R. Keen, *Wireless Direction Finding.*

In this present work the author attempted to produce a textbook and reference work for training electrical engineers who desire to specialize in the design or theory of direction finders for aircraft, shipboard, or fixed-station use. In it are combined qualitative descriptions of the practical systems in use with an analytical study of the underlying phenomena. In order to approach these objectives in this latter fashion, the author presupposes a better technical training and greater ability in mathematics than does this other previous work on the subject. Accordingly, the reader is assumed to be of either two types. He may be a well-trained electrical engineer who desires to become capable of developing new systems involving direction finder principles. Consequently, emphasis is laid upon these basic underlying facts; qualitative results are obtained; and, it is hoped, the reader is left in the position of being able to apply these facts to research and development problems which he has at hand. Alternatively, the reader may have had more limited technical training, and for his benefit the detailed mathematical derivations have been placed in footnotes or in the Appendix.

Particular attention has been paid to current trends, such as the use of ultra-high frequencies, the employment of visual and automatic direction finders, the better understanding of Adcock systems, and the analysis of the behavior of direction finders for the reception of ionosphere waves. These and other topics have been discussed as an aid to the improvement of military and peacetime commercial direction finder systems.

Restrictions have necessarily been imposed in certain fields because direction finders constitute military implements, and the specific applications resulting from current wartime needs are of course excluded from the book. Nevertheless, it will be noted by those familiar with such trends that an attempt has been made to add emphasis to the basic facts and general principle that underlie these military developments. Certain topics are given an emphasis that might be considered unwarranted at first sight were it not for the fact that the probable trends in the next few years in direction finder progress may include these developments. In this a number of workers in the field concur. The author has deliberately omitted reference to certain more recent papers on wave propagation because it was believed that the complexities of the more rigorous treatments would necessitat an undesirable change in over-all presentation methods.

A considerable amount of the original material appearing this work has been given the crucial test of application in th laboratories of the Radio Corporation of America. Much the book was originally presented by the author as a series classroom lectures for design engineers and student engineers RCA. This was carried out at, and under the auspices of, th Moore School of Electrical Engineering of the University Pennsylvania. Instruction was maintained at a graduate level with the equivalent of a bachelor's degree in electrical engineering assumed. The textbook information, with the supplementary problems and exercises, was arranged so that design problems taken from actual commercial laboratory activities were studi and the solution carried out by students.

There is included a considerable amount of material of a hand book type, for it is believed that this will be useful as a reference by engineers concerned with the design of direction finder equip ment or by those involved in the study of the simpler aspects the phenomena of wave propagation. Much of the materi presented in Chap. I is of this reference type, concerning th accepted methods of direction-finding testing. While this may be considered to be an assumption of more detailed knowledge o the part of the student than is warranted, later reference to this material can be made when the user begins to concern himself with over-all problems of test. Elsewhere numerous summaries of data are included for easy reference. For comparison purposes,

data are given in charts on the maximum range of transmission over a wide range of frequencies. Summaries are made in tabular form of phase-shift performance of resonant circuits. Circuit diagrams of commercial direction finders and representative equipments of other classifications are given with enough descriptive information so that a user of this apparatus can study the principles of operation with no other text material. Thus other systems can be analyzed because of the basic similarity of the principles involved. Instructions are given on such subjects as the establishing of standard fields for the testing of direction finders and the calibration of aircraft direction finders in flight.

The writer has benefited from the opportunity to discuss the material and the method of presentation with his associates of the Radio Corporation of America. Edward D. Blodgett, in charge of the direction finder development section, has been especially helpful in this respect. Carl G. Sontheimer has been responsible for a number of the mathematical treatments, including those relating to balancer phasing in Chap. IV. He has contributed very willingly in suggestions on method of presentation and in reading of proofs. Acknowledgment must be made of the encouragement by John B. Coleman, Chief Engineer of the Communication and Industrial Equipment Engineering Department of RCA. Much of the material in Chap. VI has been furnished through the courtesy of W. L. Webb, Chief Engineer of Bendix Radio Division of Bendix Aviation Corporation and G. O. Essex of the same company. The latter has very kindly commented on the material on these topics. Through the kind assistance of Arthur R. Weckel, Manager of Aeronautical Sales of the Sperry Gyroscope Company, the subject matter of the Mark I automatic direction finder was made available. To these and other members of the staffs of RCA, Bendix, and Sperry Gyroscope Company much of the material on aircraft calibration methods as covered in Chap. VII is due. The author acknowledges many stimulating suggestions from Major Francis L. Moseley, formerly of Sperry Gyroscope Company, during the joint development, by Sperry and RCA, of the direction finder discussed in Chapter VI.

To the publishers of the *Proceedings of the Institute of Radio Engineers*, the *Bell System Technical Journal*, *RCA Review*, *Journal of the Franklin Institute*, *Electronics*, and *Time, Inc.*, thanks are due for permission to reproduce text and illustrations.

The Director of the National Bureau of Standards has given assent to the use of illustrative matter in Chap. II, and members of his staff have suggested certain technical changes in this material for greater accuracy. Likewise the Civil Aeronautics Administration of the U.S. Department of Commerce has been helpful in granting permission to quote from certain of its publications.

DONALD S. BOND.

CAMDEN, N. J.,
March, 1944.

CONTENTS

APPENDIX

RADIO DIRECTION FINDERS

CHAPTER I

GENERAL CONSIDERATIONS

1.01. The Function of Direction Finders.—A radio direction finder is a device for determining the direction of the energy flux of an electromagnetic wave. More specifically, it is a device for measuring one component of this energy flux vector. Its principal use is in navigation, for determining the angle between the line of bearing connecting a transmitter and a receiver and a known direction in space at one or the other of those locations. Information of this sort suitably obtained from enough stations serves to locate the craft uniquely.

A direction finder when used at a receiving station consists of a directive array, a receiver having good performance characteristics, and a means for coupling the array to the latter. In the case of a transmitting direction finder the receiver is, of course, replaced by a transmitter of suitable design.

1.02. Comparison of Communication Receivers and Direction Finders.—A number of rather important differences between receivers for point-to-point or broadcast communication and direction finders may be noted.

1. In the case of a receiver the purpose is that of communication of messages, while in a direction finder the identification of direction of radio energy flow is essential. It may be true, however, that a direction finder can be used simultaneously for communication purposes.

2. In case of a communication system the modulation of the carrier is of prime importance, while in a direction finder it is usually of negligible interest insofar as the determination of direction or of bearing is concerned. The only function of the modulation is as an aid to the identification of the transmitting station.

3. Communication receivers are used between points of known location or where the precise knowledge of this information is of

little importance. On the other hand, radio direction finders are almost invariably used where one of the stations is mobile and where its location must be determined for the purpose of navigation. The term "navigation" will be understood to include position identification of vessels at sea, of aircraft, and even of portable land stations.

4. The receiver portions of a communication unit and of a direction finder may be quite similar. In general, a direction finder receiver involves obtaining all of the performance characteristics of a good receiver and in addition imposes certain requirements on overload, low r-f leakage, and proper phase relationships in the currents of the r-f circuits.

5. Communication receivers and transmitters are often nondirectional. If they do have a directive characteristic, it is merely to secure a more favorable ratio of signal to noise or to diminish the effect of interfering signals from other directions. In contrast, a direction finder system is entirely dependent upon the directive properties of its antenna array.

6. In communication work the properties of the medium through which the radio waves are propagated are of importance only in determining the field strength obtainable at the receiving point and in producing selective fading. The accuracy of performance of a direction finder is very dependent upon the medium and upon the vagaries of propagation. These latter influence the accuracy of bearings obtainable in a given design, and determine to a great measure the choice of directive antenna system in a new design to keep undesired errors to a minimum.

1.03. Classes of Direction Finders.—It is commonly supposed that a direction finder always consists of a loop antenna and a receiver. This is very far from being the case, as a direction finder may be either a transmitter or a receiver. Furthermore, the directive antenna system may be installed either on a moving craft or at a fixed location. As far as navigation is concerned, the choice of transmitting or receiving equipment connected to the directive array is dependent only on convenience in relaying the directive information to the point at which navigation is to be done. As an example: If a ship desires to learn a line of position from a shore station equipped with a directive antenna, it may transmit a signal to be picked up by the shore-station direction finder receiver. Then by means of auxiliary circuits

the information of the measurement of the line of bearing is communicated back to the ship for navigation purposes. If the shore station has a transmitter connected to the array and transmits a signal in various directions on a predetermined schedule, the radio operator aboard ship may identify the characteristic direction of this beam by employing a nondirectional receiver. This system of a rotating radio beam transmitter ("radio lighthouse") has been used extensively abroad, and the airways radio range transmitters in this country work on the same general principle.

It will be seen in Chap. VII that different types of information are furnished for navigation when the directive system is on the craft or at a fixed location. One gives a *line of bearing* measured at the craft, and the other gives a similar measurement, establishing a *line of position*, from the ground or fixed station.

A second difference exists between a directive system at fixed and mobile locations, and that is the accuracy of bearing obtainable. In most cases it is found that a ground or shore station can use a larger, more carefully chosen site, in which the residual errors are small and can be allowed for by calibration, and this calibration will hold over a long period of time. The opposite of each of these advantages is true both for ship and airplane installations.

The problem of convenience in transmitting observed data to the location where they are to be utilized for navigation has already been discussed.

1.04. Direction Finders Employing Null Methods.—Many types of direction finder systems make use of a sharp cusp in the directive pattern of the receiving or transmitting array. This is usually the position of null or minimum signal and is used because it is much sharper than the maximum that can be obtained. An example of this is the well-known figure-of-8 pattern obtained from a loop antenna. The two minima are very sharp and may often be complete nulls, while the maxima are very broad and poorly defined in practice. For systems employing a null method, the equipment must work at very low equivalent field strength. This is true even when the signal at maximum is quite strong. As a consequence the signal-to-noise performance and signal-to-interference behavior are of prime importance in such equipment. In other systems employing phase shift or phase reversal indica-

tions, these characteristic points almost invariably occur at the same positions as the nulls. Consequently the same operation at low equivalent field strength is required.

1.05. Direction Finder Receiver Performance Characteristics. The detailed consideration of direction finders in this book will be confined to receiving systems and directive arrays. When a transmitter is an essential part of the directive equipment, it will not be considered in detail here. A summary is given below of those characteristics of a receiver for direction finder use which are of importance in design. Many of them are also characteristic of good communication receivers. A superheterodyne receiver will be considered in detail, because this is the most usual type to be used with direction finders. The designation *commercial* equipment may be understood to include military designs and is to be contrasted with apparatus built for broadcast or entertainment reception.

1. *Gain.*—The amount of amplification or gain through all the stages of a direction finder receiver determines the over-all sensitivity. This, in turn, is a measure of the weakest signals to which the receiver will respond. The type of service determines whether a receiver of 100 or 500 microvolts sensitivity is adequate or whether it must be capable of receiving signals of the order of 10μv or less.

The low limit of signals to which a receiver will respond is determined almost always by the internal or external noise level. The *internal noise level* represents a signal originating from thermal agitation noise or perhaps from tube noise in the receiver. When the signal input is much less than the equivalent first circuit noise, reception is unsatisfactory or impossible. The limit on gain and sensitivity is frequently determined by the *interference noise level* in the region of the direction finder receiver and antenna array. A systematic study of reduction of interference of this sort is beyond the scope of this book, for the only manner in which receiver design can influence it is in adequate shielding against external fields, filtering of power-supply leads, and the inclusion of noise limiters to discriminate against certain types of impulsive noise.

Very frequently field strengths are expressed in "decibels below 1 volt/m" or, alternatively, in "decibels above 1 μv/m," for convenience in comparison of fields or of receiver performance.

2. *Selectivity.*—Two characteristics must be considered simultaneously in the determination of desired selectivity of a direction finder receiver. The resonant circuits must be sharp enough to suppress adjacent channel interference and spurious signal responses; and the response must be broad enough to pass the highest audio-modulating frequency required by the system without excessive attenuation. In nearly every case it is desirable to have a constant absolute band width rather than a constant percentage band width. A superheterodyne receiver lends itself very well to this requirement when the major part of the selectivity is obtained by one or more intermediate frequency amplifiers that are fixed tuned.

3. *Signal-noise Characteristic.*—As was discussed in (1) Gain above, the problem of first-circuit noise is very frequently the limiting factor in the over-all sensitivity of a receiver. One of the main problems of the receiver designer is that of choice of the antenna coupling circuit to secure most efficient utilization of the signal picked up from the antenna system by making the signal-noise ratio as large as possible.

4. *Power Output.*—Most commercial receivers do not have the requirement of large power output for driving a loud-speaker, and thus the importance of high undistorted output is minor. For headphone use, power outputs are usually satisfactory at 10 to 100 milliwatts, although for aircraft receivers pilot fatigue often requires 500 to 1000 mw. Certain fixed stand-by receivers utilize loud-speakers, but 2 to 3 watts is the usual maximum level required for them. It is desirable, however, that at low signal *inputs* to the receiver the power output be made as near its maximum asymptotic value as possible.

5. *Spurious Responses.*—A superheterodyne receiver has a number of characteristic frequencies at which interfering signals may be troublesome. These spurious response frequencies are a consequence of the double or triple frequency conversion essential to this type of receiver. Examples of these may be given when a superheterodyne having one intermediate frequency is used with the oscillator for the first converter operating *above* signal frequency. (*a*) An *image response* occurs at a frequency $f_{rf} + 2f_{if}$. This is ordinarily the strongest spurious response. (*b*) There is a response to a signal of *intermediate frequency* applied to the antenna (frequency f_{if}). (*c*) If two signals, the desired one and

an interfering one, f_{rf1} and f_{rf2}, respectively, differ in frequency by the intermediate frequency, the spurious response known as *intermodulation* is obtained, *i.e.*, $f_{rf1} - f_{rf2} = f_{if}$. (*d*) *Higher order image* responses are obtained at frequencies $2f_{osc} \pm f_{if}$, *i.e.*, at $2f_{rf} + 3f_{if}$, $2f_{rf} + f_{if}$, etc. (*e*) *Harmonic beat notes*, or "tweets," are obtained at $2f_{if}$, $3f_{if}$, etc., if these frequencies lie within the tuning range of the receiver.

6. *Overload and Automatic Volume Control.*—Many commercial direction finder receivers do not utilize a.v.c. In such cases and where the volume is adjustable by means of a manual sensitivity control, it is frequently required that the receiver should not "block" with a strong signal input when the adjustment is made for maximum sensitivity. By blocking is meant the diminution in signal output to a low or zero value, even when the power output at lower signal inputs is comparatively great. For many applications it is required that the receiver should not block entirely at inputs of 0.1, 1, or even 2 volts input to the antenna. In the case of aircraft receivers for the reception of radio range signals where the pilot must distinguish by intensity between *A* and *N* code signals, it is a further requirement that at all settings of the sensitivity control for normal listening levels the receiver output must *increase* with an *increase* in carrier input. When a.v.c. is used, the usual desideratum of flatness holds for commercial receivers as for broadcast receivers.

7. *Frequency Stability.*—The field conditions encountered in commercial receiver and direction finder service are usually much more severe than for entertainment receivers. Such factors as ambient temperature, humidity, voltage and frequency variations of the power supply, barometric pressure, and mechanical shock or vibration are factors that must be considered very carefully where the requirements are those of highly reliable service. Two factors associated with all these changes which must be carefully controlled are the resonant frequency of selective circuits and the frequency of oscillators in the equipment. Much care should be exercised for proper compensation to give good frequency stability when the receiver is once tuned to a desired point. It should also be possible to reproduce the setting of the tuning adjustment with a high degree of precision in many commercial designs.

8. *Audio Fidelity.*—As has been discussed above, the requirement of commercial receivers is primarily that of intelligibility of speech or telegraphic transmission and not pleasing tone quality. On this account, the a-f range for speech reception is generally limited to the minimum that will give adequately intelligible speech so that the extraneous noise obtained with a wide-band audio system will be diminished. This is of importance in direction finders for identification of the transmitter and for simultaneous use as a communication receiver.

9. *Circuit Isolation.*—Adequate shielding and isolation of the various stages in a receiver from each other, from the power supply, and from external disturbance are required. For stability of gain and selectivity it is necessary to do so to prevent variations in the amount of stray feedback. In the case of direction finder receivers the requirements are much more severe because feedback between certain stages of the r-f system may result in errors of apparent bearings.

1.06. Standardization of Test Procedures.—Several organizations have standardizing committees whose purpose it is to simplify and correlate a large number of different test procedures on a given class of equipment. Among these may be mentioned the Standards Committee of the Institute of Radio Engineers and the Subcommittee on Standardization on Test Equipment and Procedures of the Radio Technical Committee for Aeronautics (R.T.C.A. Subcommittee 14). The requirements of the Civil Aeronautics Board for the issuing of approved type certificates for airline radio equipment conform in general to the recommendations of the R.T.C.A. Requirements of the U.S. Navy, the U.S. Army, and other military organizations are similar enough to these specifications so that they will not be considered in detail. It is true, however, that the requirements for military use are almost invariably written individually for the specific use of the equipment.

A considerable amount of material on test methods is included in this chapter as an aid in giving an over-all picture of the final receiver characteristics that must be obtained. This, in turn, suggests the type of measuring apparatus and methods that should be used for making the tests. In later chapters, the discussion of apparatus and laboratory methods will be amplified.

1.07. Standard Test Procedures (Institute of Radio Engineers). At the date of this publication the current issue of the *Standards on Radio Receivers* of the I.R.E. is the issue of 1938. Although particular reference is made to the testing of broadcast receivers, *i.e.*, those for entertainment use, certain generalizations allow extension to the testing of direction finder receivers. This fact should be borne in mind in the study of the applicable section, "Methods of Testing Broadcast Radio Receivers."[1] A few explanatory notes should clarify the problem of direction finder testing.

1. *Input Levels.*—It will be noted that frequent reference is made to the measurement of input voltage to a receiver either as "decibels below 1 volt" or "microvolts." The use of a scale of decibels below 1 volt instead of the more commonly used microvolt scale will be found to be very useful to the set designer. The range of figures is very much less, even though the voltage ratios encountered may be of the order of 10,000,000 : 1. Stage-by-stage gain measurements may be interpreted by addition and subtraction rather than by the multiplication of amplification ratios. A logarithmic scale, such as the decibel scale, expands small differences in power or voltage ratios, and yet keeps the large ratios within bounds of conveniently used figures. A further discussion of logarithmic systems and of units of transmission is given in Secs. 1.09 to 1.12.

2. *Standard Dummy Antenna.*—The directive array is usually such an essential part of a direction finder that it must be used in conjunction with its receiver for test purposes. When no other antenna input is required, the usual means of obtaining input is with an electromagnetic field of known magnitude artificially produced. Such a means is given in (3) Standard Fields below and also in Sec. 6.17. When an auxiliary "sense" or nondirectional antenna is used, a suitable dummy antenna may be used to obtain the correct relative pickups of the directive and the nondirective systems. This choice will be determined by the ultimate use or location of the direction finder.

3. *Standard Fields.*—As an alternative to the establishing of a field of known strength by the methods of Sec. IV *A*3 (*a*) or (*b*),[2] a straight wire is often used through which current is caused to

[1] *Standards on Radio Receivers*, 1938 (New York, I.R.E., 1938), pp. 14–54.
[2] *Ibid.*, pp. 24–26.

flow from a standard signal generator. The simplicity of the relationship governing the resulting circular field at a given distance from the wire furnishes an easy means of establishing a known field strength for measurements on a loop antenna.

Other means of establishing a standard field are given in the I.R.E. *Standards*, Sec. IV *A*3.

4. *Acoustic Fidelity.*—Generally the acoustic fidelity characteristic is not checked on commercial receivers for reasons that have been given, and for that reason Sec. IV *E*5 of the *Standards* may be omitted.

5. *Signal-noise Characteristic.*—An alternative method to that of Sec. IV *E*13 (*a*) of the *Standards* for measuring the signal-noise characteristic is frequently employed for commercial receivers, and the method of conversion of it to equivalent-noise-side-band input is given below. The method of measurement is that of applying a carrier modulated to a depth of 30 per cent at 400 cycles to the input of the receiver. As the modulation is switched off and on, the carrier level is adjusted to give a 6-db change in output between these two conditions. In other words the voltage output due to *signal plus noise* is measured when modulation is on. The output due to *noise only* is measured when the carrier is on without audio modulation.

Let

$e_{1(n)}$ = equivalent-noise-side-band-input voltage (ENSI voltage)
e_c = signal carrier input voltage
$(e_c)_2$ = signal carrier input voltage to give 6-db signal-noise ratio with and without modulation
m = signal modulation factor
V_n = output voltage of noise only
V_{s+n} = output voltage of signal plus noise
V_s = output voltage of signal only

Since a root-mean-square indicator is commonly used, it is found that

$$V_s^2 + V_n^2 = (V_{s+n})^2$$

or

$$V_s = \sqrt{(V_{s+n})^2 - V_n^2} \tag{1.01}$$

For $\dfrac{V_{s+n}}{V_n} = 2$, $V_s = V_n\sqrt{3}$.

The I.R.E. definition

$$e_{1(n)} = me_c \frac{V_n}{V_s} \tag{1.02}$$

then becomes

$$e_{1(n)} = 0.3(e_c)_2 \frac{V_n}{V_n \sqrt{3}} \tag{1.03}$$

$$= 0.1 \sqrt{3}\,(e_c)_2$$

$$= 0.173(e_c)_2 \tag{1.04}$$

It should be remembered that this is a function of the over-all receiver amplitude response (usually referred to as *fidelity*).

Example.—If 6-db signal-to-noise (signal plus noise to noise) occurs at 3-μv input of 400 cycles 30 per cent modulated carrier,

$$e_{1(n)} = 0.173 \times 3 = 0.52\ \mu\text{v ENSI}$$

In the case of a direction finder receiver that includes the antenna array, an analogous definition of equivalent-noise-side-band-input field strength may be made. Here a standard field is produced, consisting of a carrier modulated to a depth of 30 per cent at 400 cycles (1000 cycles is also often used). The modulation is switched off and on, and the carrier field strength is adjusted to give a 6-db change in output between the two conditions. This gives:

Modulation on.	Signal plus noise
Modulation off.	Noise only

If one defines

E_n = ENSI field
E_c = signal carrier input field
$(E_c)_2$ = signal carrier input field to give 6-db signal-noise ratio with and without modulation

then E_n may be calculated in terms of the measured value of $(E_c)_2$ in precisely the same manner as for the case of voltage input to the receiver.

Example.—Thus if there is a 6-db change in output as the modulation is turned on and off at a field strength of 50 μv/m,

$$E_n = 0.173 \times 50 = 8.65\ \mu\text{v/m of ENSI}$$

6. *Two-signal Interference.*—The tests of Sec. IV E18, 19, and 20[1] are of some importance for commercial receivers although they

[1] *Ibid.*, pp. 48–51.

are not frequently made. However, in the case of direction finders, some very analogous measurements of interference are almost always made. Here the interfering signal is used to supply a field oriented at right angles to the field of the desired signal. Then the measurements of adjacent channel and spurious interference may be checked as in the sections of the I.R.E. *Standards* to which reference is made above.

1.08. Standard Test Procedures (Radio Technical Committee for Aeronautics).—The standards for direction finder receiving equipment adopted by the Committee on Standards of the R.T.C.A. on Jan. 13, 1941, are summarized in the following paragraphs. It will be observed that these are of the nature of test methods for the acceptance "type testing" of completed equipment whose reliability in air-line service must be proved.

1. *General Requirements.* *a. Standard test antenna.*—A standard test antenna shall consist of a capacitance of 100 micromicrofarads ± 10 per cent and a series resistance of 10 ohms. The output resistance of the signal generator shall be included in the 10 ohms specified.

In cases where the input circuit of the receiver is designed for a specific input impedance as, for example, a 72-ohm transmission line, the tests hereinafter prescribed shall be conducted at the input impedance for which the receiver is designed in lieu of the standard test antenna defined above. A notation shall be made in the test data setting forth the value of specific input impedance used.

b. Signal-to-noise tests.—The MCW signal-to-noise ratio specified in these tests shall be determined with the carrier *on*, and the modulation *on* and *off* for *signal* and *noise*, respectively. The CW signal-to-noise ratio specified in these tests shall be determined with the modulation *off*, and with the carrier *on* and *off* for *signal* and *noise*, respectively.

In cases where the specified signal to noise cannot be obtained either because of the performance characteristics or because of circuit design of the receiver, the specified tests shall be conducted with the receiver sensitivity or volume control set at the "maximum" position, and a notation to this effect, together with the actual signal-to-noise ratio obtained, included in the test data.

c. Supply voltages.—All receiver tests shall be conducted with input power voltage adjusted to 14 ± 0.25 volts for 12- to 14-volt

equipment, or to 28 ± 0.5 volts for 24- to 28-volt equipment.[1] The input voltage shall be measured at the power source end of the power cables normally supplied or recommended for use with the receiving equipment.

d. Other test conditions.—Unless otherwise specified, the *a-v-c* switch and the beat frequency oscillator switch shall be in the *off* position. The circuits of the receiving equipment shall be properly aligned and otherwise adjusted in accordance with the manufacturer's recommended practices prior to the application of the specified tests.

The resonant circuits of the receiving equipment normally varied to accomplish tuning of the receiver shall be accurately adjusted to the frequency of the source of r-f input (signal generator), unless otherwise specified. Audio-frequency inputs shall be held constant over the frequency range specified at that level established at the reference input frequency, unless otherwise specifically required by the test procedure. Due precautions shall be taken to prevent the introduction of errors resulting from the employment of headphones, voltmeters, oscilloscopes, and other test instruments across either the input or the output impedances used in connection with the specified tests. All tests shall be conducted under conditions of normal room temperature and humidity, unless otherwise specified.

2. *Receiver Tests.*—The group of tests that may properly be called "receiver tests" as applied to direction finders are summarized in Table I*A* and *B*. These are also used for the testing of communication receivers, with a few obvious exceptions.

3. *Direction Finder Tests.*—The reader may refer to Chaps. IV and VI for a discussion of aural-null and visual types of direction finders. Special reference is made in this section to loop antenna equipment.

a. Width of null—loop antenna.—Orient the loop for maximum signal response. Adjust the field strength of a standard r-f carrier (modulated 30 per cent at 400 cycles) to 1000 μv/m, and tune the radio direction finder to the frequency of the carrier. Then orient the loop to the null position as determined by the

[1] Results obtained subsequent to the date of the R.T.C.A. report indicate that more representative values of voltage are 13.25 and 26.5, respectively. For other classes of equipment, appropriate test voltages should of course be chosen.

visual indicating device. Adjust the gain of the receiver so that an output of 0.5 mw is obtained, as indicated on an output meter connected to the output terminals of the receiver. Rotate the loop and record the number of degrees of rotation to the right and left of the null position to which the loop must be turned in order to obtain an output of 50 mw into the load impedance for which the receiver is designed. Repeat this test with field strengths of 500, 250, 100, and 50 μv/m, readjusting the sensitivity of the receiver, if necessary, for each field strength specified to obtain an output of 0.5 mw in the null position. Conduct these tests at the center point of each frequency band. Plot loop setting in degrees right and left for 50-mw output vs. field strength in microvolts per meter.

b. Reciprocal bearings—loop antennas.—Orient the loop for maximum signal response. Adjust the field strength of a standard r-f carrier to 1000 μv/m and accurately tune the radio direction finder receiver to the frequency of the carrier. Orient the loop to the null position as indicated by the visual indicating device or by an output meter in the audio output circuit of the receiver. Adjust the gain of the receiver so that an output of 0.5 mw is obtained. Record the reading of the azimuth control indicator, and rotate the loop to obtain a reciprocal null as indicated by the visual indicating device or output meter. Record the azimuth control bearing and audio output reading.

Repeat the above test with field strengths of 500, 250, 100, and 50 μv/m, readjusting the sensitivity of the receiver, if necessary, for each field strength specified to obtain an output of 0.5 mw in the null position. Conduct these tests at the center point of each frequency band and record the results.

c. Interfering field selectivity—visual direction finders.—Orient the loop for maximum signal response. Adjust the field strength of a standard r-f carrier to 100 μv/m and tune the radio direction finder to the frequency of the carrier. The loop shall then be oriented to the null position as determined by the visual indicating device. Set up an interfering field, the frequency of which may be adjusted, at 90° (physically) from the desired signal field. Record the frequencies, above and below the resonant frequency, to which the interfering signal must be tuned to produce errors of 1, 3, 5, 10, and 25° in the bearing given by the visual indicating device. This test shall be made with interfering signal field

TABLE 1A.—RADIO AND AUDIO-FREQUENCY TESTS OF RECEIVERS AND DIRECTION FINDERS

Type of test	Circuit notes	Type of input and point of application	Radio frequency (for each band)	R-f input level	A-f output level,* mw	Signal-noise ratio, db	Sensitivity or a-f gain control setting	Audio-modulation frequency, cycles/sec	Type of record
1. Sensitivity (MCW-regular antenna)	.... .	Std. r-f signal† **Antenna‡**	6 equally spaced frequencies	*Measure*	50	6	Adjust	400	R-f input vs. radio frequency
2. Sensitivity (CW-regular antenna)	CW oscillator *on*	Unmod. r-f signal **Antenna**	6 equally spaced frequencies	*Measure*	50§	10	Adjust	....	R-f input vs. radio frequency
3. Sensitivity (MCW-loop antenna)	Loop at max. position	Std. r-f field‖ **Loop¶**	6 equally spaced frequencies	*Measure*	50	6	Adjust	400	R-f field strength vs. radio frequency
4. Sensitivity (CW-loop antenna)	Loop at max. position CW oscillator *on*	Unmod. r-f field **Loop**	6 equally spaced frequencies	*Measure*	50§	10	Adjust	. ...	R-f field strength vs. radio frequency
5. Selectivity (intermediate frequency)	.... .	Std. r-f signal **Input of i-f amplifier**	(*a*) Intermediate frequency (*b*) *Measure*	(*a*) Adjust at resonance (*b*) Increase by 6, 20, 40, 60 db	50	(*a*) 6 (*b*) ..	(*a*) Adjust (*b*) Fixed	400	Frequency off resonance vs. r-f input
6. Selectivity (over-all—regular antenna or loop antenna)	A.v.c. rendered inoperative	Std. r-f signal or std. r-f field **Antenna**	(*a*) High and low ends of band (at resonance) (*b*) *Measure*	(*a*) Adjust at resonance (*b*) Increase by 6, 20, 40, 60, 80 db	50	(*a*) 6 (*b*) .	(*a*) Adjust (*b*) Fixed	400	Frequency off resonance vs. r-f input

7. Intermediate-frequency rejection		(a) Std. r-f signal Antenna (b) Std. i-f signal Antenna	(a) High, center, low ends of band (b) Intermediate frequency	(a) Adjust (b) *Measure*	50	(a) 6 (b) . .	(a) Adjust (b) Fixed	400	Ratio of i-f to r-f input in db vs. radio frequency
8. Image frequency rejection		(a) Std. r-f signal Antenna (b) Std. image-freq. signal Antenna	(a) High, center, low ends of band (b) Corresponding image frequency**	(a) Adjust (b) *Measure*	50	(a) 6 (b). .	(a) Adjust (b) Fixed	400	Ratio of image frequency input to r-f input in db vs. radio frequency
9. Intermediate-frequency harmonic beats	. . . . . .	(a) Std. r-f signal Antenna (b) Unmod. r-f signal Antenna	(a) Each harmonic of intermediate frequency in band (b) Readjust slightly for beat note of max. amplitude	50, 5000, and 10,000 μv	(a) Max. undistorted†† (b) *Measure* a-f beat note output	. . . .	(a) Adjust (b) Fixed	(a) 400 (b)	Ratio of beat note output to max. undistorted output in db at each radio frequency and input
10. Rejection of other undesirable responses	. . . .	Std. r-f signal Antenna	(a) High, center, low ends of band (b) Vary from lowest frequency of band to twice highest frequency	(a) Adjust (b) *Measure* (use 2 volts forsearching)	50	(a) 6 (b). .	(a) Adjust (b) Fixed	400	Ratio of spurious response to r-f input in db
11. Noise level	Std. test antenna between antenna and ground connections	None	High, center, and low ends of band	. . . . . .	*Measure*	. . .	Max.	. .	Noise output power

TABLE 1A.—RADIO AND AUDIO-FREQUENCY TESTS OF RECEIVERS AND DIRECTION FINDERS.—(*Continued*)

Type of test	Circuit notes	Type of input and point of application	Radio frequency (for each band)	R-f input level	A-f output level,* mw	Signal-noise ratio, db	Sensitivity or a-f gain control setting	Audio-modulation frequency, cycles/sec	Type of record
12. Fidelity (over-all)	. . .	Std. r-f signal **Antenna**	High and low ends of band	(*a*) Adjust (*b*) Fixed	(*a*) 50 (*b*) *Measure*	(*a*) 20 (*b*)	(*a*) Adjust (*b*) Fixed	(*a*) 400 (*b*) 100, 200, 300, 400, 600, 800, 1000, 1250, 1500, 2000, 2500, 3000, 4000	A-f output power vs. radio frequency
13. Resonant overload and distortion	For circuits without a.v.c.	Std. r-f signal **Antenna**	Center of band	1; 3; 5; 7; 10; 30; 100, 300; 1000; 3000; 10,000; 30,000; 100,000 μv, 0.3, 1.0 v	*Measure*		Full; reduced for 50 mw at 100 μv; reduced for 50 mw at 1000 μv	400	A-f output vs. r-f input; also percentage harmonic distortion‡‡ vs. r-f input
14. Dual channel power output	For circuits with 2 separate a-f output channels	Std. r-f signal **Antenna**	Center of band	(*a*) Adjust (*b*) 1; 3, 5; 7; 10; 30, 100, 300; 1000; 3000; 10,000; 30,000; 100,000 μv, 0.3; 1.0 v	(*a*) Channel 1:50 (*b*) *Measure* for channels 1 and 2	(*a*) 6 (*b*)	(*a*) Adjust (*b*) Fixed	400	A-f output of each channel vs. r-f input
15. Automatic volume control characteristics and distortion	For circuit with a.v.c.	Std. r-f signal **Antenna**	Center of band	1; 3; 5; 7; 10; 30, 100; 300; 1000; 3000; 10,000; 30,000; 100,000 μv; 0.3; 1.0 v	*Measure*	.	Full; reduced for 50 mw at 100 μv, reduced for 50 mw at 1000 μv	400	A-f output vs. r-f input; also percentage harmonic distortion‡‡ vs. r-f input

TABLE 1A.—RADIO AND AUDIO-FREQUENCY TESTS OF RECEIVERS AND DIRECTION FINDERS.—(*Continued*)

Type of test	Circuit notes	Type of input and point of application	Radio frequency (for each band)	R-f input level	A-f output level,* mw	Signal-noise ratio, db	Sensitivity or a-f gain control setting	Audio-modulation frequency, cycles/sec	Type of record
16. **Sensitivity** control	.	Std. r-f signal **Antenna**	Center of band	*Measure*	50	. . .	(*a*) Max. (*b*) Change in steps of 10° rotation	400	**R-f input vs. angular position of sens. control (poorest band)**
17. **Fidelity** (audio)	R-f system rendered inoperative	A-f signal **Input of 1st a-f stage**	. . . .	.	(*a*) 50 (*b*) *Measure*	. . .	. . . .	(*a*) 400 (*b*) 100, 200, 300, 400, 600, 800, 1000, 1250, 1500, 2000, 2500, 3000, 4000	A-f output power vs. audio frequency
18. **Fidelity** (side tone)	For equipment using a-f system as side-tone amplifier. R-f system rendered inoperative	A-f signal **Side-tone input connection**	. . . .	. .	(*a*) 50 (*b*) *Measure*	.	. . .	(*a*) 400 (*b*) 100, 200, 300, 400, 600, 800, 1000, 1250, 1500, 2000. 2500, 3000, 4000	A-f output power vs. audio frequency

TABLE 1B.—MISCELLANEOUS RECEIVER TESTS

Type of test	Circuit notes	Type of input and point of application	Radio frequency (for each band)	A-f output level,* mw	Audio frequency (cycles/sec)	Special measurement	Type of record
19. Dual output channel coupling	Channel 1: Std. load impedance *R* Channel 2: *R*, 2*R*, ½*R* in succession Then interchange channels 1 and 2	**A-f signal** **Output load of channel 1**	....	Channel 1: 500 Channel 2: *measure*	100, 500, 1000, 1500, 2000, 3000	....	A-f output power from channel 2 vs. audio frequency for each load impedance Repeat with channels interchanged
20. Frequency range	Signal generator to be calibrated within 0.05 per cent in frequency	Std. r-f signal **Antenna**	*Measure* max. and min.	....	....	....	Satisfactory tuning range of each band
21. Warm-up drift	Preliminary alignment after 2 hr full load operation Also for CW oscillator if provided	Std. r-f signal **Antenna**	(*a*) Center of band (*b*) *Measure* change of resonant frequency at 10-min intervals from cold start Also change of beat note from CW oscillator	....	....	....	Resonant frequency change (as percentage of resonant frequency) vs. time of operation Also percentage frequency change of beat note vs. time
22. Calibration	Calibration of receiver dial and control unit dial	Std. r-f signal **Antenna**	10 equally spaced frequencies f_{rf}	....	....	*Measure* indicated frequency f_d on each dial	Deviation $f_d - f_{rf}$, in cycles, vs. radio frequency

23. Interchangeability of tubes and plug-in components	(*a*) Complete change of tubes	(*a*) Std. r-f signal **Antenna**	(*a*) Same as test (1)	(*a*) Same as test (1)	(*a*) Same as test (1)	(*a*) Recheck sensitivity test (1)	(*a*) Same as test (1)
	(*b*) Change of crystal in crystal-controlled receivers	(*b*) Std. r-f signal **Antenna**	(*b*) Same as test (1)	(*b*) Same as test (1)	(*b*) Same as test (1)	(*b*) Recheck sensitivity test (1)	(*b*) Same as test (1)
	(*c*) Change of oscillator tube	(*c*)	(*c*)	(*c*) . .	(*c*)	(*c*) *Measure* frequency change	(*c*) Frequency change
	(*d*) Change of power vibrator	(*d*)	(*d*) Entire band ¶	(*d*) . .	(*d*)	(*d*) Check for hum or r-f interference	(*d*) Note results
24. Crystal operation	For "lock-in" crystal operation	Std. r-f signal **Antenna**	Determined by crystal frequency	. . .	. . .	*Measure* frequency above and below resonance at which crystal takes control	Total frequency band of control, in kc

* The load impedance is to be the value for which the receiver or direction finder is designed.

† A standard r-f signal is a carrier voltage which is 30 per cent modulated at audio frequency. Unless otherwise noted, an audio frequency of 400 cycles/sec is to be used.

‡ Input signal is to be applied to the antenna connection through a standard test antenna.

§ Adjust for a beat note of approximately 1000 cycles/sec (800 to 1200 cycles).

‖ A standard r-f field is the radiated field due to a standard r-f signal. Its strength is to be measured at the location of the loop or other directional antenna.

¶ The term "loop" is used here to include other types of directional antennas.

** Image frequency is $f_{rf} + 2f_{if}$ if the receiver oscillator frequency is above f_{rf}. It is $f_{rf} - 2f_{if}$ if the oscillator frequency is below f_{rf}.

†† Undistorted output is considered for this test to contain 10 per cent or less of total harmonic distortion.

‡‡ Harmonic distortion in tests 13 and 15 is to be measured by means of a distortion and noise meter reading the combined output of harmonic distortion and noise. Distortion test is to be made at 3; 10; 100; 10,000; and 100,000 μv input in l-f and h-f bands.

strengths of 100 times and 1000 times the amplitude of the desired signal field strength. Conduct this test at the high and low ends of each frequency band and plot the results. The purpose of this test is to determine how near to the frequency of the desired signal an interfering signal may come, (as a function of relative field strength) without causing deviation of the indicating device from that point which is controlled by the desired signal. The interfering signal is placed 90°, physically, from the desired field in order to simulate the worst condition.

d. Accuracy of bearing—visual indicating devices.—The test setup, as outlined below, is applicable to tests of right-left and automatic direction finders. For the purposes of these tests, mount the loop assembly (loop, loop mount, rotating mechanism, etc.) on a rotatable support in such manner that the loop assembly may be rotated about the loop axis through 360° in a horizontal plane. Provide the rotatable support with a scale graduated in degrees so that the angular position of the loop assembly with reference to a lubber line may be determined by reference to this scale. It is further required that the relation between the angular rotation of the loop and the scale readings of the loop azimuth control and bearing indicator be linear, *i.e.*, no "quadrantal" correction provided. Conduct tests using the maximum length of tachometer shaft and loop transmission line recommended by the manufacturer between the various component units of the radio direction finder.

For a left-right direction finder, adjust the field strength of a standard r-f carrier to 1000 μv/m. With the loop azimuth control set at the zero reading, orient the loop to the *on-course* position, as shown by the visual indicator, by turning the loop assembly on the rotatable mount. (For convenience in making readings of the loop assembly position, the zero degree reading of the rotatable mount scale should coincide with the lubber line in this position.) Rotate the loop assembly by turning the rotatable mount through 360°, in 15° steps, and orient the loop to the *on-course* position as shown by the visual indicator at each setting of the loop assembly by adjustment of the azimuth control. Make adjustment of the azimuth control in both a clockwise and a counterclockwise direction in order to determine the amount of backlash in the azimuth control tachometer shaft. Conduct this test at the center position in the l-f band and record

the azimuth control readings (clockwise and counterclockwise) for each setting of the loop assembly.

Next orient the loop to the *on-course* position as shown by the visual indicator, and vary the output of the signal generator to produce field strengths of 50, 100, 1000, and 10,000 μv/m. Note any deviation of the visual indicator from the *on-course* position resulting from the variation in field strength, and record the number of degrees to the right or left through which the loop must be rotated to return the visual indicator to the *on-course* position. Conduct this test at five approximately equally spaced points in each frequency band.

For an automatic direction finder employing a nondirectional sense antenna set the field as above to 1000 μv/m. Orient the loop by turning the rotatable loop mount to the *on-course* position of the loop as shown by the bearing indicator. Rotate the loop assembly in a clockwise direction through 360°, in 15° steps, and record the bearing indicated at each step by the azimuth indicator. Repeat the above procedure, rotating the loop assembly in a counterclockwise direction. Conduct this test in the center (300 kc) of the "range" band.

With the r-f carrier set for a field strength of 1000 μv/m as specified above, allow the loop to "home," and note the reading of the bearing indicator. (The bearing indicator should read *zero* degrees when the loop is in this position.) Turn off the carrier and turn the loop in a clockwise direction 175° from the home position. Then turn on the carrier, record the time required for the loop to home and the final reading of the bearing indicator. Repeat this procedure, turning the loop 2° from the home position, except that the time required need not be determined if less than one second. Duplicate the above test, turning the loop in a counterclockwise direction. Conduct this test with field strengths of 50, 100, 1000, and 10,000 μv/m and at five equally spaced points in each frequency band.

Duplicate these last tests, using the "loop" sense antenna (if one is provided) instead of the nondirectional sense antenna. Set the loop at 85° instead of 175° from the home position, because of the 180° ambiguity of bearing obtained when a loop sense antenna is used.

e. Phase shift—visual direction finders.—This test is applicable to systems of either the automatic or left-right type. Check for

any malfunction resulting from phase shift between the loop and sense antenna input voltages, in the following manner. With all the circuits of the radio compass properly resonated and adjusted, set the field strength of a standard r-f carrier to 1000 μv/m. Orient the loop so that an *on-course* bearing is indicated on the visual bearing indicator.

Adjust the receiver sensitivity control to the *maximum* position and the audio level control for an output of 50 mw into the load impedance for which the receiver is designed. Successively detune the sense antenna and loop input circuits above and below resonance sufficiently to cause a 3-db decrease in the resonant output indicated by the output meter. To determine a 3-db decrease in the resonant output for detuning of the "loop," connect (or switch) the equipment to function as a receiver operating without a.v.c., and using only the loop as a source of signal pickup, set the audio level control for 50 mw output, and detune the loop circuit the amount necessary to reduce the output to 25 mw. Follow the same procedure for detuning of the sense antenna circuit, but use only the sense antenna as a source of signal input.

Next, simultaneously detune the loop and sense antenna input circuits in various combinations above and below resonance to cause a 3-db decrease in the resonant output, following the same procedure for detuning.

Conduct this test at the h-f and l-f ends of each frequency band. Repeat the test using field strengths of 100 and 100,000 μv/m. Note any deviation of the indicated *on-course* bearing resulting from the application of this test, and record the test conditions under which such deviations occur.

f. Operation of direction finders at harmonics of the beat frequency oscillator.—When an aural-null, an automatic, or a right-left direction finder is equipped with a beat frequency or CW oscillator, check to determine if the operation of this latter adversely affects the operation of the direction finder function. If investigation discloses evidence of malfunction due to the operation of the beat frequency oscillator, with particular attention being given to such of its harmonics as fall within the tunable range of the receiver, record the frequencies, degree of bearing error, and other conditions under which the malfunction is observed.

g. Loop antenna and loop circuit coupling.—Orient the loop for maximum signal response. Set the field of a standard r-f carrier to an amplitude necessary to produce an output of 50 mw into the load impedance for which the receiver is designed. So adjust the receiver sensitivity control that a signal-to-noise ratio of 6 db is obtained.

Then, without changing the adjustment of the receiver loop selector switch, connect the signal generator to the antenna connection of the receiver through a standard test antenna and apply a signal 30 per cent modulated at 400 cycles of sufficient amplitude to produce an output of 50 mw into the load impedance for which the receiver is designed. Record the ratio of the signal generator output to field strength (see Sec. 6.18). Conduct this test at the center of the "range" frequency band. In making this test, take due precautions to isolate the external connections between the signal generator and the loop antenna to prevent stray pickup of the signal generator voltage by the loop antenna.

1.09. Power, Voltage, and Current Ratios.—Increasingly it is becoming common practice to utilize a logarithmic scale of power ratios in communication work. There have been several reasons for this. In the first place, it was common practice with telephone engineers to specify transmission equivalents of telephone circuits as an indication of their figure of merit. The unit for this was initially arbitrarily known as the "mile of standard cable." This later was modified to the *transmission unit,* or T.U., which was defined in a slightly different fashion but was still of a logarithmic nature, as is the unit used at present, the decibel.

In the second place, in the field of acoustics the *sensation* of loudness is of definite physiological significance. It may be shown experimentally that a sound wave of given frequency and pressure (say 0.001 dyne/sq cm) will produce a certain sensation of loudness in the mind of a given listener, and increments of loudness sensation produced as this initial value is increased by successive increments will be less and less as the pressure is raised. To a close approximation, the Weber-Fechner law holds that the minimum detectable *change* in the stimulus is proportional to the magnitude of the stimulus itself. From this it is evident that the loudness sensation is proportional to the *logarithm* of the stimulus, in this case the stimulus being magni-

tude of the sound pressure. From this it follows that the function of interest in acoustics is the logarithm of the ratio of two sound pressures. By analogy it can be seen that in electrical circuits the logarithm of the power ratio is of importance. This is obviously true in an electrical system that delivers an acoustic output.

The third reason for the adoption of a logarithmic scale is for convenience in dealing with the large range of magnitudes encountered in communication systems. This may easily be a factor of 10^{12} or 10^{14} in power.

1.10. Units of Transmission.—There are four units of transmission that have common acceptance in present-day theoretical or practical discussions. The transmission equivalent G is defined as

$$G = \frac{1}{2} \log_e \frac{P_1}{P_2} \qquad \text{in nepers} \qquad (1.05)$$

$$G = 5 \log_e \frac{P_1}{P_2} \qquad \text{in decinepers} \qquad (1.06)$$

In other words, the decineper is $1/10$ neper. When a scale of common logarithms is used, there are two corresponding units:

$$G = \log_{10} \frac{P_1}{P_2} \qquad \text{in bels} \qquad (1.07)$$

$$G = 10 \log_{10} \frac{P_1}{P_2} \qquad \text{in decibels} \qquad (1.08)$$

It may readily be proved that

$$\left.\begin{aligned} 1 \text{ bel} &= 1.151 \text{ nepers} \\ \text{or} \qquad & \\ 1 \text{ neper} &= 8.686 \text{ decibels} \end{aligned}\right\} \qquad (1.09)$$

1.11. Extension of Definitions to Voltage and Current Ratios.—If a constant value of impedance is considered, the power developed will be proportional to the square of the voltage appearing across the impedance or to the square of the current flowing through it. Under such conditions if

$$\frac{P_1}{P_2} = \frac{E_1^2}{E_2^2} = \frac{I_1^2}{I_2^2} \qquad (1.10)$$

then the transmission equivalent may be expressed as

$$G = \log_e \frac{E_1}{E_2} = \log_e \frac{I_1}{I_2} \qquad \text{in nepers} \qquad (1.11)$$

and

$$G = 20 \log_{10} \frac{E_1}{E_2} = 20 \log_{10} \frac{I_1}{I_2} \quad \text{in decibels} \tag{1.12}$$

1.12. Application to Receiver and Direction Finder Measurements.—The use of a logarithmic scale, *i.e.*, the use of the decibel notation, is quite common in the description of the fidelity of a receiver or the response of selective filters. Radio-frequency measurements of receivers may well utilize the same scale for measurements of stage gains, selectivity, image attenuation, signal-to-noise characteristics, etc. In many cases, the impedances of the successive stages are quite high. Then the concept of voltage ratios at points of *infinite impedance* may be used to extend the notion of gain to the *voltage gain* corresponding to the value G used in Eqs. (1.11) and (1.12), without taking into account the actual magnitude of the impedance. Care should be observed when a comparison is to be made with a point in the circuit where the impedance is low. Then recourse must be made to the original definition of G in terms of *power*.

When a reference level of signal has been chosen, it then becomes possible to express sensitivities measured at various stages and on the antenna on such a scale as that of decibels below 1 volt. This system of measurement of sensitivities is finding increased acceptance among radio engineers.

Bibliography

DEPARTMENT OF COMMERCE, CIVIL AERONAUTICS ADMINISTRATOR: *Civil Aeronautics Manual* 16: *Aircraft Radio Equipment Airworthiness*, especially pp. 41–52, Dept. of Commerce, Washington, D.C., Feb. 13, 1941. Much of the material in the R.T.C.A. reference will also be found here.

HENNEY, K. (ed.): *Radio Engineering Handbook*, 3d ed., Sec. 13, by G. L. Beers, "Receiving Systems," pp. 423–458, McGraw-Hill Book Company, Inc., New York, 1941.

KEEN, R.: *Wireless Direction Finding*, 3d rev. ed.; Iliffe & Sons, Ltd., London, 1938.

MCILWAIN, K., and J. G. BRAINERD: *High Frequency Alternating Currents*, 2d ed., pp. 32–35, John Wiley & Sons, Inc., New York, 1939.

RADIO TECHNICAL COMMITTEE FOR AERONAUTICS, SUB-COMMITTEE 14: (STANDARDIZATION OF TEST EQUIPMENT AND PROCEDURES), *Receiving Equipment Test Procedures*, Radio Technical Committee for Aeronautics, Washington, D.C., Jan. 13, 1941.

TERMAN, F. E.: *Radio Engineering*, 2d ed., Chap. 1, McGraw-Hill Book Company, Inc., New York, 1937.

CHAPTER II

WAVE PROPAGATION

2.01. Factors Controlling Direction Finder Operation.—The study of direction finding equipment involves the analysis of the production of an electromagnetic field by means of an antenna and the propagation of the energy represented by this wave motion outward in space. On the first of these factors depend the efficiency of generation of a radio wave and the directive characteristics displayed. On the second, propagation, depends the usefulness of the received energy for identification of the direction of the transmitter. It will be found in the discussion that follows in this chapter that the medium through which the wave is propagated imposes variations in behavior that may affect greatly the accuracy of observations. A proper consideration of and regard for these anomalies will be required in the design and operation of direction finders.

By no means the least important factor is *range*, the distance over which usable transmission can be secured. This is a function of the amount of radiated power, the characteristics of the antenna, the frequency, as well as the properties of the medium.

In this chapter only simple antennas will be considered, but the properties of the space near the surface of the earth will be examined in detail as a function of the frequency of the radio wave disturbance. The analysis of a simple antenna allows study to be made of the process of conversion of energy of a radio transmitter into energy propagated outward into space.

2.02. Electric Field Due to a Dipole in Free Space.—If an antenna consisting of a short wire or other conductor has flowing in it an alternating current, it may be referred to as a radiating *dipole*. The study of the behavior of such a dipole in free space is essential to the analysis of other more complex radiation phenomena. For frequencies sufficiently high, radio communication between near-by aircraft or between aircraft and ground may be practical instances of this simple idealized concept.

As the name *electromagnetic wave* implies, there are present at all points in space where the wave motion exists an *electric* and a *magnetic* field. Neither can exist without the other. It may be mentioned that analysis of direction finder behavior may be carried out at will by a consideration of both or either field component alone, and the conclusions drawn will be the same.

The result for radiation due to a dipole will be given here, but the reader who desires an insight into the method of obtaining the result is referred to Appendix A for a simplified (and not wholly rigorous) derivation from first principles. There the distinction between the *induction* magnetic and electric fields on the one hand and the *radiation* magnetic and electric fields on the other is made clear. Except within the immediate vicinity of the antenna (less than a few wave lengths), only the two radiation fields need be considered.

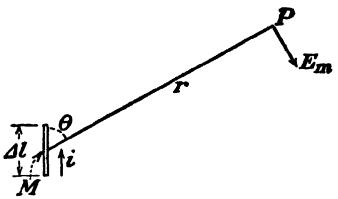


FIG. 2.01.—Radiation field due to dipole. The radiation electric field E_m is in the plane of Δl and r.

If the current in the dipole antenna of length Δl is given as a function of time t by

$$i = I_{\max} \cos \omega t \tag{2.01}$$

then the radiation electric field at a point P has an instantaneous value of

$$E_m = \frac{I_{\max} \, \Delta l \sin \theta}{rc} \, \omega \sin \omega \left(t - \frac{r}{c} \right) \tag{2.02}$$

provided the current distribution throughout the length of the conductor is uniform at any instant.

In Eq. (2.02)

$I_{\max}$ = maximum instantaneous current in the antenna in electromagnetic units (e.m.u.) (abamperes)

θ = angle between the axis of the dipole and the line joining the center M of the dipole to the point P (see Fig. 2.01)

r = distance from the dipole to P in centimeters

c = velocity of light in centimeters per second

ω = angular velocity of the alternating current i of frequency f. $\omega = 2\pi f$ where f is in cycles

Usually one is interested in the maximum value of E_m rather than its instantaneous value. Consequently

$$E_{m(\max)} = \frac{\omega I_{\max} \Delta l \sin \theta}{rc} \tag{2.03}$$

$$= \frac{2\pi I_{\max} \Delta l \sin \theta}{\lambda r} \tag{2.04}$$

since the wave length λ is given by

$$\lambda = \frac{c}{f} = \frac{2\pi c}{\omega} \tag{2.05}$$

Here the values of E_m and $E_{m(\max)}$ are in electrostatic units (e.s.u.), *viz.*, *statvolts per centimeter*, while $I_{\max}$ is in e.m.u., as given above.

When a single isolated dipole Δl with uniform current at all points in its length is considered, the electric radiation field is given by Eq. (2.04). In many practical cases, however, this distribution is not uniform. Then there is a value of Δl for the fictitious equivalent uniform distribution which gives the same field at P. This value of Δl will be designated by h_e and may be called the "effective height." It will be noted in the following equations that $I_{\max}$ refers to this fictitious length and uniform distribution, and not to the value along the actual dipole.

$$E_{m(\max)} = \frac{2\pi I_{\max} h_e \sin \theta}{\lambda r} \tag{2.06}$$

This will now be put in practical units. Since E (volts per centimeter) $= 300E$ (e.s.u.) and I (amperes) $= 10I$ (e.m.u.),

$$E_{m(\max)} = \frac{60\pi I_{\max} h_e \sin \theta}{\lambda r} \tag{2.07}$$

where $E_{m(\max)}$ is in volts per centimeter
$I_{\max}$ is in amperes
h_e and λ are in the same units
r is in centimeters

Alternatively, Eq. (2.07) applies if
$E_{m(\max)}$ is in millivolts per meter
r is in kilometers

and the other quantities are as before.

2.03. Electric Field Due to Vertical Dipole near Ground.— When the dipole is placed adjacent to and normal to a plane of

high conductivity, the method of images shows that the field at P must be the sum of the contributions due to D_1 and D_2, as shown in Fig. 2.02.

This doubles the field at P because a charge moving upward in the actual antenna has a corresponding image of opposite sign and opposite direction of motion. As a result, the *currents* in antenna and image are in the same direction. This conclusion of course does not hold for a horizontal current component. For the case of the vertical grounded dipole of effective height h_e, the field along the ground will be twice that of Eq. (2.07) or, in general,

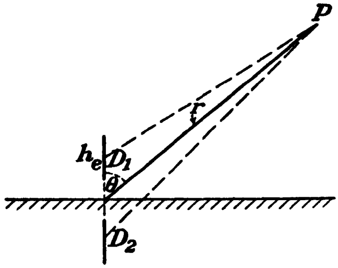


FIG. 2.02.—Dipole and image near conducting plane. In Eq. (2.08) the distance from D_1 to the plane is small. Otherwise h_e depends on this distance.

$$E_{m(\max)} = \frac{120\pi I_{\max} h_e \sin\theta}{\lambda r} \tag{2.08}$$

where the units are as before.

The *radiation resistance* R_r of an antenna may be defined so that the radiated power has a maximum value of

$$P_{r(\max)} = (I_{\max})^2 R_r \tag{2.09}$$

Then Eq. (2.08) becomes

$$E_{m(\max)} = \frac{120\pi \sin\theta}{\lambda r} \frac{h_e}{\sqrt{R_r}} \sqrt{P_{r(\max)}} \tag{2.10}$$

It will be demonstrated in Sec. 3.04 that a vertical dipole of length $\lambda/4$ near ground has a value of effective height of

$$h_e = \frac{\lambda}{2\pi} \tag{2.11}$$

and a radiation resistance of 36.57 ohms. Then for this quarter-wave antenna

$$E_{m(\max)} = \frac{60 \sin\theta}{\sqrt{36.57}\, r} \sqrt{P_{r(\max)}} \tag{2.12}$$

Since either *maximum* or *effective* values of both E_m and P_r may be used, one may denote simply

$$E_m = \frac{9.91 \sin\theta}{m} \sqrt{P_r} \tag{2.13}$$

where E_m is in millivolts per meter, r in kilometers, and P_r in watts. Alternatively,

$$E_m = \frac{6.14 \sin \theta}{r} \sqrt{P_r} \tag{2.14}$$

when r is in miles. This will be found to be an extremely useful formula and is the basis for practically all field-strength computations.

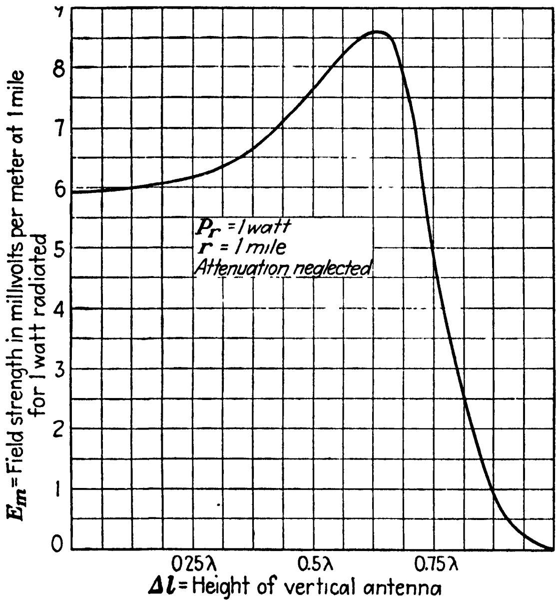


Fig. 2.03.—Electric field strength due to radiating vertical dipole near high-conductivity ground plane as function of dipole height. (*After Ballantine, Proc. I.R.E.*, **12**, 823, *December*, 1924.)

When the antenna is not a quarter of a wave length in height, the coefficient 6.14 must be modified. For values of length up to one wave length, the appropriate value is given in Fig. 2.03.

2.04. Propagation of the Ground Wave.—When a wave from a vertical quarter-wave dipole is propagated along a horizontal plane of infinite conductivity, Eq. (2.14) holds for $\theta = \pi/2$. Let the radiation field be denoted simply as E instead of E_m. Then

$$E = \frac{6.14 \sqrt{P_r}}{r} \tag{2.15}$$

with the same units as for the preceding equation. This equation must be modified when the earth's surface is considered, as it has a finite value of conductivity. The general problem was solved by Sommerfeld[1] and put into much more conveniently usable form by Norton.[2] The procedure consists of the introduction of an attenuation factor A_1. For an antenna sufficiently short so that there is uniform current distribution throughout its length, this is given as a function of two parameters by[2]

$$A_1 = fn(p, b) \tag{2.16}$$

where p is called the "numerical distance" and b the "phase constant." The quantity b is given by

$$\tan b = 5.55 \times 10^{-19} \frac{\epsilon + 1}{\sigma_{\text{emu}}} f_{\text{kc}} \tag{2.17}$$

where ϵ is the dielectric constant and σ the conductivity (in e.m.u.) of the earth's surface. Then

$$p = 1.77 \times 10^{-18} \frac{f_{\text{kc}}}{\sigma_{\text{emu}}} \frac{r}{\lambda} \cos b \tag{2.18}$$

Here r and λ are measured in the same units.

It may readily be seen that Eq. (2.18) may be written

$$p = \frac{\pi}{\epsilon + 1} \frac{r}{\lambda} \sin b \tag{2.19}$$

Consequently for b near $\pi/2$ the factor $\sin b$ may be set equal to unity in Eq. (2.19). This is the case for low conductivity at high frequencies and may be referred to as a *capacitive earth.* Conversely, at low frequencies with σ large, b is small and

$$\cos b = 1$$

in Eq. (2.18). This may be designated as a *resistive earth.*

The value of A_1 is given in Fig. 2.04 as a function of p and b. The constants σ and ϵ may be estimated from Table II and from the map of Fig. 2.05.

[1] A. SOMMERFELD, *Annalen der Physik*, **28**, 665 (1909).

[2] K. A. NORTON, The Propagation of Radio Waves over the Surface of the Earth and in the Upper Atmosphere, *Proceedings of the Institute of Radio Engineers*, **24**, 1367 (October, 1936); **25**, 1203 (September, 1937).

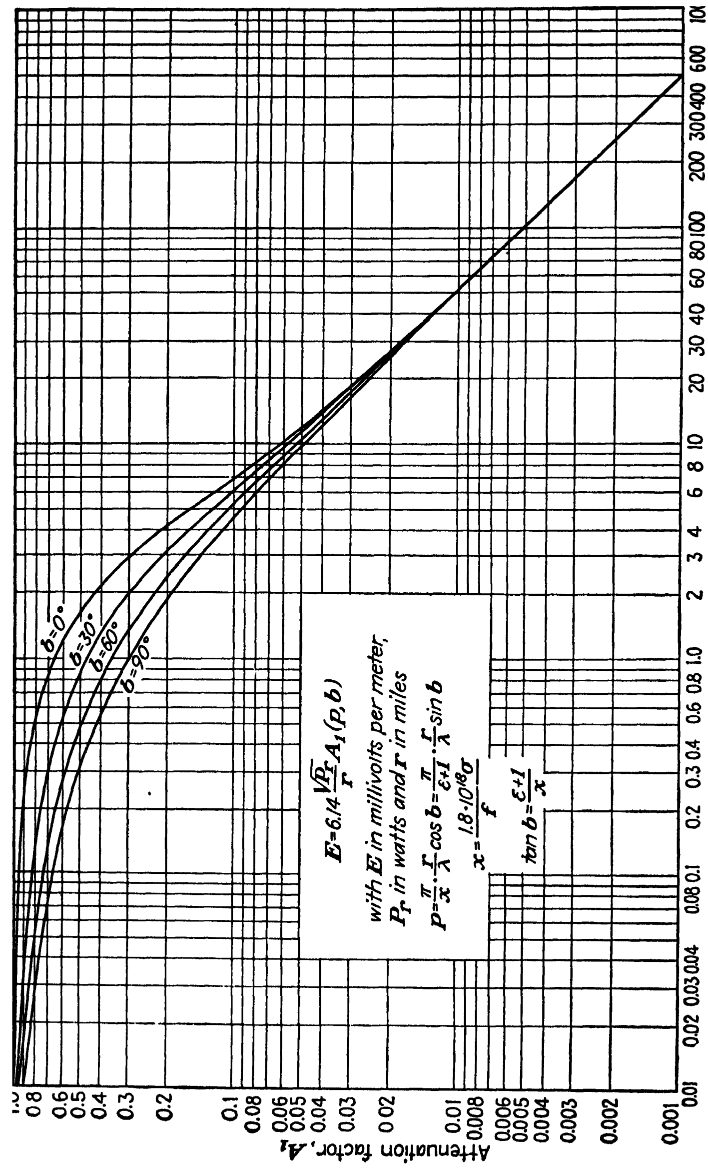


FIG. 2.04.—Attenuation factor A_1 of Sommerfeld propagation equation. (*Norton, Proc. I. R. E.*, **24**, 1367, *October*, 1936.)

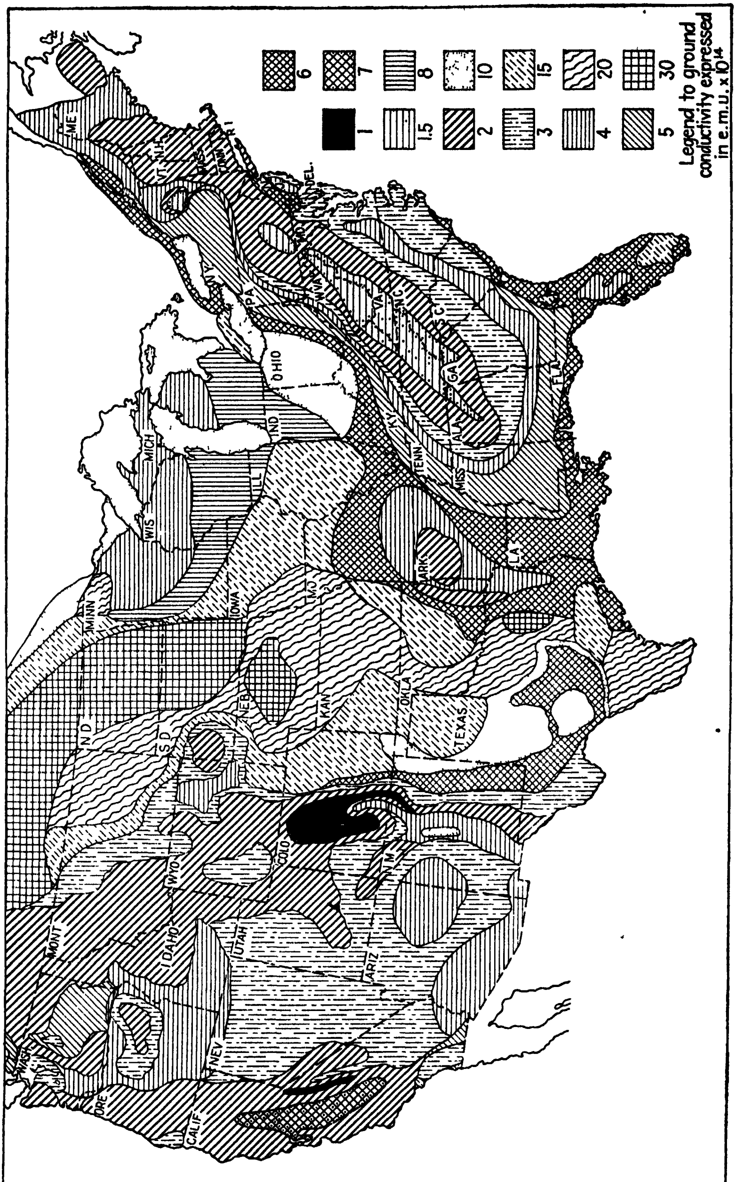


FIG. 2.05.—Ground conductivity in the United States. (*Federal Communications Commission.*)

Then the field strength is

$$E = \frac{6.14\sqrt{P_r}}{r}A_1 \tag{2.20}$$

Thus it must be remembered that the field strength is proportional to the *square root* of the *power*. If attenuation is negligible, field strength is *inversely proportional* to the *distance*. For large values of the numerical distance p, the factor A_1 approaches $1/2p$, thereby causing E to vary inversely as the *square* of the distance.

TABLE II.—TYPICAL SURFACE CONSTANTS

Type of earth surface	σ (e.m.u.)	ϵ
Sea water	5×10^{-11}	80
Fresh water	1×10^{-13}	80
High-conductivity land	3×10^{-13}	15
Moderate-conductivity land	5×10^{-14}	10
Low-conductivity land	1×10^{-14}	5

In Table II, σ expressed in e.m.u. may be replaced by $10^{-9}\sigma$ mho/cm in practical units. For instance $\sigma = 10^{-13}$ e.m.u. corresponds to $\sigma = 10^{-4}$ mho/cm, or a 1-cm cube of the material has a resistance of 10,000 ohms.

Example.—As an example of calculation of field strength, one may consider a 50-kw transmitter operating at 600 kc and having a quarter-wave vertical antenna located near the seashore. If the land has a conductivity $\sigma = 5 \times 10^{-14}$ e.m.u. and $\epsilon = 10$, the problem is to find the field strength 100 miles inland and 100 miles at sea. For the first case, from Eq. (2.17):

$$\begin{aligned} \tan b &= \frac{5.55 \times 10^{-19} \times (10 + 1) \times 600}{5 \times 10^{-14}} \\ &= 0.0733 \\ b &= 4.1° \end{aligned}$$

Then from Eq. (2.18):

$$\begin{aligned} p &= \frac{1.77 \times 10^{-18} \times 600 \times 100 \times 0.998}{5 \times 10^{-14} \times 0.62 \times 0.5} \\ &= 6.84 \end{aligned}$$

By reference to Fig. 2.04 it is found for the attenuation factor that

$$A_1 = 0.099$$

Consequently,

$$\begin{aligned} E &= \frac{6.14\sqrt{50 \times 10^3} \times 0.099}{100} \\ &= 1.36 \text{ mv/m or } 1360\ \mu\text{v/m} \end{aligned}$$

Next for the case of propagation over sea water, one finds

$$\tan b = \frac{5.55 \times 10^{-19} \times (80 + 1) \times 600}{5 \times 10^{-11}}$$
$$= 5.39 \times 10^{-4}$$
$$b = 0°$$
$$p = \frac{1.77 \times 10^{-18} \times 600 \times 100 \times 1.000}{5 \times 10^{-11} \times 0.62 \times 0.5}$$
$$= 6.85 \times 10^{-3}$$

Hence

$$A_1 = 0.999$$

This means that at 100 miles over sea water, propagation obeys accurately the inverse distance law.

$$E = \frac{6.14 \sqrt{50 \times 10^3} \times 0.999}{100}$$
$$= 13.6 \text{ mv/m or } 13{,}600\ \mu\text{v/m}$$

The field intensity for propagation over water is here 10 times as great as over land.

The attenuation of waves between 150 and 5000 kc when propagated along the surface for various values of σ and ϵ is illustrated in Figs. 2.06 to 2.08. One may note that the numerical constant is chosen for a very short antenna. This corresponds to a value of 5.90 in place of 6.14 of Eq. (2.20) as given above. A power of 1 kw is assumed. The value for other antenna heights may be estimated from Fig. 2.03.

The extensions of these results to include the minor corrections due to diffraction around a spherical earth and refraction in the lower atmosphere are given by Watson[1] and by Burrows,[2] respectively, and summarized by Norton.[3]

2.05. Polarization of Ground Waves.—The drawing of Fig. 2.09 shows that in free space the radiation from a dipole at a large distance consists of two components: (1) the electric field vector E which lies tangent to a meridian and thus normal to the radius vector r, and (2) the magnetic field vector H, tangent to a latitude circle and therefore also normal to the radius vector r, but at right angles to E.

[1] G. N. WATSON, The Diffraction of Electric Waves by the Earth, *Proceedings of the Royal Society (London)*, *A* **95,** 83 (1918). See also T. L. ECKERSLEY, *Proc. I.R.E.*, **20,** 1555 (October, 1932).

[2] C. R. BURROWS, Radio Propagation over Spherical Earth, *Proc. I.R.E.*, **23,** 470 (May, 1935).

[3] K. A. NORTON, *loc. cit.*

The *wave front* at the point P is the plane drawn through that point including E and H. In free space it is of course normal to

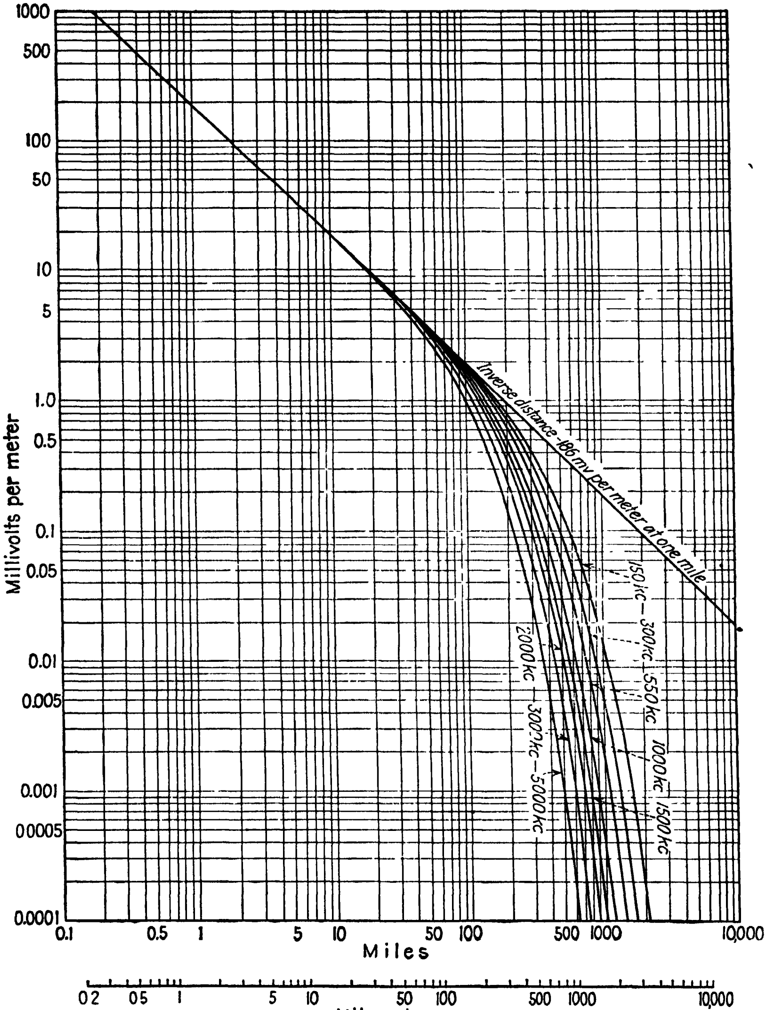


FIG. 2.06.—Ground-wave field strength as a function of distance from transmitter. A power of 1 kw from a short antenna is assumed. Propagation is over sea water for which $\sigma = 5 \times 10^{-11}$ e.m.u., and $\epsilon = 80$. (*Norton, Proc. I.R.E.*, **24**, 1367, *October*, 1936.)

r. The direction of polarization at P is identical with the direction of the vector E. The *plane of polarization* is defined to

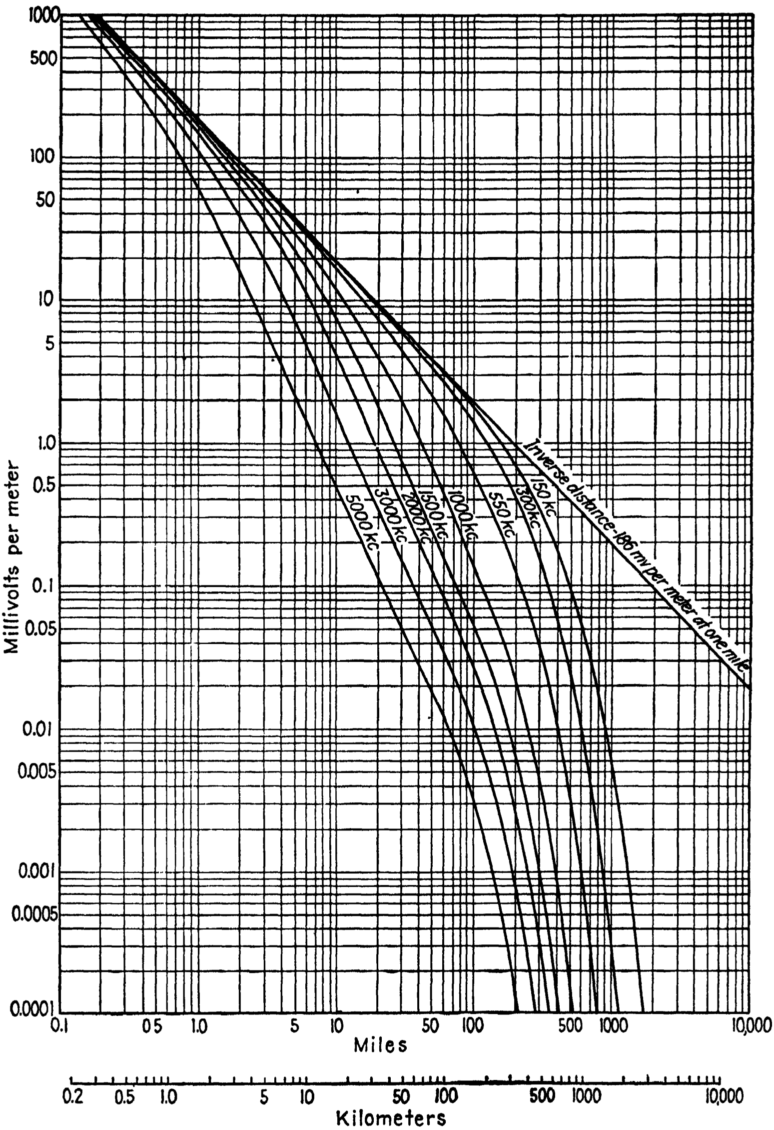


FIG. 2.07.—Ground-wave field strength as a function of distance from transmitter. A power of 1 kw from a short antenna is assumed. Propagation is over land of moderate conductivity for which $\sigma = 10^{-13}$ e.m.u., and $\epsilon = 15$. (*Norton, Proc. I.R.E.*, **24**, 1367, *October*, 1936.)

include the vectors E and r; *i.e.*, it lies along the direction of propagation and is normal to the wave front (in a homogeneous

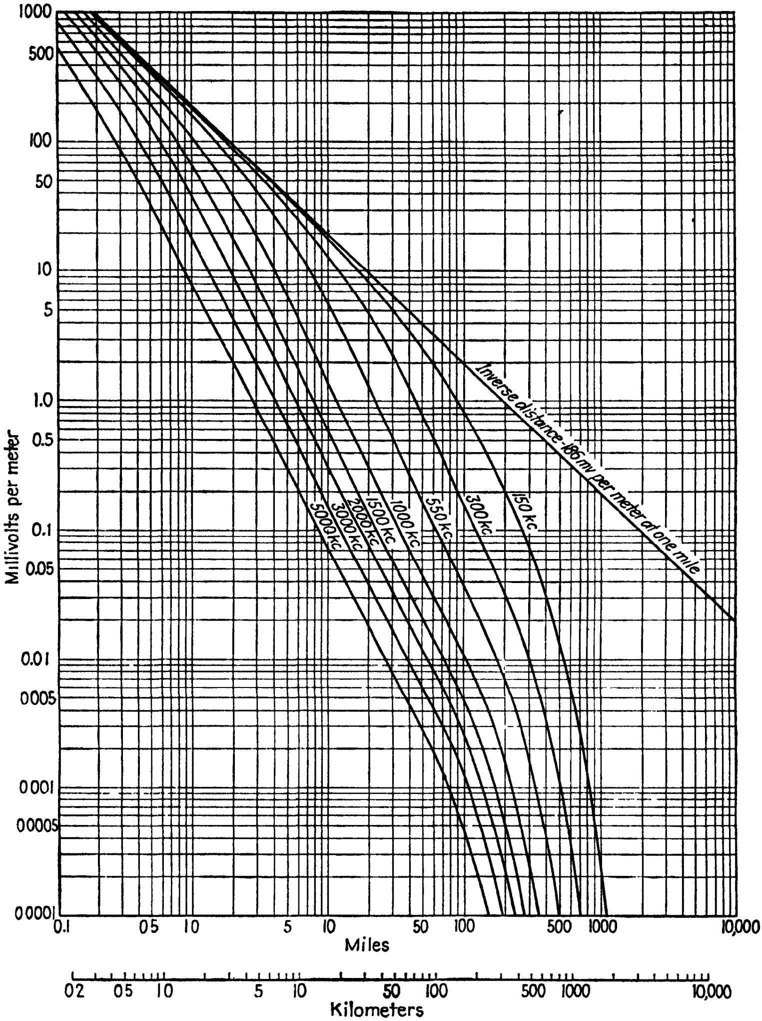


FIG. 2.08.—Ground-wave field strength as a function of distance from transmitter. A power of 1 kw from a short antenna is assumed. Propagation is over land of low conductivity for which $\sigma = 10^{-14}$ e.m.u., and $\epsilon = 5$. (*Norton, Proc. I.R.E.*, **24**, 1367, *October*, 1936.)

medium). The plane of polarization, therefore, contains the axis of the radiating dipole. It will be seen in more detailed

consideration of the behavior of direction finders that the plane of polarization of a wave is of extreme importance.

An examination will now be made of the geometric relations existing in the equatorial plane of a radiating dipole, like the *LMN* plane of Fig. 2.09. The dipole axis will be assumed to be vertical. Then *E* also is vertical and *H* is horizontal, tangent to the equator. The wave front is a vertical plane element at the point *M*, although of course it is actually part of a spherical sur-

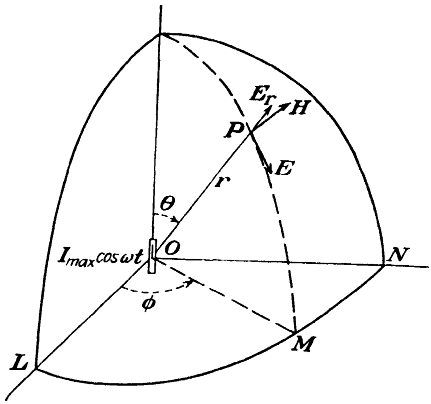


FIG. 2.09.—Relationship of wave front and plane of polarization to direction of radiating dipole.

face. The direction of polarization is vertical, and the plane of polarization is *OMP*.

When a ground plane of high conductivity is made to coincide with *LMN*, the image of the dipole is also vertical, so that the same state of directions of propagation and polarization results. Thus the *plane of polarization* from a *vertical radiator* near the earth's surface is also *vertical*. The successive wave fronts are then sections of concentric spheres and, for large distances, are sensibly plane parallel vertical planes, at right angles to the direction of propagation.

It may be remarked that the direction of polarization or the direction of *E* is vertical only for a zero-resistance ground plane. Losses in the latter cause the wave fronts to tilt forward slightly, so that *E* also has a forward tilt. The direction of *H* is unaltered. For the purposes of this discussion this effect is of little moment, although on it depends the operation of the so-called "wave antenna."

Suppose now the ground plane were chosen to coincide with *OMP* of Fig. 2.09; *i.e.*, the radiator would be a *horizontal* dipole. As a consequence, E would lie in the plane of the highly conducting ground plane. This in turn would mean that there was an electric field along the ground plane and a potential difference between adjacent points. This is obviously impossible since zero resistance is assumed. Thus in the ground plane there can be no horizontally polarized radiation propagated horizontally.

When actual values of ground conductivity are used and when the frequencies for medium- and long-wave direction finders are considered, this argument as to the attenuation of horizontally polarized waves reasonably near the earth's surface still applies.

2.06. The Ionosphere. Experimental Evidence.—It is found experimentally that radio waves are in general propagated to much greater distances than would be possible if the field strengths were given by Eq. (2.20) under all conditions. An indication of this is the well-known fact that broadcast signals are received at greater distances at night and in wintertime especially. Equation (2.20) gives no evidence that there should be diurnal or seasonal variation of field intensity.

Furthermore it is observed at night in the broadcast band, and by day or night at higher frequencies, that as one recedes from the transmitter the field intensity falls off at first in accordance with results previously given. Beyond that there is a region of low and variable field intensity, or perhaps no signal at all, and at greater distances the signal is received again with fair to extremely good field strength. This phenomenon may be described as the *skip effect*. Other observations on the apparent direction of arrival of signals beyond the *skip distance* indicate that the waves are coming downward, often at considerable angles, and are not being propagated tangentially to the earth's surface, as would be the case for the ground wave.

These facts may be explained by more than one theory of propagation, for they constitute only indirect evidence in support of any of them. Much more direct means are available, as will be discussed shortly, to show that the effect is due to a layer or series of layers of conducting material in the upper atmosphere of the earth. All the evidence goes to indicate that the conducting material consists of ionized gases and free electrons located in a region from 80 to 450 km above the earth's surface.

This ionized region, although actually a series of strata, is known collectively as the *ionosphere.* The lowest of the layers to be commonly observed is also referred to as the "Kennelly-Heaviside" layer after the two workers who independently predicted its existence. The next higher layer is often called the "Appleton" layer after its discoverer.

2.07. Origin of the Ionized Layers.—The fundamental cause of ionization in the upper atmosphere is the presence of radiation from the sun. Under the influence of ultraviolet light of sufficient intensity, appreciable numbers of atoms of a gas layer may be ionized into positive ions and free electrons. When the gas density is high, recombination into neutral atoms occurs very rapidly even though the density of the electrons in the region may be quite small. On the other hand, when the molecular density is sufficiently low so that the mean free path of the electron gas is high, long time intervals will elapse before recombination occurs, and as a result there exists a cloud of free electrons behaving as a partial conductor. This effect then has certain resemblances to the electron flow in the space-charge region of a thermionic vacuum tube.

At a height of several hundred kilometers in the earth's atmosphere two conditions are much more favorable for the production of electrons and positive ions than at the earth's surface:

1. The gas density is much less so that recombination does not occur so rapidly.

2. Ultraviolet radiation to cause ionization is much more intense.

Although the ozone content of the atmosphere is extremely small on a percentage basis, it acts to absorb a great fraction of the ultraviolet light radiated from the sun. To a lesser extent both nitrogen and molecular oxygen perform this same absorption at lower wave lengths. An excellent discussion of the ionization and recombination phenomena occurring in the ionosphere is given by Chapman.[1]

Certain of the ionosphere layers vary with time of day in electron density. This quantity may rise to maximum about noon, fall off as sunlight diminishes, and reach a low value of ionization during the night. Other portions of the atmosphere

[1] S. CHAPMAN, The Sun and the Ionosphere, *Journal of the Institution of Electrical Engineers (London)*, **88**, 400 (November, 1941).

change less rapidly owing to the slow rate of recombination that may occur. It will be observed how complex the actual phenomena are as a function of the impinging radiation to conditions in the given layer and the presence of electronic or magnetic fields when it is noted that the following factors all have a profound effect upon the behavior of the ionosphere:

1. Time of day.
2. Time of year.
3. Latitude.
4. Epoch in sunspot cycle.
5. Occurrence of magnetic storms.

2.08. Ionosphere Layers.—During the daytime there are three main layers of the ionosphere: the E, the F_1, and the F_2. The E layer has its region of maximum electron density at about 100 km. This varies somewhat between a summer day during a year of minimum sunspot activity, when it may be as low as 80 km, up to 125 km, the virtual height at the maximum of solar activity.

The F_1 layer is much higher than the previous, being usually found at about 200 km, with limits of about 140 to 250 km. It has much higher electron density than does the E layer. Like the latter its height is nearly independent of the time of year and changes relatively slowly except at sunrise and sunset. The F_2 layer varies quite rapidly with both these factors. It has a still higher electron density. The maximum height may be over 400 km at noon in June or may be as low as 250 at the same time in December. At sunset the layer descends in virtual height at the same time as the density decreases, so that F_2 and F_1 layers coalesce. Thus, at night there are the two main layers: the F, consisting of the combined F_1 and F_2 strata and located at a height of 200 to 400 km, and the lower E layer at about the same height as during the daytime. Each has a much lower electron density than it has during the day. The F layer may be only 20 per cent of the density of the F_2, while the E layer may change by so great a factor that it seems to disappear by night. The manner in which these two change with time of day and time of year is illustrated in Fig. 2.10. Corresponding to this are curves[1]

[1] GILLILAND, KIRBY, SMITH, and REYMER, Characteristics of the Ionosphere and Their Application to Radio Transmission, *Journal of Research of the National Bureau of Standards*, **18**, 645 (June, 1937); *Proc. I.R.E.*, **25**, 823 (July, 1937).

on variation of the electron density of the layers as a function of time of day and time of year as will be seen in Fig. 2.11.

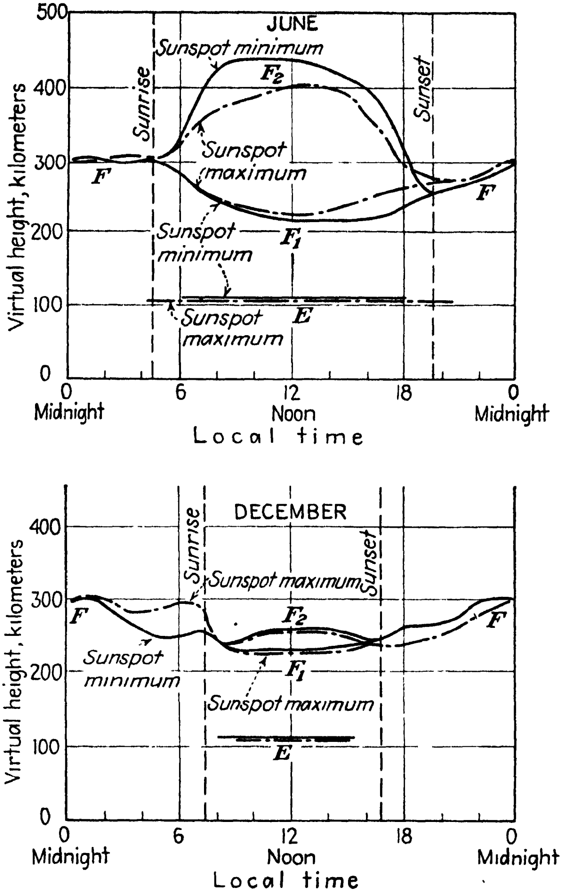


FIG. 2.10.—Ionosphere virtual heights. (*National Bureau of Standards.*)

A rough comparison can be made of the E and F_2 layers with respect to frequency of collision of a given electron with an ion, molecular density, and electron density from the following:

Layer	Collision frequency per sec	Molecular density per cc	Electron density per cc
E	10^6	10^{13}	10^5
F_2	5×10^3	5×10^{10}	7×10^5

It will thus be seen that recombination occurs much more rapidly in the E layer, where gas density may be 200 times as great as in higher layers. On the other hand, the electron den-

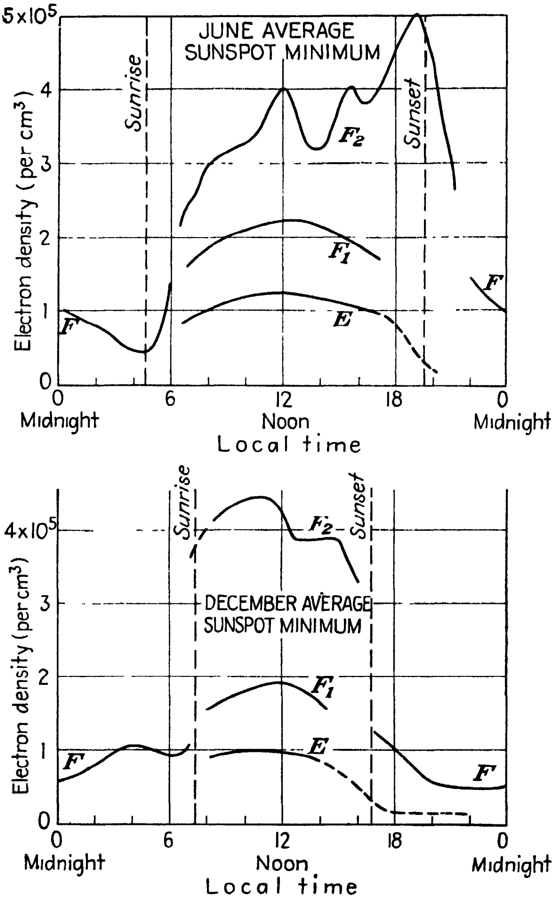


FIG. 2.11.—Ionosphere electron densities. (*National Bureau of Standards.*)

sity in the F layers is of the order of seven times as great as in the E for these average conditions of daytime behavior.

At the present time it is believed that the E layer may be identified with the free electrons of ionized molecular oxygen, while the F layers are produced by ionized nitrogen. Evidence of this is obtained from the spectrum of the aurora. This latter

indicates that molecular oxygen extends in appreciable quantities only to a height of 110 to 130 km. Nitrogen alone is found at the higher altitudes.

It will be seen from Fig. 2.11 that the electron density of each layer shows pronounced diurnal effect. In all cases the density rises rapidly at sunrise and has an upward trend as the angular elevation of the sun increases. This is especially simple in the case of the E and F_1 layers. The density of each rises to a maximum at about noon. The F_2 layer behaves in a much more complicated fashion with a series of maxima and minima during the daytime. The reasons for this are discussed by Chapman.[1]

The seasonal variations of the E and F_1 layers are as would be predicted by a consideration of the zenith angle of the sun at the particular time. Consequently, in temperate latitudes the electron density is considerably higher in summer than in winter. The F_2 layer shows a different trend of electron density during the winter and may actually be greater at certain times of day than in summer.

2.09. Propagation through an Ionized Medium.—The manner in which energy from a radio wave may be absorbed or reradiated by the ionosphere may be examined in general terms by considering a single electron in a radiation field. In this simple argument only the electric field will be taken into account. The electron will be subject to a force F due to its charge $-e$, and it will move under the influence of F alone during the time of one free path, *i.e.*, the time between collisions with gas molecules.

The force on an electron at rest due to the electric field E is

$$F = -Ee \tag{2.21}$$

or, if E is a function of time alone at a fixed point,

$$E = E_{max} \sin \omega t \tag{2.22}$$

it can be shown[2] that the electron in motion under this varying

[1] S. CHAPMAN, *loc. cit.*

[2] The equation of motion for E along the x axis is

$$m\frac{d^2x}{dt^2} = -Ee \tag{2.24}$$

if the electron mass is m.

[Footnote continued on page 46.]

field is equivalent to a current

$$i = -\frac{E_{max}e^2 \cos \omega t}{\omega m} \qquad (2.23)$$

where m is the electron mass.

Equations (2.22) and (2.23) demonstrate that the varying current due to the electron motion lags behind the field by an angle $\pi/2$ and is also sinusoidal.

The current i is equivalent to a dipole and radiates in the same manner. This energy is abstracted from the original electromagnetic wave, the electron is set in motion, and it in turn radiates a wave of the same frequency, but of a different phase.

It can be shown[1] that this results in a change in *phase* velocity of the electromagnetic wave.

One should make a distinction between the *phase velocity* and the *group velocity* of a wave disturbance. In free space they are of the same magnitude, but in a dispersing medium they may be different. The phase velocity measures the rate of motion of a "crest" or a "valley" of the wave. The velocity of energy propagation is the group velocity. It is this latter which can

---

If E is the function of time given in Eq. (2.22)

$$\frac{d^2x}{dt^2} = -E_{max}\frac{e}{m}\sin \omega t \qquad (2.25)$$

Integration gives

$$\frac{dx}{dt} = v = \frac{E_{max}e}{\omega m}\cos \omega t + c_1 \qquad (2.26)$$

Now since there is no streaming motion (steady current) of electrons due to E, c_1 must be zero. The position of the electron at any instant is given by an integration of Eq. (2.26).

$$x = \frac{E_{max}e}{\omega^2 m}\sin \omega t \qquad (2.27)$$

if the constant of integration is set equal to zero for the case that $x = 0$ when $t = 0$.

If one reverts now to the relation for the electron velocity, it is found that the current due to a *charge in motion* is

$$i = -ev \qquad (2.28)$$

since $-e$ is the charge, and thus the result of Eq. (2.23) follows directly.

[1] H. W. NICHOLS and J. C. SCHELLENG, Propagation of Electric Waves over the Earth, *Bell System Technical Journal*, **4**, 215 (1925), especially p. 222. See also P. O. PEDERSON, The Refractive Index of Space with Free Electrons, *Experimental Wireless and Wireless Engineer*, **7**, 16 (January, 1930).

never exceed that of light in free space. An example of the difference is the phenomenon of motion of water waves behind the bow wave of a ship. Individual crests may move forward until they encounter the bow wave, where they disappear. The energy of the wave motion cannot propagate itself ahead of the bow wave, which in turn does not lie ahead of the vessel when the speed of the latter is sufficiently great. Here the phase velocity (motion of individual ripples) exceeds the group velocity (motion of the bow wave).

If the index of refraction

$$\mu = \frac{\text{velocity in free space}}{\text{phase velocity in ionized medium}} \tag{2.29}$$

then in the absence of a magnetic field the result is

$$\mu^2 = 1 - \frac{4\pi e^2 N}{m\omega^2} \tag{2.30}$$

where N is the number of free electrons per cubic centimeter. Since

$$\frac{4\pi e^2}{m} = 3.2 \times 10^9 \tag{2.31}$$

$$\mu^2 = 1 - \frac{3.2 \times 10^9 N}{\omega^2}$$

$$= 1 - \frac{81.3N}{f_{\text{kc}}{}^2} \tag{2.32}$$

It will be noted that μ^2 has a value less than unity. This means that the phase velocity is greater than that of light in free space. This phenomenon is characteristic of the anomalous dispersion of light also. The *group* velocity, that of propagation of *energy*, remains less than the velocity of light in free space.

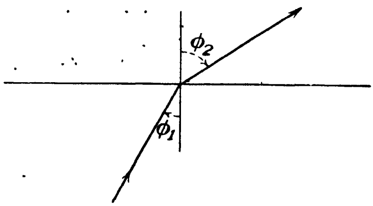


FIG. 2.12.—Refraction at boundary of ionosphere layer.

Snell's law of refraction may be written as

$$\frac{\sin \phi_1}{\sin \phi_2} = \mu \tag{2.33}$$

for a ray traveling from a medium of index of refraction unity to one of μ, as shown in Fig. 2.12. This is a well-known result from

elementary physical optics. There will be total reflection at the interface if

$$\frac{\sin \phi_1}{\mu} > 1$$

Consequently the *critical angle* is the value of ϕ_1 at which $\sin \phi_2 = 1$, or if one denotes ϕ_1 at the critical angle by ϕ_1'

$$\sin \phi_1' = \mu \tag{2.34}$$

For decreasing values of μ, the critical angle diminishes, with the result that a wave propagated upward into the ionosphere layer will be returned to earth even when normal incidence is approached.

If Eqs. (2.32) and (2.34) are combined, the critical angle ϕ_1' in terms of the frequency of wave may be found.

$$\begin{aligned}\frac{81.3N}{f_{kc}^2} &= 1 - \sin^2 \phi_1' \\ &= \cos^2 \phi_1' \end{aligned} \tag{2.35}$$

Thus the *highest* frequency which will be reflected from the layer when the wave is incident at the angle ϕ_1' is

$$f_{kc}' = \frac{9.02 \sqrt{N}}{\cos \phi_1'} \tag{2.36}$$

Example.—It is desired to find the maximum frequency at which reflection will occur from the E layer at noon in December. The conditions are as given in Figs. 2.10–2.11, and an angle of incidence of 60° is assumed. Here $N = 10^5$ per cc.

$$\begin{aligned} f_{kc}' &= \frac{9.02 \times 3.16 \times 10^2}{0.5} \\ &= 5700 \text{ kc} \end{aligned}$$

Both because of the usual experimental means of determining this limiting frequency and because of the ease of expressing the result, it is customary to define the value of f' for vertical incidence ($\phi_1' = 0$) as the *critical frequency* for that layer. The critical frequency is thus a measure of the electron density. This has a maximum value, obtained from Eq. (2.36) of

$$\begin{aligned} N &= \frac{f_c^2}{81.3} \\ &= 0.0124 f_c^2 \end{aligned} \tag{2.37}$$

where f_c is in kilocycles per second. It was by this means that the values of electron density in Fig. 2.11 were obtained.

2.10. Critical Frequencies.—When virtual height is measured as a function of frequency it is found that the apparent value rises very rapidly as the frequency is increased to the critical frequency, above which there is no reflection. This is illustrated in Fig. 2.13 for a typical condition on a winter day.

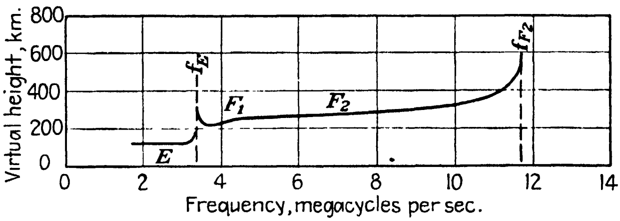


Fig. 2.13.—Typical virtual-height characteristic of ionosphere showing critical frequencies. (*National Bureau of Standards, Letter Circular LC*-614.)

The values of f_E and f_{F_2} are the critical frequencies for the E and F_2 layers, respectively, and for vertical incidence as described in Sec. 2.09. Above f_E the wave penetrates into the higher layer and will be reflected if it lies below f_{F_2}.

For frequencies just above f_E, the wave is retarded by a large amount in passing through the E layer, with the result that the virtual height is much greater than the height of the actual layer at which reflection takes place. It will be noted that the velocity here is the *group* velocity, or velocity of energy propagation, not the *phase* velocity as used in the definition of index of refraction in Eq. (2.29).

Typical values of critical frequencies are given in Fig. 2.14 for the same range of conditions as for Fig. 2.10 at the latitude of Washington, D.C., and typical of conditions throughout the continental United States. The values for the F layers are for the ordinary ray (see discussion on the effect of the earth's magnetic field in Sec. 2.13). The critical frequency for another component, the extraordinary ray, is about 750 kc higher than for the ordinary ray. This difference does not exist in the case of f_E.

During the period from 1937 to the beginning of 1942, curves similar to those of Figs. 2.10 and 2.14 appeared monthly in the *Proceedings of the Institute of Radio Engineers* as a record of

observations. Together with these data on virtual heights and critical frequencies, curves on *maximum usable frequency* were given, and also predictions for this latter for a later time.

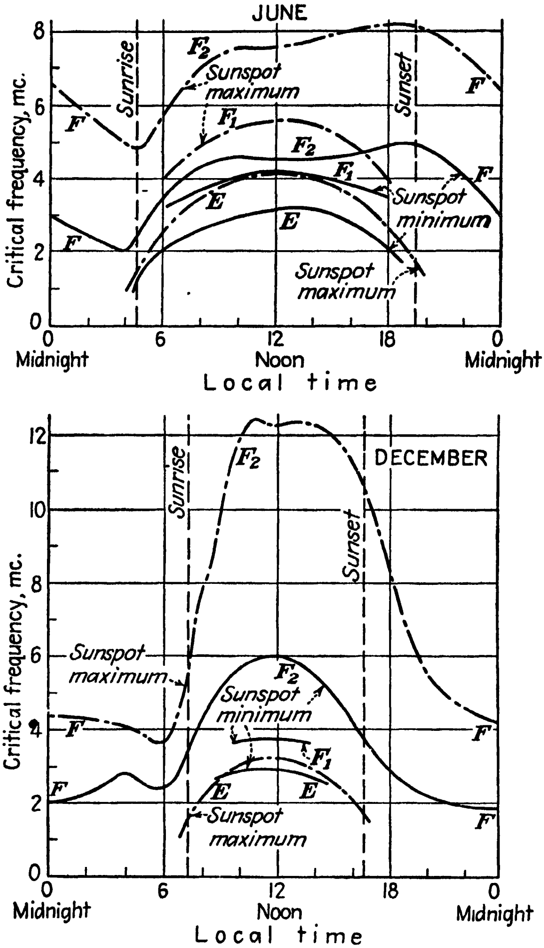


FIG. 2.14.—Ionosphere critical frequencies. (*National Bureau of Standards.*)

2.11. Maximum Usable Frequencies.—When a radio wave is propagated along the earth's surface or obliquely upward, it will strike the ionosphere layer at an angle ϕ_1 (in Fig. 2.12) greater than zero, and perhaps approaching 90° or grazing incidence. Under these conditions the *maximum usable frequency* is greater

than the critical frequency previously discussed. Thus, for a single reflection from the ionosphere, the *maximum usable frequency increases as the transmission distance increases.* This is illustrated in Fig. 2.15. Thus reception by reflection from the F_2 layer at a point 2000 km from a transmitter at Washington becomes possible at a higher frequency than at Chicago because ϕ_c is greater than ϕ_b.

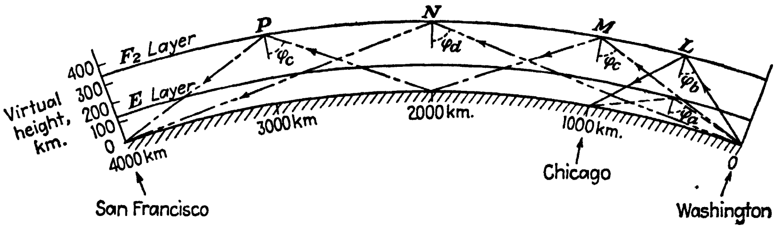


FIG. 2.15.—Example of one-hop and multiple-hop sky-wave long-distance transmission.

Transmission may take place by paths involving one or more ionosphere reflections. For example, Fig. 2.15 illustrates a one-hop path between Washington and San Francisco, with reflection taking place at N; and also a two-hop route, with reflections at M and P. Considerations that determine the path by which waves will arrive with the greatest intensity include the following:

1. The transmitted ray must not be too nearly tangential to the earth's surface at the sending and receiving ends. Usually the lower limit is about 3.5°. In other words, sky waves nearly always arrive along a path directed downward by at least this *minimum grazing angle.* When the wave is too close to the earth's surface, attenuation due to the finite conductivity of the earth is the limiting factor.

2. The angle of incidence ϕ_1 must exceed the value given by Eq. (2.35) at each reflection. If the critical frequency f_c for the particular layer is known, then from Eqs. (2.35) and (2.37) the desired condition is found to be

$$\cos \phi_1 \gtreqless \frac{f_c}{f} \tag{2.38}$$

where f is the operating frequency.

3. Because of absorption in the ionosphere below the virtual point of reflection and because it is actually *refraction* with

scattering that is involved, the strongest signals generally occur for transmission over a path having the smallest number of hops and consequently the smallest distance of travel through the ionosphere. This virtual height is less for large ϕ_1 than for nearly vertical incidence. When the wave is traveling well above the surface of the earth and not in the ionosphere, the field intensity obeys the inverse-distance law of Eq. (2.14).

Table III.—Typical Average Ratio of Maximum Usable Frequency to Critical Frequency
(One-hop transmission)

Distance, km.	500	1000	1500	2000	2500	3000	3500	4000
Miles	310	620	930	1240	1550	1860	2170	2480
Winter:								
Midnight, F	1.2	1.5	1.8	2.3	2.8	2.8	2.9	
Noon, F_2	1.2	1.6	2.1	2.6	2.9	3.2	3.4	
Summer:								
Midnight, F	1.2	1.4	1.7	2.0	2.4	2.6	2.8	
Noon, F_2	1.2	1.5	1.8	2.2	2.5	2.7	2.9	
Noon, F_1	1.3	2.0	2.7	3.2	3.6			
Noon, E	2.0	3.4	4.4					
Sporadic E*	2.5	4.2	5.1					

* Sporadic E transmission has no critical frequency. The values given are ratios of maximum usable frequency to the approximate upper limit of frequency of the stronger sporadic E reflections at vertical incidence.

4. The highest possible frequency should be chosen (for frequencies above 1500 kc), because it is found that attenuation in the ionosphere *decreases* as the frequency rises. This will be evident when the behavior of an oscillating electron in the earth's magnetic field is studied. The optimum frequency is usually not this maximum usable frequency but a value between 50 and 85 per cent of the latter. Lower figures result in excessive attenuation, and a value much above 85 per cent will result in occasional failures to secure transmission at all, when the skip distance increases above its mean value for short periods. It should be remembered that the *distance* at which a given frequency is the *maximum usable frequency* is also the *minimum* distance over which that frequency is receivable.

5. The ionosphere conditions of importance are those prevailing at the points of reflection. This means for single-hop reception that the critical frequency and ionosphere heights at

N of Fig. 2.15 must be determined for the local time at N. For multihop transmission, the conditions at M, P, etc., must be considered. If one is in daylight and the other in darkness, the conditions may be quite different, reflection possibly taking place

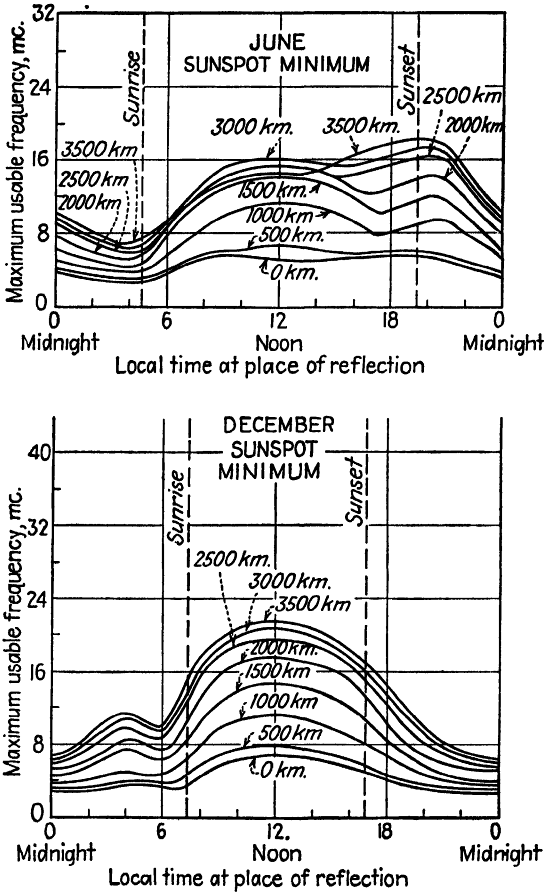


FIG. 2.16.—Maximum usable frequencies as a function of time of day and season for a minimum in the sunspot cycle. (*National Bureau of Standards.*)

at different layers. For multihop transmission, the smallest of the several maximum usable frequencies is to be used.

As an aid to the estimate of the maximum usable frequency in terms of the critical frequency, Table III may be used. This applies to one-hop transmission. It can be applied repeatedly

to successive legs of multihop paths. Where there is no entry in the table, the distance exceeds the possible value for one-hop transmission under the limitations imposed above.

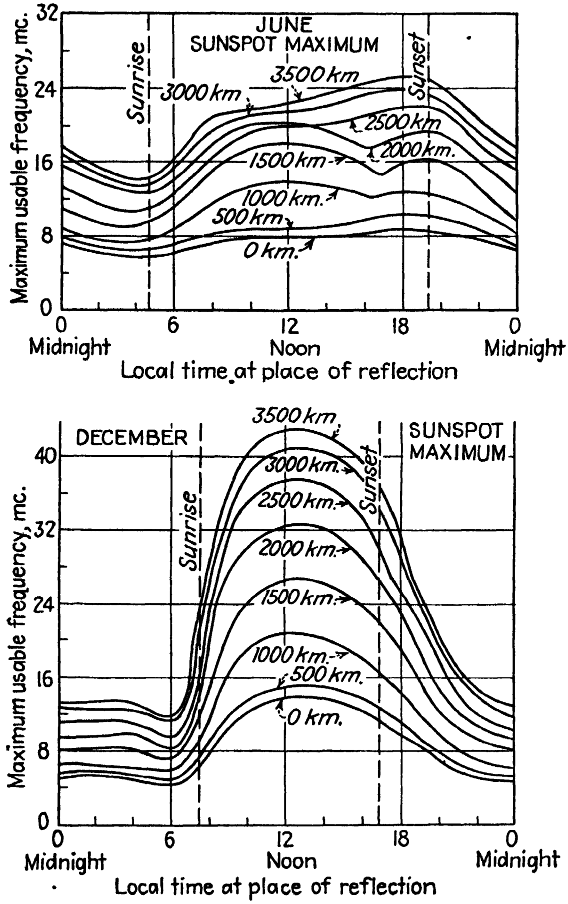


FIG. 2.17.—Maximum usable frequencies as a function of time of day and season for a maximum in the sunspot cycle. (*National Bureau of Standards.*)

Values of maximum usable frequencies are given from more elaborate calculations in Figs. 2.16 and 2.17 for the same seasons and solar activity as in Figs. 2.10 and 2.14. Reference was made in Sec. 2.10 to the regularly published values of these data.

2.12. Example of Choice of Optimum Frequency.—If the best operating frequencies for transmission from Washington, D.C., to Chicago are desired,

data from Table III may be used to prepare a chart like that below. It is desirable in most cases to keep the number of different frequencies to a minimum. The longitudes are

Washington, D.C. .... 77°4′
Chicago, Ill .... 87°37′

The point of reflection is thus at 82°21′ and has a local time 30 min less than Eastern standard time. Note that the astronomical 24-hr day is used (0000 designates midnight; 1200, noon; 1850, 6:50 P.M.; etc.).

Month and year	Frequency, mc	Local time at mid-point of path		Eastern standard time		Path and layer
		From	To	From	To	
June, 1937 (sunspot max).	6	2100	0700	2130	0730	1-hop F
	11	0700	2100	0730	2130	1-hop F_2 or 1-hop E
December, 1937 (max)	4.5	1900	0800	1930	0830	1-hop F
	10	0800	0930	0830	1000	1-hop F_2
	16	0930	1530	1000	1600	1-hop F_2
	10	1530	1900	1600	1930	1-hop F
June, 1944 (min)	3	2100	0700	2130	0730	1-hop F
	8	0700	2100	0730	2130	1-hop E
December, 1944 (min)	3	1900	0730	1930	0800	1-hop F
	5	0730	0930	0800	1000	1-hop F_2
	8	0930	1530	1000	1600	1-hop F_2
	5	1530	1900	1600	1930	1-hop F

The calculations become somewhat more involved when more than one hop must be considered. This is especially true for east-west paths, where part of the transmission may be in daylight and part in darkness. For an example of sky-wave propagation over a 4000-km two-hop or three-hop path, see "Radio Transmission and the Ionosphere."[1] For a more general dis-

[1] NATIONAL BUREAU OF STANDARDS, *Letter Circular* LC-614, U.S. Department of Commerce, Washington, D.C., Oct. 23, 1940. Extensive bibliography. Table III and the example given in this section were adapted from this paper.

cussion, reference may be made to Smith, Kirby, and Gilliland.[1]

2.13. Effects of the Earth's Magnetic Field. Absorption and Polarization.—The magnetic field of the earth can be shown to be sufficient to have a profound effect on the propagation of a wave through an ionized region in the field. An electron moving in accordance with Eq. (2.27) then has a force normal to x and to the component H_z of the earth's field H which is perpendicular to the x direction. This follows from the well-known Motor Rule of electrical engineering. There will be a y component of motion such that the velocity in the y direction v_y differs by $\pi/2$ in time phase from v [*i.e.*, v of Eq. (2.26)]. The resultant motion of the electron for small values of H_z will be an ellipse.[2]

As demonstrated in Eq. (2.44), the eccentricity is great when the frequency is high, while the ratio of minor to major axes varies inversely with frequency. The straight-line motion of

[1] SMITH, KIRBY, and GILLILAND, Application of Graphs of Maximum Usable Frequency to Communication Problems, *J. of Research Nat. Bur. of Standards*, **22**, 81 (January, 1939).

[2] This may be seen as follows: If the current along the x axis of Eq. (2.23) is denoted by i_x, then the transverse force f_y is

$$f_y = i_x H_z \tag{2.39}$$

$$= -\frac{H_z E_{\max} e^2}{\omega m} \cos \omega t \tag{2.40}$$

The equation of motion along the y axis is

$$m \frac{d^2 y}{dt^2} = -\frac{H_z E_{\max} e^2}{\omega m} \cos \omega t \tag{2.41}$$

Two successive integrations carried out as in Eq. (2.26) and (2.27) give

$$y = \frac{H_z E_{\max} e^2}{\omega^3 m^2} \cos \omega t \tag{2.42}$$

If one denotes

$$x_0 = \frac{E_{\max} e}{\omega^2 m}$$

and

$$y_0 = \frac{H_z E_{\max} e^2}{\omega^3 m^2} \tag{2.43}$$

it is seen that

$$\frac{y_0}{x_0} = \frac{H_z e}{\omega m} \tag{2.44}$$

In general x_0 and y_0 are not equal. Equations (2.27) and (2.42) indicate consequent elliptical motion of the electron. The ratio of y_0 to x_0 is a measure of the eccentricity of the elliptical path of the electron.

the electron at very high frequencies changes to more and more of an elliptical one as the frequency decreases.

Equation (2.44) is actually valid only for $y_0 << x_0$ because the y motion results in a current that produces motion along x. More detailed analysis would show that this latter effect causes the electron to spiral outward when a *resonance frequency* is reached at which

$$\omega_0 = \frac{H_z e}{mc} \tag{2.45}$$

where H_z is in e.m.u. (gausses) and e in e.s.u. For the appropriate direction in the earth's field at 180 km above the earth's surface and 40° latitude, H_z is about 0.52 gauss. The quantity

$$\frac{e}{m} = 5.279 \times 10^{17} \text{ e.s.u./gram}$$

$$\omega_0 = \frac{0.52 \times 5.279 \times 10^{17}}{3 \times 10^{10}}$$

$$= 9.2 \times 10^7$$

$$f_0 = \frac{9.2 \times 10^7}{2\pi} = 1460 \text{ kc} \tag{2.46}$$

It may be shown that the energy corresponding to the y component of motion is obtained from the impinging electromagnetic wave. Some of this is reradiated as a *horizontal component* of polarization if x is the vertical direction. This results in the change of plane of polarization of a wave passing through the ionosphere. As will be seen later, a consequence of this is the type of error in direction finder bearings known as *night effect*. Both the x and y components of motion contribute to the absorption of energy. If the moving electron collides with a molecule before reradiating all this energy, the remainder is lost to the radio wave. This results in attenuation of the wave. Equation (2.43) shows that the amplitudes and hence the absorption rise with decreasing frequency until the resonance frequency f_0 of Eq. (2.46) is reached. Here the attenuation is a maximum.

Below the frequency f_0 the rather surprising conclusion is reached that the magnetic field of the earth acts to *reduce* the attenuation.[1] For a frequency f considerably below f_0, the absorption coefficient k_H is related to the corresponding quantity

[1] NICHOLS and SCHELLENG, *Bell System Tech. J.*, **4**, 229–231 (1925).

k for no magnetic field in the following manner:

$$\frac{k_H}{k} = \frac{1}{\left(\frac{f_0}{f} - 1\right)^2} \tag{2.47}$$

Thus, at $f = 150$ kc, the absorption of energy in the ionosphere is only 1.3 per cent of the value obtained if the earth's magnetic field were not present. The motion of the electron is no longer elliptical, and the average velocities along x and y are much reduced. As will be seen later, this permits long-wave, long-distance communication by means of the sky wave as well as the ground wave. The region of poorest transmission of waves through the ionosphere is seen to be near the h-f end of the standard broadcast band. This will be illustrated further in Sec. 2.14.

2.14. Distance Ranges of Ground and Sky Waves.—A comprehensive picture of the behavior of ground and sky waves necessitates a better means of comparing the two types than has been afforded by the foregoing discussion. In particular the location of the "skip zone" and the comparison of the propagation characteristics of very low and high frequencies need further consideration. As a means of doing so, the *distance range* may be plotted. This is not a uniquely defined quantity but represents the limits of distance over which communication may be possible. The following assumptions are made:

1. The receiving equipment has as good signal-to-noise characteristics as would represent good engineering practice at each frequency.
2. Receiver sensitivity (see *Gain*, Sec. 1.05) is high enough so that the signal-to-noise behavior is the limiting factor.
3. Radio telegraph communication is assumed. Broadcast entertainment reception ranges are generally less favorable because greater field strengths are required.
4. The transmitter radiates 1 kw of power. The very low radiation efficiencies of l-f antennas must be considered.
5. Transmitting and receiving antennas are nondirectional.
6. Over a given path, the received field strength is proportional to $\sqrt{P_r}$. (However it is not safe to extrapolate a change of power in terms of change in distance range.)
7. There are no abnormal magnetic disturbances or ionosphere irregularities (except sporadic-E reflections).

8. Atmospheric conditions typical of temperate latitudes are assumed. During electrical storms or generally in the tropics, the distance ranges will be less favorable.

9. The average minimum field strengths to fulfill these conditions may be taken to be as given in Table IV.

TABLE IV.—MINIMUM FIELD STRENGTHS

Time	Frequency			
	100 kc	1 mc	5 mc	10 mc
	Field strength, μv/m			
Summer day	60	10	10	3
Summer night	100	50	15	1
Winter day	25	1	2	1
Winter night	35	5	1	1

The results for summer and winter at a time about midway between maximum and minimum in the sunspot cycle are given in Figs. 2.18 to 2.21. This method of representation was used by the National Bureau of Standards,[1] but the results given here were independently estimated. The limits of transmission at the l-f end, where the ground wave predominates, were found from Figs. 2.06 and 2.07 for sea water and moderate conductivity land, respectively. Here the exact estimate of minimum usable field strength is not important because of the rapid variation of signal intensity with distance.

At the other extreme in frequency, the skip distance contour is determined from the measured results of maximum usable frequency.[2] The *Day* graphs refer to noon conditions, while midnight results are shown in the others. The progressive

[1] NATIONAL BUREAU OF STANDARDS, *Letter Circular LC*-615, U.S. Department of Commerce, Washington, D.C., Oct. 25, 1940. Includes bibliography of works on experiments of long-distance transmission over a wide range of frequencies. This paper is mainly a summary of all the results cited in its bibliography.

[2] NATIONAL BUREAU OF STANDARDS, The Ionosphere and Radio Transmission, January, 1941, with Predictions for April, 1941, *Proc. I.R.E.*, **29**, 32 (January, 1941). Also High-frequency Radio Transmission Conditions, July, 1941, with Predictions for October, 1941, *Proc. I.R.E.*, **29**, 467 (August, 1941).

diurnal and seasonal changes follow the trends shown in Figs. 2.10, 2.14, 2.16, and 2.17.

For day conditions there is a range of frequencies from about 1 mc up to the skip-distance contour in which appreciable amounts of ionosphere waves are added to the ground-wave component.

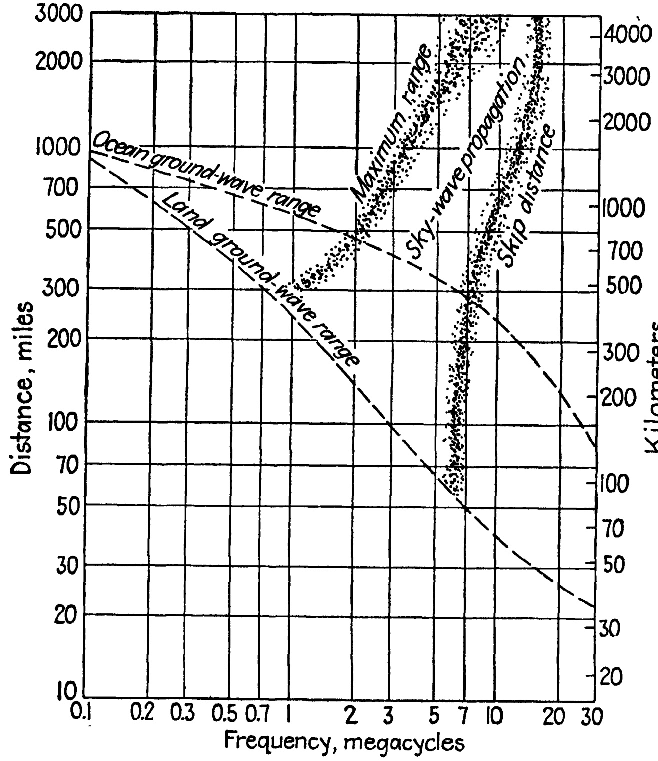


FIG. 2.18.—Average distance range for summer daylight conditions. Middle of cycle of solar activity.

At night this region extends down to much lower frequencies. This is the region in which "night effect" is so frequently observed in loop direction finders, as will be studied in Sec. 3.17. Because of the variable nature of the attenuation of a wave propagated through the ionosphere, only a very rough estimate can be made of the maximum range of transmission in this region. Here the field intensity falls off slowly with increasing distance, so that the limit chosen in Table IV affects the range greatly.

Data on long-distance field intensities at short waves by sky-wave paths are available in terms of "quasi-maximum" values. These are defined as the field strengths that are exceeded by the instantaneous values only 5 per cent of the time. Curves

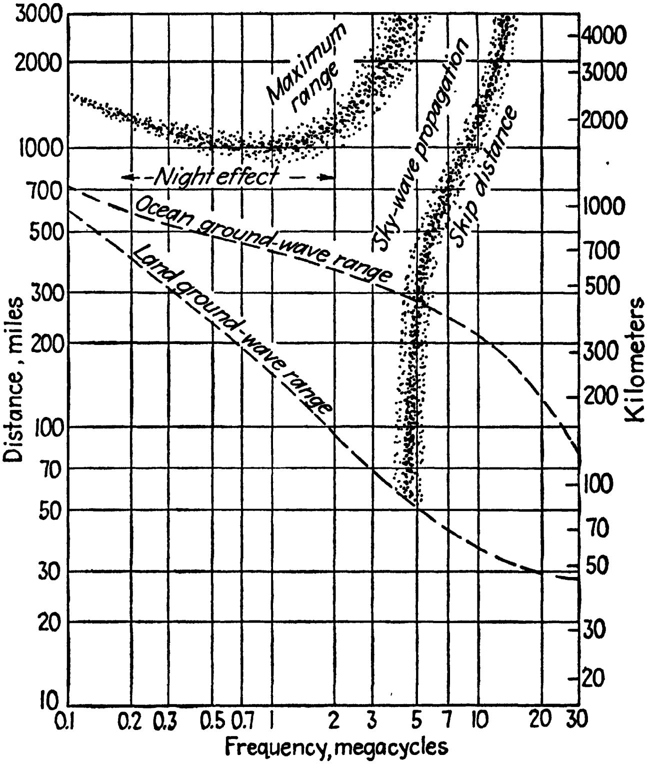


FIG. 2.19.—Average distance range for summer night conditions. Middle of cycle of solar activity.

are given by the International Radio Consulting Committee (C.C.I.R.).[1] The boundary *maximum range* is consequently a very variable quantity as will be seen in Figs. 2.18 to 2.21.

In summer, reception may occasionally be possible in the skip zone at *higher* frequencies than the maximum usable value. The propagation in such cases is by way of the sporadic-*E* layer.

[1] Report of Committee on Radio Wave Propagation, *Proc. I.R.E.*, **26**, 1193 (October, 1938), Figs. 3–5. Additional results also used were given by W. Ross, Ground and Ionosphere Rays, *Wireless Engineer*, **14**, 306 (June, 1937).

This is actually not a layer in the ordinary sense. Strong reflections are observed on these occasions from the E layer at frequencies far above that predicted for vertical incidence by Eq. (2.38). Probably the phenomenon is due to reflection at a

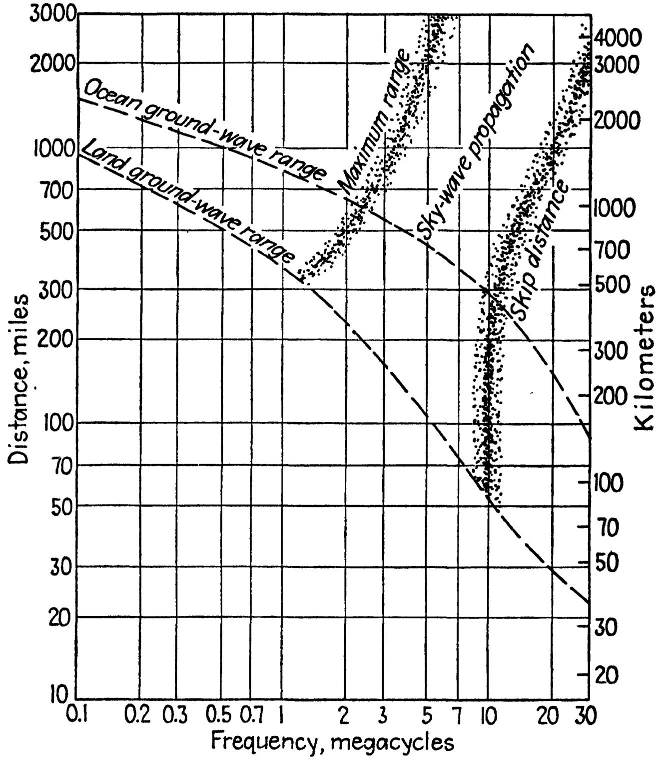


FIG. 2.20.—Average distance range for winter daylight conditions. Middle of cycle of solar activity.

stratum where the electron density changes quite rapidly, although this may not be the layer of maximum electron density.

2.15. Propagation of Ultra-high Frequency Waves.—The foregoing discussion shows that above a certain frequency at a given angle of incidence on the ionosphere layer, the radio wave is no longer reflected (or refracted) back to the earth. Instead it passes on through the ionized layer and is lost. The spectrum of *ultra-high frequencies* may be defined at the present state of the art as being roughly those above 25 to 40 mc, which are above

the maximum usable frequency of ionosphere reflection. The frequency of demarcation is inexact, of course, because of the variability of the upper limit of reflections.

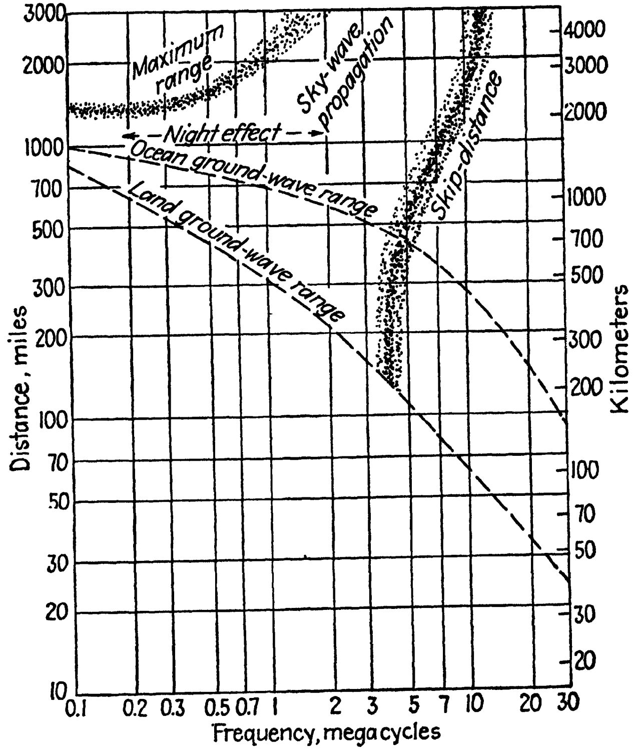


FIG. 2.21.—Average distance range for winter night conditions. Middle of cycle of solar activity.

Ultra-high frequencies are characterized by the fact that propagation is essentially along optical paths. In general, transmitting and receiving antennas must be within line of sight with respect to the horizon. Propagation beyond this distance gives very low field strengths.

Optical path transmission may be considered by reference to Fig. 2.22. Two antennas A and B are at heights h_1 and h_2 above a plane earth surface and are separated by r along the surface. Propagation is assumed to be from A to B, and the antennas are point sources or very short dipoles and have the same planes of polarization.

2.16. Propagation over Plane Earth of Infinite Conductivity.—It will be assumed for the elementary derivation that the earth plane has infinite (or, strictly, finite but high) conductivity and that $r >> h_1$ or h_2, so that ϕ_1 is large. Then for either vertical or horizontal polarization, reflection will take place with a 180° phase change. The signal at B will be the resultant of two waves: one a direct transmitted ray along a path of distance r_1, and the other over a distance r_2 with the reflection mentioned. The vectors representing the wave at B are equal in magnitude if there is no loss on reflection (neglecting the variation in field strength in the additional distance $r_2 - r_1$ compared to r_1 since nearly grazing incidence is assumed). However these vectors differ in *phase* owing to the fact that the path difference $r_2 - r_1$ is not negligible in comparison with λ.

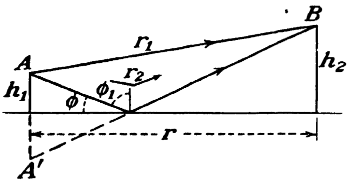


FIG. 2.22.—Paths of direct and reflected rays between elevated antennas near earth's surface.

From the geometry of the image A' of Fig. 2.22, it is seen that

$$r_1 = \sqrt{(h_1 - h_2)^2 + r^2} \tag{2.48}$$

$$r_2 = \sqrt{(h_1 + h_2)^2 + r^2} \tag{2.49}$$

The first of these may be written

$$r_1 = r\sqrt{1 + \frac{(h_1 - h_2)^2}{r^2}} \tag{2.50}$$

$$r_1 = r\left[1 + \frac{(h_1 - h_2)^2}{2r^2} - \frac{(h_1 - h_2)^4}{8r^4} + \cdots\right] \tag{2.51}$$

Since $\frac{(h_1 - h_2)^2}{r^2} << 1$, the approximation for this series is

$$r_1 = r + \frac{(h_1 - h_2)^2}{2r} \tag{2.52}$$

Similarly,

$$r_2 = r + \frac{(h_1 + h_2)^2}{2r} \tag{2.53}$$

The path difference is thus

$$r_2 - r_1 = \frac{(h_1 + h_2)^2 - (h_1 - h_2)^2}{2r}$$

$$= \frac{2h_1h_2}{r} \tag{2.54}$$

The phase difference ψ is related to this path difference as follows:

$$\frac{\psi}{2\pi} = \frac{r_2 - r_1}{\lambda} \tag{2.55}$$

or

$$\psi = \frac{4\pi h_1 h_2}{\lambda r} \tag{2.56}$$

The angle ψ represents the departure from exact phase opposition, as is shown in Fig. 2.23.

The resultant E is also shown. It is readily seen that this field at B is

$$E = 2E_1 \sin \frac{\psi}{2} \tag{2.57}$$

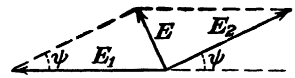


FIG. 2.23.—Phase relationship of direct and reflected rays at receiving point.

in terms of E_1 the direct wave component from A. From Eq. (2.57) .

$$E = 2E_1 \sin \frac{2\pi h_1 h_2}{\lambda r} \tag{2.58}$$

However for nearly grazing incidence ψ is small, and this angle may be set equal to its sine so that

$$E = E_1 \frac{4\pi h_1 h_2}{\lambda r} \tag{2.59}$$

The following conclusions may be drawn from Eq. (2.59):

1. For fixed antenna locations and radiated power (the antennas being varied appropriately in length to be a given fraction of a wave length), the field strength is directly proportional to the frequency.

2. The signal strength increases with the heights of the antennas. This must be reconsidered however when the approximation $\sin \psi = \psi$ is not ustified. When ϕ_1, the angle of incidence, is appreciably less than 90° there will be a series of maxima and minima as h_2 is varied.

3. Since E_1 varies inversely with distance in free space as Eq. (2.07) shows, the field strength E in the present case varies *inversely* as the *square* of the distance.

A half-wave dipole in free space is the counterpart of the quarter-wave dipole near the earth's surface (Sec. 2.03) as far as the radiation for a given current is concerned. However, the

power required to establish this field is doubled, so that the radiation resistance R_r of Eq. (2.10) is also doubled. When the appropriate value of effective height (or length) is used it is found that

$$E_1 = \frac{7.00\sqrt{P_r}}{r} \tag{2.60}$$

with E_1 in millivolts per meter, P_r in watts, and r in kilometers. Then Eq. (2.59) becomes

$$E = \frac{4\pi \times 7.00 \times 10^{-3}\sqrt{P_r}\,h_1h_2}{\lambda r^2} \tag{2.61}$$

$$= \frac{8.80 \times 10^{-2}\sqrt{P_r}\,h_1h_2}{\lambda r^2} \tag{2.62}$$

where h_1, h_2, and λ are in *meters*, but r is in *kilometers*.

2.17. Propagation over Plane Earth of Finite Conductivity.—In many practical cases we cannot make the simplifying assumption of Sec. 2.16 that $\sigma = \infty$, but rather that the conductivity is finite and that we must take into account the dielectric constant ϵ. Let us define ϵ_0 as

$$\epsilon_0 = \epsilon_{esu} - j\frac{2\sigma_{esu}}{f_{cycles}} \tag{2.63}$$

The quantity ϵ_0 is called the *complex dielectric constant.* Here f_{cycles} refers to cycles *per second.* Where σ is in e.m.u. as previously defined, the factor c^2 must be included in the last term. Normally ϵ is expressed in e.s.u. so that $\epsilon = 1$ for free space. $c = 3 \times 10^{10}$.

$$\epsilon_0 = \epsilon - j\frac{2\sigma c^2}{f} \tag{2.64}$$

$$= \epsilon - j18 \times 10^{14}\frac{\sigma}{f_{mc}} \tag{2.65}$$

Fresnel's laws of reflection in optics for any plane surface give the ratio of reflected to incident light. The results apply equally well to a radio wave because the derivation is based upon principles that apply correctly to any type of electromagnetic waves. For the electric vector in the plane of incidence this reflection coefficient may be denoted by K_V (*i.e.*, *vertical* polarization of the radio wave). The corresponding component normal to the plane

of incidence is K_H. For the angle of incidence ϕ_1 measured from the normal drawn from the surface, the results are

$$K_V = \frac{\epsilon_0 \cos \phi_1 - \sqrt{\epsilon_0 - \sin^2 \phi_1}}{\epsilon_0 \cos \phi_1 + \sqrt{\epsilon_0 - \sin^2 \phi_1}} \tag{2.66}$$

and

$$K_H = \frac{\cos \phi_1 - \sqrt{\epsilon_0 - \sin^2 \phi_1}}{\cos \phi_1 + \sqrt{\epsilon_0 - \sin^2 \phi_1}} \tag{2.67}$$

The derivation of these is carried out in works on physical optics[1] and for the complex value of ϵ_0 by Trevor and Carter.[1]

In terms of the angle ϕ between the earth's surface and the incident ray, since $\phi = \pi/2 - \phi_1$

$$K_V = \frac{\epsilon_0 \sin \phi - \sqrt{\epsilon_0 - 1 + \sin^2 \phi}}{\epsilon_0 \sin \phi + \sqrt{\epsilon_0 - 1 + \sin^2 \phi}} \tag{2.68}$$

$$K_H = \frac{\sin \phi - \sqrt{\epsilon_0 - 1 + \sin^2 \phi}}{\sin \phi + \sqrt{\epsilon_0 - 1 + \sin^2 \phi}} \tag{2.69}$$

In general the values of K_V and K_H are complex, *i.e.*, are of the form $x + jy$. This indicates that there is a phase shift θ upon reflection which is not π. This depends on the value of the complex dielectric constant ϵ_0.

It will be instructive to study the amplitude factor A and the phase shift θ at reflection for the V and the H components. The manner in which the reflected wave combines with the direct wave can then be seen much more clearly than when the results are in the form of Eqs. (2.68) and (2.69). K_V and K_H may be written

$$\left.\begin{aligned} K_V &= A_V e^{j\theta_V} \\ K_H &= A_H e^{j\theta_H} \end{aligned}\right\} \tag{2.70}$$

Then from Eqs. (2.68) and (2.69) for any angle of incidence, one may calculate both A and θ for each plane of polarization.

2.18. Example of Calculation of Amplitude and Phase Shift at Reflection. As a specific example, a determination of A_V and θ_V is to be made for the following conditions:

[1] P. DRUDE, *The Theory of Optics* (tr. by Mann and Millikan), pp. 278–284, Longmans, Green and Company, New York, 1925. B. TREVOR and P. S. CARTER, Notes on Propagation of Waves below Ten Meters in Length, *Proc. I.R.E.*, **21**, 387 (March, 1933), Appendix.

$$\epsilon = 7$$
$$\sigma = 5 \times 10^{-14} \text{ e.m.u.}$$
$$f = 30 \text{ mc}$$
$$\phi = 5°$$

From Eq. (2.65) it is found that

$$\epsilon_0 = 7 - j\frac{18 \times 10^{14} \times 5 \times 10^{-14}}{30}$$
$$= 7 - j3$$

Equation (2.68) gives

$$K_V = \frac{(7 - j3)0.0872 - \sqrt{(7 - j3) - 1 + 7.6 \times 10^{-3}}}{(7 - j3)0.0872 + \sqrt{(7 - j3) - 1 + 7.6 \times 10^{-3}}}$$
$$= \frac{0.610 - j0.262 - \sqrt{6.01 - j3}}{0.610 - j0.262 + \sqrt{6.01 - j3}}$$

But by means of the usual transformation to polar form,[1] it may be seen that

$$6.01 - j3 = 6.72e^{-j0.463}$$

and it follows[2] that

$$\sqrt{6.01 - j3} = 2.59e^{-j0.232}$$

Thus, finally,

$$\sqrt{6.01 - j3} = 2.59 \cos (0.232) - j2.59 \sin (0.232)$$
$$= 2.52 - j0.597$$
$$K_V = \frac{(0.610 - 2.52) + j(0.597 - 0.262)}{(0.610 + 2.52) - j(0.597 + 0.262)}$$
$$= \frac{-1.91 + j0.335}{3.13 - j0.859}$$
$$= -\frac{1.94e^{-j0.173}}{3.24e^{-j0.2675}}$$
$$= -0.598e^{j0.094}$$

Thus, for this case, the magnitude and phase of K_V are

$$A_V = 0.598$$
$$\theta_V = -174.6°$$

2.19. Comparison of Reflection Characteristics for Vertical and Horizontal Polarization.—The values of A_V and θ_V (for vertical polarization) as well as A_H and θ_H (for horizontal polarization) as a function of ϕ are given in Figs. 2.24 and 2.25. Three types of surface are assumed, as follows:

[1] That is, $x + jy = re^{j\alpha}$ where $r = \sqrt{x^2 + y^2}$ and $\tan \alpha = y/x$.
[2] Since $(re^{j\alpha})^n = r^n e^{jn\alpha}$.

Curve	ϵ	σ, e.m.u.	f, mc	ϵ_0
1	25	3.2×10^{-13}	30	$25 - j19.2$
2	7	5×10^{-14}	30	$7 - j3$
3	80	5×10^{-11}	30	$80 - j3000$

Further examination of the A_V curves discloses that there is an angle ϕ at which A_V is a minimum.

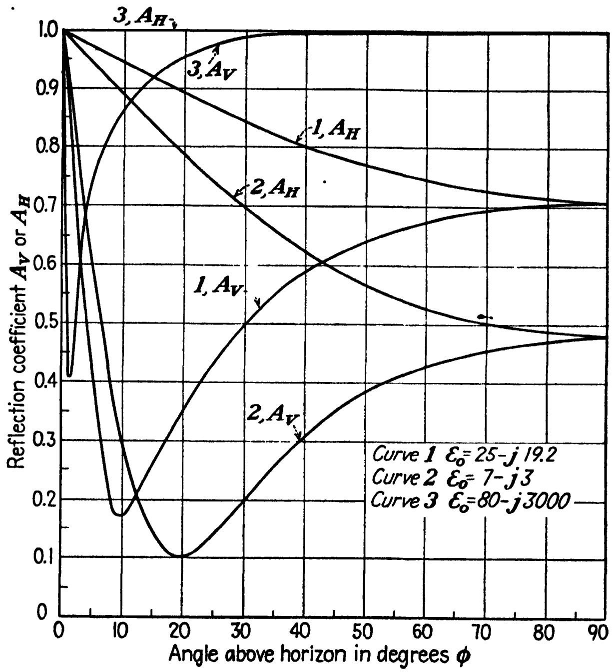


FIG. 2.24.—Magnitude of reflection coefficient for imperfectly conducting earth as function of angle of incidence. (*Feldman, Proc. I.R.E.*, **21**, 764, *June*, 1933).

Now it is a well-known fact in optics that, when polarized light is incident on a reflecting surface, *e.g.*, a glass plate, reflection does not take place at a certain angle of incidence and plane of polarization. This is illustrated in *a* of Fig. 2.26. If the index of refraction of the glass is μ, then this angle ϕ_{null}, known as the *Brewster angle*, is given by

$$\cot \phi_{\text{null}} = \mu \tag{2.71}$$

An application of this principle is seen in the Nörrenberg polariscope, where two such reflecting plates are used in cascade.

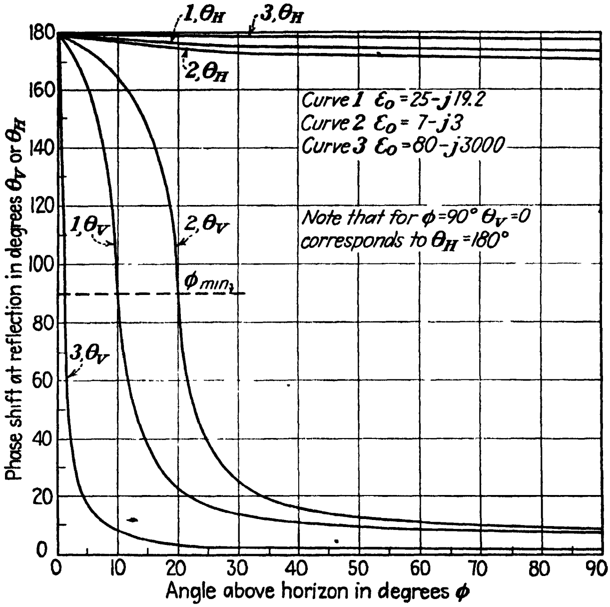


FIG. 2.25.—Phase angle of reflection coefficient for imperfectly conducting earth as function of angle of incidence. (*Adapted from Feldman, Proc. I.R.E.*, **21**, 764, *June*, 1933.)

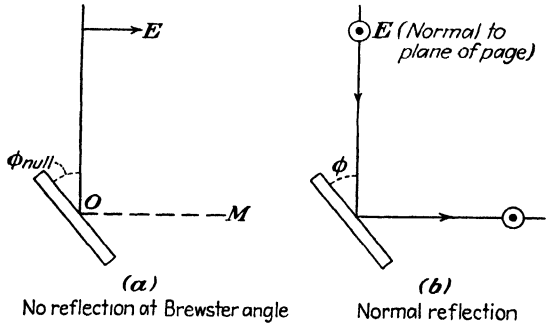


FIG. 2.26.—Reflection of polarized wave at Brewster angle.

By analogy with the foregoing condition for the reflection of light at a nonmetallic surface ($\sigma = 0$), for which $A_V = 0$ at the Brewster angle, there is an angle of incidence ϕ_{min} for the radio wave case known as the *pseudo-Brewster angle.* Here A_V will be a minimum but not necessarily zero. At grazing incidence

for either vertical or horizontal polarization, the phase shift is 180° when σ is large and all the energy is reflected. For the case of horizontal polarization, θ_H changes slowly from this value to 160 to 175° as normal incidence is approached. In the case of sea water, θ_H approaches 178°, and A_H is approximately unity at all values of ϕ. For vertically polarized waves θ_V varies from 180°, through 90° at the pseudo-Brewster angle, to a small angle

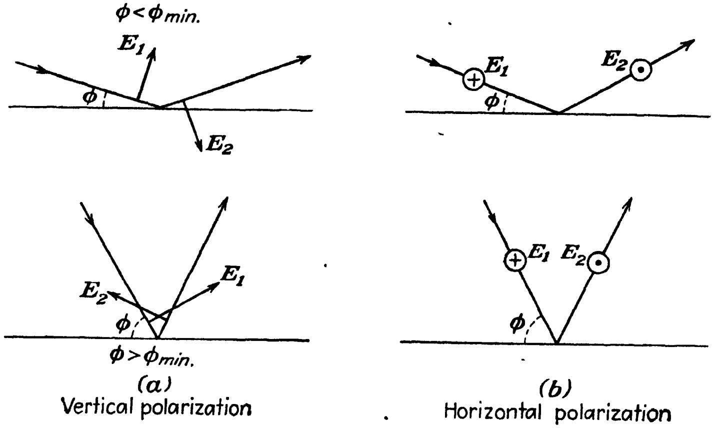


FIG. 2.27.—Phase changes at reflection from earth's surface.

(5 to 20°) at normal incidence. For sea water θ_V at $\phi = 90°$ is about 2°.

It will be noted that the cases of V and H components at $\phi = 90°$ merge together, because the plane of incidence is indeterminate. The values of θ_V and θ_H differ by 180° only because of the assumed vector directions. This is illustrated in Fig. 2.27.

2.20. Field Strength near the Earth's Surface.—The small values of A_V near grazing incidence account for the higher field strength for vertical polarization in comparison with horizontal when transmission is between two elevated antennas at ultrahigh frequencies. The expressions for the magnitude of the field strength under these conditions may be derived in terms of the magnitude of E_1, the field strength in free space. The analysis is made in Appendix B, with a result for vertical polarization of

$$|E_V| = \frac{|E_1|}{r} \sqrt{\frac{4\epsilon_0^2}{\epsilon_0 - 1} (h_1 + h_2)^2 + \left(\frac{4\pi h_1 h_2}{\lambda}\right)^2} \qquad (2.72)$$

where the magnitudes are denoted by $|E_V|$ and $|E_1|$.

If a comparison is made with the case for $\sigma = \infty$ of Sec. 2.16, it is seen that the effect of finite earth conductivity is to add the term

$$\frac{4\epsilon_0^2(h_1 + h_2)^2}{\epsilon_0 - 1}$$

in the radicand.

Example.—$\sigma = 10^{-14}$ e.m.u., $\epsilon = 15$, $f = 100$ mc, and $h_1 = h_2 = 1$ m

$$\begin{aligned}\epsilon_0 &= 15 - j\frac{18 \times 10^{14} \times 10^{-14}}{100} \\ &= 15 - j0.18\end{aligned}$$

and the second term may be neglected, so that $\epsilon_0 = \epsilon$, approximately. Then from Eq. (2.72)

$$\begin{aligned}|E_V| &= \frac{|E_1|}{r}\sqrt{\frac{4 \times 15^2 \times 4}{14} + \left(\frac{4\pi}{3}\right)^2} \\ &= \frac{|E_1|}{r}\sqrt{257 + 17.5} \\ &= 16.6\,\frac{|E_1|}{r}\end{aligned}$$

This result may be compared with that for infinite conductivity, where

$$\begin{aligned}|E_V| &= \frac{|E_1|}{r}\frac{4\pi}{3} \\ &= 4.18\,\frac{|E_1|}{r}\end{aligned}$$

It thus may be concluded that the field strength for the case of *low conductivity* land is $16.6/4.18 = 3.96$ times as great (or 11.9 db higher) as for infinite conductivity. The cause of this is, of course, the reduction in amplitude of the reflected wave causing destructive interference.

For the case of horizontal polarization, the result analogous to Eq. (2.72) is

$$|E_H| = \frac{|E_1|}{r}\sqrt{\frac{4(h_1 + h_2)^2}{\epsilon_0 - 1} + \left(\frac{4\pi h_1 h_2}{\lambda}\right)^2} \qquad (2.73)$$

If now the previous example is considered for horizontal polarization it is seen that

$$\begin{aligned}|E_H| &= \frac{|E_1|}{r}\sqrt{\frac{4 \times 4}{14} + \left(\frac{4\pi}{3}\right)^2} \\ &= \frac{|E_1|}{r}\sqrt{1.14 + 17.5} \\ &= 4.32\,\frac{|E_1|}{r}\end{aligned}$$

Thus, a horizontally polarized wave is only slightly stronger (0.2 db), owing to finite σ, than for the case where $\sigma = \infty$. E_H is 11.7 db below E_V.

This example illustrates the fact that with ground of finite conductivity, the vertical component is stronger than the horizontal for antennas near the surface. This effect is also very pronounced near the surface of sea water, as Figs. 2.24 and 2.25 will show.

2.21. Propagation over a Spherical Earth.—When the actual shape of the earth's surface is taken into consideration, it is found that the transmission is modified by (1) the geometry of the

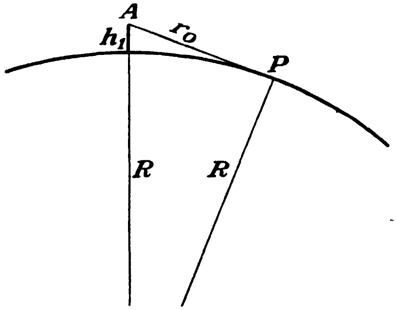


FIG. 2.28.—Distance to horizon from elevated antenna.

paths of the rays within the line of sight; (2) diffraction effects, which allow propagation beyond the horizon; and (3) refraction of the waves in the atmosphere, which also permits extension of the range beyond the horizon. Although these latter two effects permit transmission somewhat beyond line of sight, signal strengths are usually very much weaker and variable.

One may consider first the determination of the optical range from an elevated antenna to the horizon. Figure 2.28 illustrates an antenna at A at a height h_1 above the earth's sphere, the latter being of radius R. From the figure, it is evident that

$$(h_1 + R)^2 = R^2 + r_0^2 \tag{2.74}$$

where r_0 is the distance to the horizon P as seen from A. Because R is large in comparison with h_1, r_0 can be used as the arc or the tangent distance without appreciable error. Thus

$$r_0 = \sqrt{2h_1R + h_1^2} \tag{2.75}$$

For instance if $h_1 = 1000$ m, since $2R = 1.283 \times 10^7$ m, the error

in neglecting the h_1^2 term will be less than 1 part in 10^4. Consequently,

$$r_0 = \sqrt{2h_1R} \tag{2.76}$$

In order to take into account refraction in the earth's atmosphere, an *effective radius* of the earth is defined by multiplying R by a factor k. The effective radius is greater than R, owing to the fact that the diminishing atmospheric density causes a horizontally propagated ray to bend down toward the earth

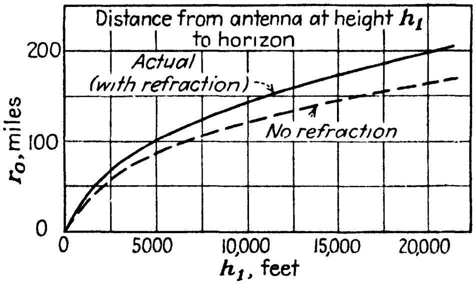


FIG. 2.29.—Line-of-sight range for ultra-high-frequency propagation. The distance from the antenna of height h_1 to the horizon is the range r_0.

instead of proceeding parallel to a tangent. This causes the apparent horizon to be farther removed. The factor has a value[1] of about $k = 1.33$. Then from Eq. (2.76)

$$\begin{aligned} r_0 &= \sqrt{2kRh_1} & (2.77)\\ &= \sqrt{1.33 \times 1.283 \times 10^7 h_1} \\ &= 4.13\sqrt{h_1} & (2.78)\end{aligned}$$

where r_0 is in kilometers and h_1 in meters.

When h_1 is in feet and r_0 in miles, the result is

$$r_{0(\text{miles})} = 1.41\sqrt{h_{1(\text{feet})}} \tag{2.79}$$

or

$$r_{0(\text{miles})} = \sqrt{2h_{1(\text{feet})}} \tag{2.80}$$

This is a very useful practical result for estimating the range of ultra-high-frequency transmission. These results are illustrated in Fig. 2.29.

[1] C. R. BURROWS, Radio Propagation over Spherical Earth, *Proc. I.R.E.*, **23**, 470 (May, 1935).

For transmission between two elevated antennas, the limit of optical range is the sum of the values of r_0 for the two individually. In this case

$$r_{0(\text{miles})} = \sqrt{2h_1} + \sqrt{2h_2} \tag{2.81}$$

where h_1 and h_2 are in feet.

The behavior of waves beyond the horizon is a matter of some conjecture, because of the irregular changes with time and dependence on random reflections and interference. It can merely be indicated in general that the attenuation goes up very rapidly with frequency. For line of sight the field strength varies as $1/r^2$ at these frequencies. At 40 mc, beyond the line of sight, it was found experimentally that E varied as $1/r^{3.6}$, while at 400 mc the relationship was $1/r_h^9$, where r_h is the distance beyond the horizon.[1] Throughout the discussion of propagation of radio waves it has been assumed that reception has been carried out with an antenna having the same sense of polarization as that of the transmitting antenna. If such is not the case, an appropriate factor should be included to give the magnitude of the voltage developed in the receiver. The same considerations apply to the directive radiation patterns of both antennas, as will be evident from Chap. III.

Bibliography

BREIT, G., and M. TUVE: Note on a Radio Method of Estimating the Height of the Conducting Layer, *Terrestrial Magnetism and Atmospheric Electricity*, **30**, 15 (March, 1925).

———, ———: A Test of the Existence of the Conducting Layer, *Physical Review*, **28**, 554 (September, 1926).

BROWN, G. H.: A Comparison of Vertically and Horizontally Polarized Waves at Ultra-high Frequencies, prepared for Panel 9, National Television System Committee, by RCA Mfg. Co., Sept. 25, 1940, as *Wave Polarization for Television*, pp. 9–29 and corrections pp. 1–3.

BURROWS, C. R., A. DECINO, and L. E. HUNT: Ultra-short Waves in Urban Territory, *Electrical Engineering*, **54**, 115 (January, 1935).

———, ———, ———: Ultra-short-wave Propagation over Land, *Proc. I.R.E.*, **23**, 1507 (December, 1935).

EVERITT, W. L.: *Communication Engineering*, 2d ed., McGraw-Hill Book Company, Inc., New York, 1937.

[1] H. H. BEVERAGE, Some Notes on Ultra-high Frequency Propagation, *RCA Review*, **1**, 76 (January, 1937). Also B. TREVOR and R. W. GEORGE, Notes on Propagation at a Wave Length of Seventy-three Centimeters, *Proc. I.R.E.*, **23**, 461 (May, 1935).

FELDMAN, C. B.: The Optical Behavior of the Ground for Short Radio Waves, *Proc. I.R.E.*, **21**, 764 (June, 1933).

INSTITUTE OF RADIO ENGINEERS: *Standards on Radio Wave Propagation—Definitions of Terms*, Institute of Radio Engineers, New York, 1942.

———: *Standards on Radio Wave Propagation—Measuring Methods*, Institute of Radio Engineers, New York, 1942.

NORTON, K. A.: The Effect of Frequency on the Signal Range of an Ultra-high Frequency Radio Station with Particular Reference to a Television Broadcast Service, *Television Hearing*, before the Federal Communications Commission, Mar. 20, 1940.

———: Some Characteristics of Ultra-high Frequency Ground Wave Propagation over Land, *Television Hearing*, before the Federal Communications Commission, Jan. 15, 1940.

-: A Theory of Tropospheric Wave Propagation, *Hearing in the Matter of Aural Broadcasting on Frequencies above* 25,000 *Kilocycles*, before the Federal Communications Commission, Mar. 18, 1940.

Report of Committee on Radio Propagation Data, *Proc. I.R.E.*, **21**, 1419 (October, 1933).

TERMAN, F. E.: *Radio Engineering*, 2d ed., Chap. 14, McGraw-Hill Book Company, Inc., New York, 1937.

CHAPTER III

DIRECTIVE ANTENNA SYSTEMS

3.01. General Properties of Directive Systems.—Antennas that do not have spherical or axial symmetry of radiation or reception may be of use in direction finders. Certain of these *directive antennas* have properties especially well suited for this type of operation. The suitability of the *directive pattern* depends upon the rapidity or uniformity of variation of amplitude or phase with space angle and upon the type and simplicity of the amplitude function. It may be noted that many of the directive patterns suited for direction finder use are also of utility at both the transmitter and receiver in point-to-point communication service, where the greatest amount of energy is to be radiated in a given direction, and the greatest received signal-to-interference and -noise ratio is to be obtained.

The directive systems for transmitters and for receivers may be studied together, for there is no essential difference in mode of operation. It may be true, however, that certain concepts—like radiation resistance in the case of transmitting antennas—may be of more use in one case than the other. The identity of behavior of antennas for the two uses is an illustration of a very general theorem of radiation systems given by Rayleigh and applied to the case of radio transmission by Carson.[1] This is referred to as the "Rayleigh-Carson reciprocity theorem." Another and similar conclusion is made in the Sommerfeld-Pfrang theorem with certain restrictions pointed out by Carson. The reciprocity theorem is

If an electromotive force is inserted at a given point in an antenna A_1 and the resulting current measured at a certain point in a receiving antenna A_2, then an equal current (both as regards amplitude and phase) will be received at the point in A_1 if the same electromotive force is inserted at the point in A_2.

[1] J. R. Carson, Reciprocal Theorems in Radio Communication, *Proc. I.R.E.*, **17**, 952 (June, 1929). See, however, A. Alford, Coupled Networks in Radio Frequency Circuits, *Proc. I.R.E.*, **29**, 55 (February, 1941).

In a directive antenna system there are several factors that describe its behavior for practical direction finding. These include:

1. The directive pattern.

2. The relative scale factor of the directive pattern. This may be described by the effective height, the pickup factor, or the standard radiated field value.

3. The polarization pattern. This describes the behavior of the directive pattern for various states of polarization of the wave arriving at a receiving array. The result may be summarized by suitable definition of a figure of merit, the "standard wave error," or, alternatively, the horizontal-vertical pickup ratio.

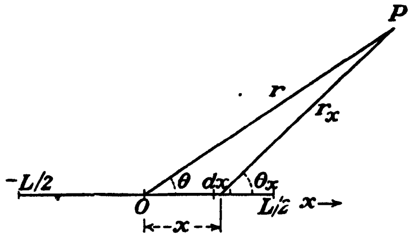


FIG. 3.01.—Radiation from an extended dipole.

The discussion that follows treats first the several cases of simple antenna systems having useful directive properties and then examples of multielement arrays made up of two or more of these simple arrays spaced appropriately.

3.02. Extended Dipole in Space.—The analysis of Sec. 2.02 for a very short dipole may be extended to the case where the length of the straight wire or dipole is comparable to the wave length. In Fig. 3.01 the dipole of length L is made to coincide with the x axis. Then, if dx denotes an infinitesimal radiating length, it may be used in place of Δl of Eq. (2.04) or h_e of (2.07) Now I_{max}, the time amplitude of the current, may vary from point to point on the dipole. Thus the contribution to the field at P due to dx is

$$dE_{max} = \frac{60\pi I_{max}(x) \sin \theta_x}{\lambda r_x} dx \qquad (3.01)$$

as was shown in Eq. (2.07). When r is sufficiently large, two approximations may be made.

and

$$\left.\begin{aligned} r_x &= r - x\cos\theta \doteq r \\ \theta_x &\doteq \theta \end{aligned}\right\} \tag{3.02}$$

Thus

$$dE_{max} = \frac{60\pi I_{max}(x)\sin\theta}{\lambda r}\,dx \tag{3.03}$$

Now it becomes necessary to assume a current distribution along the wire, *i.e.*, the value of the amplitude I_{max} at each point, the current being taken to be everywhere in time phase. The cases to be considered are those for which L is an integral number of half wave lengths. If there is no end loading, the currents at

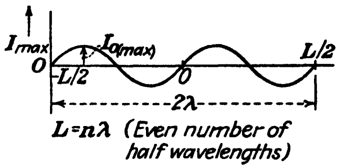


FIG. 3.02.—Current distribution along dipole whose length is an even number of half wave lengths.

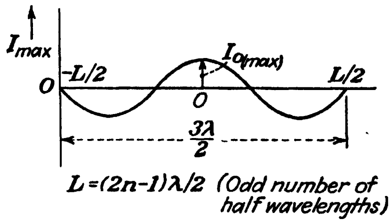


FIG. 3.03.—Current distribution along dipole whose length is an odd number of half wave lengths.

$x = \pm L/2$ are zero, and elsewhere the current will follow the usual relationship for standing waves on a line. Thus, for an *even* number of half waves, $I = 0$ at the center, while for L an *odd* number of half wave lengths long, the maximum current will be at the center. This is illustrated in Figs. 3.02 and 3.03.

The case where L is an *odd* number of half wave lengths will be considered first. For it

$$I_{max}(x) = I_{0(max)}\cos\frac{2\pi}{\lambda}x \tag{3.04}$$

where $I_{0(max)}$ is now the current amplitude at $x = 0$.

It is shown in Appendix C that the integration that sums up the contributions dE_{max} due to all the elements of current gives a final result for the field strength in this case of

$$E_{max} = \frac{60 I_{0(max)}}{r}\,\frac{1}{\sin\theta}\cos\left(\frac{m\pi}{2}\cos\theta\right) \tag{3.05}$$

Here E_{max} is the time amplitude of the field strength at a distance

r, for m an odd integer representing the dipole length in multiples of $\lambda/2$.

If the amplitude factor $60I_{0(\max)}/r$ is denoted by K_0, one finds

$$E_{\max} = K_0 \frac{\cos\left(\frac{m\pi}{2}\cos\theta\right)}{\sin\theta} \tag{3.06}$$

Equation (3.06) holds for an antenna an odd number of half waves long. For an even number (*i.e.*, an integral number of wave lengths) the corresponding result may be shown to be

$$E_{\max} = K_0 \frac{\sin\left(\frac{m\pi}{2}\cos\theta\right)}{\sin\theta} \tag{3.07}$$

The case for $L = \lambda/2$ is of especial importance in direction finding. For it

$$E_{\max} = K_0 \frac{\cos\left(\frac{\pi}{2}\cos\theta\right)}{\sin\theta} \tag{3.08}$$

This is plotted in Fig. 3.04 for the half-wave dipole, and for comparison the function $\sin\theta$ for an infinitesimal dipole, the proper

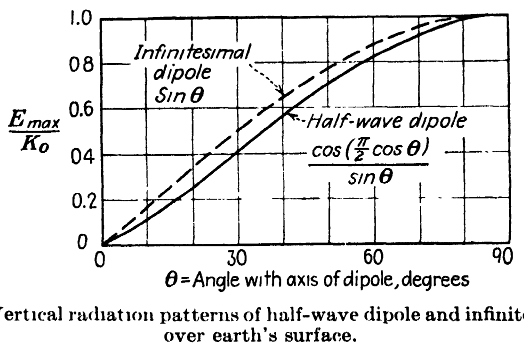


FIG. 3.04.—Vertical radiation patterns of half-wave dipole and infinitesimal dipole over earth's surface.

proportionality factor being chosen for the latter to give the same field in the normal plane bisecting the dipole. It will be noted that the directive pattern of the $\lambda/2$ dipole is quite close to that of a short antenna. In practice, this approximation is frequently made.

For longer straight wires, the results begin to differ markedly. This is illustrated by means of polar diagrams in Fig. 3.05, which

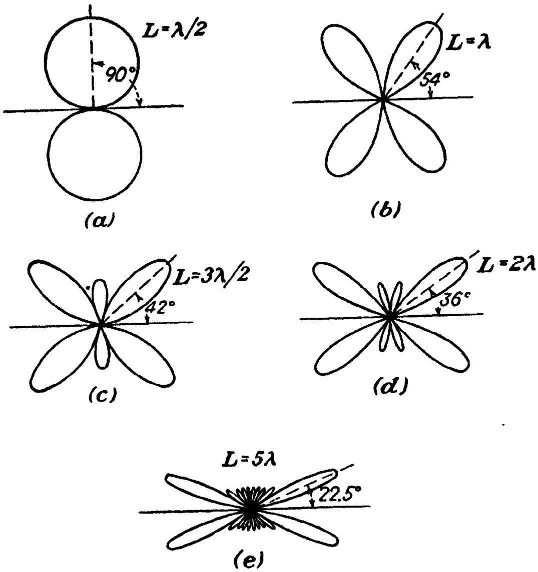


FIG. 3.05.—Radiation patterns of long antennas. (*Carter, Hansell, and Lindenblad.*)

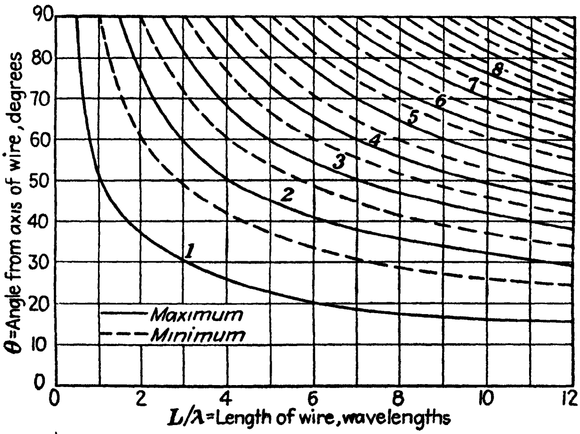


FIG. 3.06.—Lobe maxima and minima of radiation patterns of long antennas.

were calculated from Eqs. (3.06) and (3.07). It will be noted that more lobes appear for the longer wires. For integral multiples

of $\lambda/2$, the number of lobes on one side of the axis equals the number of half waves in the length of the antenna. Each polar diagram is a section of a figure of revolution about the wire as an axis, and thus each possesses *axial symmetry*.

The locations of the maxima and minima are shown in Fig. 3.06, which was taken from Carter, Hansell, and Lindenblad.[1]

3.03. Vertical Wire over Perfect Earth.—Analysis of the behavior of a straight vertical wire or antenna above the earth's

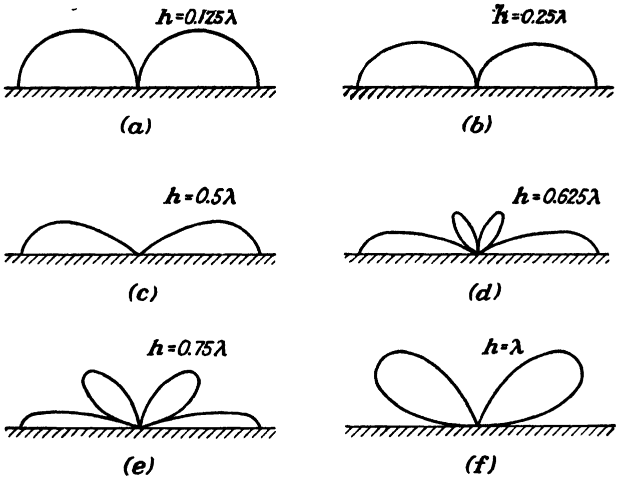


FIG. 3.07.—Vertical radiation patterns of antennas up to one wave length in height over earth of infinite conductivity.

surface is facilitated by an assumption[2] of current distribution as was done in Sec. 3.02. When there is no top loading and the antenna is of small cross section, the current can be taken to increase sinusoidally from the open end. The conducting plane representing the earth's surface results in the presence of an image antenna having the appropriate current distribution and sense of flow (see Sec. 2.03).

[1] CARTER, HANSELL, and LINDENBLAD, Development of Directive Transmitting Antennas by R.C.A. Communications, Inc., *Proc. I.R.E.*, **19**, 1773 (October, 1931). Figure 3.05 is also taken from this paper.

[2] The solution is possible without this assumption, but the analysis becomes much more involved. See, for example, J. A. STRATTON and L. J. CHU, Steady-state Solutions of Electromagnetic Field Problems, *Journal of Applied Physics*, **12**, 230 (March, 1941).

A quantitative consideration shows the general resemblance to the case of the long wire in space. Specific practical situations

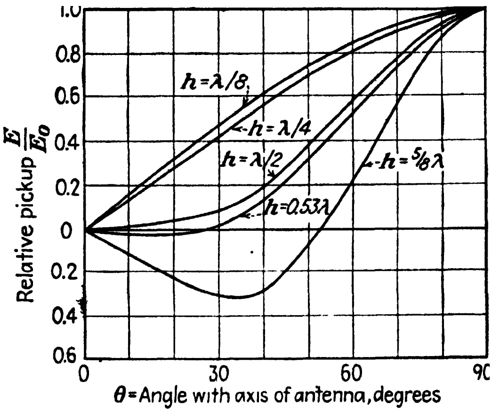


Fig. 3.08.—Comparison of high-angle radiation of vertical antennas over earth of infinite conductivity. The antenna height is h.

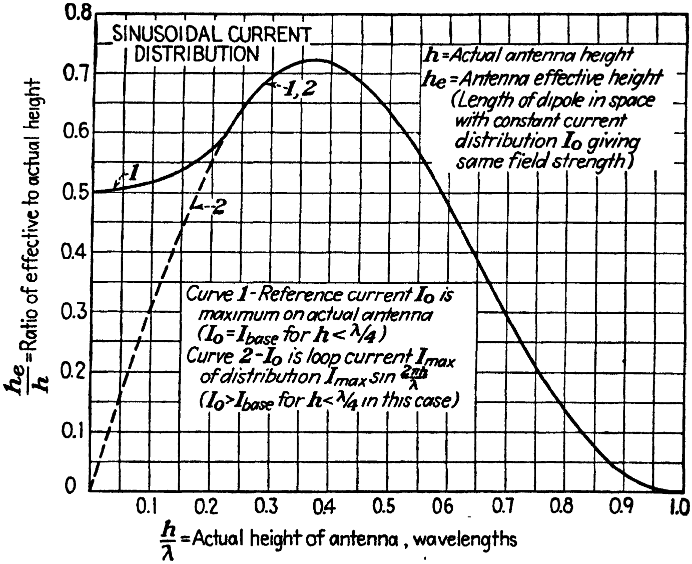


Fig. 3.09.—Effective height along horizon of vertical antenna above plane earth of infinite conductivity.

give radiation patterns as shown in Fig. 3.07 for various values of height h up to one wave length.

This may also be seen from the plot[1] of *relative* amplitudes in rectangular coordinates of Fig. 3.08. Here all the curves are adjusted by an appropriate scale factor to give unit radiation in the direction of the main lobe. The negative values of ordinates have no especial significance other than to emphasize the continuity of the amplitude function. It will be observed that if the curve lies everywhere above the zero axis, there are no subsidiary lobes. In other cases the null values of θ are the intersections with the axis. Since the main lobe has its maximum in the horizontal plane up to the greatest length shown in this figure, but not for case *f* of Fig. 3.07, the relative values at $\theta = 90°$ are given by Fig. 2.03 for constant power and by Fig. 3.09 for constant current.

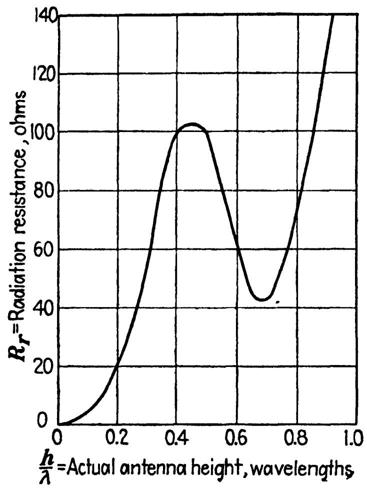


FIG. 3.10.—Radiation resistance of vertical antenna near surface of earth, referred to current loop value.

Radiation resistance for lengths up to one wave length is illustrated in Fig. 3.10 and is referred to the loop current, *i.e.*, $I_{0(max)}$, the maximum value of a sinusoidal distribution increasing from zero at the top of the antenna. For values of height less than $\lambda/4$ this is a virtual value and is greater than the current at the base.

3.04. Effective Height of Vertical Wire.—The value of effective height may be computed by much simpler means than those involved in the analysis of radiation resistance of Fig. 3.10. The two quantities R_r and h_e then permit field-strength computations by means of Eq. (2.10). The expression for effective height *along the earth's* surface may be obtained, with a certain lack of rigor, by assuming that the dipole moment[2] of the fictitious

[1] G. H. BROWN, A Critical Study of the Characteristics of Broadcast Antennas as Affected by Antenna Current Distribution, *Proc. I.R.E.*, **24**, 48 (January, 1936).

[2] The *dipole moment* is the product of the length by the current flowing in the dipole, or a corresponding summation for nonuniform distribution of current.

antenna of height h_e and of uniform current I_0 is equal to the moment of the actual length h and the mean value of the actual current $\bar{I}$. That is,

$$h_e I_0 = h\bar{I} \tag{3.09}$$

The quantity $\bar{I}$ denotes the mean value, averaged over the length of the antenna, of the amplitudes of the alternating antenna current I. Since the variation of I with time need not be considered here, the notation of I for I_{max} of preceding sections will be used.

The value of h_e depends upon the arbitrary choice of I_0, the comparison uniform current distribution. Three possibilities suggest themselves:

1. I_0 = maximum value of I on antenna
2. $I_0 = I_{loop}$
3. $I_0 = I_{base}$

It will be seen by a comparison of Figs. 3.11 and 3.12 that I_{loop} does not occur on the physical antenna for $h < \lambda/4$. The first

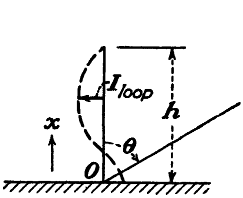


FIG. 3.11.—Current distribution along vertical antenna of height greater than $\lambda/4$.

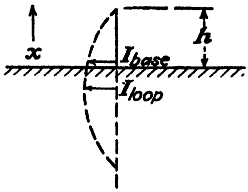


FIG. 3.12.—Current distribution along vertical antenna of height less than $\lambda/4$.

of these cases will be considered by choosing I_0 equal to the maximum value on the actual antenna. Then

$$\left.\begin{aligned} I_0 &= I_{base} \text{ for } h \lesseqgtr \frac{\lambda}{4} \\ I_0 &= I_{loop} \text{ for } h \gtreqless \frac{\lambda}{4} \end{aligned}\right\} \tag{3.10}$$

Then, as shown in Appendix C, the effective height is given by

$$h_e = \frac{\lambda}{\pi} \sin^2\left(\frac{\pi h}{\lambda}\right) \qquad \text{for } h \gtreqless \frac{\lambda}{4} \tag{3.11}$$

$$h_e = \frac{\lambda}{\pi \sin \dfrac{2\pi h}{\lambda}} \sin^2\left(\frac{\pi h}{\lambda}\right) \qquad \text{for } h \lesseqgtr \frac{\lambda}{4} \tag{3.12}$$

This is illustrated in curve 1 of Fig. 3.09. When the actual antenna height is expressed in fractions of a wave length, one may write

$$\eta = \frac{h}{\lambda} \tag{3.13}$$

Thus from Eq. (3.11):

$$\frac{h_e}{h} = \frac{\sin^2 \pi\eta}{\pi\eta} \qquad \text{for } h \gtreqqless \frac{\lambda}{4} \tag{3.14}$$

and from Eq. (3.12):

$$\frac{h_e}{h} = \frac{\sin^2 \pi\eta}{\pi\eta \sin 2\pi\eta} \qquad \text{for } h \lesseqqgtr \frac{\lambda}{4} \tag{3.15}$$

The last equation may be written

$$\frac{h_e}{h} = \frac{1}{2} \cdot \frac{\sin^2 \pi\eta}{\pi^2\eta^2} \cdot \frac{2\pi\eta}{\sin 2\pi\eta} \tag{3.16}$$

Then as the antenna becomes very short in comparison with the wave length, each of the last two factors approaches unity because each is of the form $(\sin x)/x$, and the latter approaches unity as x approaches zero. Then

$$\lim_{\eta \to 0} \frac{h_e}{h} = \frac{1}{2} \tag{3.17}$$

This shows that a very short vertical antenna near ground has an effective height which is half the physical height.

The second case ($I_0 = I_{\text{loop}}$) gives an effective height for any length in accordance with Eqs. (3.11) and (3.14). This is curve 2 of Fig. 3.09, and it coincides with curve 1 for actual heights greater than one-quarter wave length.

The third case ($I_0 = I_{\text{base}}$) is usually of interest where this is the maximum current at any point on the antenna, *i.e.*, for $h \lesseqqgtr \lambda/4$. It is then given by Eqs. (3.12) and (3.15).

It may be remarked that h_e is actually a function of θ, the angle of elevation from the horizontal. This value of h_e gives the radiation in any direction. The result given by Norton[1] for the general case appears in Appendix C.

[1] K. A. NORTON, The Propagation of Radio Waves over the Surface of the Earth and in the Upper Atmosphere, *Proc. I.R.E.*, **24**, 1367 (October, 1936). See also H. E. GIHRING and G. H. BROWN, General Considerations of Tower Antennas for Broadcast Use, *Proc. I.R.E.*, **23**, 311 (April, 1935).

Example.—A broadcast station antenna is frequently a vertical radiator of physical length 0.58λ. This choice is made for fading considerations when high-angle radiation is to be kept to a minimum. Assume that one wishes to compute the effective height in terms of the loop current I_{loop}. The latter is measured at a point 0.25λ from the top, or 0.33λ above the earth's surface. Equation (3.14) applies.

$$\eta = \frac{h}{\lambda} = 0.58$$

$$\frac{h_e}{h} = \frac{\sin^2 (0.58\pi)}{0.58\pi} = \frac{0.938}{1.825} = 0.514$$

Consequently,

$$h_e = 0.514 \times 0.58\lambda = 0.298\lambda$$

3.05. Loop Antenna.—When an antenna consisting of one or more turns of a closed loop is considered, important directive properties are found. One may analyze first a rectangular single-turn loop of dimensions much less than λ as in Fig. 3.13.

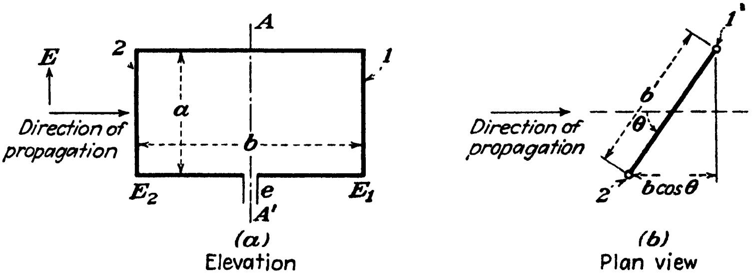


FIG. 3.13.—Loop antenna in radiation field.

The loop may be rotated about the axis AA', the latter coinciding with the plane of polarization. The second figure shows the plan view. The field strengths at two points $b \cos \theta$ apart, owing to a wave propagated in the direction shown, are

$$\left. \begin{aligned} E_1 &= E_{max} \cos \omega t \\ E_2 &= E_{max} \cos \left(\omega t + \frac{2\pi b \cos \theta}{\lambda} \right) \end{aligned} \right\} \tag{3.18}$$

The vertical conductors 1 and 2 pick up voltages proportional to a:

$$\left. \begin{aligned} e_1 &= E_1 a \\ e_2 &= E_2 a \end{aligned} \right\} \tag{3.19}$$

This follows because I is constant in the loop for $a = h << \lambda$. These voltages are *approximately* π out of phase at the terminals where the loop is broken, but there is a resultant e due to the phase change in the distance $b \cos \theta$.

$$e = (E_1 - E_2)a \tag{3.20}$$

$$e = E_{max}\, a \left[\cos \omega t - \cos \omega t \cos \left(\frac{2\pi b \cos \theta}{\lambda} \right) + \sin \omega t \sin \left(\frac{2\pi b \cos \theta}{\lambda} \right) \right] \tag{3.21}$$

If one sets

$$\psi = \frac{2\pi b \cos \theta}{\lambda} \tag{3.22}$$

Eq. (3.21) becomes

$$e = E_{max}\, a[\cos \omega t(1 - \cos \psi) + \sin \omega t \sin \psi] \tag{3.23}$$

Inasmuch as the loop dimensions are small compared to the wave length, the quantities $1 - \cos \psi$ and $\sin \psi$ may be compared for ψ quite small.

$$\left. \begin{aligned} 1 - \cos \psi &= \frac{\psi^2}{2!} - \frac{\psi^4}{4!} + \cdots \\ \sin \psi &= \psi - \frac{\psi^3}{3!} + \cdots \end{aligned} \right\} \tag{3.24}$$

so that

$$\frac{1 - \cos \psi}{\sin \psi} \doteq \frac{\psi}{2} \tag{3.25}$$

For example if $b = 1$ m, $\lambda = 300$ m, and $\theta = 0$, then

$$\psi = \frac{2\pi \times 1}{300} = 0.021$$

and the error of neglecting $1 - \cos \psi$ in comparison with $\sin \psi$ in computing the magnitude of e in Eq. (3.23) cannot exceed 0.0002. Thus

$$e = E_{max}\, a \sin \omega t \sin \psi \tag{3.26}$$

or making the approximation

$$\psi \doteq \sin \psi = \frac{2\pi b \cos \theta}{\lambda} \tag{3.27}$$

$$e = \frac{2\pi ab\, E_{max}}{\lambda} \cos \theta \sin \omega t \tag{3.28}$$

But ab is the area of the loop A. Furthermore, if there are N turns connected in series, the output voltage will be N times as great.

$$e = \frac{2\pi N A E_{max}}{\lambda} \cos \theta \sin \omega t \tag{3.29}$$

Several points will be noted in Eq. (3.29):

1. Since e is proportional to $\sin \omega t$, it is 90° out of phase with the electric field E_1. This is of great importance in direction finders in which the output of a loop is combined with that of a vertical antenna in the proper phase.

2. The voltage e varies as $\cos \theta$, giving the figure-of-8 pattern of Fig. 3.14.

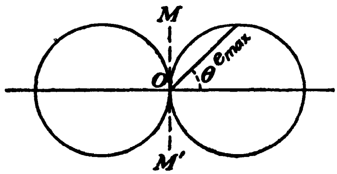


FIG. 3.14.—Directive pattern (figure of 8) of loop antenna.

3. The voltage pickup varies as the loop area. It can be easily demonstrated that for any shape of plane loop, it is the area that enters into the equation corresponding to Eq. (3.29). This demonstration involves breaking the area into elements $dx\,dy$, for each of which e is given by Eq. (3.29), and then summing up over the whole loop, the currents canceling everywhere except along the periphery.

4. The voltage e is directly proportional to the frequency. If the effective height is defined as the voltage amplitude for unit field when $\theta = 0$,

$$h_e = \frac{2\pi N A}{\lambda} = \frac{2\pi N A f}{c} \tag{3.30}$$

Example.—A circular loop 24 in. in diameter with eight turns operates at 1500 kc ($\lambda = 200$ m). The value of h_e is required. The loop diameter $d = 0.61$ m, so that $A = 0.292$ m².

$$h_e = \frac{2\pi \times 8 \times 0.292}{200} = 0.0734 \text{ m}$$

Thus a straight vertical wire above ground of $h_e = 7.34$ cm would give the same pickup. By Fig. 3.09 for a very short antenna, $h = 2h_e = 14.7$ cm. This illustrates the small pickup from a loop antenna of moderate dimensions.

3.06. Two-element Arrays of Point Sources.—A fictitious "point source" having equal radiating properties in all directions may be assumed for the purpose of simplifying the analysis of

arrays of a number of elements. When this is done formulas may be obtained for directivity as a function of the spacing and phasing of the currents in these point sources. Then superimposed upon this space function will be that due to the directivity of the individual elements if they consist of finite sources like those of Secs. 3.02 to 3.05.

If two point sources are separated by a distance d and have flowing in them currents having a phase difference α, the field at a distant point P of Fig. 3.15 may be determined. The con-

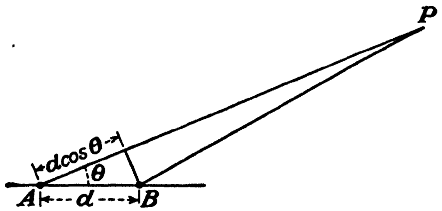


FIG. 3.15.—Radiation from two point sources.

cept of the current flowing in a point source will be taken to mean the limiting case, as the dimensions diminish, of a radiator of constant dipole moment. In the limit this would radiate equally in all directions. The field at P due to A is

$$E_1 = KI_1 \cos \omega t$$

and due to B,

$$\left. \begin{aligned} E_1 &= KI_1 \cos \omega t \\ E_2 &= KI_2 \cos (\omega t + \alpha + \psi) \end{aligned} \right\} \tag{3.31}$$

where I_1 and I_2 are the maximum values of the currents, α the phase difference in the currents, and ψ the phase difference due to the path difference $d \cos \theta$, *viz.*,

$$\psi = \frac{2\pi}{\lambda} d \cos \theta \tag{3.32}$$

K is an appropriate constant of proportionality.

It is instructive and more compact in form at this point to utilize exponential notation for Eq. (3.31) by writing

$$\left. \begin{aligned} E_1 &= KI_1 e^{j\omega t} \\ E_2 &= KI_2 e^{j(\omega t + \alpha + \psi)} \end{aligned} \right\} \tag{3.33}$$

provided it is understood that the real part of the time function is

to be taken in each case. The resultant field is

$$E = E_1 + E_2$$
$$= Ke^{j\omega t}(I_1 + I_2 e^{j(\alpha+\psi)}) \qquad (3.34)$$

Or, if

$$I_2 = nI_1 \qquad (3.35)$$
$$E = KI_1 e^{j\omega t}(1 + ne^{j(\alpha+\psi)}) \qquad (3.36)$$

Now the magnitude of this vector can be found by setting $t = 0$ in Eq. (3.36), giving

$$E_{max} = KI_1(1 + ne^{j(\alpha+\psi)}) \qquad (3.37)$$

The vector E_0/KI_1 is given in Fig. 3.16. Its components are obviously $1 + n \cos (\alpha + \psi)$ and $jn \sin (\alpha + \psi)$, respectively.

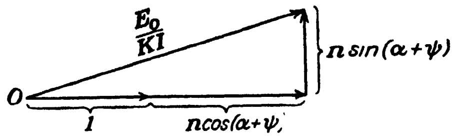


FIG. 3.16.—Phase relations between fields from two point sources. Here $I = I_1$.

This vector in turn has a length

$$|E| = KI_1\sqrt{[1 + n \cos (\alpha + \psi)]^2 + n^2 \sin^2 (\alpha + \psi)} \qquad (3.38)$$
$$= KI_1 \sqrt{1 + 2n \cos (\alpha + \psi) + n^2 \cos^2 (\alpha + \psi) + n^2 \sin^2 (\alpha + \psi)} \qquad (3.39)$$
$$= KI_1\sqrt{1 + 2n \cos (\alpha + \psi) + n^2} \qquad (3.40)$$

This is the desired result. In the important special case where the currents are equal $n = 1$ and

$$|E| = 2KI \cos \frac{\alpha + \psi}{2} \qquad (3.41)$$
$$= 2KI \cos \left(\frac{\alpha}{2} + \frac{\pi}{\lambda} d \cos \theta\right) \qquad (3.42)$$

For example if $\alpha = \pi/2$ and $d = \lambda/4$, one has

$$|E| = 2KI \cos \left[\frac{\pi}{4} (1 + \cos \theta)\right]$$

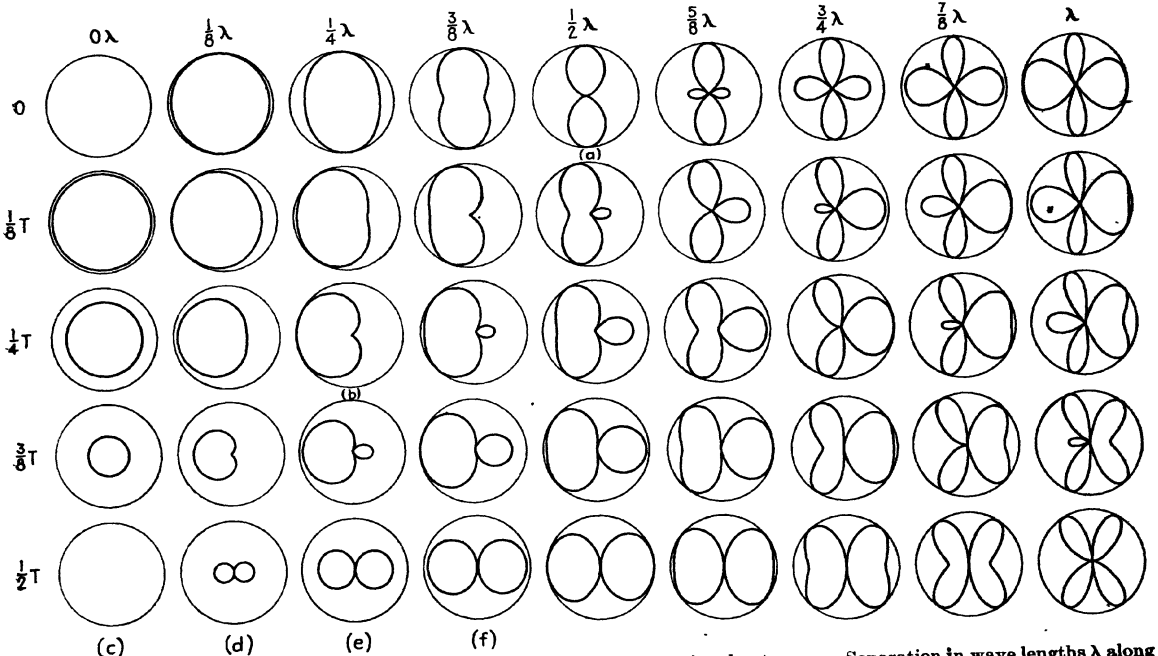


FIG. 3.17.—Directive-amplitude diagrams for an array of two nondirectional antennas. Separation in wave lengths λ along the top, phase difference in fractions of a period T at the left.

Curve a: Separation $d = \frac{1}{2}\lambda$, phase difference $\alpha = 0$. This is a typical pattern having two null directions.

Curve b: Separation $d = \frac{1}{4}\lambda$, phase difference $\alpha = 90°$ or $\frac{1}{4}\ T$. This pattern has only a single null. (*Southworth*, *Proc. I.R.E.*, **18**, 1502, *September*, 1930.)

and this has typical values as follows:

θ	$\|E\|/2KI$
0	0
$\frac{\pi}{2}$	0.707
π	1.000
$\frac{3\pi}{2}$	0.707

The actual function is plotted in Fig. 3.17 as curve *b*, since this value of α corresponds to a phase difference of one-quarter period ($\frac{1}{4}T$). It will be noted that this directive pattern has a single null. This combination of antennas is only one means of producing such a pattern. Another will be discussed in Sec. 3.08. A number of other cases are plotted[1] in Fig. 3.17 for values of α between 0 and π and d from 0 to λ.

3.07. Three-dimensional Array.—When two elements were considered in the previous section, the directivity of each was neglected or spherical symmetry assumed. Consequently, there was equal radiation in all directions in a plane bisecting AB in Fig. 3.15, the plane being normal to the plane of the page. It is often of advantage to be able to control the radiation in all directions as well as in the plane ABP. Obviously a three-dimensional array of radiating point sources is a means of obtaining this.

Such an analysis can be carried out practically by choosing a regular lattice-type of array as shown in Fig. 3.18. Along each axis the point sources are equally spaced. Their number and spacing and the phasing of the currents flowing in them are chosen to fit the desired result. Most broadside and end-fire arrays of high directivity for point-to-point communication make use of this general system. The literature on this problem is rather extensive.

The general formula involves the quantities:

θ = elevation angle
Φ = azimuth angle

[1] G. C. SOUTHWORTH, Certain Factors Affecting the Gain of Directive Antennas, *Proc. I.R.E.*, **18**, 1502 (September, 1930); also, R. M. FOSTER, Directive Diagrams of Antenna Arrays, *Bell System Tech. J.*, **5**, 292 (April, 1926).

N_x, N_y, and N_z = number of point sources along x, y, and z axes, respectively

a_x, a_y, and a_z = separation of successive sources along x, y, and z axes, respectively, in multiples of the wave length λ

b_x, b_y, and b_z = phase difference between currents in successive sources along x, y, and z axes, respectively, in multiples of one period (2π radians)

The result is[1]

$$E = K \frac{\sin N_x\pi(a_x \cos \Phi \cos \theta + b_x)}{N_x \sin \pi(a_x \cos \Phi \cos \theta + b_x)} \cdot \frac{\sin N_y\pi(a_y \sin \Phi \cos \theta + b_y)}{N_y \sin \pi(a_y \sin \Phi \cos \theta + b_y)} \cdot \frac{\sin N_z\pi(a_z \sin \theta + b_z)}{N_z \sin \pi(a_z \sin \theta + b_z)} \qquad (3.43)$$

3.08. Loop and Vertical Antennas.—A type of two-element array that is of great importance in direction finding is the combination of a vertical loop and an antenna that is nondirectional

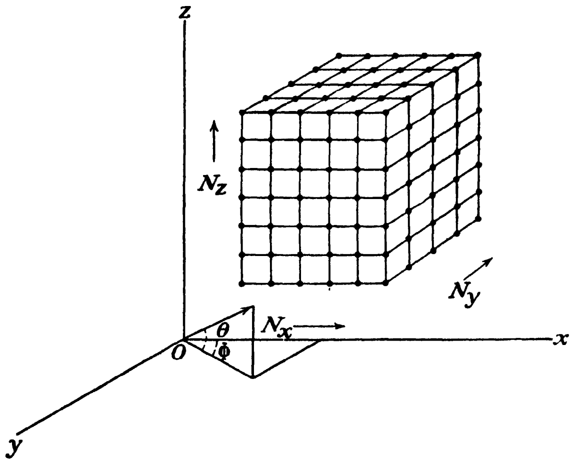


FIG. 3.18.—Three-dimensional array of point sources. Phase shifts between successive sources in multiples of one period are b_x, b_y, and b_z. The separations of successive sources are $a_x\lambda$, $a_y\lambda$, and $a_z\lambda$. (*Southworth, Proc. I.R.E.*, **18**, 1502, *September*, 1930.)

in the horizontal plane. The separation of the two will be assumed to be such a small fraction of a wave length as to intro-

[1] *Ibid*

duce no relative phase shift. This is almost always met in practice with a loop-type direction finder having a vertical "sense" antenna.

In this case the directive patterns are, respectively,

$$\left.\begin{aligned} E_1 &= \cos\theta \cos\omega t \\ \text{and} \qquad E_2 &= n\cos(\omega t + \alpha) \end{aligned}\right\} \tag{3.44}$$

where the constant of proportionality has been ignored. The quantity n is the ratio of the maxima of the second and the first antenna patterns. The phase constant α includes the phase difference of $\pi/2$ between the electric field and the loop terminal voltage as was discussed on page 89.

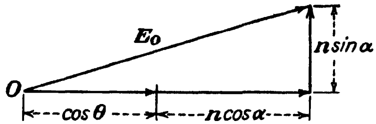


FIG. 3.19.—Phase relations between loop and vertical antenna voltages.

The resultant of the two vectors E_1 and E_2 has a magnitude[1] of

$$|E| = \sqrt{n^2 + \cos^2\theta + 2n\cos\theta\cos\alpha} \tag{3.45}$$

From this general result one may proceed to several special cases of importance. When $\alpha = 0$, the quantities E_1 and E_2 (representing either radiated fields or voltages picked up in receiving antennas) are in phase or π out of phase, depending on θ, and Eq. (3.44) becomes

$$|E| = \cos\theta + n \tag{3.50}$$

[1] This may be seen by a method similar to that used in deriving Eq. (3.40). If exponential notation is used, Eq. (3.44) becomes

$$\left.\begin{aligned} E_1 &= \cos\theta\, e^{j\omega t} \\ E_2 &= n e^{j(\omega t + \alpha)} \end{aligned}\right\} \tag{3.46}$$

The resultant is

$$\begin{aligned} E &= E_1 + E_2 \\ &= e^{j\omega t}(\cos\theta + n e^{j\alpha}) \end{aligned} \tag{3.47}$$

Figure 3.19 shows that the magnitude E_0 is

$$E_0 = \cos\theta + n e^{j\alpha} \tag{3.48}$$

This has a length of

$$|E| = \sqrt{(\cos\theta + n\cos\alpha)^2 + n^2\sin^2\alpha} \tag{3.49}$$

and the result given above follows directly.

This is illustrated in Fig. 3.20 for various values of n. The case for $n = 1$ is that of a *cardioid*. It provides means of resolving the ambiguity as to direction of arrival of the waves to the loop

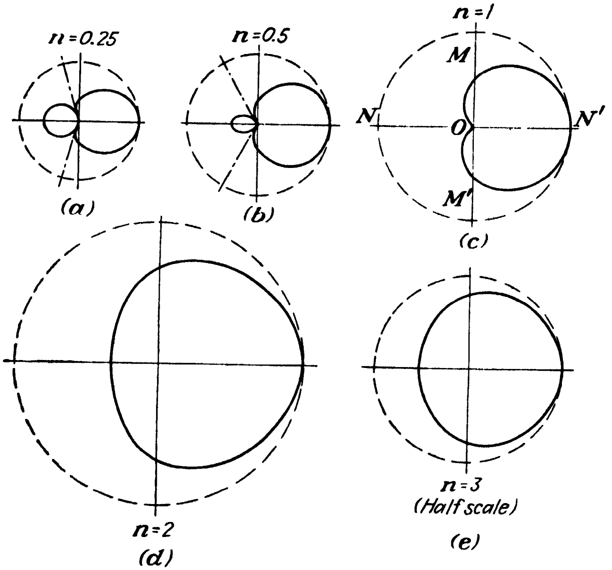


FIG. 3.20.—Directive patterns of loop and vertical antennas for various values of relative pickup.

alone. In Fig. 3.14 there is no way of distinguishing between OM and OM' of the loop alone, while with this combination of loop and vertical antenna, the minimum direction ON is uniquely

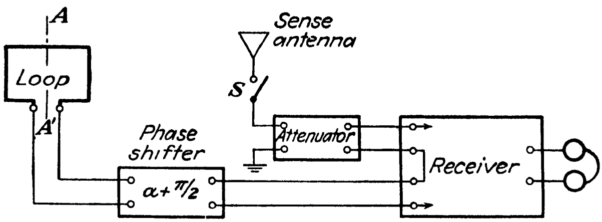


FIG. 3.21.—Circuit for obtaining bilateral and unilateral bearings by means of an aural-null direction finder.

defined. It therefore gives the "sense" of arrival of the signal, and accordingly the nondirectional antenna used with the loop is called a "sense antenna."

3.09. Bilateral and Unilateral Bearings.—Application of this is seen in the circuit of Fig. 3.21, which is adapted for taking aural-null bearings with the loop alone ("bilateral") or with loop and sense antennas ("unilateral"). Operation consists in rotating the loop to a minimum signal position with switch S open, thereby establishing accurately the *pair* of bearings OM and OM'. Then S is closed and the loop rotated in a predetermined direction, *e.g.*, toward higher readings on the azimuth scale, by approximately 90° from the first null. If the signal has increased,[1] the original direction, *e.g.*, OM, was the proper bilateral bearing.

The attenuator allows variation of n to give a high maximum-to-minimum ratio along the unilateral null line NON'. Its adjustment is not critical. No attempt is made to secure *accurate* bearings on the minimum ON. This is due to the fact that it is a null only for n exactly unity. For $n < 1$, it is actually a maximum of the smaller lobe, and there are two null lines symmetrically disposed about ON and diverging by greater amounts as n decreases. Furthermore the slope of the curve near ON is much less than for a cosine pattern. For the cardioid Eq. (3.50) shows this to be

$$\frac{d|E|}{d\theta} = -\frac{1}{2}\sin\theta \tag{3.51}$$

the factor ½ having been included to give the same maximum amplitude as for the figure of 8. At $\theta = 0$, Eq. (3.51) becomes

$$\frac{d|E|}{d\theta} = 0 \tag{3.52}$$

For the loop pattern

$$E = \cos\theta \tag{3.53}$$

and at its minimum $\theta = \pm\pi/2$, so that

$$\frac{dE}{d\theta} = -\sin\theta = \pm 1 \tag{3.54}$$

at these angles.

3.10. Undesired Effects Due to Vertical Antenna Pickup.—The curves of Fig. 3.20 for $n < 1$ illustrate the effect known as *nonopposite minima*. When a small amount of stray signal is

[1] This convention applies to most shipboard direction finders. The opposite is true of aircraft direction finders in most cases.

inadvertently picked up by an improperly shielded receiver or when the loop and its transmission lines exhibit pickup that is independent of loop orientation, the result is to make the null positions be less than 180° apart. Direction finders are particularly susceptible to small amounts of vertical signal. For example, if the stray vertical pickup is 40 db below the maximum loop signal, $n = 0.01$ and each minimum will occur at an angle $\Delta\theta$ from the proper line of nulls, where

$$\sin \Delta\theta = n \tag{3.55}$$

and for this case

$$\Delta\theta = 0.57°$$

and the minima differ from 180° by $2\Delta\theta$ or 1.1°.

In contrast to the case of equal phase given in Eq. (3.50), if $\alpha = \pi/2$ in Eq. (3.45):

$$|E| = \sqrt{n^2 + \cos^2 \theta} \tag{3.56}$$

This will be seen to have no null directions. In the case where $n = 1$

$$|E| = \sqrt{1 + \cos^2 \theta} \tag{3.57}$$

This is plotted in Fig. 3.22. It will be considered further in a later discussion of balancer circuits for aural-null direction finders.

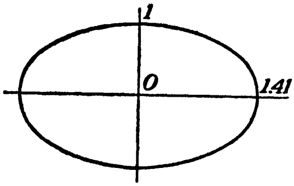


FIG. 3.22.—Loop pattern with the addition of nondirectional quadrature voltage. There are no null points under these conditions.

3.11. Two Parallel Loops.—A type of two-element array, which has been used somewhat for direction finding when polarization errors must be kept to a minimum at high frequencies, is the *parallel loop array*. It usually consists of two loops rigidly fixed to the ends of a boom which may be rotated about its center. This is illustrated in Fig. 3.23, where a plan view of the two loops A and B is shown. The loops are separated by a distance d. All dimensions are assumed to be small in comparison with λ.

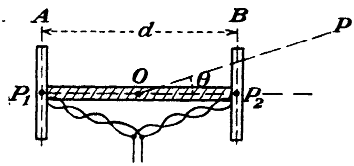


FIG. 3.23.—Parallel coaxial loop direction finder (plan view), often referred to as spaced-loop direction finder.

If the directive pattern for two point sources P_1 and P_2 is considered, Eq. (3.42) gives

$$|E| = 2E_{max}h_e' \cos\left(\frac{\alpha}{2} + \frac{\pi}{\lambda} d \cos\theta\right) \quad (3.58)$$

if one lets $KI = E_{max}h_e'$ in Eq. (3.31). Then for each loop the directive pattern is

$$h_e' = h_e \sin\theta \quad (3.59)$$

where h_e is defined for a loop by Eq. (3.30).

Now, if the loops are connected series opposing ($\alpha = \pi$ at $\theta = \pm\pi/2$), the final result[1] for the directivity is

$$\frac{|E|}{E_{max}} = h_e \frac{\pi d}{\lambda} \sin 2\theta \quad (3.60)$$

This pattern has *four* minima as is shown in Fig. 3.24. One will note that the maximum value of $|E|$ is obtained at $\theta = \pi/4$, $3\pi/4$, $5\pi/4$, and $7\pi/4$, and is given in terms of E_{max} as

$$\left.\frac{|E|}{E_{max}}\right]_{\frac{\pi}{4}} = h_e \frac{\pi d}{\lambda} \quad (3.65)$$

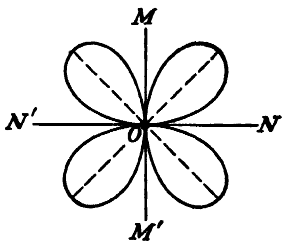


FIG. 3.24.—Directive pattern of parallel coaxial loop direction finder.

where h_e is the corresponding amplitude factor for one loop alone. Thus the pickup is much less than that of a single loop.

[1] This may be shown since Eq. (3.58) may be written

$$|E| = 2E_{max}h_e \sin\theta \cos\left(\frac{\alpha}{2} + \frac{\pi}{\lambda} d \cos\theta\right) \quad (3.61)$$

$$\frac{|E|}{E_{max}} = 2h_e \sin\theta \left[\cos\left(\frac{\pi d}{\lambda}\cos\theta\right)\cos\frac{\alpha}{2} - \sin\left(\frac{\pi d}{\lambda}\cos\theta\right)\sin\frac{\alpha}{2}\right] \quad (3.62)$$

Now, if the loops are connected with outputs π out of phase (at $\theta = \pm\pi/2$), $\alpha = \pi$ and

$$\frac{|E|}{E_{max}} = -2h_e \sin\theta \sin\left(\frac{\pi d}{\lambda}\cos\theta\right) \quad (3.63)$$

If $d << \lambda$, the approximation holds that

$$\frac{|E|}{E_{max}} = -h_e \frac{2\pi d}{\lambda} \sin\theta \cos\theta \quad (3.64)$$

and the result of Eq. (3.60) follows if the negative sign is ignored.

Example.—If the loops are 10 m apart and the frequency is 1000 kc, the relative pickup is

$$\frac{E}{E_{\text{loop}}} = \frac{\pi d}{\lambda}$$
$$= \frac{\pi \times 10}{300}$$
$$= 0.105$$

In other words, the two loops have a pickup 19.6 db below that of a single loop of the same size as each.

The merit of such a system for short-wave direction finding or operation at lower frequencies in the presence of night effect lies in the fact that one pair of nulls, the *principal nulls* (those in the plane of the loops), is much less affected by the abnormally polarized component of the received wave than is a single loop. This is discussed in detail in Sec. 3.14.

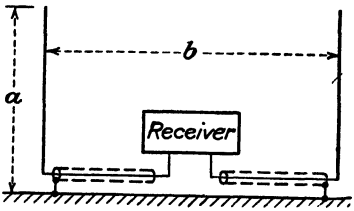


FIG. 3.25.—Adcock direction finder employing shielded transmission lines and direct coupling.

3.12. Directive Properties of Adcock Antennas.—The horizontal members of a loop contribute nothing to the directional properties for a wave arriving in the horizontal plane. In fact, they are responsible for bearing errors due to *night effect* as will be seen in Sec. 3.13. If these horizontal conductors could be eliminated or their effect nullified, accuracy would be improved. In the case of a single-turn loop this can be done by removing the upper conductor, and shielding or balancing out the effect of the lower horizontal wire. Such a directive array is known as an *Adcock antenna*.

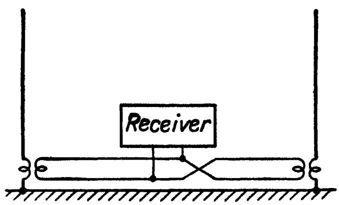


FIG. 3.26.—Adcock direction finder employing coupling transformers at bases of vertical conductors.

Two types of Adcock systems are shown in Figs. 3.25 and 3.26. It can readily be seen that the pickup is the same as that of a loop of one turn of length and width a and b, respectively. Hence the effective height, from Eq. (3.30), is

$$h_e = \frac{2\pi ab}{\lambda} = \frac{2\pi A}{\lambda} \tag{3.66}$$

since $N = 1$. A multiturn loop is usually tuned to resonance by means of a capacitor directly or through a coupling transformer. Consequently, it delivers a terminal voltage greater than the open-circuit value due to this resonant rise, the factor for a directly tuned loop being the Q of the loop winding. Furthermore the number of turns N may be considerable. On the other hand, an Adcock is limited to $N = 1$ and is usually operated as an untuned antenna. The pickup factor is much less (in the limit by the ratio $1/NQ$) compared to a loop of the same size. As a result, Adcock antennas are made quite large to compensate for this lower efficiency. The dimension b may be as much as $\lambda/5$. Such arrays are not adapted to shipboard or aircraft use, but are generally employed at fixed ground stations for both medium and short waves (200 kc to 20 mc). At the higher end of this frequency range, however, progress is being made in adapting Adcock antenna systems for such use aboard mobile craft.

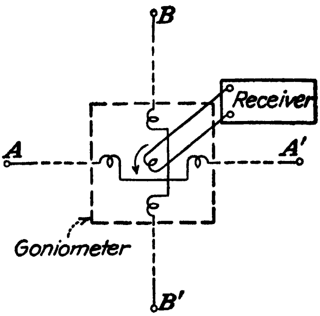


FIG. 3.27.—Adcock or fixed loop array with goniometer (Bellini-Tosi system).

The arrays themselves are often left fixed in position and are erected in pairs at right angles to each other, with coupling to each obtained by means of a rotating pickup coil system or *goniometer*, used to read the bearing.[1] This is shown in Fig. 3.27. The goniometer is ordinarily made a part of the direction finder receiver unit. Its coils are connected by suitable transmission lines to the antenna pairs AA' and BB'.

The details of design and the resulting performance of Adcock antennas, including coupling means, shielding and balancing, and the use of goniometers, have been intensively studied because of the great practical importance of the system. It will be treated in greater detail in later sections after the subject of *polarization errors* is investigated.

[1] R. KEEN, *Wireless Direction Finding*, Chaps. 5 and 7, 3d rev. ed., Iliffe & Sons, Ltd., London, 1938.

3.13. Polarization Errors. Night Effect.—The analysis of Sec. 3.05 assumes that the waves were being propagated horizontally toward a loop arranged to rotate about a vertical axis AA'. It was seen, however, in Chap. II that over large distances the major portion of the received energy is by way of the sky wave. At the receiving point this may be coming downward at a very considerable angle, and so the simple derivation for loop behavior is not strictly true. One may consider that the arriving wave consists of two components: one horizontally propagated and the other directed vertically downward. It is obvious that any diagonally directed wave can be resolved into these two components.

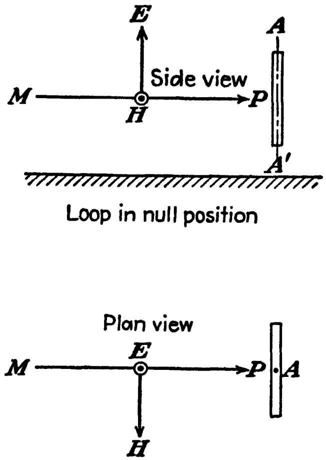


FIG. 3.28.—Loop and field relations—horizontally propagated component.

The horizontally propagated component is shown in Fig. 3.28 in both side and plan views. The electrical field vector E is vertical, while the magnetic field H is horizontal for the case of vertical polarization. If a loop is employed it is obvious that the antenna will be in a position of minimum pickup when its plane is at right angles to the direction of propagation. This is true because all the conductors lie in the plane of the wave front. It is usually simpler to consider the behavior in terms of the magnetic component H. The loop pickup will be zero when H is parallel to the plane of the loop. It is evident that the same conclusions will be reached whether the H or the E component is analyzed.

Next, the downwardly directed ray of Fig. 3.29 may be studied. The direction MP is the same as for the case of horizontal propagation and serves to define an azimuth direction in this case. Here the plane of polarization lies along MP. The vector H lies in the plane of the loop when the latter is in the position shown. This therefore is the null angle, and it will be seen to be the same as for the horizontally propagated component of Fig. 3.28. This case of the downwardly propagated component may be called that of the "normally polarized wave."

In contrast, one may take the case where the plane of polarization of the downwardly directed ray is rotated 90° with respect to the direction *MP*. This is the case of Fig. 3.30. Since *H* lies along the line *MP*, the loop will have its position of minimum when its plane coincides with *MP*. It will be observed that this component gives an apparent bearing 90° *displaced in azimuth* from that of the two preceding cases and, consequently, is

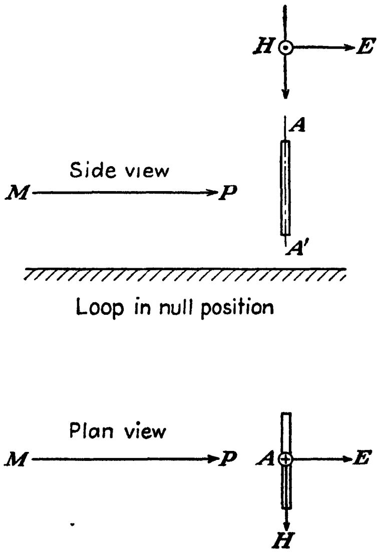


FIG. 3.29.—Loop and field relations—normally polarized component propagated vertically downward.

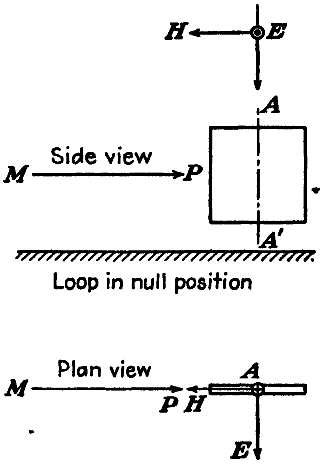


FIG. 3.30.—Loop and field relations—abnormally polarized component propagated vertically downward.

referred to as the "abnormally polarized wave." It is this component which accounts for the errors in medium-wave direction finding at night known as "night effect" and for the major errors at all times on short-wave direction finders.

The horizontally propagated component, whether vertically or horizontally polarized, cannot give rise to night effect or short-wave polarization errors under any conditions. Only the downwardly directed radiation from the ionosphere, or in certain cases from aircraft transmitters, will produce this effect. The whole class of direction finder deviations of this type, with loops

or other types of antenna arrays, may be called "polarization errors."

Night effect may change very greatly in magnitude over a short time of observation because of the rapidity of changes in ionosphere conditions. Experimentally, the phenomenon may be identified in a number of different ways. Several of them may occur at the same time, but the presence of any one is sufficient evidence of the probable existence of night effect. Under such circumstances reliance should not be placed on the accuracy of bearing. The characteristics of night effect with an aural-null direction finder are

1. Displaced minima, which may include indefiniteness of the minimum or a well-defined null point displaced from the proper bearing. In severe cases of night effect this displacement or deviation may be 90°.

2. Broad minima, poorly defined but not displaced.

3. Shifting of the null or minimum point during the time of observation or over a few minutes.

4. Abnormal balancer setting in an aural-null direction finder as described in Chap. IV, indicating the presence of a large amount of the abnormally polarized component. It is this latter which may give rise to a greater or lesser amount of quadrature reradiated component.

5. Fading. As was discussed in the section on Sky Waves, this is due to the interference between the latter and the ground wave,[1] and therefore indicates that the downward coming component is of very appreciable magnitude.

3.14. Loop Polarization Error.—From the foregoing it is evident that, when a wave is traveling diagonally downward toward a vertical loop, an error in bearing will result if the plane of polarization does not coincide with the vertical plane of incidence. The magnitude of the bearing error for any combination of angles of incidence and polarization may be calculated. It will be assumed that the loop is remote from the surface of the earth. The effect of the presence of the earth's surface is usually small enough so that this assumption is justified.

If the xz plane is taken horizontal in Fig. 3.31, with the loop at the origin, the incident wave is propagated along PO, with an

[1] Fading may also occur owing to the interference among sky-wave components that have followed different paths.

angle of incidence β. The plane of polarization (*i.e.*, that containing the electric field vector E) is assumed to make an angle α with the xy plane. For convenience the analysis will be made

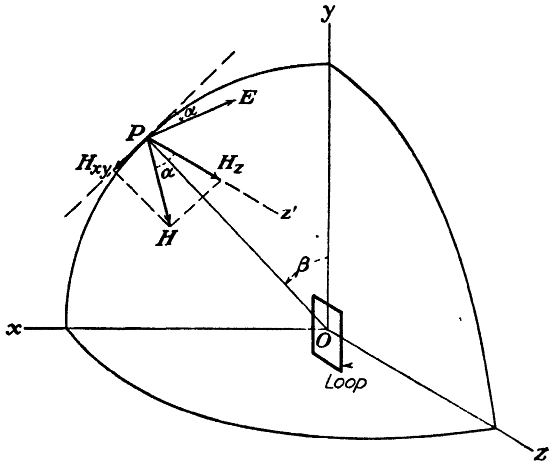


FIG. 3.31.—Vector relations for wave propagated obliquely downward on loop antenna.

in terms of the components of the magnetic field H, which also makes an angle α with Pz' drawn parallel to Oz. The z component of H is

$$H_z = H \cos \alpha \tag{3.67}$$

while the component normal to H_z, lying in the xy plane and tangent to the circle at P, is

$$H_{xy} = H \sin \alpha \tag{3.68}$$

This quantity may be resolved into x and y components:

$$H_x = H_{xy} \cos \beta$$
$$= H \sin \alpha \cos \beta \tag{3.69}$$
$$H_y = H_{xy} \sin \beta$$
$$= H \sin \alpha \sin \beta \tag{3.70}$$

The component H_y contributes no voltage to the loop whose axis lies along Oy, since no flux due to this passes through the loop in any position. Hence only H_x and H_z need be considered.

If the wave is propagated horizontally along Ox, $\beta = \pi/2$ and $H_x = 0$, leaving H_z the only component acting on the loop. The

plan view of Fig. 3.32 shows the loop in the null position, for which there is no pickup due to H_z. But when $\beta \neq \pi/2$, H_x and H_z give a resultant H_{xz}. Thus the loop must be rotated through the angle δ to the position where its plane is parallel to H_{xz}.

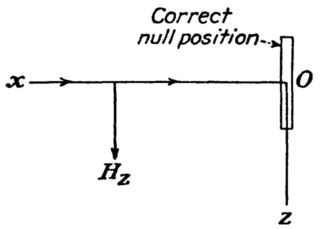


FIG. 3.32.—Plan view of loop in correct null position for horizontal propagation.

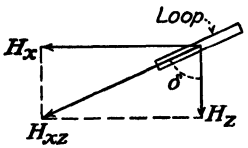


FIG. 3.33.—Deviation error of loop due to abnormally polarized downward component.

The angle δ shown in Fig. 3.33 is the *deviation error* due to polarization effect.

$$\tan \delta = \frac{H_x}{H_z} \tag{3.71}$$

$$= \frac{H \sin \alpha \cos \beta}{H \cos \alpha} \tag{3.72}$$

$$= \tan \alpha \cos \beta \tag{3.73}$$

From Eq. (3.73) it is evident that waves propagated horizontally will not contribute polarization error for any α, since $\cos \beta = 0$.

Just as is the case in radio receiver measurements, where a "standard signal" is defined in order to give typical measurements, so also may one define a "standard wave" in direction finder discussions. It is a wave downwardly directed at an angle of 45° ($\beta = \pi/4$) with plane of polarization at an angle of 45° to the plane of incidence ($\alpha = \pi/4$). The components identified above as H_x and H_z are assumed to be in such time phase as to make δ a maximum.[1] The *standard wave error* is defined as the value of δ for such a standard wave. From Eq. (3.73) for a loop antenna,

[1] A clear understanding that this phase relationship between H_x and H_z may produce greater errors than when the two vectors are in time phase was not fully realized by many workers in the field until about 1941. For this reason, many papers on the subject obtain values of standard wave errors that are entirely too optimistic.

$$\begin{aligned}\tan \delta &= \tan \frac{\pi}{4} \cos \frac{\pi}{4} \\ &= 0.707 \\ \delta &= 35.2° \end{aligned} \tag{3.74}$$

This value of standard wave error is almost independent of the presence of the earth of finite σ.

The parallel loop direction finder has very small standard wave error. This is true along the line of the principal nulls. Under such conditions the loops are *parallel* to H_x, so that this latter gives no pickup. Thus the abnormally polarized component does not cause an error. Proper balancing of the loop circuits is required to make the induced voltage due to H_z be zero in the direction given.

3.15. Adcock Polarization Errors.—The considerable number of types of Adcock direction finders that have been investigated have all been designed with one main objective, that of reduction of polarization errors for all conditions of reception and site. The calculation of standard wave error for Adcock arrays is much more complicated than the foregoing analysis of the simple loop. It requires consideration of the finite ground conductivity, the accuracy of balance of antennas and coupling means, the vertical pickup pattern, and other factors. When the *standard* wave error is known, the wave error for other angles of incidence and states of polarization is still an involved function to calculate.

Accordingly there have been several approaches to the problem of evaluating the relative merit of different direction finder systems:

1. The direct measurement of polarization error as a function of angle of incidence for one or more states of polarization may be carried out. This is accomplished by means of an elevated transmitter. Often a plane polarized wave with equal vertical and horizontal components is used. Experimental difficulties are especially severe at the lower frequencies and for large angles of elevation. Towers, aircraft, and captive balloons have been employed to support the transmitter. Such proximity effects as parallax introduce questions as to the reliability of the resulting data.

2. Measurement may be made as in the previous method but only at 45° incidence. Then from the theoretical variation of

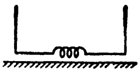
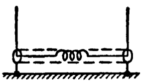
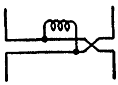
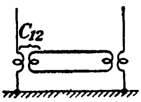
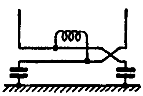
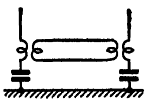
Type	Diagram	Dimensions, meters		Standard wave error, degrees (at 1000 kc, $\sigma = 1.7 \times 10^{-13}$ emu)	Pickup factor, meters
		a = height of system	h' = height above ground of horizontal members		
Loop		$\ll \lambda$	$\ll \lambda$	35 (not affected by σ)	10–20 (1 m sq.) proper number of turns to fit λ used, typical Q, varies as f
U		24	0.5	12	100–200, varies as f^3
Shielded U		24	0.5	6 (most favorable)	
Elevated or H		24	15.0	2 (not greatly affected by σ)	100–200, varies as f^3
Coupled		24	0.5	1 (untuned antenna system C_{12} = 10 $\mu\mu$f)	50–100, varies as f^4
Balanced		24	2.0	6 (untuned antenna system)	100–200, varies as f^3
Balanced coupled		24	2.0	< 1 (untuned antenna system)	50–100

Fig. 3.34.—Relative pickup factors and standard wave errors for loops and Adcock antennas, based on experimental measurements. (*Barfield, J. Inst. Elec. Engrs.* (*London*), **76**, 423, *April*, 1935.)

error at other elevations, the whole characteristic may be determined. This semiempirical method is much more rapid than the first, but it is subject to the same difficulties of technique.

3. Measurements may be made in the horizontal plane of the relative pickup factors $h_{e(V)}$ and $h_{e(H)}$ for pure vertical and horizontal polarization. The experimental method is very much simpler since the test transmitter may be located near the earth's surface. The interpretation of results in terms of the polarization error characteristic and the standard wave error is open to some question in this method.

An analysis of several practical Adcock systems was carried out by Barfield.[1] The calculated results were checked experimentally over a wide frequency range. Only the simple case of plane polarization was actually used in defining the standard wave error and consequently the errors are somewhat low for the reason noted above.[2] The comparison of the various types is still reasonably accurate. This is given in Fig. 3.34 with the case of a single loop included.

Improvements in design and changes in measuring methods since the time of the Barfield paper cited have provided practical Adcock systems having standard wave errors of the order of 5°. With careful choice of site and installation and with skilled operators, this has probably been improved by a factor of two in certain cases; but other limits in over-all accuracy, notably lateral deviation, then act to prevent both greater accuracy of measurement of wave error and practical utilization of this greater accuracy.

An experimental comparison of the observed bearings taken with a loop and with the shielded-U Adcock and with the balanced-coupled Adcock systems was reported by Watson-Watt.[3] The results represented several thousand observations on each type, the loop and the Adcock readings being taken simultaneously. Figure 3.35 shows the comparison at two locations, the percentage of observations having a certain deviation from the true bearing of the station being indicated. The superiority

[1] R. H. BARFIELD, Some Principles Underlying the Design of Spaced-aerial Direction Finders, *J. Inst. Elec. Engrs. (London)*, **76**, 423 (April, 1935).

[2] See footnote, p. 106.

[3] R. A. WATSON-WATT, Polarization Errors in Direction Finders, *Wireless Engineer*, **13**, 3 (January, 1936).

of the Adcocks under conditions of night effect is strikingly illustrated.

3.16. Comparison of Accuracy of Loop, Adcock, and Spaced-loop Systems.—In any practical case of reception from a distant station, the prediction of the actual bearing error becomes difficult or completely impossible because of the complexities of the propagation phenomena. At most, one can merely set down

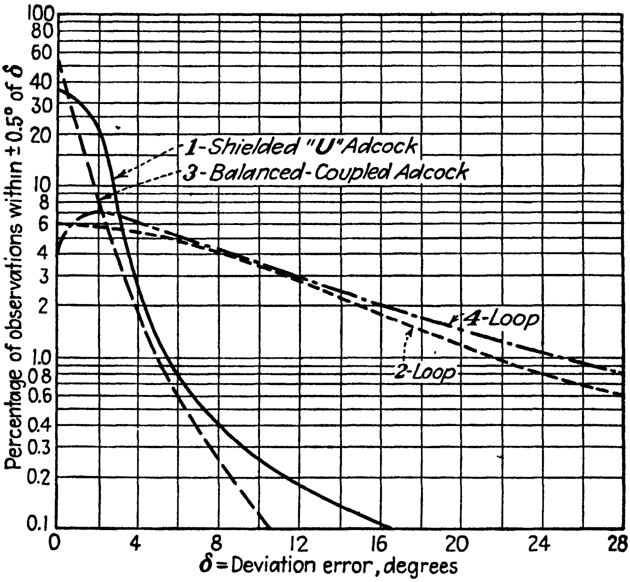


FIG. 3.35.—Experimental comparison of deviation errors of loops and Adcock direction finders. Curves 1 and 2: Shielded-U Adcock system and loop at Chelmsford. Transmitter at Kalundborg, 820 km distant. Operating frequency 238 kc. Results of 3500 simultaneous pairs of observations. Curves 3 and 4: Balanced-coupled Adcock system and similar loop at Slough. Same transmitter and distance. Results of 3500 simultaneous pairs of observations. (*Watson-Watt, Wireless Engineer*, **13**, 3, *January*, 1936.)

certain general rules for determining the relative merits of various types of direction finders. The principal types to be compared are (1) simple loop, (2) Adcock, and (3) spaced-loop systems. Both the ground wave and the ionosphere wave should be included in the analysis. When only a horizontally propagated component is received at the direction finder location, it is almost completely vertically polarized if the ray has traveled near the earth's surface for a reasonable distance. Under such conditions all three

types of direction finders are about equally accurate when polarization error is considered. This is the condition for which the ground wave is predominant, and there is a negligible amount of ionosphere wave.

The study of sky-wave propagation in Chap. II showed that the arriving wave after one or more ionosphere reflections was incident at a very appreciable downward angle. At 200 miles from transmitter to direction finder, for example, it might be 60°. Thus polarization error may become very great beyond the range in which the ground wave is predominant. In fact it may be

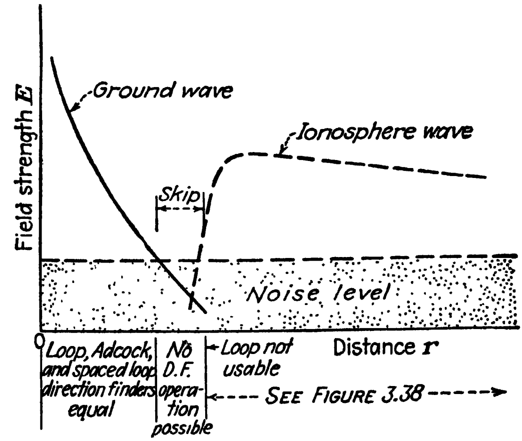


FIG. 3.36.—Comparison of accuracy of loop, Adcock, and spaced-loop direction finders on ground or ionosphere waves. Skip effect present. Noise level due either to internal receiver noise or to static.

stated broadly that a simple loop is useless on sky-wave reception, since the errors become excessive if the ionosphere component is more than 1 per cent of the direct ray.

3.17. Direction Finding with Ground and Ionosphere Waves.— A diagrammatic representation of the comparison out to the zone of pure ionosphere waves is given in Fig. 3.36 for the case of the existence of a skip zone and in Fig. 3.37 for the case in which the ground and sky waves may overlap. The former, of course, is for the higher frequencies in the range 3 to 30 mc and the latter for the lower end of this range and extending below 1 mc. The scales of field strengths and distances are arbitrary. The limit imposed by receiver noise or static level is shown. Actual cases of the relative amplitudes of ground and sky waves from

0.3 to 6 mc have been given by Ross.[1] For the frequencies in the standard broadcast band and lower, reference may be made to an earlier paper.[2]

The ground-wave curve may also be calculated as in Chap. II to give the approximate inner boundary of the skip zone, while the outer limit may be estimated from Sec. 2.11. It is evident that the skip zone is narrower for greater transmitter power and greater height of either transmitter or direction finder.

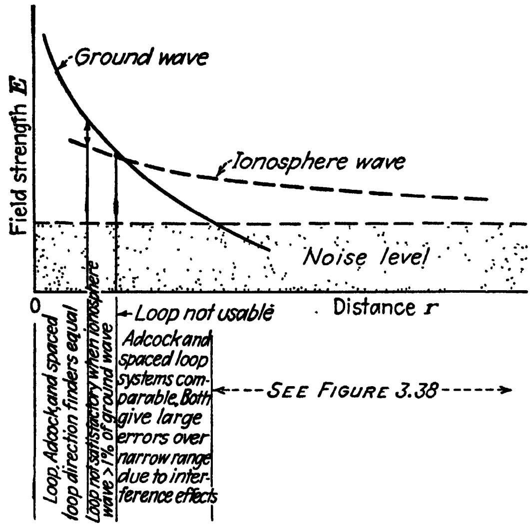


FIG. 3.37.—Comparison of accuracy of loop, Adcock, and spaced-loop direction finders on ground or ionosphere waves. No skip effect. Noise level due either to internal receiver noise or to static.

In the skip zone of Fig. 3.36 no direction finder operation is possible. It may be possible to obtain a bearing due to scattered signals in this zone, but such a virtual source may be in nearly any direction and bears no relation to the true source. In the case of highly directive beam transmission, the scattering source may be some point along the beam and may give a bearing more than 90° in error.

[1] W. Ross, Ground and Ionospheric Rays, *Wireless Engineer*, **14**, 306 (June, 1937).

[2] Report of Committee on Radio Propagation Data, *Proc. I.R.E.*, **21**, 1419 (October, 1933).

On the other hand there may be a considerable zone of overlap as shown in Fig. 3.37. The region where accuracy begins to be affected by the downcoming sky wave depends upon the pickup factor for nearly vertical incidence and upon the polarization error of the direction finder. The simple loop is much worse in both these respects than the Adcock or the spaced loops. This accounts for its much worse night effect. This latter is usually understood to mean the bearing errors at the lower frequencies when the direction finder receives only ground wave by day but an appreciable amount of sky wave by night.

There is a small region in the zone of comparable magnitudes of ground and sky waves for which either an Adcock or a spaced-loop system gives poor results owing to interference between the two wave components. In general, though, they are both fairly satisfactory in the zone shown in Fig. 3.37.

3.18. Direction Finding with Ionosphere Waves Only.—The large downward angle of the ionosphere rays may be seen from Fig. 3.38 for propagation over a plane earth. The approximate boundaries of the various. ionosphere layers are shown. For example, for F_2 reflection at 4 mc with the transmitter 200 miles distant, the ray may be incident on the antenna at a downward angle of 65°. With certain states of polarization the bearing errors may thus be quite large. Figure 3.38 shows that the spaced-loop system is decidedly superior to the Adcock for the steeper angles of arrival. At the greater distances this difference in performance diminishes, until for angles of less than 45° the Adcock is substantially as good as the spaced-loop equipment. It may thus be concluded that through this region direction finder errors due to polarization effect diminish with increasing distance.. The simple loop cannot be used in this region.

Both the Adcock and the spaced loops show errors that are not due to the cause just studied, but rather due to actual *lateral deviation* of the wave in its propagation path.[1] The magnitude of this effect is greatest for small distances when only the ionosphere wave is received. For example, at 50 miles it may give bearing errors up to 30° with a probable value of 7°. For generality, the reflecting point in the ionosphere may be considered to be dis-

[1] R. H. BARFIELD and W. ROSS, The Measurement of the Lateral Deviation of Radio Waves by Means of a Spaced-loop Direction Finder, *J. Inst. Elec. Engrs. (London)*, **83**, 98 (July, 1938).

placed laterally from the symmetrical point between the direction finder and the transmitter by a probable value of 3 miles, with a maximum of about 12 miles. If this apparent lateral displace-

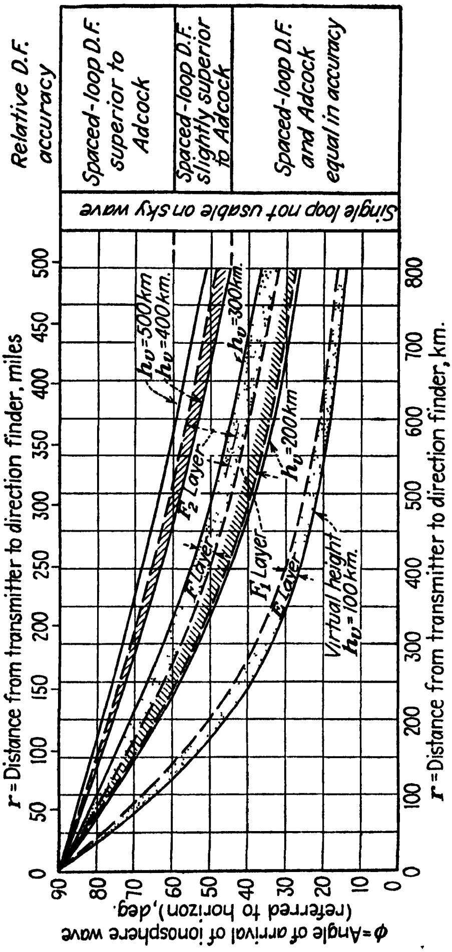


FIG. 3.38.—Comparison of direction-finder accuracy with ionosphere waves, showing downward angle of arrival as a function of distance of transmitter (plane earth). Operation beyond the skip distance is assumed; *i.e.*, the frequency is less than the maximum usable frequency. The Adcock system considered has a standard wave error of 5°. Lateral deviation and site errors are ignored.

ment is denoted by y and the separation of sending and receiving points by r, it is easily seen that the bearing error δ is given by

$$\tan \delta = \frac{2y}{r} \tag{3.75}$$

At 500 miles this gives a probable value of δ of 0.7° and a maximum of 2.5°.

3.19. Observed Adcock Accuracy.—Results that illustrate the foregoing principles when applied to a ground station Adcock system have been obtained as a function of distance of the transmitter.[1] A 50-watt aircraft transmitter was used in the 4- to 6-mc band. Flights were made from each of three direction finder stations to a distance of greater than 600 miles. Each direction finder was located at a carefully chosen site and employed the equipment developed by the Western Electric Company. A cathode-ray tube forming a part of the Western

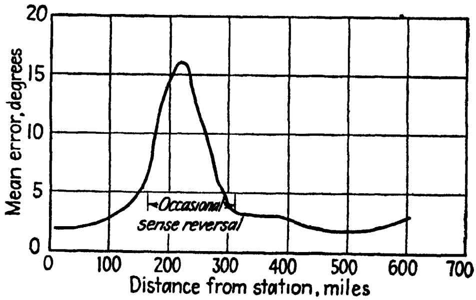


FIG. 3.39.—Typical experimental values of Adcock direction finder errors. Transmitter located in airplane. The zone of large errors where ground and ionosphere waves are both present (and the latter are downwardly incident at large angles) is shown. Compare Fig. 3.37. (*Adapted from C.A.A.*)

Electric azimuth indicating radio receiver served to give instantaneous bearing indications. Such a device gives at the same time a measure of the reliability of the bearing, because varying azimuth readings with fading present show that a bearing should be discarded.

The results for a large number of readings taken in December, 1942, during the day showed average errors as a function of distance as follows:

Distance, Miles	Average Error, Deg.
0–75	±5
75–300	±15
300–600	±3

[1] RADIO DEVELOPMENT SECTION, CIVIL AERONAUTICS ADMINISTRATION, *Report on Triangulation Tests Conducted with the New York, Pittsburgh, and Washington Direction Finder Stations*, publication of U.S. Department of Commerce, January, 1943.

The average of all bearings taken by one direction finder (New York) in daytime when there is no skip effect is shown in Fig. 3.39. The first portion of the curve represents a predominant ground wave. Between 100 and 300 miles the ionosphere component becomes of great importance, and it is downwardly incident at a high angle. Lateral deviation may also contribute in this region of bad errors. Beyond 300 miles the errors diminish very greatly. It was found that many readings in the 100- to 300-mile range showed about the same errors but with the *sense reversed.*

Bibliography

BALLANTINE, S.: On the Optimum Transmitting Wave-length for a Vertical Antenna over Perfect Earth, *Proc. I.R.E.*, **12**, 823 (December, 1924).

BARFIELD, R. H.: Recent Developments in Direction Finding Apparatus, *Exp. Wireless and Wireless Eng.*, **7**, 262 (May, 1930).

BARFIELD, R. H., and R. A. FEREDAY: An Improved Medium-wave Adcock Direction Finder, *J. Inst. Elec. Engrs. (London)*, **81**, 676 (November, 1937).

BARFIELD, R. H., and W. ROSS: A Short-wave Adcock Direction Finder, *J. Inst. Elec. Engrs. (London)*, **81**, 682 (November, 1937).

COLEBROOK, F. M.: The Application of Transmission-line Theory to Closed Aerials, *J. Inst. Elec. Engrs. (London)*, **83**, 403 (September, 1938).

ECKERSLEY, T. L.: Scattering, Polarization Errors, and the Accuracy of Short-wave Direction Finding, *Marconi Rev.*, **53**, 1 (March-April, 1935).

NAMBA, S., E. ISO, and S. UENO: Polarization of High-frequency Waves and Their Direction Finding, *Proc. I.R.E.*, **19**, 2000 (November, 1931).

ROSS, W.: The Calibration of Four-aerial Adcock Direction Finders, *J. Inst. Elec. Engrs. (London)*, **85**, 192 (August, 1939).

SANDRETTO, P. C.: *Principles of Aeronautical Radio Engineering*, 1st ed., Chaps. IV, VIII, McGraw-Hill Book Company, Inc., New York, 1942.

SMITH-ROSE, R. L.: Radio Direction Finding by Transmission and Reception, *Proc. I.R.E.*, **17**, 425 (March, 1929). (Extensive bibliography of earlier work.)

SMITH-ROSE, R. L., and R. H. BARFIELD: The Cause and Elimination of Night Errors in Radio Direction Finding, *J. Inst. Elec. Engrs. (London)*, **64**, 831 (August, 1926).

SMITH-ROSE, R. L., and H. G. HOPKINS: Radio Direction Finding on Wavelengths between 6 and 10 Meters, *J. Inst. Elec. Engrs. (London)*, **83**, 87 (July, 1938).

Symposium on Radio Direction Finding, *J. Inst. Elec. Engrs. (London)*, **85**, 203 (August, 1939).

CHAPTER IV

AURAL-NULL DIRECTION FINDERS

4.01. Components and Types of Operation.—An aural-null direction finder comprises essentially a directive array combined with a sensitive and highly stable receiver. For mobile installations, as on shipboard or aircraft, a loop antenna is almost invariably used. Then the elements consist of

1. The loop antenna.
2. A nondirectional, vertical, or "sense" antenna.
3. A loop tuning and coupling circuit.
4. A sense coupling circuit.
5. A balancer circuit (usually used on shipboard only).
6. A receiver.

Most direction finders of this type are arranged for three types of operation:

1. *Communication Reception of Modulated Continuous Wave or Continuous Wave Signals.*—This is often carried out by means of the nondirectional vertical antenna alone, or the loop may be used at or near its maximum.

//2. *Bilateral Operation.*—Here the signal is picked up on the loop, which has of course two directions of null pickup. The result is an accurate bearing but with 180° ambiguity. If a balancer circuit is used, the signal is also coupled into the loop input circuit in phase quadrature from the nondirectional antenna and is adjusted in amplitude to give the sharpest loop minima. Either modulated continuous wave or continuous wave reception is possible.

3. *Unilateral Reception.*—This is also referred to as *sense determination* or operation with a *cardioid pattern.* Signals from the loop and the vertical antennas are combined in proper phase relationship to give a single null pattern. This mode of operation permits identification of the appropriate null as determined in *bilateral* operation, but the accuracy of the unilateral null is insufficient to allow precise bearing determinations by this means alone.

Loop circuits are almost invariably tuned either directly by means of a capacitor or through one or more coupling transformers. Satisfactory operation is easily obtained at distances up to 35 ft separation between the loop and the receiver proper. In modern direction finders the loop antenna is always shielded and is usually balanced to ground. These precautions serve to minimize antenna effect and in the case of aircraft direction finders to reduce precipitation static to a minimum (see Sec. 6.08). When the vertical antenna is coupled into the receiver at the same time as the loop feeds in, it is important to establish the correct phase relationship between the signals for use either in balancing or sense determination. In the former the purpose of the antenna signal is to balance out voltage picked up by the loop or circuits and in time quadrature to the desired signal. In the case of the sense circuit the antenna should feed a voltage to the receiver in time phase with that of the loop circuit in order to produce a cardioid pattern.

4.02. Phase Relations in Series Resonant Circuits.—The loop antenna of a directly tuned input circuit may be coupled to the

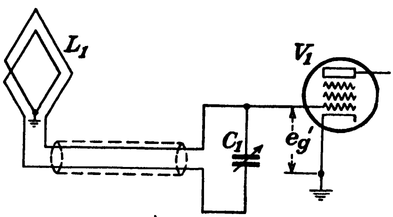


FIG. 4.01.—Balanced loop directly coupled to receiver input.

first r-f amplifier by several means, one of the most common circuits being that of Fig. 4.01. Here the loop has the mid-point grounded. A shielded transmission line couples the balanced loop output to tuning capacitor C_1, which itself is symmetrical with respect to ground. The r-f amplifier is "single-sided," *i.e.*, not push-pull, and is arranged to utilize one-half the voltage appearing across C_1. It will be seen later that this failure to apply the full voltage to V_1 is not ordinarily a disadvantage when signal-noise ratio instead of gain is of prime importance.

Regardless of the precise means of coupling to V_1, the circuit may be replaced by the equivalent series arrangement of Fig. 4.02. The generator e_1 represents the open-circuit voltage of the

loop as given in Eq. (3.29). This voltage differs in time phase from the radiation electric field E by 90°, as was discussed in Sec. 3.05.

It is of importance to trace the further phase shift that occurs between e_1 and the output terminals across C, both at resonance and when the circuit is detuned.

The ratio $\omega L/r$ will be defined as the Q, or figure of merit, of the circuit at the frequency $f = \omega/2\pi$. Here r is the resistance at that frequency. Then for any other frequency $\omega_0/2\pi$ the corresponding Q will be called Q_0. Since Q is found to be nearly constant over a considerable frequency range, it follows that

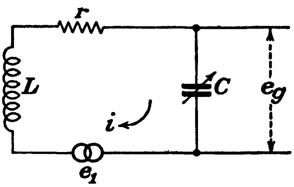


FIG. 4.02.—Series resonant circuit.

$$\frac{r}{r_0} = \frac{\omega}{\omega_0} \tag{4.01}$$

i.e., the r-f resistance is proportional to frequency.

The loop is the equivalent of an inductance L in series with which is the resistance r. Distributed capacity of the loop and the capacity of the transmission line are assumed to be included in C. Then it is evident that

$$i\left(r + j\omega L - \frac{j}{\omega C}\right) = e_1 \tag{4.02}$$

and the voltage across C is

$$e_g = i\left(-\frac{j}{\omega C}\right) \tag{4.03}$$

If the value of Q as defined above is inserted

$$\frac{e_1}{e_g} = \frac{\dfrac{\omega L}{Q} + j\omega L - \dfrac{j}{\omega C}}{-\dfrac{j}{\omega C}} \tag{4.04}$$

$$= 1 - \omega^2 LC\left(1 - \frac{j}{Q}\right) \tag{4.05}$$

It will be noted that advantage results from the use of Q because this is nearly independent of frequency.

Equation (4.05) is of the form

$$z = a + jb$$

whose phase angle ϕ is given by

$$\tan \phi = \frac{b}{a}$$

Consequently,

$$\tan \phi = \frac{\omega^2 LC}{Q(1 - \omega^2 LC)} \tag{4.06}$$

The resonant frequency of the circuit $f_0 = \omega_0/2\pi$ is such that

$$\left.\begin{aligned} \omega_0 L - \frac{1}{\omega_0 C} &= 0 \\ \text{or} \qquad LC &= \frac{1}{\omega_0^2} \end{aligned}\right\} \tag{4.07}$$

Hence

$$\tan \phi = \frac{\left(\frac{\omega}{\omega_0}\right)^2}{Q\left[1 - \left(\frac{\omega}{\omega_0}\right)^2\right]} \tag{4.08}$$

$$= \frac{1}{Q\left(\frac{\omega_0^2 - \omega^2}{\omega^2}\right)} \tag{4.09}$$

If the function β is defined as

$$\beta = \frac{\omega_0^2 - \omega^2}{\omega^2} \tag{4.10}$$

then

$$\tan \phi = \frac{1}{Q\beta} \tag{4.11}$$

The significance of β may be seen by writing

$$\beta = \frac{(\omega_0 - \omega)(\omega_0 + \omega)}{\omega^2}$$

$$\doteq \frac{2(\omega_0 - \omega)}{\omega_0} = \frac{2\,\Delta f}{f_0} \tag{4.12}$$

for frequencies near resonance since the factor

$$\frac{\omega_0 + \omega}{\omega^2} \doteq \frac{2}{\omega} \doteq \frac{2}{\omega_0} \tag{4.13}$$

Thus the fractional deviation *from resonance*

$$\frac{\Delta f}{f_0} = \frac{\beta}{2} \tag{4.14}$$

The phase shift is illustrated in Fig. 4.03.

The selectivity characteristic of this same circuit will be determined so that the phase shift may be interpreted in terms of attenuation from the resonant gain as well as in terms of the detuning function β. At resonance Eq. (4.05) becomes

$$\frac{e_1}{e_{g(r)}} = 1 - \omega_0^2 LC\left(1 - \frac{j}{Q}\right)$$

$$= \frac{j}{Q} \tag{4.15}$$

when the value of LC from Eq. (4.07) is inserted. This result gives the well-known result that the voltage across either C or L in a series resonant circuit is Q times the input voltage. The selectivity function U may be defined as

$$U = \frac{e_{g(r)}}{e_g} \tag{4.16}$$

$$= \frac{Q}{j}\left[1 - \frac{\omega^2}{\omega_0^2}\left(1 - \frac{j}{Q}\right)\right] \tag{4.17}$$

$$= \frac{\omega^2}{\omega_0^2}\left[1 + jQ\left(1 - \frac{\omega_0^2}{\omega^2}\right)\right] \tag{4.18}$$

U has a magnitude u of

$$u = \frac{\omega^2}{\omega_0^2}\sqrt{1 + Q^2\beta^2} \tag{4.19}$$

since $1 - \frac{\omega_0^2}{\omega^2} = -\beta.$

For Q reasonably high and $Q\beta$ small (for instance, $Q > 20$ and $Q\beta \lesseqgtr 5$), the error will not be great if the factor ω^2/ω_0^2 is set equal to unity in Eq. (4.19). The approximate result

$$u = \sqrt{1 + Q^2\beta^2} \tag{4.20}$$

is also shown in Fig. 4.03.

For example, when the response is -3 db or 70.7 per cent of the resonant amplitude, $Q\beta = \pm 1$, and $\phi = 90° \pm 45°$. This illus-

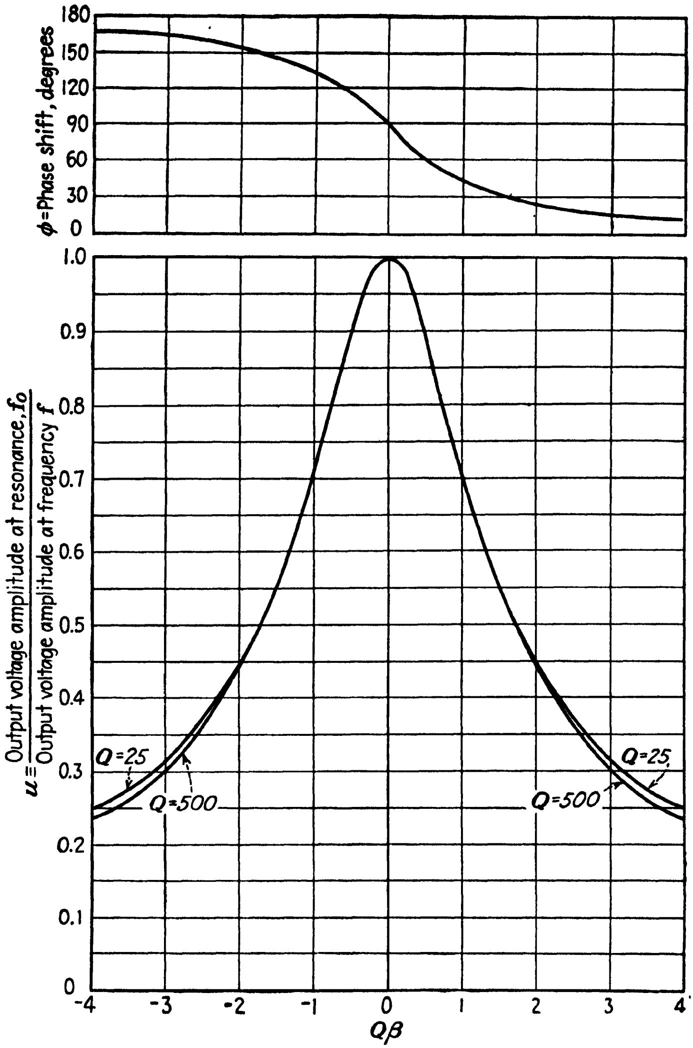


FIG. 4.03.—Phase-shift and selectivity characteristics of series resonant circuit. $Q = \omega L/r$ and $\beta = 2\Delta f/f_0$. (*Adapted from Terman, Radio Engineering.*)

trates that, if a resonant circuit is sensitive to small amounts of phase shift, care must be exercised to prevent detuning due to such causes as poor tracking.

4.03. Two Coupled Resonant Circuits.—A double-tuned circuit fed from a high-impedance source is shown in Fig. 4.04. Coupling is by means of the mutual inductance M. The two circuits are resonant at the same frequency. The phase shift between output voltage e_2 and input current i_p may be found by the method of Appendix D. The result may be expressed in terms of

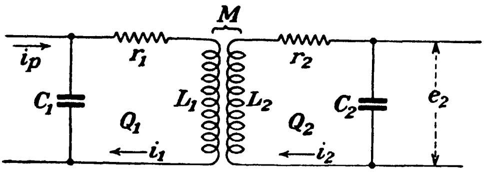


FIG. 4.04.—Two circuits resonant at the same frequency with mutual inductance coupling.

the Q factors of the circuits, the coefficient of coupling k, and the detuning factor β of Eq. (4.10) or (4.14).

The geometric mean Q is defined as

$$\bar{Q} = \sqrt{Q_1 Q_2} \tag{4.21}$$

and the arithmetic mean

$$Q_m = \tfrac{1}{2}(Q_1 + Q_2) \tag{4.22}$$

The coefficient of coupling

$$k = \frac{M}{\sqrt{L_1 L_2}} \tag{4.23}$$

The result for the phase shift is

$$\tan \phi = \frac{1 + Q^2(k^2 - \beta^2)}{2Q_m \beta} \tag{4.24}$$

For any value of k and for resonance, $\beta = 0$ and $\phi = 90°$. The condition of *critical coupling* is that for which the gain at resonance is a maximum, as will be seen from the consideration of the selectivity curve. For this case

$$\bar{Q}k = 1 \tag{4.25}$$

Then in Eq. (4.24)

$$\tan \phi = \frac{2 - \bar{Q}^2\beta^2}{2Q_m\beta} \tag{4.26}$$

For the limiting case of very loose coupling, k approaches zero, and

$$\tan \phi = \frac{1 - \bar{Q}^2\beta^2}{2Q_m\beta} \tag{4.27}$$

For 100 per cent coupling, $k = 1$ and

$$\tan \phi = \frac{1 + \bar{Q}^2(1 - \beta^2)}{2Q_m\beta} \tag{4.28}$$

These cases are illustrated in Fig. 4.05 for $Q_1 = Q_2$ with the values of ϕ measured on scale A.

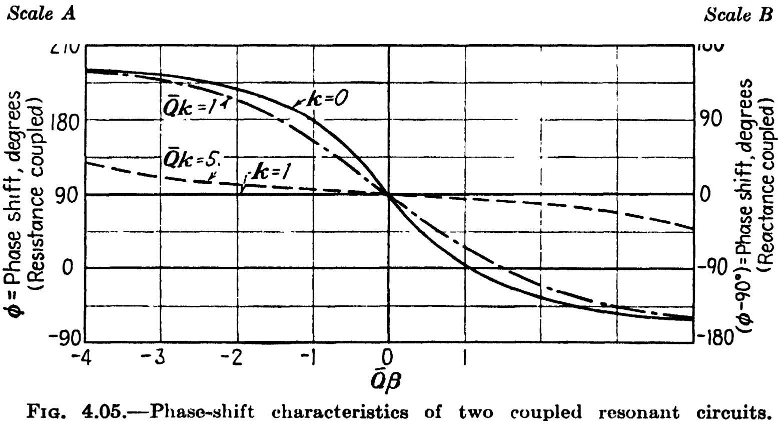


FIG. 4.05.—Phase-shift characteristics of two coupled resonant circuits. Scale A: resistance coupling as in Fig. 4.07, scale B: reactance coupling as in Fig. 4.08.

On this same scale of $\bar{Q}\beta$ the selectivity function u for various values of coupling $\bar{Q}k$ is given in Fig. 4.06. Only one-half the curve is shown, as it is symmetrical with respect to the u axis. For comparison, u for a single resonant circuit is repeated.

The result for the value of the phase shift in a pair of coupled resonant circuits applies for the comparison of input current i_p to output voltage e_2. This may be extended immediately to the case for the phase shift through an amplifier stage with a high plate impedance tube as in Fig. 4.07. Then the phase shift between grid and plate circuits is 180°, so that Eq. (4.24) applies also to this case.

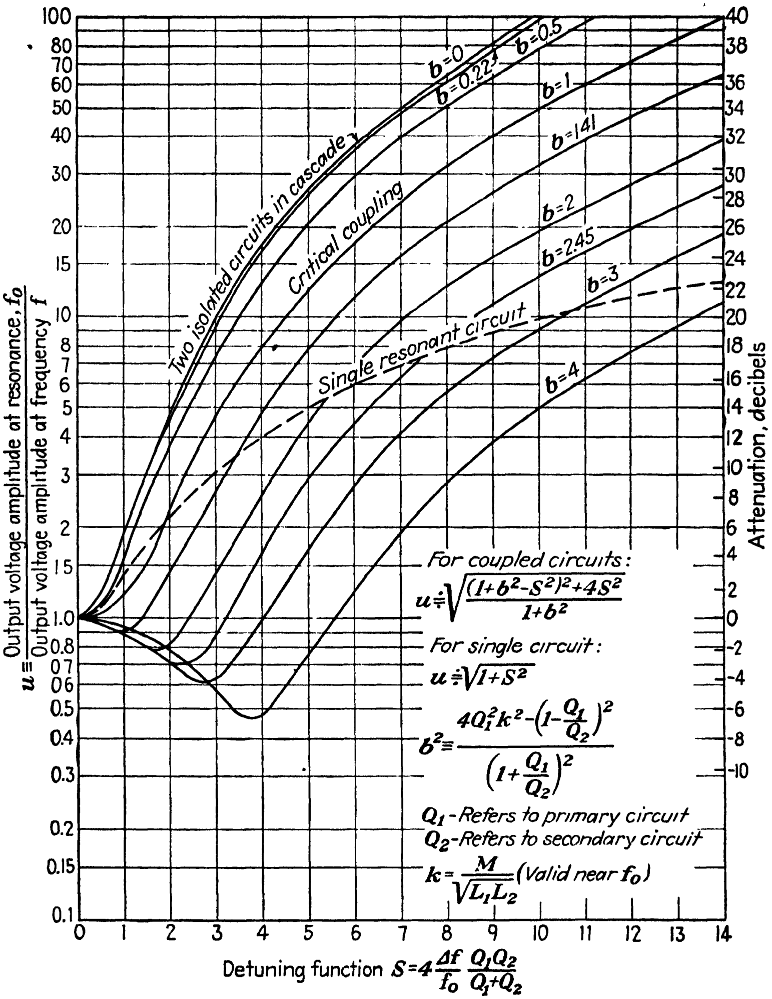


FIG. 4.06.—Selectivity characteristics of two coupled resonant circuits. Single resonant circuit shown for comparison. If $Q_1 = Q_2$ then $S = Q\beta$ and $b = Qk$. (*Maynard, Electronics*, **10**, 15, *February*, 1937.)

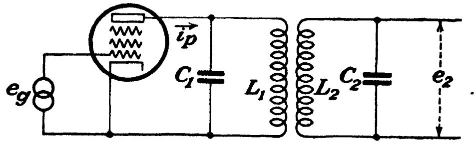


FIG. 4.07.—High plate impedance amplifier feeding two coupled resonant circuits.

For a circuit in which a low-impedance generator is coupled to the input of the double-tuned transformer by means of a pure

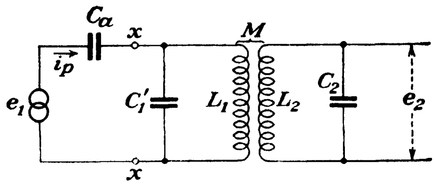


FIG. 4.08.—Low-impedance generator with series reactance feeding two coupled resonant circuits.

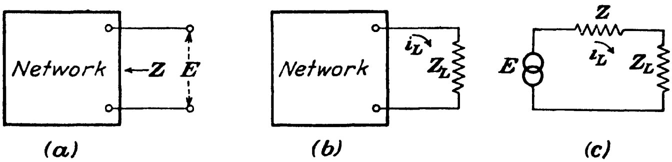


FIG. 4.09.—Equivalent networks of Thévenin's theorem.

reactance, the results are modified considerably. In Fig. 4.08 if the coupling capacitor is C_a, i_p may be found by applying Thévenin's theorem.[1]

In Fig. 4.10 the open-circuit voltage at xx due to e_1 is simply e_1, and the impedance across these terminals is $1/j\omega C_a$. Consequently if i_p flows from an infinite impedance generator

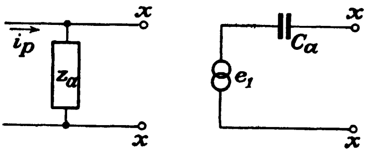


FIG. 4.10.—Equivalent input circuit of generator with series capacity.

$$\left.\begin{aligned} Z_a &= \frac{1}{j\omega C_a} \\ \text{and} \qquad e_1 &= i_p \frac{1}{j\omega C_a} \end{aligned}\right\} \qquad (4.29)$$

Now if C_1' and C_a together tune the primary to resonance, then in the previous notation

$$C_1 = C_1' + C_a \qquad (4.30)$$

[1] In Thévenin's theorem, one considers a network containing linear elements and one or more sources of e.m.f. and having one pair of accessible terminals. The voltage across these terminals with no external load is E, and the impedance measured at this same point is Z when all the internal sources of e.m.f. are short-circuited. Then the current that flows through an external load impedance Z_L connected across the terminals of the network is the same as if Z_L were connected in series with Z to a generator of voltage E. This equivalence is illustrated in Fig. 4.09.

and the circuit of Fig. 4.08 is the equivalent of 4.04, provided a phase shift of 90° between e_1 and i_p is considered. The over-all phase shift between e_1 and e_2 is 90° or $\pi/2$ more than given by Eq. (4.24) or

$$\tan\left(\phi - \frac{\pi}{2}\right) = \frac{1 + \bar{Q}^2(k^2 - \beta^2)}{2Q_m\beta} \tag{4.31}$$

Hence at resonance the phase shift is 180° (or 0° depending on the assumed sign of e_2). With a suitable scale displacement Fig. 4.05 still applies (scale B).

4.04. Capacity-coupled Single Resonant Circuit.—In certain direction finder circuits, a single tuned circuit is fed through a small capacitor from a low-impedance generator. This is typical of a high-impedance, or "top-coupled," antenna circuit and is illustrated in Fig. 4.11.

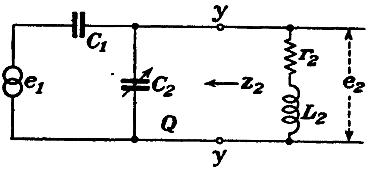


FIG. 4.11.—Capacity-coupled single resonant circuit.

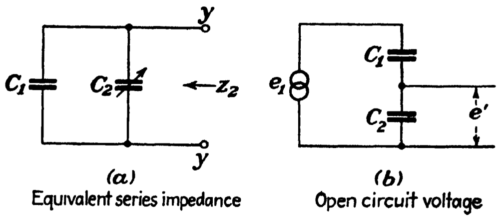


FIG. 4.12.—Circuits equivalent to input of Fig. 4.11.

The phase shift may be computed by determining the vector value of e_2/e_1 by an application of Thévenin's theorem. Figure 4.12 gives the open-circuit impedance Z_2 and voltage e' across the terminals yy of Fig. 4.11.

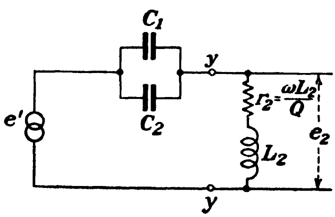


FIG. 4.13.—Series circuit replacing two-mesh capacity-coupled circuit.

$$\left.\begin{aligned} Z_2 &= \frac{1}{j\omega(C_1 + C_2)} \\ e' &= e_1 \frac{C_1}{C_1 + C_2} \end{aligned}\right\} \tag{4.32}$$

Then the equivalent series circuit is that of Fig. 4.13, for which

$$\frac{e_2}{e'} = \frac{j\omega L_2\left(1 - \frac{j}{Q}\right)}{j\omega L_2\left[1 - \frac{j}{Q} - \frac{1}{\omega^2 L_2(C_1 + C_2)}\right]} \tag{4.33}$$

If the resonant angular velocity is ω_0, then

$$\omega_0^2 = \frac{1}{L_2(C_1 + C_2)} \tag{4.34}$$

This gives

$$\frac{e_2}{e_1} = \frac{C_1}{C_1 + C_2}\left(\frac{1 - \frac{j}{Q}}{1 - \frac{j}{Q} - \frac{\omega_0^2}{\omega^2}}\right) \tag{4.35}$$

By simplification, if the approximation is made that $Q^2 >> 1$, Eq. (4.35) becomes

$$\frac{e_1}{e_2} = \frac{C_1 + C_2}{C_1}\left[1 - \frac{\omega_0^2}{\omega^2}\left(1 + \frac{j}{Q}\right)\right] \tag{4.36}$$

The phase shift ϕ is then given by

$$\tan\phi = \frac{\omega_0^2/\omega^2}{Q\left(\frac{\omega_0^2}{\omega^2} - 1\right)} \tag{4.37}$$

From Eq. (4.10) this is

$$\tan\phi = \frac{\beta + 1}{Q\beta} \tag{4.38}$$

For the usual case for which $\beta << 1$, this result becomes identical with that of Sec. 4.02, and Fig. 4.03 applies.

4.05. Coupled Resonant Circuit with Low- or High-frequency Primary.—An input circuit that simulates the behavior of any

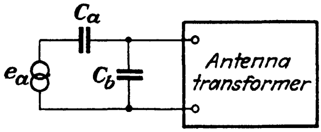


FIG. 4.14.—Capacity-coupled antenna input circuit.

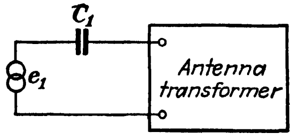


FIG. 4.15.—Equivalent series dummy antenna.

capacity antenna coupled to a receiver input is shown in Fig. 4.14. This in turn can be replaced by a network in which all the capacity is in series, as in Fig. 4.15, and an appropriate value of input

voltage is used. C_1 and e_1 represent such values, where

$$\left.\begin{aligned} C_1 &= C_a + C_b \\ \text{and by Thévenin's theorem,} \quad e_1 &= e_a \frac{C_a}{C_a + C_b} \end{aligned}\right\} \quad (4.39)$$

When the antenna transformer consists of a secondary coil tunable over the r-f range coupled to a primary tuned approximately to a fixed frequency outside the r-f band, the circuit is that of Fig. 4.16.

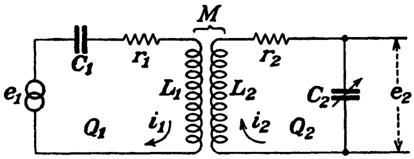


FIG. 4.16.—Coupled circuit with tunable resonant secondary and primary tuned to a frequency outside secondary tuning range.

The computation of phase shift at any frequency is rather complex and will not be carried through. The value of ϕ at resonance (denoted by ϕ_r), as computed for Fig. 4.16, is found to be given by

$$\tan \phi_r = \frac{Q_2 k^2}{1 - \theta_1} + Q_1(1 - \theta_1) \quad (4.40)$$

where

$$\theta_1 = \frac{f_p^2}{f_0^2} \quad (4.41)$$

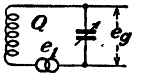
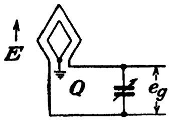
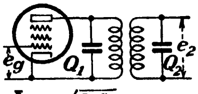
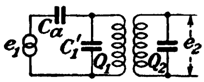
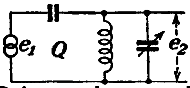
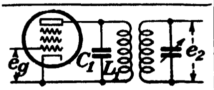
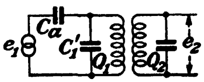
f_p being the resonant frequency of the primary with the secondary of the transformer open-circuited.

Example.—As an application of this result, one may compute the phase shift at resonance in an antenna transformer for which $Q_1 = 50$, $Q_2 = 100$, $k = 30$ per cent, $f = 1000$ kc, and $f_p = 400$ kc. Then

$$\begin{aligned} \theta_1 &= (400/1000)^2 = 0.16. \\ \tan \phi_r &= \frac{100 \times 0.09}{0.84} + 50 \times 0.84 \\ &= 10.72 + 42 \\ &= 52.7 \\ \phi_r &= 88.9^\circ \end{aligned}$$

It will be readily seen from Eq. (4.40) that the phase shift at resonance is normally very close to 90° for the circuit in which the

TABLE V.—PHASE-SHIFT CHARACTERISTICS OF R-F CIRCUITS

Type	Configuration	Phase shift at resonance ϕ_r	Phase shift ϕ
1. Series resonant circuit (Sec. 4.02)	 Reference phase: e_1	90°	$\tan\phi = \frac{1}{Q\beta}$
2. Directly tuned loop (Sec. 4.02)	 Reference phase: E	0°	$\tan\left(\phi - \frac{\pi}{2}\right) = \frac{1}{Q\beta}$
3. Two coupled resonant circuits from high plate resistance amplifier (primary and secondary resonant at same frequency) (Sec. 4.03)	 $\bar{Q} = \sqrt{Q_1Q_2}$ $Q_m = \frac{1}{2}(Q_1 + Q_2)$ Reference phase: e_g	90°	$\tan\phi = \frac{1 + \bar{Q}^2(k^2 - \beta^2)}{2Q_m\beta}$
4. Two coupled resonant circuits (primary and secondary resonant at same frequency) with reactive input coupling (Sec. 4.03)	 $\bar{Q} = \sqrt{Q_1Q_2}$ $Q_m = \frac{1}{2}(Q_1 + Q_2)$ Reference phase: e_1 or E	0°	$\tan\left(\phi - \frac{\pi}{2}\right) = \frac{1 + \bar{Q}^2(k^2 - \beta^2)}{2Q_m\beta}$
5 Capacity-coupled single resonant circuit (Sec. 4.04)	 Reference phase: e_1 or E	90°	$\tan\phi = \frac{\beta + 1}{Q\beta}$
6. Coupled resonant circuit having l-f or h-f primary from high plate resistance amplifier (Sec. 4.05)	 $f_p = \frac{1}{2\pi\sqrt{L_1C_1}} >> f_0$ or $<< f_0$ Reference phase: e_g	0°	
7. Coupled resonant circuit having l-f or h-f primary with reactive input coupling (Sec. 4.05)	 $f_p = \frac{1}{2\pi\sqrt{L_1(C_a + C_1')}}$ $>> f_0$ or $<< f_0$ Reference phase: e_1 or E	90°	

primary incorporates a series reactance C_1. This phase shift is of positive or negative sign according as $f_p < f_0$ or $f_p > f_0$. On the other hand, the situation is altered radically if a high plate resistance tube be considered. This is actually illustrated by Fig. 4.07 if the primary is resonant at a high or a low frequency. The analysis for such a case may be carried out by analogy with that of Sec. 4.03, giving the conclusion that at resonance the phase shift through such an r-f interstage circuit is approximately zero.

4.06. Summary of Phase-shift Characteristics.—The cases considered in the previous sections include many of the commonly used loop and nondirectional antenna input circuit and r-f interstage coupling means. In the case of antenna circuits the reference phase is naturally the electric field E. This is the same in phase as input e_1 of Type 1, 4, 5, or 7 of Table V. Consequently, the results are the same whether an antenna is used or a low-impedance generator is the input source. Type 2 compares the output phase to the field E explicitly.

In the summary of Table V the algebraic sign of ϕ_r is not considered. The Q factors are assumed not to be too low (perhaps greater than 20). The phase shift ϕ is between input and output voltages or between the r-f field and the output voltage as noted. The detuning factor

$$\beta = \frac{2\,\Delta f}{f_0} = \frac{f_0^2 - f^2}{f^2} \tag{4.42}$$

where f_0 is the resonant frequency.

4.07. Example of Shipboard Direction Finder Circuits.—The foregoing principles are illustrated by the circuits of several direction finders in current use. The first of these is an aural-null system for marine service. It incorporates means for obtaining bilateral bearings including a balancer circuit, and means for obtaining "sense." The basic circuit for one band is shown in Fig. 4.17.

Bilateral Operation.—Under these conditions this circuit contains the loop inductance L_1 together with two auxiliary coils L_3 and L_4. All these are resonated by means of capacitor C_1, which is balanced with respect to ground. As was seen in Sec. 3.05, the phase of the loop terminal voltage e is 90° with respect to the incident radiation field. Then the circuit $L_1L_3L_4C_1$,

resonant at signal frequency, is the equivalent of Fig. 4.02, and a phase shift between input and output of 90° will exist at resonance. The total phase shift due to both these causes is thus 0° or 180°, dependent upon the orientation of the loop. The output of the loop circuit is balanced to ground but is fed to the single-sided amplifier V_1 in such a fashion that only half of the voltage developed across C_1 is utilized. This diminishes the gain of the system by 6 db but has practically no effect upon signal-noise ratio when the gain of V_1 is sufficient, as will be seen in Sec. 5.03.

The balancer system consists of a nondirectional vertical antenna coupled through a series capacitor C_3 to the circuit

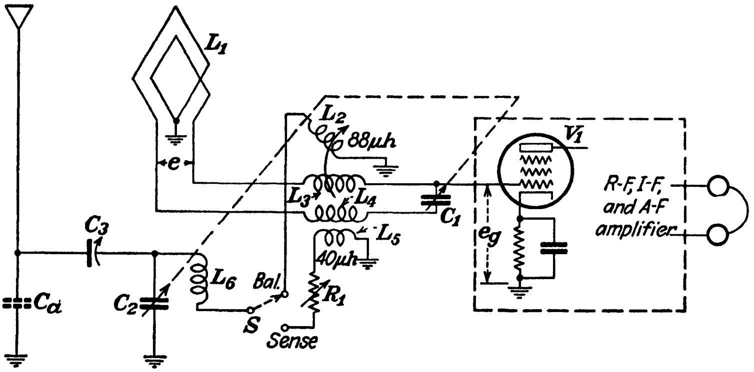


FIG. 4.17.—Circuit of shipboard direction finder showing balancer and sense connections.

$L_2L_6C_2$. This circuit in turn is coupled by a variable mutual inductance to L_3 in the loop circuit. Capacitor C_2, together with the parallel combination of C_3 and C_a, resonates this circuit at a frequency 15 to 20 per cent below signal frequency. Switch S is on position *Bal* for balancing operation. The coupling between L_2 and L_3 may be adjusted from 0 to a rather large value, and its polarity may be reversed. The balancer and the loop circuits together constitute two coupled resonant circuits, one resonating at signal frequency and the other tuned somewhat below. A rigorous analysis similar to that of Appendix D applies to the phase shift in this circuit, but because of the small frequency difference between primary and secondary, one may consider it to be equivalent to the case of Sec. 4.03 in which the two are both resonated to a frequency below that of the signal. It

will be noted in Sec. 4.03 that at resonance the phase shift is 0° between two resonant circuits, the primary of which is coupled through a reactance from a low-impedance generator. At a lower frequency this phase difference approaches 90°. This means that there will be approximately a 90° shift between the antenna and the point at which e_g is measured. The loop and antenna voltages at e_g are 90° apart in phase. As a consequence, the balancer may be used to neutralize any pickup in the loop when this pickup voltage is in 90° time phase with respect to the desired signal. This may be due to antenna effect or to a quadrature reradiated field.

The effect of quadrature (90° time phase) voltage in diminishing the sharpness of the minima of the loop pickup pattern was noted in Sec. 3.10. The proper magnitude and polarity of the introduced balancer voltage together serve to make these broad minima become sharp, well-defined nulls.

Sense Operation.—For eliminating the 180° ambiguity that occurs in bilateral operation as described above, the direction finder may be used to give "sense." This is done by means of the same antenna circuit as was described for the balancer, except that switch S is set appropriately to connect L_5 and R_1 into the antenna resonant circuit. L_5 is smaller in inductance than L_2 by such an amount that circuit $L_5L_6C_2$ resonates at signal frequency. Here the phase conditions are those of Sec. 4.03 where both circuits are resonant at signal frequency. There is, therefore, a 0° phase shift between radiation field and the grid of tube V_1. The sense antenna voltage thus mixes with loop signal at this grid with either a 0 or 180° phase relationship. These are the conditions under which a cardioid may be obtained, for the reasons analyzed in Sec. 3.08. The resistor R_1 performs two functions. In the first place, it broadens out the response curve of the antenna circuit by lowering the Q so that the phase shifts relatively slowly on either side of the resonance frequency. In the second place, R_1 serves to adjust the relative magnitudes of the antenna and loop voltages. This allows choice of any of the pickup patterns shown in Fig. 3.20. If R_1 is made an operating adjustment, it may be set to give approximately a cardioid. However, in many direction finders it is set at one frequency only on each band. Then at other frequencies the cardioid is not perfect, but there is an easily distinguishable difference

between amplitudes at 90 and 270° azimuth positions. This difference is sufficient to establish sense uniquely.

4.08. Example of Aircraft Direction Finder.—A second example of aural-null direction finder is illustrated in Figs. 4.18 to 4.20 for equipment for aircraft use. These three illustrations represent the manner in which the individual circuits are switched as one chooses nondirectional, bilateral, and sense operation, respectively. This latter is frequently referred to as "unilateral" operation. Because aircraft installations are much less likely to have much quadrature field radiation present and since precision of obtaining bearings is somewhat less than for shipboard use, no balancer is provided in this equipment.

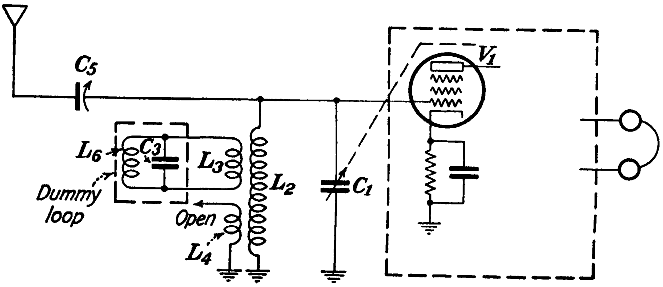


FIG. 4.18.—Circuit of aircraft direction finder—nondirectional operation.

In Fig. 4.18 nondirectional operation is obtained. The equipment serves as a straight receiver fed from the antenna. This latter is capacity coupled through C_5 to the resonant circuit L_2C_1. The loop antenna is shorted, and a dummy loop L_6C_3 is connected in its place. C_1 is a section of the gang capacitor. Tube V_1 is the first r-f amplifier and feeds through conventional r-f, i-f, and audio stages to the headphones.

In Fig. 4.19 the circuit is set up for bilateral operation. Loop L_1 couples through primary L_3 to the tuned circuit L_2C_1. The antenna is short-circuited, and in its place is substituted a capacitor C_4 to maintain the circuit at resonance. L_1 and L_3 resonate with C_0, the capacity of the transmission line, at a frequency above the highest in the tuning range. This loop circuit is thus in the category of Sec. 4.05. The phase shift is the same as for Fig. 4.16 since the algebraic sign of the series reactance is not important. This means that the phase shift

between e, the loop terminal voltage, and e_g is 90°. When the additional shift between radiation field and the loop is considered, the total phase shift will be 0° (or 180°).

The phase shift through the loop circuit becomes of importance when unilateral operation shown in Fig. 4.20 is analyzed. The

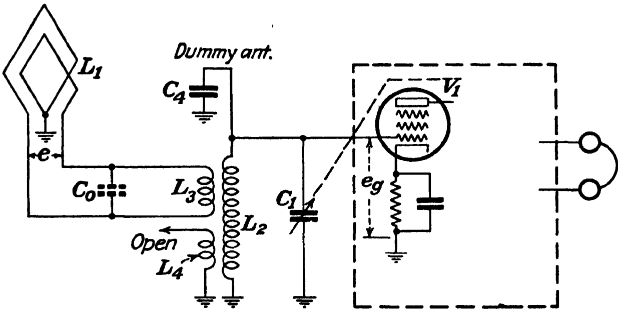


FIG. 4.19.—Circuit of aircraft direction finder—bilateral operation.

antenna circuit is resonated by means of gang capacitor section C_2, not used in previous types of operation. This sense circuit is thus the equivalent of that of Fig. 4.17, with 0° phase shift between antenna and the grid of V_1. Resistor R_1 is an operating control to secure a proper cardioid pattern. It will be evident

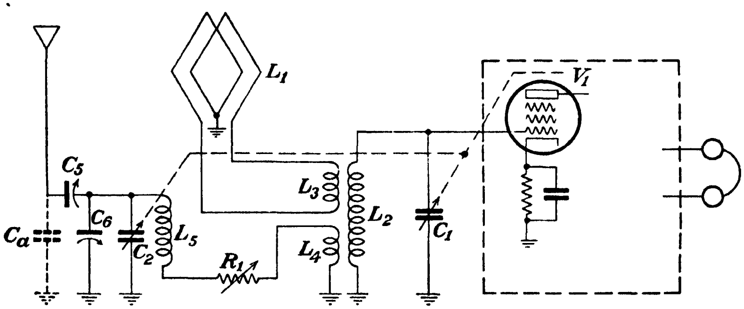


FIG. 4.20.—Circuit of aircraft direction finder—sense or unilateral operation.

from a comparison of phase shifts that loop and antenna signals combine at the grid of V_1 in phase.

4.09. Example of Direction Finder with Loop Amplifier.—The third typical example of a direction finder circuit is that of Fig. 4.21. Although this is not ordinarily used as an aural-null type of direction finder, it has application in such a use, and the phase

relations must be considered for other and more elaborate operations as described in Chap. VI. The loop channel involves two amplifier tubes V_2 and V_3. Loop L_1 couples to primary L_3 of a transformer having high coefficient of coupling and high secondary Q. The voltage at the grid of V_2 is in phase with the radiation field. In the plate circuit of V_2 is a parallel resonant network L_4C_5 tuned to a frequency far outside the receiver band. Its tuning is fixed. If it resonates below signal frequency, it appears as a capacitor with a 90° phase change of output voltage with respect to grid voltage. The total phase shift between radiation field and the grid of V_3 is thus 90°. This latter tube in

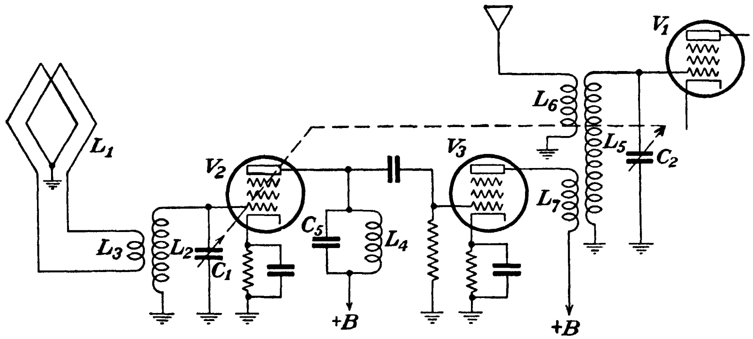


FIG. 4.21.—Circuit of direction finder with loop amplifier.

turn couples through transformer L_7L_5, where the primary circuit resonates above the tuning range. The fact that the phase shift through such a stage with a high plate resistance tube is 0° is shown in Sec. 4.05. This means that the over-all phase shift between the radiation field and the grid of V_1 is 90° (or 270°). The antenna is coupled to the circuit L_5C_2 by means of the l-f or h-f primary L_6. This voltage therefore undergoes a 90° phase shift through the transformer. Consequently, loop and antenna are in phase, and the circuit may be used for obtaining unilateral or sense indication.

4.10. Adjustment of Shipboard Direction Finders.—A loop-type direction finder for marine use generally requires considerable care in installation, in adjustment, and in calibration in order to give satisfactory operation. Installation includes the choice of loop location with respect to fixed structures and rigging on the ship, and also the addition of compensators to

reduce residual bearing errors to a minimum. The procedure may well be illustrated by a consideration of one specific type of direction finder as illustrated in Fig. 4.17 and described in Sec. 4.07. This is used at frequencies of 1500 kc and below. One may assume that the loop location has been chosen.

Adjustment of Nondirectional Antenna.—With the ship in the clear and all rigging secured and grounded suitably for sea duty, the nondirectional antenna is adjusted to give the proper pickup. This is done by checking balancer operation through the complete equipment. Sufficient nondirectional antenna pickup is required to give adequate balancer voltage at the h-f end of the highest tuning band. This maximum amount of balancer is required in taking bearings on stations off the beam of the ship, and such a station (1400 to 1500 kc) should be chosen for this adjustment.

It is conventional to calibrate the balancer coupling adjustment (between L_2 and L_3 of Fig. 4.17) on an arbitrary scale of -50 to 0 to $+50$. Then the proper balancer setting should be between 30 and 50 on this scale, with either algebraic sign. The only objectionable effect of too much nondirectional antenna pickup is that the balancer adjustment becomes quite critical when there is only a small amount of quadrature voltage to be balanced out. This occurs at low frequencies and for stations off the bow or stern.

It is desirable to have a symmetrical antenna for this purpose to secure a nondirectional pattern. For this reason, the antenna should be a vertical wire or a flat-top *T* antenna.

Throughout all these operations the tuning of the balancer circuit $L_2L_6C_2C_3C_a$ should be 15 to 20 per cent below signal frequency, but this adjustment is not critical. This may be rechecked subsequent to the sense circuit alignment described later.

Sense Adjustment.—The sense circuit is adjusted with the antenna chosen for proper balancer operation as described above. Over a large frequency range no attempt is usually made to secure a perfect cardioid. Rather, any of the patterns of Fig. 3.20 may be used provided it gives unmistakable difference in "front-to-back ratio," *i.e.*, shows considerable difference between the response along *ON* and *ON'*. The relative magnitudes of loop and sense voltages are determined by the original circuit

design, the accuracy of tracking of the L_5L_6 circuit with the loop, and the setting of R_1. This latter of course varies the antenna stage gain by changing the Q of the resonant circuit. In the particular equipment described, there is a variable resistor R_1 for each tuning band, and each adjustment is an alignment control. It is not adjusted in actual operation.

Alignment.—The steps in r-f alignment for each band may be outlined as follows:

1. The receiver is connected to the loop and sense antennas that are part of the shipboard installation.

2. The sense control R_1 is set at the position of minimum resistance.

3. A suitable standard signal generator is coupled very loosely to the sense antenna post of the direction finder, with the antenna connected.

4. The balancer coupling adjustment is set at maximum (± 50 divisions), as this has a small effect on circuit tuning. Switch S of Fig. 4.17 is then thrown to *sense* by pressing the push button. The r-f circuits, including the loop, may then be aligned at the h-f and l-f tracking points by the conventional method for superheterodyne receivers.

5. The signal generator is disconnected, and an actual station of known bearing approximately in the middle of the band is then tuned in. Then with switch S set for bilateral operation and with balancer connected, the loop is rotated until a null bearing is observed. Since the bearing of the station is known, the correct null may be chosen.

6. The convention as to polarity of "sense" voltage is that the minimum or null of the *cardioid* pattern should occur when the scale reading in step 5 is *decreased* by 90°. The loop is set to this azimuth and R_1 adjusted for minimum output. The proper cardioid pattern is thus chosen at this one frequency.

7. A recheck is made with stations at other frequencies in the band to determine that the setting of R_1 of step 6 gives adequate front-to-back ratio at these frequencies.

4.11. Loop Site Errors.—In Sec. 3.13 one source of error of direction finder bearings was considered, namely polarization errors. There are other external sources of erroneous bearings due to the presence of large absorbing masses, due to coast-line refraction, etc. Generally these are not within the control of

the user, although he may estimate the magnitude of the resulting error.

On the other hand, certain local effects produce deviation of direction finders. Here special reference will be made to loop-type installations aboard ship. There are two principal sources of local errors. The first of these results in *nonopposite minima*, as discussed in Sec. 3.10. The displaced minima result from pickup of signal which combines in phase with the loop output but which is nondirectional in character. This is referred to as *antenna effect*. Design faults of the receiver, or inadequate shielding and grounding of the loop and transmission line may contribute to this effect. The main part of the antenna effect voltage consists of a component in quadrature with the loop signal, but such causes as improper loop alignment will result in a zero phase component. In a direction finder properly installed and aligned for shipboard or aircraft use, the antenna effect should produce no more of a deviation than 0.5° from exact opposition of the minima.

A far more important source of error, and the principal one causing shipboard direction finder deviation, is *reradiation*. This also has two components: an in-phase one, producing deviation; and a quadrature signal, requiring balancer displacement. In the case of the first component, one must rotate the loop through a certain angle, the deviation angle, in order to secure a minimum or a null. In the case of the quadrature component, the balancer circuit of Sec. 4.07 allows the operator to introduce a second voltage exactly out of phase with the undesired pickup, so that the latter may be balanced out. This is a necessity for sharp, clean aural-null bearings.

Reradiation results from the currents induced in vertical elements or loop structures aboard the ship. The currents are induced by the signal from the distant station, and set up local "induction" fields, which in turn react upon the direction finder loop. As has been seen in Chap. II, the induction fields predominate over the radiation field since the direction finder loop is near by; but for convenience, the resulting fields at the direction finder will be classed as radiation fields. This gives rise to the term *reradiation*.

Analysis will show that the effects of reradiation depend upon

1. *Electrical Conductivity.*—If the closed loop of rigging or of structure of the ship has low resistance, the resulting deviation is apt to be considerable. The magnetic properties of the structure are not of importance. If deviation is present, it is essential that it remain constant. This in turn means that connections in rigging, contacts between metal structures, etc., should be properly treated so that the electrical properties are not affected by corrosion or vibration.

2. *Location.*—The size of the reradiating structure and its proximity to the direction finder loop are of great moment in determining the magnitude of deviation and balancer displacement. At the time of calibration and operation of a loop direction finder, it is desirable to have rigging, railings, cranes, and other metallic structures made ready for sea duty. Other adjacent antennas should be open-circuited, unless tests during calibration have shown that their resonant frequencies are far enough removed from direction finder operating frequencies as to cause no trouble. In the case of closed loop structures formed by rigging, it is a good empirical rule to space each from the direction finder by a distance greater than twice the largest dimension of the rigging structure. Although much of the following analysis assumes reradiated components to be exactly in quadrature or in phase, it must be remembered that, when the offending part of the structure of the vessel is spaced by an appreciable fraction of a wave length, there will be an additional change in phase due to the time of propagation over this path.

3. *Natural Frequency.*—The vertical elements and loop structures present reactive impedance under most conditions, because the natural frequency of each does not coincide with the operating frequency. The phase and magnitude of the reradiated field are dependent upon this natural frequency in a manner that will be discussed presently.

Deviation errors may be reduced and the variation of the residual deviations maintained small by several means: (1) proper location of the loop, *i.e.*, in the clear of other structures, and symmetrically located; (2) treatment of rigging by breaking up with insulators and by solid bonding; (3) use of electrical compensators consisting of closed loops to introduce a deviation equal and opposite to an initial deviation; (4) use of mechanical compensators, rather infrequent on shipboard; and (5) employ-

ment of calibration curves for the residual deviations as a function of frequency.

4.12. Effects of the Ship Structure.—If a signal from a distant station is being received on a shipboard direction finder, one may estimate the changes in magnitude and direction of arrival of the fields at the loop as the ship is turned. As is shown in Table VI, the direct signal is unaffected in magnitude and arrives from the true direction. As a result, the deviation is zero. On the other

TABLE VI.—SIGNAL COMPONENTS AT DIRECTION FINDER FOR DIFFERENT AZIMUTHS

Signal field	Magnitude	Direction	Deviation
Direct	Constant	Varying	None
Reradiated,			
From vertical elements.......	Constant	Constant	Semicircular
From loops (closed or open)..	Varying	Constant	Quadrantal

hand, reradiated fields from vertical elements or local loop structures arrive from a constant direction referred to the bow of the ship because these structures serve as virtual sources. In the case of vertical elements, the magnitude also is approximately constant because it always is in the same field due to the received signal. The pickup by a loop structure varies with azimuth for the same reason as for the loop of the direction finder. The first of these reradiated components results in semicircular deviation; the second, in quadrantal deviation.

As an example, one may consider a loop abaft a mast aboard ship. If the natural frequency of the mast is either much less than or much greater than signal frequency, it appears as a pure reactance, and the current flowing as a result of the impinging field from the distant transmitter is 90° out of phase with respect to the field itself. The reradiated field is in phase with the current, and hence is 90° out of phase with the original direct field.[1] This quadrature field causes balancer displacement. However,

[1] The first of these conclusions, that the current is 90° out of phase with the incident radiation field follows from Eqs. (2.01) and (2.02) by an application of the reciprocity theorem. Since the direction finder loop may be analyzed in terms of its response to the induction magnetic field set up by the current in the mast, Eqs. (A.10) and (A.13) in Appendix A show that this field and the current are in phase.

if the phase is not exactly 90° (and it never is in practical cases, owing to the proximity of signal frequency to natural frequency), then there will be some in-phase component, resulting in deviation. Because the reradiated field is of constant magnitude, a maximum signal will be picked up in the direction finder loop when the plane of the latter is fore and aft. This is the condition for obtaining a bearing on a station off the beam. Hence the deviation error will be greatest off the two beams, and a semicircular deviation curve results.

In contrast, a loop structure, such as a closed loop of rigging surrounding the direction finder loop, will behave in an entirely different fashion. The loop has a reactive impedance except at the natural frequency, and currents flow in the two individual verticals as was the case for the nonresonant vertical mast. The resultant of these currents is 90° out of phase with either, as was seen in Eq. (3.28) for the case of a receiving loop. The reradiation is thus 90° out of phase with either current. As a consequence, the closed loop structure, operating far below or far above its natural resonant frequency, reradiates an in-phase field. The algebraic sign of the resultant deviation is dependent upon the natural frequency compared to signal frequency.

As a specific example, for a fore-and-aft closed loop, pickup from a distant station is maximum when the transmitter lies dead ahead or dead astern. Pickup in the loop structure is zero off the beams. Then for a direction finder loop located with its center in the plane of this closed loop, coupling to this reradiating system is zero when the direction finder is taking a bearing on a station dead ahead. The combination of these two effects results in the fact that the deviation becomes zero at 0, 90, 180, and 270°. It attains a maximum value at some intermediate angle in each of the four quadrants. This is the explanation of quadrantal error.

By far the most important source of quadrantal error on most shipboard installations is the so-called *mast-hull* loop. This consists of the hull or the deck of the vessel with two vertical elements: masts, stacks, funnels, etc. These three sides make up an open loop which is completed by the capacity between the upper ends of the vertical elements. Because of this small capacity, the mast-hull loop has a natural frequency above the highest conventionally used aboard vessels, 1500 kc.

Most of the other loops are closed structures of rigging, railing, etc. Since these then behave as an inductance in series with a low resistance, their natural frequency is below the direction finder band. The algebraic sign of quadrantal error resulting from closed loops then is opposite to that for the mast-hull system. Other open loops, such as rigging broken with insulators, generally form h-f systems like the mast-hull structure.

TABLE VII.—DEVIATION AND BALANCER DISPLACEMENT DUE TO RERADIATING STRUCTURES

Type of conductor	Natural frequency (referred to signal frequency)	Deviation				Balancer displacement
		Quadrant 1	Quadrant 2	Quadrant 3	Quadrant 4	
Vertical element (including other antennas and antenna effect of closed loop and mast-hull loop)	Above *f*	. .	. .	. .	. .	Semicircular
	At *f*	+	+	−	−	
	Below *f*	. .	. .	. .	. .	Semicircular
Loop elements:						
Closed loops* (including hull) . .	Below *f*	−	+	−	+	
Open loops* (mast-hull loop)*	Above *f*	+	−	+	−	
	At *f*	. .	. .	. .	. .	Large
	Below *f*	−	+	−	+	

* Natural frequency assumed to be far removed from signal frequency. Additional phase shift due to propagation time ignored.

Table VII summarizes the conditions of deviation and balancer behavior to be expected from these ideal structures. By this latter is meant that when the natural frequency is assumed above or below the operating frequency, it is far enough removed as to give a pure in-phase or quadrature field as the case may be. In the case of loop elements, the algebraic signs are for the loop structure surrounding the direction finder loop and lying in the fore-and-aft plane. The opposite sign will occur if the direction finder is entirely fore or aft. The algebraic sign is also reversed for a closed loop which is athwartship.

In Table VII balancer displacement is not indicated for nonresonant loop elements. In the case of the mast-hull loop, it

always occurs however, because of the antenna effect of the latter. The two masts included in the mast-hull loop are unequal in pickup, and consequently give a differential reradiated field like that of a single vertical element. Under most circumstances, the mast-hull loop will resonate above the signal frequency, but the other cases are shown for completeness. It should not be believed that, as the resonance of this structure is approached, the quadrantal deviation will diminish. Rather it will be found that the deviation becomes continually worse as resonance is approached, on account of the larger circulating current. Only in the immediate vicinity of the natural resonance will the deviation drop, and at the same time the balancer displacement become very large. In larger vessels with large top-side structures, the resonance point may be near enough to signal frequency so that above 1000 or 1200 kc operation is somewhat unsatisfactory.

The hull itself constitutes a closed vertical loop giving quadrantal deviation of the opposite algebraic sign to the mast-hull structure. It is of lesser importance in most conditions and may be noticed mainly in the way it varies with the draught of the vessel.

4.13. Compensation and Calibration.—It is evident from Table VII how a closed loop can be used to compensate for the

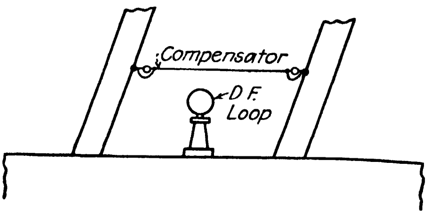


FIG. 4.22.—Location of compensator to reduce deviation of shipboard direction finder. Deviation is assumed to be due to a mast-hull type of loop structure.

open mast-hull structure. Since this latter is the principal source of deviation, compensation for it is usually made, because the usual procedure of relocation of the loop is relatively insignificant in the presence of such a large structure. A compensator may consist of one or more conductors stretched between the two masts that make up the mast-hull loop. A typical situation is shown in Fig. 4.22 where the loop lies within the mast-hull loop, and consequently the compensator is placed directly over the

direction finder itself. The location, the number of parallel conductors, and their electrical resistance determine the magnitude and the shape of the compensation curve. It is usually good practice to check the compensator near the lowest important frequency in the direction finder band, and readjust to secure a relatively small magnitude of quadrantal error at this frequency. If the direction finder loop is placed on the center line of the vessel, but before or abaft the mast-hull loop, the compensator should be left in the same position between the masts as before, in order to secure the proper algebraic sign of compensation. Alternatively, the compensator structure may be constructed athwartship to form a closed loop surrounding the direction finder.

If the quadrantal deviation curve has the usual form of a double sine curve but is not symmetrical with respect to the fore-and-aft line, the compensator loop may be placed parallel to the proper pair of bearings which correspond to zero on the deviation curves.

Two precautions should be observed in the use of compensators. Overcompensation not only results in deviation that may be comparable in magnitude to the original amount, but it also causes loss of signal. The compensators serve only by virtue of the absorption that they produce in certain directions. In the second place, care should be taken to ensure that the electrical conductivity of the compensator loop does not change with time. Corrosion may cause electrical contacts to become poor and the surface conductivity of the conductors to diminish. Proper attention should be paid to welding and brazing of joints and to the use of phosphor-bronze or galvanized-steel conductors for the loops.

After the desired amount of compensation has been made, calibration should be carried out at a number of frequencies distributed through the direction finder band. The rigging of the ship should be properly secured for sea duty. The vessel itself should be in the clear and free from metal structures at a dock. Calibration points should be made at enough bearings so that the points may be checked and found to lie on a smooth deviation curve. Recalibration should be carried out periodically, and after every major change of ship's structure in the vicinity of the direction finder loop.

It is conventional to give the algebraic sign of the deviation so that

$$(\text{Observed bearing}) + (\text{deviation}) = (\text{correct bearing}) \quad (4.43)$$

Aboard ship the reference point (0° bearing) is the bow. Measurements are made in a clockwise direction up to 360°. This same is true aboard aircraft. On shore stations the reference bearing is the North point.

4.14. Calculation of Deviation Error without Balancer.—When a direction finder is set up in the vicinity of conducting objects, errors may result from reradiation fields (or secondary induction

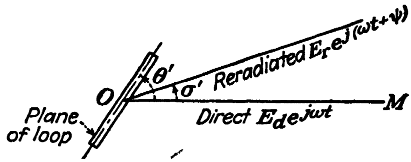


FIG. 4.23.—Directions of arrival of direct and reradiated waves.

fields) from these conductors. This problem becomes of especial importance aboard ship, as was discussed in the previous sections, both because the effects are very marked and because the desired accuracy is high. The apparent direction and time phase of the undesired field are characteristic of the location and nature of the conductor and the frequency.

The nomenclature to describe the situation is as follows:

The direct signal may be represented by

$$e_d = E_d e^{j\omega t} \quad (4.44)$$

and the undesired signal, which will be referred to as "reradiated signal," is

$$e_r = E_r e^{j(\omega t+\psi)} \quad (4.45)$$

where ψ is the time phase difference. e_r will be assumed to be arriving at an angle σ' with respect to the direct signal e_d. The angle between e_d and the plane of the loop is θ', as shown in Fig. 4.23. The reradiated component may be resolved into two components: one in time phase with the direct signal, and the other differing in phase by a time angle of 90°. The first of these will always give rise to bearing error, and the second is the quadrature component to be neutralized by an appropriate

balancer circuit. The effectiveness of the latter will be considered below.

The components of e_r may be derived from Eq. (4.45) since

$$e_r = E_r e^{j\omega t}(\cos \psi + j \sin \psi) \tag{4.46}$$

The in-phase component is thus

$$e_{r0} = E_r \cos \psi \, e^{j\omega t} \tag{4.47}$$

and the quadrature component

$$e_{rq} = jE_r \sin \psi \, e^{j\omega t} \tag{4.48}$$

Here the operator j is associated with the time function and as usual denotes a 90° phase shift. It should be remembered that e_{r0} and e_{rq} both arrive from the direction of e_r, making a space angle σ' with e_d.

The components of the same phase as the direct signal are e_d and e_{r0}. If the maximum value of this vector sum be denoted by e_0

$$e_0 e^{j\omega t} = e_d + e_{r0} \tag{4.49}$$
$$= (E_d + E_r \cos \psi)e^{j\omega t} \tag{4.50}$$
$$e_0 = E_d + E_r \cos \psi \tag{4.51}$$

The corresponding quadrature component is e_q where

$$e_q j e^{j\omega t} = e_{rq} \tag{4.52}$$
$$e_q = E_r \sin \psi \tag{4.53}$$

The *space vector diagrams* are given in Fig. 4.24. The apparent direction of arrival of the wave represented by e_0 makes an angle

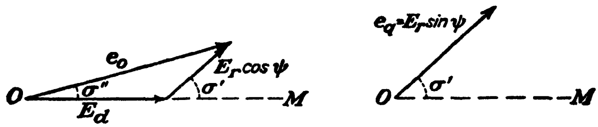


FIG. 4.24.—Apparent direction of arrival of in-phase and quadrature wave components. The angle σ'' represents deviation error.

σ'' with the actual direction of the station. It is evident that

$$\tan \sigma'' = \frac{E_r \cos \psi \sin \sigma'}{E_d + E_r \cos \psi \cos \sigma'} \tag{4.54}$$

$$= \frac{\sin \sigma'}{\dfrac{E_d}{E_r \cos \psi} + \cos \sigma'} \tag{4.55}$$

If a new reference direction *ON* is chosen, making an angle of σ'' with *OM*, then in Fig. 4.25, the angle between e_0 and e_q may be denoted by σ, and that between e_0 and the plane of the loop by θ. Then

and

$$\left.\begin{aligned}\theta &= \theta' - \sigma'' \\ \sigma &= \sigma' - \sigma''\end{aligned}\right\} \tag{4.56}$$

The total loop pickup is

$$e_L = e_0 \cos \theta + je_q \cos (\theta - \sigma) \tag{4.57}$$

The *phase vector diagram* (not the space pattern) is shown in Fig. 4.26. For convenience $|e_L|$ will be denoted simply by e_L.

$$e_L^2 = e_0^2 \cos^2 \theta + e_q^2 \cos^2 (\theta - \sigma) \tag{4.58}$$

The output of the loop will be a function of e_L^2 and will be a null when $e_L = 0$. In Eq. (4.58) it is evident that a *null* will be

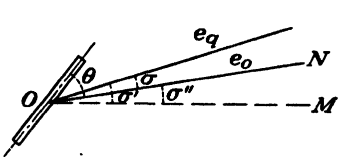


FIG. 4.25.

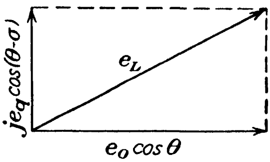


FIG. 4.26.

FIG. 4.25.—Directions of arrival of various components: *MO* is path of direct wave; *NO* is apparent direction of resultant of direct and in-phase reradiated component; and e_q is the quadrature reradiated component.

FIG. 4.26.—Phase vector diagram of loop input components.

obtained only if $\sigma = 0$ or π. Maxima and minima may be found by differentiating Eq. (4.58):

$$2e_L \frac{de_L}{d\theta} = -2e_0^2 \cos \theta \sin \theta - 2e_q^2 \cos (\theta - \sigma) \sin (\theta - \sigma) \tag{4.59}$$

$$\left.\begin{aligned}\frac{de_L}{d\theta} &= -\frac{e_0^2 \cos \theta \sin \theta + e_q^2 \cos (\theta - \sigma) \sin (\theta - \sigma)}{e_L} \\ &= 0\end{aligned}\right\} \tag{4.60}$$

Since for $\sigma \neq 0$ or π, $e_L \neq 0$, then

$$e_0^2 \sin 2\theta + e_q^2 \sin 2(\theta - \sigma) = 0 \tag{4.61}$$

If one lets

$$n = \frac{e_0}{e_q} \tag{4.62}$$

$$n^2 \sin 2\theta + \sin 2\theta \cos 2\sigma - \cos 2\theta \sin 2\sigma = 0 \tag{4.63}$$

$$\tan 2\theta = \frac{\sin 2\sigma}{n^2 + \cos 2\sigma} \tag{4.64}$$

Here σ is the angle between the direction of the resultant of all in-phase components (direct and reradiated) and the direction of the quadrature component. It differs from σ', the angle between e_d and e_r by the bearing error σ'' where the latter is given by Eq. (4.55).

Alternatively Eq. (4.64) may be written as a function of the single angle θ,

$$\tan 2\theta = \frac{2 \tan \theta}{1 - \tan^2 \theta}$$

If M is defined as

$$M = \frac{\sin 2\sigma}{n^2 + \cos 2\sigma} \tag{4.65}$$

$$2 \tan \theta = M(1 - \tan^2 \theta) \tag{4.66}$$

$$\tan^2 \theta + \frac{2}{M} \tan \theta - 1 = 0 \tag{4.67}$$

$$\tan \theta = -\frac{1}{M} \pm \sqrt{1 + \frac{1}{M^2}} \tag{4.68}$$

It can be shown that the minima of e_L occur when the radical of Eq. (4.68) has the positive sign. Thus

$$\tan \theta_{\min} = \sqrt{1 + \frac{1}{M^2}} - \frac{1}{M} \tag{4.69}$$

and this gives two minima, differing in angle by π.

4.15. Deviation Error with Balancer.—If now a signal voltage derived from a nondirectional antenna is added, one may determine the conditions under which this signal will serve as a balancer to give sharp nulls instead of broad minima. Ideally the phase of the balancer should be $\pi/2$ with respect to the loop signal at the point where the two mix. Suppose the actual balancer phase is α. Then the balancer voltage may be represented by

$$e_b = E_b e^{j(\omega t + \alpha)} \tag{4.70}$$

$$= E_b e^{j\omega t}(\cos \alpha + j \sin \alpha) \tag{4.71}$$

The in-phase component is

$$\left.\begin{aligned} e_{b0}e^{j\omega t} &= E_b e^{j\omega t} \cos \alpha \\ e_{b0} &= E_b \cos \alpha \end{aligned}\right\} \tag{4.72}$$

and the quadrature component is

$$\left.\begin{aligned} je_{b_q}e^{j\omega t} &= jE_b e^{j\omega t} \sin \alpha \\ e_{b_q} &= E_b \sin \alpha \end{aligned}\right\} \tag{4.73}$$

In other words e_{b0} is in phase with e_0, and e_{bq} is in phase with e_q. Then e_0 becomes

$$\left.\begin{aligned} e_0' &= E_d + E_r \cos \psi + E_b \cos \alpha \\ &= e_0 + E_b \cos \alpha \end{aligned}\right\} \tag{4.74}$$

and for the corresponding sum of quadrature components

$$e_q' = e_q + E_b \sin \alpha \tag{4.75}$$

The total loop output voltage is

$$e_L' = e_0 \cos \theta + E_b \cos \alpha + j[e_q \cos (\theta - \sigma) + E_b \sin \alpha] \tag{4.76}$$

This will give a null under the necessary and sufficient condition that the real and the imaginary parts are both zero. If this corresponding value of θ is denoted by θ_0:

$$\left.\begin{aligned} e_0 \cos \theta_0 + E_b \cos \alpha &= 0 \\ e_q \cos (\theta_0 - \sigma) + E_b \sin \alpha &= 0 \end{aligned}\right\} \tag{4.77}$$

$$\begin{aligned} \tan \alpha &= \frac{e_q \cos (\theta_0 - \sigma)}{e_0 \cos \theta_0} \\ &= \frac{\cos \theta_0 \cos \sigma + \sin \theta_0 \sin \sigma}{n \cos \theta_0} \\ &= \frac{\cos \sigma + \sin \sigma \tan \theta_0}{n} \end{aligned} \tag{4.78}$$

$$\tan \theta_0 = \frac{n \tan \alpha - \cos \sigma}{\sin \sigma} \tag{4.79}$$

Example.—One may consider a shipboard direction finder loop located just abaft the mainmast. This latter gives rise to quadrature phase reradiated signal as shown in Tables VI and VII. Bearings are to be taken on a station 45° off the bow. The quadrature signal is half the magnitude of the direct signal. It is required to compute the bearing error with no balancer and then with a balancer of phase $\alpha = 60°$.

Here $\sigma = 45°$, $n = 2$, and with no balancer, Eq. (4.64) applies. The minimum (not the null) is given by

$$\tan 2\theta = \frac{\sin 90°}{4 + \cos 90°} = 0.25$$
$$2\theta = 14.0° \text{ or } 194.0°$$
$$\theta = 7.0° \text{ or } 97.0°$$

Thus the error, referred to a true θ of 90° is 7.0°. With the balancer, from Eq. (4.79)

$$\tan \theta_0 = \frac{2 \tan 60° - \cos 45°}{\sin 45°} = \frac{2 \times 1.732 - 0.707}{0.707} = 3.895$$
$$\theta_0 = 75.6° \text{ or } 255.6°$$

instead of 90° (or 270°). Thus the error of the null with the balancer is 14.4° and is worse than that of the broad minimum of the earlier case. This is, of course, because the balancer adds a component of in-phase voltage as it balances out the quadrature component. The importance of supplying a balancer voltage of the correct phase is thus emphasized.

Bibliography

KEEN, R.: *Wireless Direction Finding*, 3d rev. ed., especially Chap. 11, Iliffe & Sons, Ltd., London, 1938.

MAYNARD, J. E.: Universal Performance Curves for Tuned Transformers, *Electronics*, **10**, 15 (February, 1937).

SHEA, T. E.: *Transmission Networks and Wave Filters*, 1st ed., D. Van Nostrand Company, Inc., New York, 1929.

SMITH, F. LANGFORD: *The Radiotron Designer's Handbook*, 3d ed., especially pp. 115–139, Wireless Press for Amalgamated Wireless Valve Company, Sydney, Australia, c. 1941.

TERMAN, F. E.: *Radio Engineering*, 2d ed., McGraw-Hill Book Company, Inc., New York, 1937.

CHAPTER V

PERFORMANCE CHARACTERISTICS OF LOOP INPUT CIRCUITS

5.01. Fluctuation Noise in Direction Finders and Receivers.—When high-gain amplifiers came into use, it became evident that the amplification could not be increased indefinitely to make the amplifier or receiver sensitive to weaker and weaker signals. It was found that there exists a lower limit to the level of signals that can be used on account of so-called "fluctuation phenomena." In the case of a receiver having an audio output system, these fluctuation voltages result in a hiss or noise output. In other classes of receivers or amplifiers there are corresponding output components occupying a wide frequency band in the last circuit of the unit. This, for example, is true in the video output channel of a television receiver. It is customary to refer to these background fluctuation voltage components as *fluctuation noise.* Strictly speaking, this would be true only if the components lay within the a-f pass band of the receiver.

Fluctuation phenomena result from the granular nature of electric charges flowing in a metallic resistor or in the evacuated space surrounding the cathode of a high-vacuum tube. Statistical considerations show that there are deviations in the instantaneous flow of electrons in a conductor from the mean value of zero, even when no voltage is applied. Similarly, the space current of a vacuum tube varies above and below the mean or d-c value by amounts related to the Gauss error function curve. These variations in current may be interpreted as an a-c component superimposed upon a steady d-c component in the case of vacuum tubes or simply as an a-c component in the case of a resistor.

Fluctuation noise found in the output of a receiver or amplifier may be due to three causes:

1. Thermal agitation noise in the resistive component of circuit elements.

2. Noise due to the flow of space current in vacuum tubes.
3. Fluctuation noise entering the receiver with the signal.

The last-named source of noise voltage is in general beyond the control of the amplifier designer, and, as a result, attention will be confined to the first two sources.

5.02. Thermal Agitation Noise.—The output noise voltage of an amplifier due to fluctuation phenomena (Brownian movements) that are present in the first circuit is given by the expression:

$$\overline{V_r^2} = 4kT \int_0^\infty RG^2\, df \qquad (5.01)$$

where $\overline{V_r^2}$ = mean-square output voltage.
k = Boltzmann's constant = 1.37×10^{-23} watt-sec/deg.
T = temperature, deg K.
R = resistive component in ohms of the input impedance as measured across the input terminals of the amplifier.
G = total voltage gain of the amplifier.
f = frequency, cycles.

Both R and G are functions of the frequency f in general. If the amplifier has a constant gain G over a frequency band Δf,

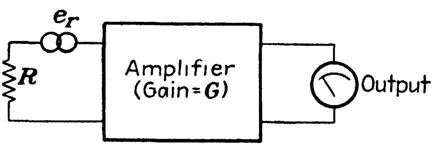


FIG. 5.01.—Equivalent amplifier circuit for thermal agitation noise, showing generator e_r and noise-free resistor R.

and the gain is zero for other frequencies, and if R is substantially constant over this band,

$$\overline{V_r^2} = 4kTRG^2\,\Delta f \qquad (5.02)$$

The equivalent voltage introduced in series with the input impedance and the grid circuit of the first tube of the amplifier may be defined as

$$e_r = \frac{V_r}{G} \qquad (5.03)$$

as shown in Fig. 5.01.

Consequently,

$$\overline{e_r^2} = 4kTR\,\Delta f \qquad (5.04)$$

For a system at room temperature, one may set

$$T = 290°\text{K.} = 17°\text{C.}$$

Then Eq. (5.04) becomes

$$\overline{e_r^2} = 1.59 \times 10^{-20} R \, \Delta f \tag{5.05}$$

where $\overline{e_r^2}$ is in (volts)^2, and R and Δf are in ohms and cycles, respectively.

This may be expressed more compactly if e_r is considered to be furnishing a power to R given by

$$\left.\begin{aligned} W_r &= \frac{\overline{e_r^2}}{R} \\ &= 1.59 \times 10^{-20} \, \Delta f \end{aligned}\right\} \tag{5.06}$$

The equivalent thermal agitation power for any circuit and any resistance is, thus,

$$\text{Thermal agitation power} = 1.59 \times 10^{-20} \text{ watts/cycle}$$

More detailed consideration will show that frequency conversion does not affect the validity of the result, nor does detection in the presence of a strong carrier. Only the total band width, determined by all the selective circuits, determines the equivalent thermal agitation noise power.

Example.—For a total band width of 10 kc, the thermal agitation power is

$$W_r = 1.59 \times 10^{-20} \times 10^4 = 1.59 \times 10^{-16} \text{ watts}$$

This is 135.8 db below a zero level of 6 mw. By Eq. (5.05) the equivalent r-m-s thermal agitation noise input voltage for an input resistance of 1 megohm is

$$\begin{aligned} \bar{e}_r &= \sqrt{1.59 \times 10^{-20} \times 10^6 \times 10^4} \\ &= 12.6 \ \mu\text{v} \end{aligned}$$

Alternatively, the r-m-s thermal agitation current may be calculated.

$$\bar{i}_r = g\bar{e}_r \tag{5.07}$$

where the conductance g is $1/R$. Then Eq. (5.04) becomes

$$\left.\begin{aligned} \overline{i_r^2} &= 4kTg \, \Delta f \\ &= 1.59 \times 10^{-20} g \, \Delta f \end{aligned}\right\} \tag{5.08}$$

5.03. Shot Effect, Tube Noise.—The amplifier output noise voltage corresponding to V_r, but due to *shot effect* or tube noise, may be calculated in a similar manner for a diode or multielement vacuum tube. If the temperature of the cathode of a diode or triode is sufficiently high so that emission is not temperature-limited, it can be shown that the mean-square a-c component of plate current is

$$\overline{i_p^2} = 4\theta k T_k g_s \, \Delta f \tag{5.09}$$

where g_s is the a-c conductance of the tube connected as a diode, θ is a constant whose value is approximately 0.644 over the normal range of anode potentials, and T_k is the cathode temperature.

The approximate equivalent of Eq. (5.08) for a space-charge-limited diode is

$$\overline{i_p^2} = 1.59 \times 10^{-20} \frac{T_k}{T} \theta g_s \, \Delta f \tag{5.10}$$

For an oxide-coated cathode operating at 800°C.,

$$\begin{aligned} \overline{i_p^2} &= 1.59 \times 10^{-20} \times 2.39 g_s \, \Delta f \\ &= 3.79 \times 10^{-20} g_s \, \Delta f \end{aligned} \tag{5.11}$$

Equation (5.09) is valid for a diode or a triode. With suitable modifications it may be applied to multigrid tubes. In the case of a triode, if the ratio of the control grid–plate transconductance S_{gp} to the a-c conductance of the equivalent diode g_s be defined as s.

$$s = \frac{S_{gp}}{g_s} \tag{5.12}$$

and

$$\overline{i_p^2} = \frac{4\theta k T_k S_{gp} \, \Delta f}{s} \tag{5.13}$$

The equivalent voltage in the grid circuit $\overline{e_i}$ is given by

$$\begin{aligned} \overline{e_i^2} &= \frac{\overline{i_p^2}}{S_{gp}^2} \\ &= \frac{4\theta k T_k \, \Delta f}{s S_{gp}} \end{aligned} \tag{5.14}$$

Then, if there is a fictitious resistance R_{eq} in the grid circuit and at temperature T, it will produce the same noise magnitude as

the shot effect noise of Eq. (5.14) provided

$$\overline{e_i^2} = \overline{e_r^2} \tag{5.15}$$

where $\overline{e_r^2}$ is given by Eq. (5.04) for $R = R_{eq}$

$$R_{eq} = \frac{\theta T_k}{sS_{gp}T} \tag{5.16}$$

The advantage of a tube with low cathode temperature T_k is evident. Consequently, for a given S_{gp} an oxide-coated cathode is superior to a thoriated tungsten filament. Likewise a high value of S_{gp} is desirable to keep R_{eq} small.

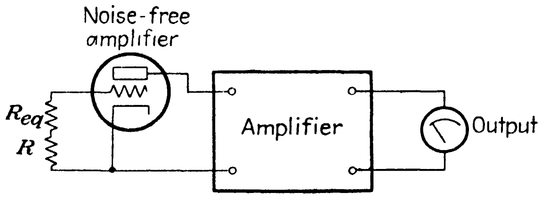


FIG. 5.02.—Equivalent amplifier circuit for thermal agitation and tube noise. R_{eq} is chosen to give thermal noise equal to that of the actual tube noise of the amplifier.

If a receiver has an input circuit of tuned impedance R, the relative contributions of thermal agitation noise and shot effect noise can be determined from R and R_{eq} in series as shown in Fig. 5.02. The total noise voltage $\bar{e}_t$ is

$$\bar{e}_t = \sqrt{\overline{e_r^2} + \overline{e_i^2}} \tag{5.17}$$

$$= \sqrt{1.59 \times 10^{-20}\,\Delta f(R + R_{eq})} \tag{5.18}$$

while that due to the input circuit alone is

$$\bar{e}_r = \sqrt{1.59 \times 10^{-20}\,\Delta f R} \tag{5.19}$$

In order to secure the least amount of tube noise, *i.e.*, to make the fluctuation noise depend only upon the input circuit, the ratio of $\bar{e}_t$ to $\bar{e}_r$ should be as near unity as possible.

$$\frac{\bar{e}_t}{\bar{e}_r} = \sqrt{\frac{R + R_{eq}}{R}}$$

$$= \sqrt{1 + \frac{R_{eq}}{R}} \tag{5.20}$$

TABLE VIII.—NOISE-EQUIVALENT RESISTANCE OF AMPLIFIERS AND CONVERTERS

Type	Application	Voltages			Currents			Transconductance, micromhos	Noise equivalent calculated, ohms	Resistance measured, ohms
		Plate, volts	Screen, volts	Bias, volts	Plate, ma	Screen, ma	Cathode, ma			
6SK7	Pentode amplifier	250	100	−3	9.2	2.4	11.6	2,000	10,500	9,400–11,500
6SJ7	Pentode amplifier	250	100	−3	3	0.8	3.8	1,650	5,800	5,800
6SG7	Pentode amplifier	250	125	−1	11.8	4.4	16.2	4,700	3,300	
6AC7/1852	Pentode amplifier	300	150	−2	10	2.5	12.5	9,000	720	600–760
956	Pentode amplifier	250	100	−3	5.5	1.8	7.3	1,800	9,400	
1T4	Pentode amplifier	90	45	0	2.0	0.65	2.65	750	20,000	
6SA7	Frequency converter	250	100	0	3.4	8.0	11.9	450‡	240,000	210,000
6K8	Frequency converter	250	100	−3	2.5	6.0	8.5†	350‡	290,000	
1R5	Frequency converter	90	45	0	0.8	1.8	2.75	250‡	170,000	
6L7	Pentagrid mixer	250	100	−3	2.4	7.1	9.5	375‡	255,000	210,000
6J5	Triode amplifier	250	...	−8	9.0	....	....	2,600	960	1,250
955	Triode amplifier	180	...	−5	4.5	....	....	2,000	1,250	
6AC7/1852	Triode amplifier	150	150	−2	....	....	12.5	11,200	220	200
6AC7/1852	Pentode mixer	300	150	−1*	5.2	1.3	6.5	3,400‡	2,750	3,000
6SG7	Pentode mixer	250	125	−1*	3.0	1.1	4.1	1,180‡	13,000	
956	Pentode mixer	250	100	−1*	2.3	0.8	3.1	650‡	33,000	
6J5	Triode mixer	100	...	−1*	2.1	....	.....	620‡	6,500	
6AC7/1852	Triode mixer	150	150	−1*	....	....	6.5	4,200‡	950	
955	Triode mixer	150	...	−1*	2.8	....	.....	660‡	6,100	

(*Harris, RCA Rev.*, **5**, 505, *April*, 1941.)

* At peak of oscillator cycle.

† Hexode section only. Triode section takes its current from a separate part of the cathode.

‡ Conversion transconductance value.

It is possible to realize values of $\overline{e_t}/\overline{e_r}$ approximately equal to unity for direction finder receivers in the lower frequency bands. But at the higher frequencies it may rise very considerably above unity. For these conditions the proper choice of tube function, tube type, and operating conditions becomes of great importance.

Returning now to Eq. (5.16), one finds that s lies between 0.5 and 1.0 for most triodes. A very typical value will be assumed, namely $s = 0.95$. Then for the conditions of Eq. (5.11)

$$\frac{T_k}{T}\theta = 2.39$$

Whence for a triode used as an amplifier,

$$R_{eq} = \frac{2.5}{S_{gp}} \tag{5.21}$$

Similar equations for multigrid amplifiers and for converters have been given by Harris.[1] Typical calculated and measured values are given in Table VIII.

5.04. Example of Fluctuation Noise Calculation.—Suppose a 6SK7 pentode is used as an r-f amplifier in a receiver and is coupled to an input circuit having a tuned impedance of 15,000 ohms over the total band width of 15 kc. The relative contributions of tube noise and thermal agitation noise are to be determined. Thermal noise is fixed by the design of the input circuit. It is found that for standard conditions of $E_B = 250$ volts, $E_{G2} = 100$ volts, and $E_{G1} = -3$ volts, $R_{eq} = 10{,}500$ ohms for the 6SK7. Then from Eq. (5.20):

$$\frac{\overline{e_t}}{\overline{e_r}} = \sqrt{1 + \frac{10{,}500}{15{,}000}}$$
$$= 1.31$$

Thus the noise is worse by 2.3 db than it would be with a "noise-free" tube. This is frequently stated as being "2.3 db above thermal noise." If a 6AC7 were substituted, $R_{eq} = 720$ ohms, and

$$\frac{\overline{e_t}}{\overline{e_r}} = \sqrt{1 + \frac{720}{15{,}000}}$$
$$= 1.03$$

Practically, the 6AC7 represents such a "noise-free" tube under these circuit conditions because of its high S_{gp}. In the original case, from Eq. (5.18)

[1] W. A. HARRIS, Fluctuations in Vacuum-tube Amplifiers and Input Systems, *RCA Rev.*, **5**, 505 (April, 1941).

$$\begin{aligned}\bar{e}_t &= \sqrt{1.59 \times 10^{-20}(R + R_{eq})\,\Delta f} \\ &= \sqrt{1.59 \times 10^{-20} \times 25{,}500 \times 15 \times 10^3} \\ &= 24.6 \times 10^{-7} \\ &= 2.46\ \mu\text{v}\end{aligned}$$

When the 6AC7 is substituted, $\bar{e}_t$ will diminish by 2.3 db to 1.88 μv.

5.05. Signal-noise Characteristics of Antenna and Loop Circuits.—A general type of antenna or loop coupling circuit is shown in Fig. 5.03. In this a generator produces an input *signal* voltage $e_{1(s)}$. The corresponding voltage $e_{g(s)}$ due to $e_{1(s)}$ may be found if the circuit gain G is known. If the impedance Z is a

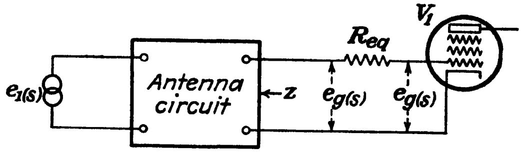


FIG. 5.03.—Equivalent antenna circuit with input signal $e_{1(s)}$. Tube noise is represented by the equivalent resistor R_{eq} in the grid circuit.

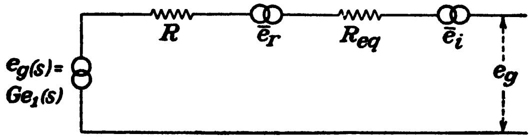


FIG. 5.04.—Equivalent grid circuit, showing signal, thermal-agitation, and tube-noise generators.

pure resistance R over the pass band Δf of the entire receiver, the equivalent circuit is shown in Fig. 5.04 for an input impedance of the grid of tube V_1 that is quite high, as is almost always the case for l-f and m-f direction finders. The component of e_g due to signal is

$$e_{g(s)} = Ge_{1(s)} \tag{5.22}$$

Present at the same time is fluctuation noise consisting of thermal agitation noise voltage $\bar{e}_r$ in R, given by Eq. (5.05), and shot-effect tube noise $\bar{e}_t$ of Eq. (5.14). As was done in Sec. 5.03, the tube noise may be considered to be equal to the thermal agitation noise in a fictitious resistor R_{eq}. The total fluctuation noise at the grid terminals is found from Eq. (5.18).

$$e_{g(n)} = 1.26 \times 10^{-10} \sqrt{\Delta f(R + R_{eq})} \tag{5.23}$$

where $e_{g(n)}$ is in volts; Δf is in cycles per second, and the resistances are in ohms.

The signal-noise ratio at the grid of the tube is the same as if a noise generator $e_{g(n)}/G$ were connected into the input circuit of Fig. 5.03. If this fictitious generator is designated by $e_{1(n)}$, the signal-noise ratio γ is

$$\gamma = \frac{e_{1(s)}}{e_{1(n)}} = \frac{G}{1.26 \times 10^{-10} \sqrt{\Delta f(R + R_{eq})}} e_{1(s)} \tag{5.24}$$

$$= 7.93 \times 10^{9} \frac{G}{\sqrt{\Delta f(R + R_{eq})}} e_{1(s)} \tag{5.25}$$

When the signal is a modulated carrier, the total side-band component for a modulation factor m determines the amount V_s of output of the receiver, and likewise if the total noise $e_{1(n)}$ modulates the same carrier by such an amount as to give an output V_n, the signal-noise ratio

$$\gamma = \frac{V_s}{V_n} = \frac{me_c}{e_{1(n)}} \tag{5.26}$$

where the carrier amplitude is e_c. Here me_c is the total side-band component of signal $e_{1(s)}$. This is independent of the detection or frequency conversion characteristic of the receiver. From Eq. (5.26)

$$e_{1(n)} = me_c \frac{V_n}{V_s} \tag{5.27}$$

It will be noted that $e_{1(n)}$ may be identified with the equivalent-noise-side-band-input voltage of Eq. (1.02), and e_c, V_n, and V_s with the same quantities as defined on page 9.

$$\begin{aligned} e_{1(n)} &= \frac{e_{1(s)}}{\gamma} \\ &= \frac{1.26 \times 10^{-10} \sqrt{\Delta f(R + R_{eq})}}{G} \end{aligned} \tag{5.28}$$

For a constant value of receiver band width Δf (twice the *audio* band width), and for the impedance of the tuned antenna circuit constant, the equivalent-noise-side-band input varies inversely with antenna stage gain.

In the case of loop direction finders at frequencies below 1500 kc, shot effect noise may be neglected in comparison with

thermal noise when the first tube stage is an r-f amplifier of moderate to high gain. Under such conditions R_{eq} may be set equal to zero in Eq. (5.28). This will be done in the results that follow.

5.06. Signal-noise Ratio of Directly Tuned Loop.—The gain and signal-to-noise ratio of the directly tuned loop of such a type as that of Fig. 4.01 may be analyzed by means of the equivalent circuit of Fig. 4.02. At resonance

$$\omega^2 = \omega_0^2 = \frac{1}{LC} \tag{5.29}$$

and thus from Eq. (4.05)

$$\frac{e_1}{e_g} = \frac{j}{Q} \tag{5.30}$$

The gain of the series resonant circuit, when the output is measured across C, is

$$G = \left|\frac{e_g}{e_1}\right| = Q \tag{5.31}$$

The parallel tuned circuit consisting of C and the loop has an impedance, measured at resonance across the terminals of C, of

$$R = Q\omega_0 L \tag{5.32}$$

Consequently for a signal $e_{1(s)} = e_1$ introduced in series with the loop, the signal-noise ratio is

$$\gamma = \frac{7.93 \times 10^9}{\sqrt{\Delta f}} \frac{Q}{\sqrt{Q\omega_0 L}} e_{1(s)} \tag{5.33}$$

as given by Eq. (5.25).

$$\gamma = \frac{7.93 \times 10^9}{\sqrt{\Delta f}} \sqrt{\frac{Q}{\omega_0 L}}\, e_{1(s)} \tag{5.34}$$

Here Δf and $\omega_0/2\pi$ are in cycles per second, L in henrys, and $e_{1(s)}$ in volts.

In terms of the field intensity E_s and the loop dimensions, Eq. (3.30) gives for the voltage at the maximum position of the loop,

$$\gamma = \frac{7.93 \times 10^9 \times 2\pi NAf_0}{c\sqrt{\Delta f}} \sqrt{\frac{Q}{\omega_0 L}}\, E_s \tag{5.35}$$

$$= \frac{66.3}{\sqrt{\Delta f}} NA \sqrt{\frac{Qf_0}{L}}\, E_s \tag{5.36}$$

It will be seen that the signal-noise ratio γ varies as the square root of the Q factor of the loop circuit and also as the square root of the operating frequency. In the case of a solenoid winding, to a close approximation L is proportional to N^2, provided the other dimensions are fixed. Consequently, for this case $N/\sqrt{L}$ is constant, and the conclusion may then be drawn that the signal-noise ratio is independent of the inductance, provided a suitable C is chosen for each case to resonate the circuit.

For loops that do not have a simple solenoid winding of fixed dimensions, the quantity $N/\sqrt{L}$ may not be constant. It is desirable to choose a winding that will give the maximum number of turns for a value of L fixed by C and the desired tuning range. When a ferromagnetic material is inserted to form the proper core for the loop, an improvement in γ may frequently be realized, although often at the expense of increased weight.

The equivalent-noise-side-band-input field as defined in Sec. 1.07 gives a relationship analogous to Eq. (5.28):

$$E_n = \frac{E_s}{\gamma} \tag{5.37}$$

where E_n may be identified with the same quantity of page 10.

$$E_n = \frac{1.51 \times 10^{-2}\sqrt{\Delta f}}{NA}\sqrt{\frac{L}{Qf_0}} \tag{5.38}$$

This is the desired result for the equivalent-noise-side-band-input field.

Example.—A loop 21 in. in diameter wound with 6 turns has a Q of 100. The inductance $L = 60\ \mu h$. At 1000 kc the ENSI field is to be computed for a receiver audio response of width $\Delta f/2 = 3000$ cycles. It will be observed that the total band width Δf of the r-f system from which components of the fluctuation noise spectrum are obtained is twice this audio band.

$$E_n = \frac{1.51 \times 10^{-2}\sqrt{60} \times 10}{6 \times 0.223}\sqrt{\frac{60 \times 10^{-6}}{10^2 \times 10^6}}$$

since $A = 0.223$ m².

$$E_n = 0.678 \times 10^{-6}\ \text{v/m}$$
$$= 0.678\ \mu\text{v/m}$$

If one wishes to compute the carrier field $(E_c)_2$ which when modulated 30 per cent gives a 6-db increase in output over the unmodulated value (*i.e.*,

6-db signal plus noise to noise), by Eq. (1.04)

$$(E_c)_2 = \frac{E_n}{0.173} \tag{5.39}$$

$$= \frac{0.678}{0.173} = 3.92 \ \mu\text{v/m}$$

5.07. Gain and Signal-noise Ratio of Loop with Coupling Transformer.—For multiband direction finders and for loop

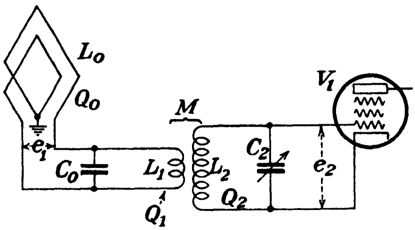


FIG. 5.05.—Coupled loop input circuit.

locations remote from the receiver, it is common practice to couple the loop through a two-wire transmission line to the primary of a two-winding transformer. The secondary of this latter is tuned by means of a section of the gang variable capacitor. By the use of a different coupling transformer for each band, a wide range of frequencies may be covered by a single loop. The circuit is represented in Fig. 5.05.

The equivalent circuit for a generator of voltage e_1 introduced in series with L_0 is shown in Fig. 5.06. In each of the figures,

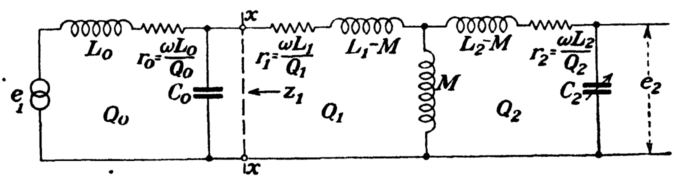


FIG. 5.06.—Circuit equivalent to Fig. 5.05.

C_0 represents the shunt capacity of the two-wire shielded transmission line connecting the loop to the receiver input, together with distributed capacity of L_0 and L_1. The circuit will be analyzed by a consideration of the network to the left of points xx in Fig. 5.06.

The impedance of a parallel resonant circuit at any frequency may be shown to be

$$Z_1 = \frac{\sqrt{\frac{L_0}{C_0}}\,(Q_0 - j)}{\frac{\omega}{\omega_l} + jQ_0\left(\frac{\omega}{\omega_l} - \frac{\omega_l}{\omega}\right)} \tag{5.40}$$

where $f_l = \omega_l/2\pi$ is the resonant frequency of L_0 and C_0. Since the distributed capacity of L_1 is usually much less than the transmission line capacity, f_l may be called the "resonant frequency" of the loop and transmission line.

A quantity L_l may be defined so that

$$Z_1 = j\omega L_l \tag{5.41}$$

L_l may be a function of frequency.
Then

$$L_l = \frac{\omega_l\sqrt{\frac{L_0}{C_0}}\,(Q_0 - j)}{j\omega^2\left[1 + jQ_0\left(1 - \frac{\omega_l^2}{\omega^2}\right)\right]} \tag{5.42}$$

Since $\omega_l = 1/\sqrt{L_0C_0}$

$$L_l = \frac{\frac{\omega_l^2}{\omega^2}L_0(Q_0 - j)}{\left[j - Q_0\left(1 - \frac{\omega_l^2}{\omega^2}\right)\right]} \tag{5.43}$$

If ω_l is not too near ω,

$$\left[Q_0\left(1 - \frac{\omega_l^2}{\omega^2}\right)\right]^2 >> 1$$

and $Q_0^2 >> 1$.

$$L_l = L_0\frac{\frac{\omega_l^2}{\omega^2}}{\frac{\omega_l^2}{\omega^2} - 1} \tag{5.44}$$

The function θ_l will be defined to be

$$\theta_l = \frac{\omega^2}{\omega_l^2} \tag{5.45}$$

$$L_l = \frac{L_0}{1 - \theta_l} \tag{5.46}$$

Thus, the impedance Z_1 is represented by an apparent inductance that varies with frequency in accordance with Eq. (5.46).

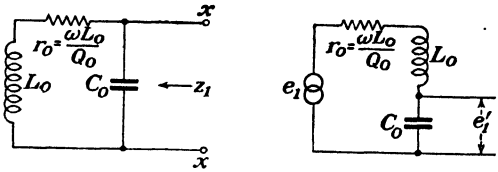


FIG. 5.07.—Circuits equivalent to input of Fig. 5.06. (a) Equivalent series impedance, (b) open-circuit voltage.

From the second circuit of Fig. 5.07, it is found that

$$
\begin{aligned}
e_1' &= e_1 \frac{\dfrac{1}{j\omega C_0}}{j\omega L_0\left(1 - \dfrac{j}{Q_0}\right) + \dfrac{1}{j\omega C_0}} \\
&= e_1 \frac{1}{1 - \dfrac{\omega^2}{\omega_l^2}\left(1 - \dfrac{j}{Q_0}\right)}
\end{aligned}
\tag{5.47}
$$

To the same degree of approximation as before

$$
e_1' = \frac{e_1}{1 - \theta_l} \tag{5.48}
$$

One will note that for ω_l far enough removed from ω, the Q of the loop does not enter into the results.

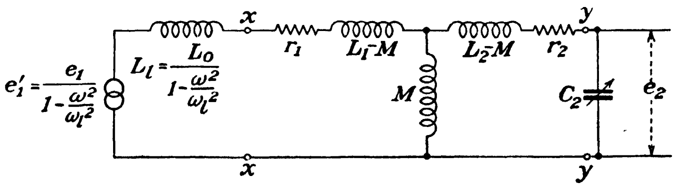


FIG. 5.08.—Two-mesh circuit derived from Fig. 5.06 by application of Thévenin's theorem.

With the results obtained in Eqs. (5.46) and (5.48) one may consider the equivalent circuit shown in Fig. 5.08. The first mesh is almost always resonant above the tuning band, so that the analysis of Sec. 4.05 may be applied, using the value of e_1'

instead of e_1. Thévenin's theorem may be applied again by consideration of the points yy.

The impedance Z_s measured across those terminals may be computed from Fig. 5.09.

$$Z_s = r_2 + j\omega(L_2 - M) + \frac{j\omega M[r_1 + j\omega(L_l + L_1 - M)]}{r_1 + j\omega(L_l + L_1)} \quad (5.49)$$

$$= r_2 + j\omega L_2 + \frac{\omega^2 M^2 r_1}{r_1^2 + \omega^2(L_l + L_1)^2} - \frac{j\omega^3 M^2(L_l + L_1)}{r_1^2 + \omega^2(L_l + L_1)^2} \quad (5.50)$$

Here the effect of the finite Q of the loop is neglected because L_0 and C_0 constitute a parallel resonant circuit having a resistive

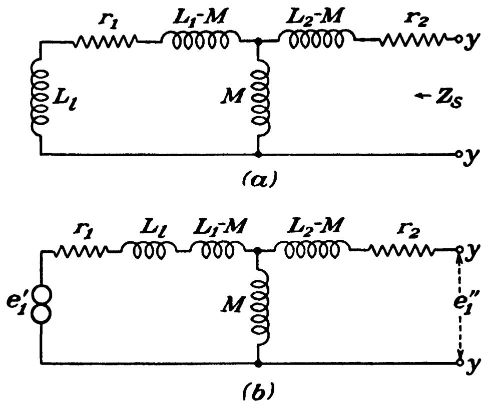


FIG. 5.09.—Circuits equivalent to input of Fig. 5.08 (to left of points yy). (a) Equivalent series impedance, (b) open-circuit voltage.

component large in comparison with r_1 even at a frequency considerably removed from f_l. In the denominator of each of the last terms of Eq. (5.50), r_1^2 may be neglected so that

$$Z_s = r_2 + \Delta r_2 + j\omega L_2\left(1 - \frac{\Delta L_2}{L_2}\right) \quad (5.51)$$

where

$$\Delta r_2 = \frac{M^2}{(L_l + L_1)^2} r_1$$

and

$$\Delta L_2 = \frac{M^2}{L_l + L_1} \quad (5.52)$$

The effective inductance included in Z_s is

$$L_s = L_2\left(1 - \frac{\Delta L_2}{L_2}\right)$$
$$= L_2\left[1 - \frac{M^2}{(L_l + L_1)L_2}\right]$$
$$= L_2\left[1 - \frac{k^2}{1 + \frac{L_0}{L_1}\frac{1}{(1-\theta_l)}}\right] \tag{5.53}$$

where L_l has the value given in Eq. (5.46) and k is the coefficient of coupling. If one defines

$$P = \frac{1}{1 + \frac{L_0}{L_1}\frac{1}{(1-\theta_l)}} \tag{5.54}$$

$$L_s = L_2(1 - k^2P) \tag{5.55}$$

The corresponding resistive component is

$$r_s = r_2 + \Delta r_2$$
$$= r_2 + \frac{k^2L_1L_2}{(L_l + L_1)^2}r_1$$
$$= r_2 + \frac{k^2L_2}{L_1\left[1 + \frac{L_0}{L_1}\frac{1}{(1-\theta_l)}\right]^2}r_1 \tag{5.56}$$
$$= r_2 + k^2\frac{L_2}{L_1}P^2r_1 \tag{5.57}$$

The effective Q factor is

$$Q_s = \frac{\omega L_2(1 - k^2P)}{\frac{\omega L_2}{Q_2} + \frac{\omega L_2}{Q_1}k^2P^2} \tag{5.58}$$
$$= \frac{Q_2(1 - k^2P)}{1 + \frac{Q_2}{Q_1}k^2P^2} \tag{5.59}$$

The open-circuit voltage e_1'' in Fig. 5.09 is

$$e_1'' = e_1'\frac{j\omega M}{j\omega\left[L_1\left(1 - \frac{j}{Q_1}\right) + \frac{L_0}{1-\theta_l}\right]} \tag{5.60}$$

$$e_1'' = e_1' \frac{M}{L_1\left[1 + \frac{L_0}{L_1}\frac{1}{(1 - \theta_l)}\right]} \tag{5.61}$$

since $\left(1 - \frac{j}{Q_1}\right)$ is approximately equal to unity. Thus

$$\frac{e_1''}{e_1'} = k\sqrt{\frac{L_2}{L_1}}\,P \tag{5.62}$$

Then in the equivalent circuit of Fig. 5.10 the output voltage e_2 at resonance is given by Eq. (5.31):

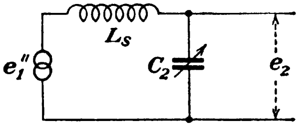


FIG. 5.10.—Simple series circuit derived from Fig. 5.06 by two successive applications of Thévenin's theorem.

$$\frac{e_2}{e_1''} = Q_s \tag{5.63}$$

Q_s is given by Eq. (5.59) and may be measured by appropriate means (such as a Q meter) as the apparent secondary Q factor with primary and loop circuit connected. It will be noted that L_s does not enter explicitly into Eq. (5.63).

$$\frac{e_2}{e_1'} = k\sqrt{\frac{L_2}{L_1}}\,Q_2P \tag{5.64}$$

and by Eq. (5.48) the gain referred to the loop terminal voltage is

$$G = \frac{e_2}{e_1} = k\sqrt{\frac{L_2}{L_1}}\frac{Q_sP}{(1 - \theta_l)} \tag{5.65}$$

or

$$G = k\sqrt{\frac{L_2}{L_1}}\frac{Q_2P(1 - k^2P)}{(1 - \theta_l)\left(1 + \frac{Q_2}{Q_1}k^2P^2\right)} \tag{5.66}$$

The equivalent-noise-side-band input may next be determined. From Eq. (5.28) for $R_{eq} = 0$ and $R = Q_s\omega L_s$,

$$e_{1(n)} = 1.26 \times 10^{-10}\sqrt{\Delta f}\,\frac{\sqrt{Q_s\omega L_2(1 - k^2P)}}{k\sqrt{\frac{L_2}{L_1}}\frac{Q_sP}{(1 - \theta_l)}} \tag{5.67}$$

$$= 1.26 \times 10^{-10}\sqrt{\Delta f}\sqrt{\frac{\omega L_1(1 - k^2P)}{Q_sP^2}}\,\frac{(1 - \theta_l)}{k}$$

$$= 1.26 \times 10^{-10}\sqrt{\Delta f}\sqrt{\frac{\omega L_1}{Q_2}\left(\frac{1}{P^2} + \frac{Q_2}{Q_1}k^2\right)}\,\frac{(1 - \theta_l)}{k} \tag{5.68}$$

From $e_{1(n)}$ the equivalent-noise-side-band-input field E_n defined on page 10 may be found in terms of the effective height h_e.

$$E_n = \frac{e_{1(n)}}{h_e} \tag{5.69}$$

From this, the value of $(E_c)_2$, the signal carrier input field for 6-db signal-noise ratio, is

$$(E_c)_2 = \frac{e_{1(n)}}{0.173 h_e} \tag{5.70}$$

Example.—Consider a loop system with the following constants:

$L_0 = 60\ \mu h$	$Q_1 = 100$
$L_1 = 60\ \mu h$	$Q_2 = 100$
$L_2 = 240\ \mu h$	$k = 0.707$
$f = 2000$ kc	$f = 1000$ kc
$\Delta f = 6$ kc (total)	

The gain and equivalent-noise-side-band-input voltage are to be computed for the operating frequency f.

$$\theta_l = \frac{f^2}{f_l^2} = 0.25$$

$$P = \frac{1}{1 + \frac{1}{(1 - 0.25)}} = 0.43$$

$$Q_s = \frac{100(1 - 0.5 \times 0.43)}{1 + 0.5 \times 0.185} = 71.8$$

$$G = 0.707 \sqrt{\frac{240}{60}}\, \frac{71.8 \times 0.43}{0.75} = 58.2$$

$$\begin{aligned} e_{1(n)} &= 1.26 \times 10^{-10} \sqrt{6000} \sqrt{\frac{2\pi \times 60}{100} \left(\frac{1}{0.185} + 0.5\right)}\, \frac{0.75}{0.707} \\ &= 1.26 \times 10^{-10} \times 77.5 \sqrt{22.25} \times 1.06 \\ &= 0.049\ \mu v \end{aligned}$$

In the foregoing example, if the loop has the dimensions given on page 162, $h_e = 0.028$ m. Consequently,

$$(E_c)_2 = \frac{0.049}{0.173 \times 0.028} = 10.1\ \mu v/m$$

If this is compared with the corresponding result for the same loop directly tuned, as given on page 163, it is found that the signal-noise ratio is poorer by a factor of 2.58 or 8.2 db.

It is instructive to compare the values of $e_{1(n)}$ as the primary inductance L_1 is varied. This is shown in Fig. 5.11, with gain G as computed by Eq. (5.66) also shown. One may observe that the equivalent-noise-side-band-input voltage goes through a broad minimum at $L_1 = L_0$. When the loop

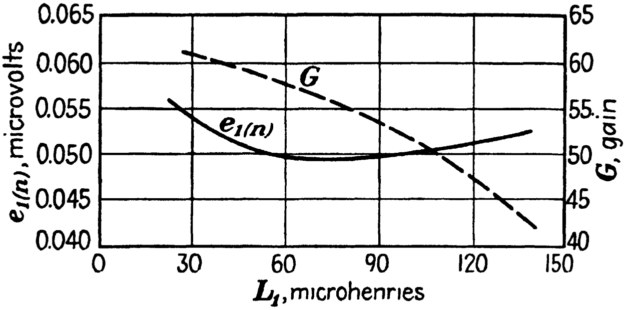


FIG. 5.11.—Example of variation of $e_{1(n)}$, the equivalent-noise-side-band-input voltage, and G, the gain of a loop system employing a coupling transformer. A broad minimum of $e_{1(n)}$ is found for the transformer primary inductance L_1 equal to the loop inductance.

resonant frequency is far enough removed from signal frequency, this is a satisfactory approximation and is often made in practice.

Bibliography

JOHNSON, J. B., and F. B. LLEWELLYN: Limits to Amplification, *Electrical Engineering*, **53**, 1449 (November, 1934).

LEVY, G. F.: Loop Antennas for Aircraft, *Proc. I.R.E.*, **31**, 56 (February, 1943).

LLEWELLYN, F. B.: A Study of Noise in Vacuum Tubes and Attached Circuits, *Proc. I.R.E.*, **18**, 243 (February, 1930).

———: A Rapid Method of Estimating the Signal-to-noise Ratio of a High Gain Receiver, *Proc. I.R.E.*, **19**, 416 (March, 1931).

MOULLIN, E. B., and H. D. M. ELLIS: Spontaneous Background Noise in Amplifiers due to Thermal Agitation and Shot Effects, *J. Inst. Elec. Engrs.* (*London*), **74**, 323, 348 (April, 1934).

NORTH, D. O.: The Absolute Sensitivity of Radio Receivers, *RCA Rev.*, **6**, 332 (January, 1942).

SANDRETTO, P. C.: *Principles of Aeronautical Radio Engineering*, 1st ed., Chap. IV, McGraw-Hill Book Company, Inc., New York, 1942.

ZIEGLER, M.: Noise in Amplifiers, *Philips Technical Review*, **2**, 136 (May, 1937), 329 (November, 1937).

CHAPTER VI

VISUAL DIRECTION FINDERS

6.01. General Classes of Visual Direction Finders.—In distinction to the direction finders described in Chap. IV, there are numerous types in which the proper bearing is determined by means of a visual device. The operator is not required to listen for a minimum signal as in an aural-null type, reception with phones being needed only for station identification or for monitoring. The purpose of a visual system of the type discussed in this chapter is two-fold: (1) to provide greater convenience or accuracy in indication of bearings and (2) to permit simple resolution of the 180° ambiguity in bearings that occurs in the accurate null determination with an aural device.

Visual direction finders may be grouped in two main classes. *Automatic direction finders* indicate directly on a 360° scale the station bearing. *Right-left* types utilize a zero-center meter or similar indicator and indicate deviations in bearing from the manually established loop position.

Aural-null direction finders are sometimes provided with a tuning indicator or output meter. However, this will not be classed as a visual direction finder inasmuch as the condition of giving "sense," or of elimination of 180° ambiguity, is not fulfilled.

6.02. Historical Summary.—Practical visual indicating means for direction finding date back to about 1925, when Goldschmidt and Braillard[1] devised a system employing a spinning loop and a synchronously rotated transparent cylindrical scale, calibrated to read the bearing. A galvanometer located centrally within the cylinder projected a spot of light on the surface of the latter. The galvanometer was connected to the direction finder receiver output, and the light spot traced a line to indicate maxima and minima in the loop pattern. The complications in the optical system to allow the scale to be read at high speeds are obvious.

[1] Goldschmidt and Braillard, U.S. Pat. 1525177, issued Feb. 3, 1925.

This was improved upon by Leib,[1] who used stroboscopic illumination of the scale by means of a neon lamp arranged to flash at the maximum signal bearing. Both these systems constitute visual indicators of a very crude type. An automatic system was proposed by Leib[2] in which a relay connected in the receiver output served to control a unidirectional loop-orienting motor to bring the array to a position of maximum or minimum signal. A much improved version incorporating a reversible driving system is the basis of the standard automatic direction finder in very extensive use at the present time and described in detail in this chapter.

Other developments of historical interest and illustrative of phase-reversal and phase-shift indicator means are summarized by Tuska[3] as follows:

Henri Busignies[4] has described a radio compass (*i.e.*, a visual direction finder) in which an antenna is alternately connected to a pair of crossed loops so that a pair of cardioid response patterns are obtained. The receiver output is synchronously connected to first one then the other of a pair of meter coils. The effect of this four-fold commutation is to rotate the response pattern around the antenna. The meter coils, which are fastened together, assume a position corresponding to the direction of propagation of the received wave, and a suitable pointer indicates the wave source.

In a U.S. patent,[5] entitled "Magnetic and Radioelectric Goniometry," Lucien Levy discloses an interesting type of radio direction finder. A loop and alternator armature are rotated in synchronism. The currents derived in the output of a receiver, connected to the loop, have a phase which is a function of the wave front intercepted by the loop. The alternator phase is fixed with respect to the loop. If the phase displacement is measured, the phase angle is a function of the radio bearing. In a modification of this system, Levy describes (*loc. cit.*) an arrangement in which crossed loops are alternately keyed by currents corresponding to sin ωt and cos ωt. These currents, being independent of the direction of the received signals, are used as a reference phase. The phase of the received signals, after demodulation, is compared to the reference phase to indicate the radio bearing.

[1] A. LEIB, U.S. Pat. 1799238, issued Apr. 7, 1931.

[2] ———, U.S. Pat. 1850080, issued Mar. 22, 1932.

[3] C. D. TUSKA, Radio in Navigation, *Journal of the Franklin Institute*, **228**, 433 (October, 1939); 581 (November, 1939), especially pp. 582–585.

[4] H. BUSIGNIES, U.S. Pat. 1741282, issued Dec. 31, 1929.

[5] L. LEVY, U.S. Pat. 1844859, issued Feb. 9, 1932.

The Levy disclosure has been improved by Dieckmann and Berndorfer,[1] Hell,[2] Scheppmann,[3] and others. The improvements have resulted in a "left-right" meter. The left-right has had widespread use in aircraft in the United States. The device indicates whether the craft carrying the instrument is headed to the left or right or on a desired course.

The first successful commercial automatic direction finder in general use in the United States was developed in 1937 jointly by Radio Corporation of America and Sperry Gyroscope Company.[4] Later designs have embodied these same general principles.

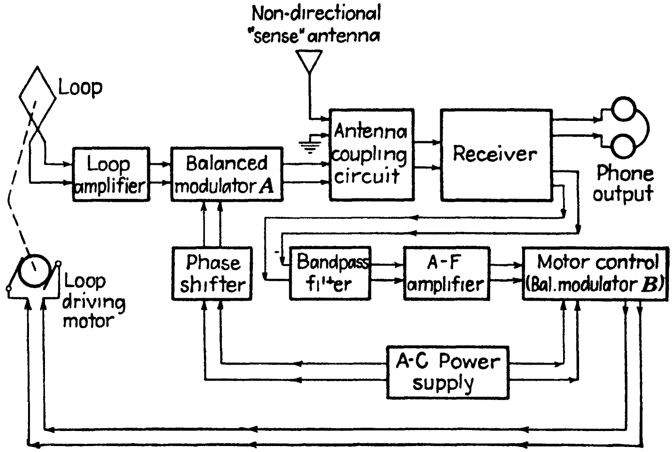


FIG. 6.01.—Typical circuit elements of automatic direction finder.

6.03. Automatic Direction Finders.—In order to study the detailed circuit of a self-orienting automatic direction finder as described in Sec. 6.02, it becomes important to study two topics concerned with circuit operation: (1) balanced modulator circuits and (2) relations of carrier and side-band vectors. First, however, an examination may be made of a block diagram of the direction finder system in which balanced modulators occur. This is shown in Fig. 6.01.

[1] M. DIECKMANN and F. BERNDORFER, German Pat. 517432, issued Feb. 4, 1932.

[2] R. HELL, Direktzeigendes funkentelegraphisches Peilverfahren, *Zeitschrift für Hochfrequenztechnik*, **33**, 138 (April, 1929).

[3] W. SCHEPPMANN, U.S. Pat. 1961598, issued June 5, 1934.

[4] An Automatic Direction Finder, *Communications*, **18**, 10 (October, 1938).

The a-c supply serves to modulate the r-f carrier in the loop channel by means of balanced modulator A. In this the inputs consist of the large amplitude local a-c signal and a much smaller r-f signal. The difference in amplitude and the fact that two different frequencies are fed in are points of importance.

Balanced modulator B is supplied with voltage directly from the a-c supply and also with signal *of this same frequency* from the output of the a-f amplifier. Here the two amplitudes may be comparable. Phase relationships become of importance for this case. Each of these two types of system will be taken up in the following discussion.

6.04. Two-signal Balanced Modulators (Unequal Amplitudes). A very general type of circuit of this type employs two nonlinear

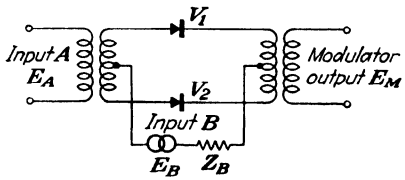


FIG. 6.02.—Circuit of two-element balanced modulator.

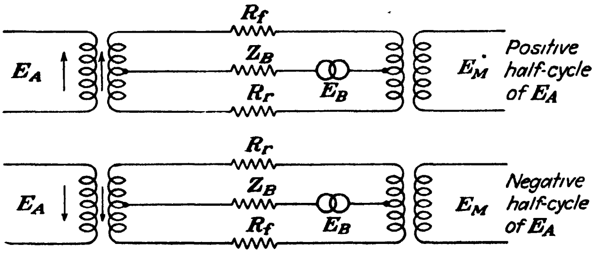


FIG. 6.03.—Equivalent circuit of balanced modulator when V_1 and V_2 have forward resistance R_f and reverse resistance R_r.

elements V_1 and V_2 as in Fig. 6.02. It will be assumed here that $|E_A| >> |E_B|$ to simplify the analysis. The frequencies of components present will be the same without this limitation, however.

A further assumption will be made that V_1 or V_2 behaves in nonlinear fashion so as to exhibit a forward resistance R_f during one half cycle of E_A and a reverse resistance R_r when E_A polarizes it in the opposite sense. For these two cases the circuits are as shown in Fig. 6.03.

Hence, if the input and the modulator output impedances are Z_A, Z_B, and Z_M, the equivalent circuits of Fig. 6.04 may be substituted when the rectification efficiency is high so that

$$R_f << |Z_A + Z_B + Z_M| << R_r \tag{6.01}$$

The current that flows in Z_M is

$$i_M = \frac{e_B}{Z_A + Z_B + Z_M} f(t) \tag{6.02}$$

where e_B is the instantaneous value of E_B and

$$f(t) = \begin{Bmatrix} 1 \text{ for positive half cycles of } E_A \\ -1 \text{ for negative half cycles of } E_A \end{Bmatrix} \tag{6.03}$$

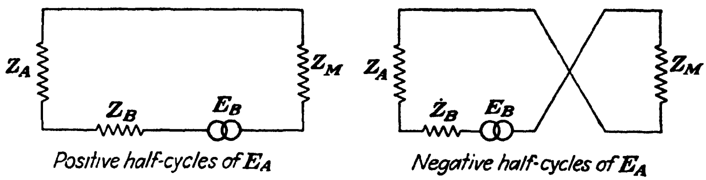


FIG. 6.04.—Equivalent circuit of balanced modulator for $R_f = 0$ and $R_r = \infty$.

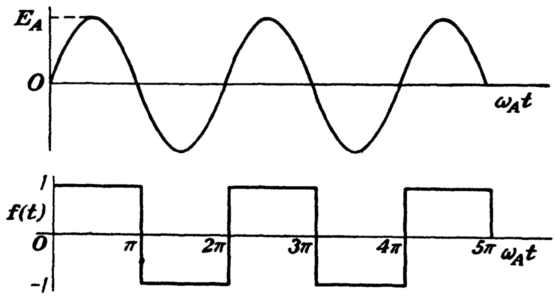


FIG. 6.05.—Value of $f(t)$ as function of e_A, the larger input to modulator.

By a Fourier analysis for $f(t)$ as a function of $\omega_A t$ as shown in Fig. 6.05, one may easily demonstrate that the following function satisfies Eq. (6.03):

$$f(t) = \frac{4}{\pi}\left(\cos \omega_A t - \frac{1}{3} \cos 3\omega_A t + \frac{1}{5} \cos 5\omega_A t - \cdots\right) \tag{6.04}$$

If

$$e_B = E_B \cos \omega_B t \tag{6.05}$$

$$i_M = \frac{4E_B}{\pi(Z_A + Z_B + Z_M)}$$
$$\cos \omega_B t \left(\cos \omega_A t - \frac{1}{3} \cos 3\omega_A t + \frac{1}{5} \cos 5\omega_A t - \cdots \right) \quad (6.06)$$

If one denotes this coefficient by

$$I_0 = \frac{E_B}{Z_A + Z_B + Z_M} \quad (6.07)$$

the result is

$$i_M = \frac{2}{\pi} I_0 \Big\{ [\cos (\omega_A + \omega_B)t + \cos (\omega_A - \omega_B)t]$$
$$- \frac{1}{3} [\cos (3\omega_A + \omega_B)t + \cos (3\omega_A - \omega_B)t]$$
$$+ \frac{1}{5} [\cos (5\omega_A + \omega_B)t + \cos (5\omega_A - \omega_B)t] - \cdots \Big\} \quad (6.08)$$

Thus there are side-band components symmetrically disposed with respect to the odd harmonics of the input E_A. Neither E_A itself nor any of its harmonics is present. This may be illustrated if one designates the E_A input and its harmonic frequencies (including direct current) by

$$\frac{a\omega_A}{2\pi}, \quad \text{where } a = 0, 1, 2, 3, \cdots$$

and the E_B input and harmonics by

$$\frac{b\omega_B}{2\pi}, \quad \text{where } b = 0, 1, 2, 3, \cdots$$

Then such a pair of terms as

$$\cos (3\omega_A + \omega_B)t + \cos (3\omega_A - \omega_B)t$$

would be identified by $(3\omega_A \pm \omega_B)$ in which $a = 3$ and $b = 1$. The two algebraic signs identify upper and lower side-band components, and the order of taking the difference is immaterial. The latter means that no limitation is imposed upon the relative magnitudes of ω_A and ω_B. The various magnitudes are summarized in Table IX.

TABLE IX.—VALUES OF $\frac{i_{M(\max)}}{I}$ FOR EACH COMPONENT

$\pm b$ \ a	0	1	2	3	4	5
0	0	0	0	0	0	0
1	0	$\frac{2}{\pi}$	0	$\frac{2}{3\pi}$	0	$\frac{2}{5\pi}$
2	0	0	0	0	0	0
3	0	0	0	0	0	0
4	0	0	0	0	0	0
5	0	0	0	0	0	0

It will be observed that I_0 is a function of Z_A, Z_B, and Z_M. Consequently, if these impedances are functions of frequency, I_0 must be evaluated for the particular frequency component under

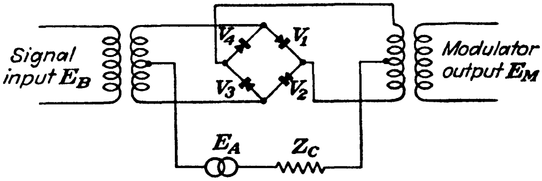


FIG. 6.06.—Circuit of four-element balanced ring modulator.

investigation. From this, the modulator output voltage may be readily calculated.

Other combinations of two nonlinear elements may be analyzed in similar fashion either for balanced or unbalanced circuits. However, for applications to direction finders the case considered is the most important two-element system.

Four-element balanced modulators of symmetrical type are also of interest. Of these the most common is the *balanced ring modulator*. Variations of this may be analyzed by analogy. In Fig. 6.06, V_1, V_2, V_3, and V_4 are the nonlinear elements of the same type as in the previous example. It will be assumed that V_1 and V_3 have the value R_f when E_A has a polarity given by the arrow, while V_2 and V_4 have the high reverse resistance R_r. On the other, or negative, half cycle of E_A, the pairs of resistance values are interchanged. As in Fig. 6.02, symmetry shows that E_A alone will produce no output in E_M. Consequently, Fig. 6.06 may be redrawn for the two carrier conditions as in Fig. 6.07, provided Eq. (6.01) holds.

This illustrates that such a ring modulator is essentially a reversing-switch type. The equivalent networks are given in Fig. 6.08. The current in Z_M is given by Eq. (6.02) where $f(t)$

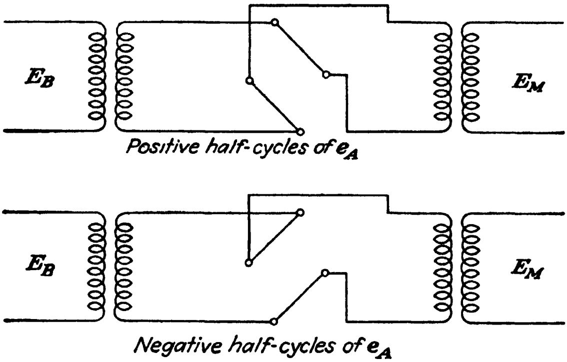


FIG. 6.07.—Equivalent circuit of ring modulator for $R_f = 0$ and $R_r = \infty$.

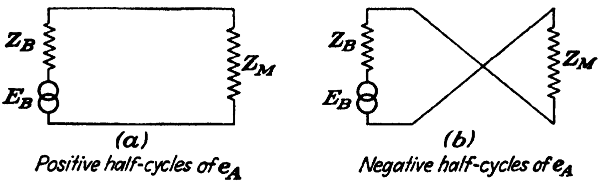


FIG. 6.08.—Circuit impedances in ring modulator.

has the same form as before. Then for e_B a sinusoidal function as in Eq. (6.05)

$$i_M = \frac{4E_B}{\pi(Z_B + Z_M)} \cos \omega_B t \left(\cos \omega_A t - \frac{1}{3} \cos 3\omega_A t + \frac{1}{5} \cos 5\omega_A t - \cdots \right) \qquad (6.09)$$

If

$$I_0 = \frac{E_B}{Z_B + Z_M} \qquad (6.10)$$

$$i_M = \frac{2I_0}{\pi} \left\{ [\cos (\omega_A + \omega_B)t + \cos (\omega_A - \omega_B)t] - \frac{1}{3} [\cos (3\omega_A + \omega_B)t + \cos (3\omega_A - \omega_B)t] + \frac{1}{5} [\cos (5\omega_A + \omega_B)t + \cos (5\omega_A - \omega_B)t] - \cdots \right\} \qquad (6.11)$$

This may be tabulated as in Table IX for the new value of I_0.

6.05. Single Frequency Balanced Modulators.—The modulator systems considered in Sec. 6.04 were supplied with two signals of different frequencies. The important case arises especially in a-f or power frequency modulator circuits when the two signals are of the *same* frequency, but where the phase may vary. A circuit similar to Fig. 6.02 may be analyzed without any limitation imposed upon the relative amplitudes of E_A and E_B. The characteristics of V_1 and V_2 will be expressed as power series:

$$\left.\begin{aligned} i_q &= q_1e_q + q_2e_q^2 + q_3e_q^3 + \cdots + q_ke_q^k \\ i_s &= s_1e_s + s_2e_s^2 + s_3e_s^3 + \cdots + s_ke_s^k \end{aligned}\right\} \qquad (6.12)$$

where e_q is the instantaneous input voltage to V_1, and i_q the corresponding output current; e_s and i_s refer to V_2.

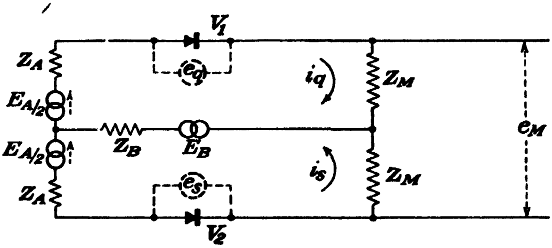


FIG. 6.09.—Equivalent circuit of single-frequency two-element balanced modulator.

The circuit of Fig. 6.02 may be redrawn in accordance with Fig. 6.09. The voltages e_q and e_s are related to the applied voltages as follows:

$$\left.\begin{aligned} e_q &= e_B + \frac{e_A}{2} \\ e_s &= e_B - \frac{e_A}{2} \end{aligned}\right\} \qquad (6.13)$$

where

$$\left.\begin{aligned} e_A &= E_A \cos \omega t \\ e_B &= E_B \cos (\omega t + \phi) \end{aligned}\right\} \qquad (6.14)$$

since these are assumed to be of the same frequency. ϕ is the phase difference between the two inputs.

Then a rather extended analysis would show that

$$\frac{e_M}{Z_M} = E_AE_B(H_1 \cos \phi + H_3 \cos 3\phi + H_5 \cos 5\phi + \cdots) \qquad (6.15)$$

where $H_1, H_3, \ldots$ are functions of the coefficients $q_1, q_2, \ldots$. Thus the phase relationship between E_A and E_B determines the magnitude and polarity of the d-c component. When $\phi = 0$, e_M has a maximum value of one polarity; for $\phi = \pi$, e_M is maximum in magnitude and of the opposite polarity. For $\phi = \pi/2$ or $3\pi/2$, $e_M = 0$.

The foregoing can be understood better by the study of several simple cases. For a characteristic involving no powers above the second, one need consider only the *even* powers, omitting the original d-c term. Hence for $q_2 = s_2$,

$$\left.\begin{aligned} i_q &= q_2 e_q^2 \\ i_s &= q_2 e_s^2 \end{aligned}\right\} \tag{6.16}$$

$$\begin{aligned} e_M &= (i_q - i_s) Z_M \\ &= Z_M q_2 \left[\left(e_B + \frac{e_A}{2} \right)^2 - \left(e_B - \frac{e_A}{2} \right)^2 \right] \\ &= 2 q_2 e_A e_B Z_M \end{aligned} \tag{6.17}$$

From Eq. (6.14),

$$e_M = q_2 Z_M E_A E_B [\cos (2\omega t + \phi) + \cos \phi] \tag{6.18}$$

$$\frac{e_M}{Z_M} = q_2 E_A E_B \cos \phi + \cdots \tag{6.19}$$

where only the d-c term is given. Hence in Eq. (6.15):

$$\left.\begin{aligned} H_1 &= q_2 \\ H_3, H_5, \cdots &= 0 \end{aligned}\right\} \tag{6.20}$$

For characteristics up to the 6th degree, the coefficients are given in Table X, K_{max} denoting the degree, assuming $E_A = E_B = 1$.

TABLE X.—MAGNITUDES OF COEFFICIENTS IN EQUATION (6.15)

	Degree of equation, K_{max}					
	1	2	3	4	5	6
H_1	0	q_2	q_2	$q_2 + 1\frac{5}{8}q_4$	$q_2 + 1\frac{5}{8}q_4$	$q_2 + 1\frac{5}{8}q_4 + 345/64 q_6$
H_3	0	0	0	0	0	$5/32 q_6$

If $q_2, q_4, \ldots$ diminish quite rapidly, only H_1 need be considered, and Eq. (6.15) reduces to the approximate relation:

$$\frac{e_M}{Z_M} = E_A E_B H_1 \cos \phi \tag{6.21}$$

Whether E_B *reverses* in phase or whether it varies continuously in phase, Eq. (6.21) applies to show the behavior of this type of balanced modulator. The automatic direction finder to be described utilizes the two conditions of $\phi = 0$ and $\phi = \pi$. Adjustments are provided to secure these particular phase relations to produce maximum angular sensitivity.

6.06. Carrier and Side-band Relations in an Amplitude Modulated Carrier Wave.—The circuit in the loop channel designated as balanced modulator A in Fig. 6.01 is of the type

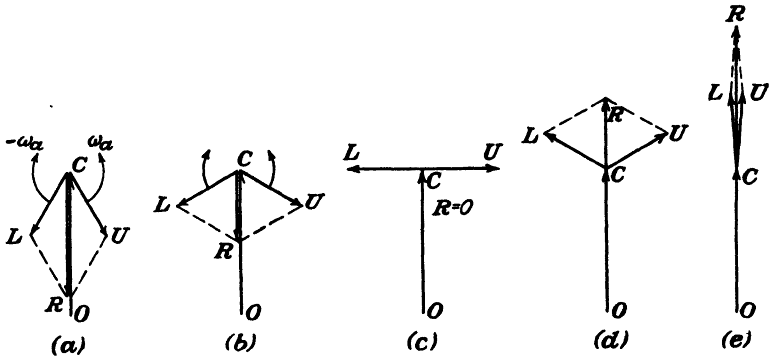


FIG. 6.10.—Carrier and side-band vectors for amplitude modulated wave at successive time intervals in a-f cycle.

discussed in Sec. 6.04. The large amplitude signal E_A is of the a-c power supply frequency, while E_B is the r-f carrier. From the analysis given, it is seen that side bands of the r-f carrier appear in the output, but the carrier itself is suppressed. Then the carrier is resupplied from the antenna by means of the antenna coupling circuit. The phase relationships among the components may best be analyzed by considering the carrier and side-band vectors.

In a normal modulated carrier system the carrier may be represented as a rotating vector C in the conventional manner for an a-c wave. If it is imagined that one examines it "stroboscopically" at intervals equal to its period, the lower and upper side-band components (L and U) will be vectors rotating more slowly or more rapidly than the carrier vector, so that L will

appear to rotate in one direction and U in the other, with an angular velocity $-\omega_a$ or ω_a, where $\omega_a/2\pi$ is the audio-modulation frequency. Furthermore, it is characteristic of amplitude modulation that the vector sum of L and U always lies along C. The vectors, viewed stroboscopically, for various portions of the audio cycle are shown in Fig. 6.10. It will be noted that R, the resultant of L and U, is a vector of varying length but always in the same direction as C (or 180° reversed).

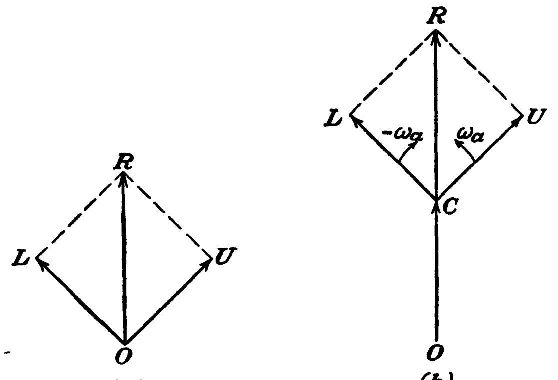


FIG. 6.11.—Vector diagrams of side bands and resupplied carrier for loop position A.

This is the only phase relationship that can be specified, inasmuch as C, L, and U are of different frequencies. When the carrier is suppressed, the output of balanced modulator A continues to be represented by the vectors L and U of Fig. 6.11 for the same phase of incoming carrier as before. This may be compared with d of Fig. 6.10.

The r-f carrier in the loop channel reverses when the loop is rotated through a null point. The 180° zones on the two sides of a null may be identified as "loop position A" and "loop position B." When the carrier of fixed phase is resupplied from the antenna channel, the result will be as in b of Fig. 6.11.

Since the reversal of loop position causes a 180° reversal of all r-f components, the case analogous to a of Fig. 6.11 is given in Fig. 6.12. Then when carrier of the *original phase* is resupplied

from the antenna channel, one has the result of b in Fig. 6.12. The a-f envelope of the carrier is clearly reversed. This is illustrated in Fig. 6.13.

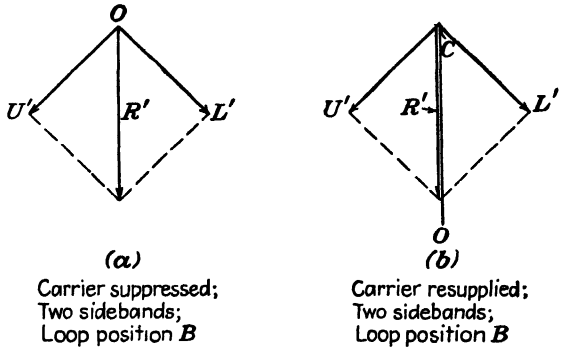


FIG. 6.12.—Vector diagrams of side bands and resupplied carrier for loop position B.

The phase of the a-f voltage at the detector of the receiver is thus changed by 180° when the loop is reversed. The general conclusion may be drawn for a system of this sort that *reversal of r-f phase in the loop channel reverses the phase of the audio signal.* The principal visual direction finder systems described in this

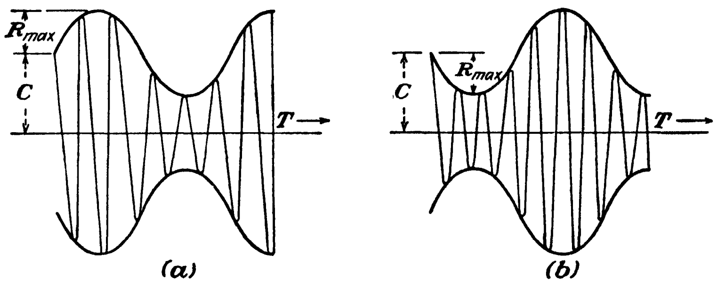


FIG. 6.13.—Modulated carrier wave for two positions of loop. (*a*) Loop position A; vectors as in Fig. 6.11*b*. (*b*) Loop position B; vectors as in Fig. 6.12*b*

chapter function by virtue of this effect. When the loop is on one side of the line of nulls (bearings 0 to 180°), audio output from the receiver is of one phase; when the loop is on the other side of the null points (bearings between 180 and 360°), the audio output is of the opposite phase.

6.07. Motor Control Circuits.—The reversing of the a-f phase is employed to cause the loop to be driven by a reversible electric motor to a point of null loop signal pickup. Because of the fact that this motion may be in one direction when the initial position of the loop is between 0 and 180° and in the opposite direction for bearings 180 to 360°, it is evident that the loop will always drive to the 0° null. This is indicated in Fig. 6.14. In the special case where the loop is exactly 180° off the "correct" null, the audio output of modulation frequency is again zero, and hence there is no restoring motor torque. Any slight electrical disturbance will be sufficient to upset this balance momentarily, and the resultant motor torque in a properly designed motor control circuit will be sufficient to start the loop in motion, so that audio control voltage will be developed and drive the loop toward the correct null. Conditions at the 180°, or "false," null are analogous to those of balancing a pencil on its point.

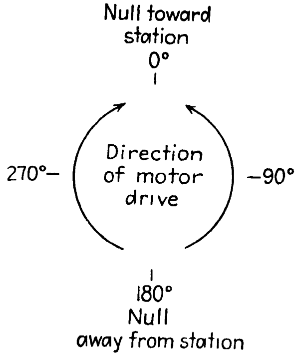


FIG. 6.14.—Direction of rotation of loop control system of direction finder having "sense" (*i.e.*, without 180° ambiguity).

Now it is a well-known fact that a two-phase a-c motor (often used as a capacitor-type motor) requires that its two fields be excited by two voltages of the same frequency but of 90° phase difference. If this difference is of one algebraic sign, the motor will rotate in one direction, while if the sign is reversed, the direction of rotation will be also reversed, as shown in Fig. 6.15.

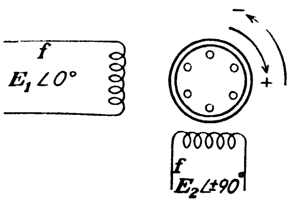


FIG. 6.15.—Two-phase induction motor. E_1 is the voltage of reference phase, while E_2 is the reversing-phase voltage derived from the motor control circuit.

Thus such a motor may be used for a reversible drive with the receiver output as voltage E_2 and a voltage E_1 serving as a reference phase and derived from the same source as used for modulator *A*. The requirement of adequate power of course necessitates a suitable a-f amplifier connected as shown in Fig. 6.01. For aircraft automatic direction finders, 5 to 30 watts maximum power

may be required, and this can be obtained from a class *A* or *B* output stage.

The band-pass filter serves to attenuate speech and other modulation components that may be present on the carrier, to prevent excessive motor heating or overloading of the a-f amplifier. The motor control amplifier and the motor itself constitute a phase comparing system like the type of modulators described in Sec. 6.05. These, therefore, perform the function of modulator *B* of Fig. 6.01.

This system has three limitations. One results from the fact that one field of the two-phase motor is excited continuously. In small-size units operating near full power this means unnecessary heating and low efficiency of power conversion. In the second place, the efficiency of the high-level audio amplifier is somewhat low. Especially for aircraft applications, where size and a-c power supply are limited, this is a serious disadvantage. Lastly, no provision is made to keep the mechanical system from oscillating or "hunting" about its equilibrium position. The cure for this is one of the main problems of the design of *servo devices* or *electromechanical follow-up systems.* This will be treated more fully later.

6.08. Mark I Aircraft Automatic Direction Finder.—A complete equipment embodying the foregoing principles has been commercially available to serve as (1) a receiver, (2) a self-orienting automatic direction finder, (3) an aural-null loop-type direction finder. The main fields of use are for commercial air transport and military service, where continuous and automatic nonambiguous bearing indications with simultaneous headphone reception are required. This direction finder, the RCA-Sperry Mark I system, gives direct indications on a horizontal azimuth dial, navigation scales being provided so that relative, magnetic, or true bearings may be read directly, without the necessity of mental calculations. The importance of this will be evident from the discussion of Navigation in Chap. VII. The automatic direction finder makes provision for operation under conditions of precipitation or dust static such as are frequently encountered in high-speed aircraft.

The various units in the Mark I equipment are shown in Fig. 6.16 illustrating the interconnections. It will be seen that the loop driving motor, part of the loop and motor drive assembly,

drives the pointer of the control and indicator unit by means of a flexible tachometer-type drive shaft. The receiver is remotely tuned from the control unit by means of this same type of drive shaft. Only the control and indicator unit is visible to the pilots or navigator. A typical installation in the cockpit of a Douglas DST (or DC-3) transport plane is shown in Fig. 6.17. Views

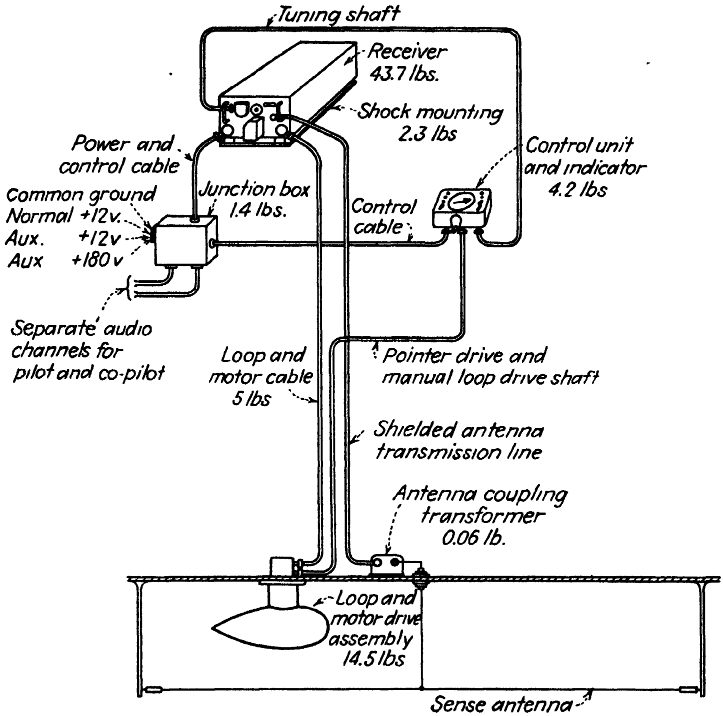


FIG. 6.16.—Equipment arrangement of RCA-Sperry Mark I automatic direction finder.

of the receiver unit (containing the principal electrical circuits), the control and indicator unit, and the loop assembly are shown in Figs. 6.18 to 6.20.

When the equipment is used as an automatic direction finder, it is necessary only to tune in the desired station. The azimuth indicating pointer on the control unit then revolves and comes to rest with the arrow pointing in the actual direction of the station.

The relative bearing or the magnetic bearing may then be read off the proper scale directly. There is no 180° ambiguity, and direction finder operation is entirely independent of volume control settings.

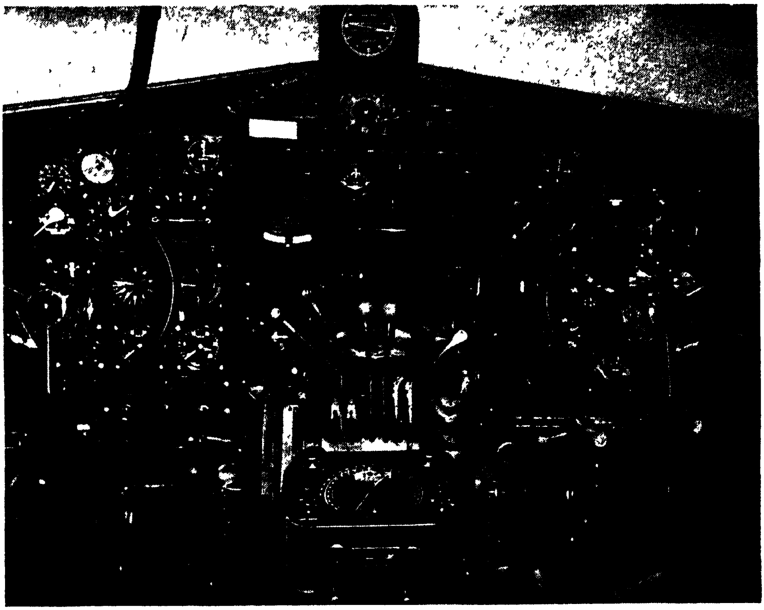


Fig. 6.17.—Control and indicator unit of Mark I automatic direction finder installed in type DST transport plane of American Airlines. All controls are readily operated by either pilot. (*Courtesy of Sperry Gyroscope Company.*)

Reference may be made to the schematic diagram of Fig. 6.21 for the details of circuit operation. Four types of operation may be considered:

1. Reception (nondirectional).
2. Automatic direction finding (with nondirectional sense antenna).
3. Automatic direction finding (antistatic).
4. Aural-null direction finding.

Section 6.09 describes reception with the conventional nondirectional or *T* antenna. Under these conditions, the apparatus is a highly selective superheterodyne receiver suitable for operation in the aircraft radio range and marine band (*X*, 200 to 500 kc)

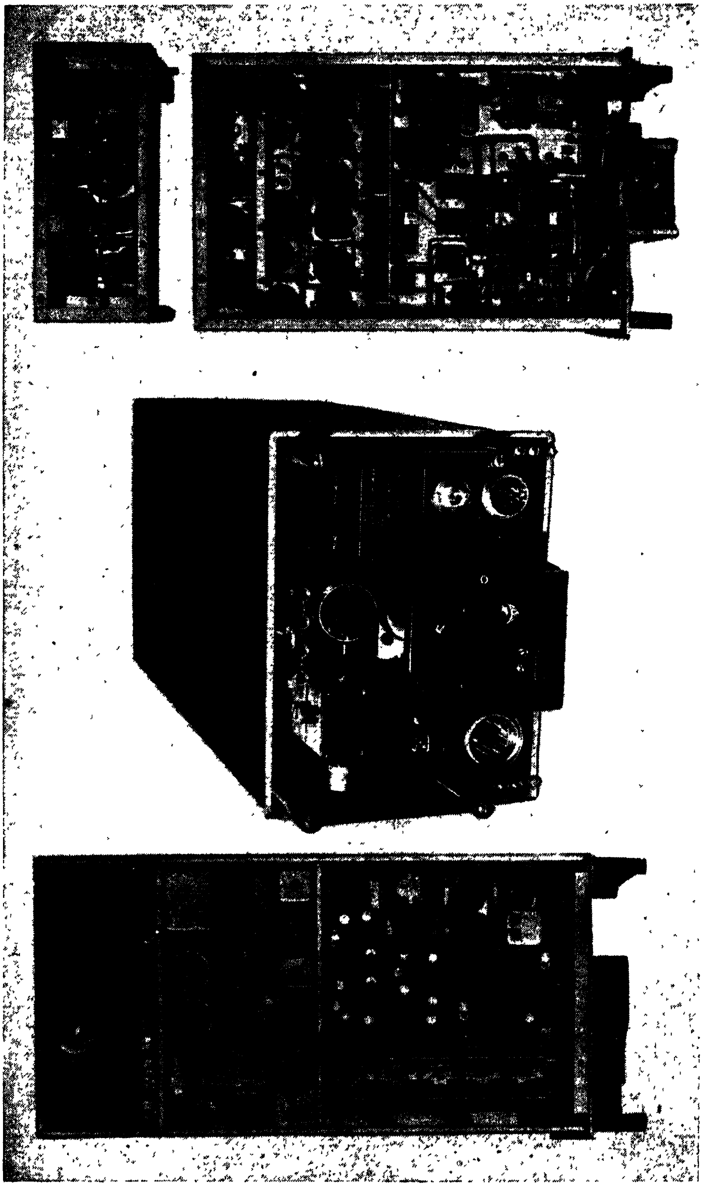


Fig. 6.18.—Receiver unit of Mark I automatic direction finder. It is of the form factor known commercially as a "single ATR" unit. The r-f circuits are in the front section. The i-f, a-f, and motor control circuits are behind. The power unit is located in the rear and is detachable as shown. (*Courtesy of Radio Corporation of America.*)

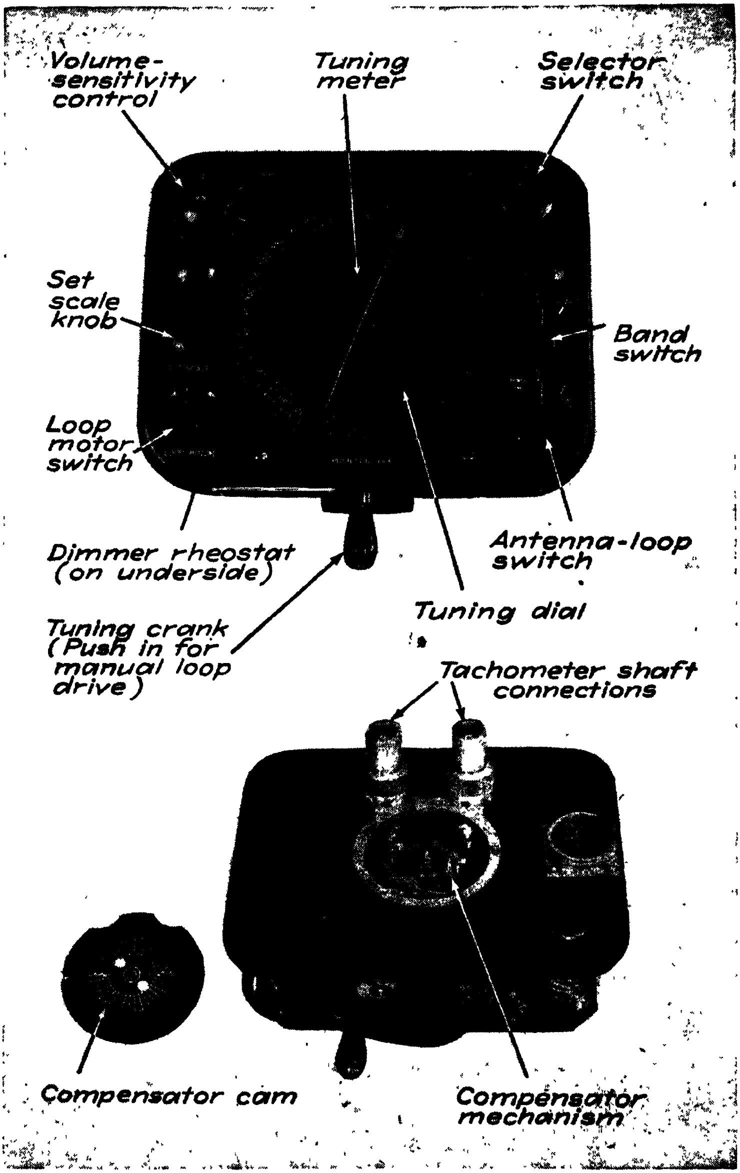


FIG. 6.19.—Control and indicator unit of Mark I automatic direction finder. (*Courtesy of Sperry Gyroscope Company.*)

and in the broadcast band (A, 550 to 1500 kc). Operation is described for the X band only, except where that for the A band is considerably different.

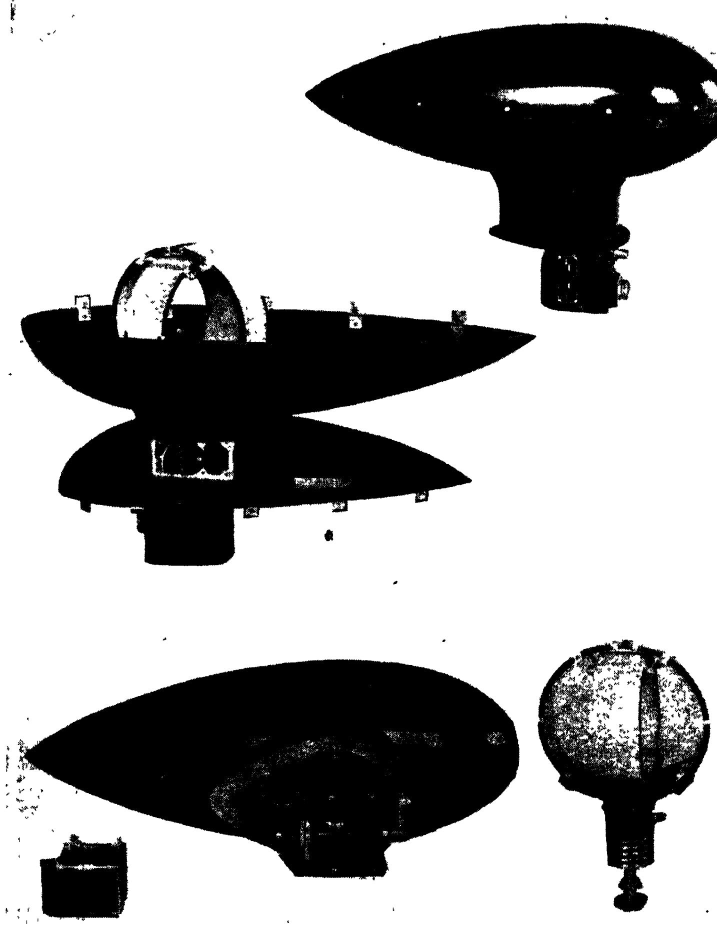


FIG. 6.20.—Loop assembly of Mark I automatic direction finder. The null and sense loops are shown. The loop driving motor and antihunt generator, having a common shaft, may be seen in the lower left view. (*Courtesy of Sperry Gyroscope Company.*)

In Sec. 6.10 operation as an automatic direction finder with a nondirectional sense antenna is analyzed. Here the sequence of

circuits of Fig. 6.01 is employed. The input from the loop (referred to as the *null loop*) is amplified and put through balanced modulator *A*, which suppresses the carrier and provides double side bands. The latter result from the presence of a 100-cycle modulating voltage obtained from the same power source as for power to operate the a-c loop drive motor. The side bands are combined with the input carrier from the sense or nondirectional antenna, and the resultant is fed into the superheterodyne receiver circuits. Thus the signal passing through the receiver has impressed on it the 100-cycle amplitude variation due to the side bands; and as the loop is rotated from one side of the null to the other, the 100-cycle envelope reverses in phase. The signal is detected and amplified to furnish audio headphone output of speech components present on the original carrier, while the 100-cycle component obtained from the local modulator is filtered out, amplified, and used to actuate a motor control circuit. This, however, is not an audio amplifier but a thyratron-controlled circuit to accomplish the same result at much higher power efficiency.

An alternate mode of operation is discussed in Sec. 6.11, for the case when rain, snow, or dust static renders an unshielded antenna completely unusable. The shielded null loop is still capable of functioning, but there is substituted an auxiliary or *sense loop* in place of the sense antenna. Automatic operation is retained, but the freedom from 180° ambiguity is sacrificed under this one condition.

Lastly, aural-null operation as described in Chap. IV is possible, as shown in Sec. 6.12. This may be used in emergencies for direction finding in case of failure of any portion of the automatic system, or may be used for reception, with the loop at maximum, during periods of precipitation static.

6.09. Nondirectional Reception with the Mark I Direction Finder. *Radio-frequency Circuits.*—Signal from the nondirectional antenna is fed into antenna coupling transformer (*L*3, *L*4 of Fig. 6.21) and by the low-capacity transmission line to the low-impedance side of antenna transformer secondary winding *L*11, after passing through switches *S*9 and *S*9*A*, relay *RE*1, antenna blocking capacitor *C*35, and band switch *S*4. Section *C*2 of the gang capacitor tunes this circuit to resonance. Adjustable capacitor *C*10 is shunted across *C*2 on this band for trimming

purposes at the h-f alignment point (450 kc). The inductance of *L*11 is adjustable by means of a magnetite core for alignment at the l-f point (220 kc) as well. Capacitor *C*8 is shunted across the antenna transmission line on the *X* band only.[1] Primary windings *L*9 and *L*10 are inoperative for nondirectional reception, *L*9 being open-circuited by relay *RE*1, and *L*10 connecting to tubes *V*2 and *V*3, which are blocked by having the *B* supply cut off by *S*8*A*.

The grid of tube *V*4 is connected to a tap on *L*11. The circuit design permits high signal-noise ratio with good image attenuation. No band switching is required in the antenna coupling transformer unit. Radio-frequency phase shift through the antenna input system is similar to that of cases 5 or 7 of Table V. This characteristic becomes of importance when the antenna is used for "sense" in direction finder operation.

From the plate of *V*4, the signal is fed to the primary *L*38 of r-f transformer 1. On the *X* band, antiresonant circuit *L*45, *C*99 attenuates signals of intermediate frequency which may be present on the antenna. On both bands a similar i-f trap *L*39, *C*34 is in the screen-grid circuit of *V*4. Secondary *L*14 of r-f transformer 1 is tuned by *C*3 of the gang capacitor. Trimmer capacitor *C*12 and an inductance adjustment allow alignment at two frequencies.

*C*73 resonates with *L*38 below the lowest frequency in the *X* band to give high gain at the low end of the band, while *C*75 produces the coupling required to equalize the h-f gain. A small link winding *L*15 magnetically coupled to *L*14 transfers r-f signal to the low-impedance side of *L*17 of r-f transformer 2. This in turn is tuned by *C*4 of the gang capacitor. A tap on *L*17 connects to the r-f signal grid of converter-oscillator tube *V*5. (On the *A* band the grid is connected to the high-impedance end of *L*16 to equalize over-all sensitivities in the two bands.) The circuit employed results in much greater r-f selectivity and spurious response attenuation than would be possible if only one gang-tuned circuit were used to couple *V*4 and *V*5.

On the *X* band the r-f oscillator grid winding *L*21, tuned by gang capacitor *C*5, is magnetically coupled to plate winding *L*20

[1] Independent adjustments are provided on the two frequency bands, so that alignment adjustments in one band will have no effect upon the other. Consequently, either band may be aligned first.

and is also coupled by oscillator grid-to-plate coupling elements *C*76, *C*79, *R*35. On the *A* band magnetic coupling only is used between *L*18 and *L*19. A tracking circuit *C*79, *L*41 is required on the *X* band to secure proper l-f alignment, while on the *A* band only capacitor *C*78 is required.

Intermediate-frequency Amplifier.—Signal at intermediate frequency is fed into the first i-f transformer *IF*1 in conventional manner, and from a tap on the secondary to the grid of first i-f amplifier *V*6. The tap is used because the full stage gain is not required. This i-f transformer, as well as the other two, employs adjustable magnetite cores that permit adjustment by variation of the inductances. From the plate of *V*6, energy is coupled through a similar i-f transformer *IF*2 to the grid of *V*7.

Since *V*7 serves simultaneously as an i-f and an a-f amplifier, the progress of the signal will be traced in detail. At intermediate frequency *C*66 by-passes the low-impedance side of secondary *L*25 to ground and to cathode via *C*44. Intermediate-frequency signal consequently appears on the primary *L*27 of the third i-f transformer *IF*-3, whose low-impedance side is similarly returned to ground through *C*64. Secondary *L*26 feeds diode plate *D*1 of *V*7 directly. *R*30 is the load across which a-f voltage is developed. To prevent audio distortion, *R*30 returns directly to the cathode. *C*90, *R*33, and the series combination of *C*47 and *C*66 serve as an i-f filter.

First Headphone Audio-frequency Amplifier.—The audio voltage on *R*30 feeds through *C*47 to the high side of grid resistor *R*38. At audio frequency this point is effectively at grid potential, *L*25 having low, and *C*66 having high impedance. *V*7 then serves as an a-f amplifier with plate load resistance *R*58. The impedance of *C*64 is high enough to have small effect at audio frequency, and it constitutes an i-f filter. The portion of the amplified audio frequency across *R*58 is fed into the headphone audio amplifier through coupling capacitor *C*56. *R*71 and *C*96 make up an i-f and a-f plate filter for *V*7. To prevent a-f distortion, screen voltage for *V*7 is obtained separately from the *B* supply through the high resistance *R*39, by-passed by *C*43, with a bleeder to ground *R*72.

Automatic Volume Control.—The action of the a.v.c. may next be considered. At all times the grid of *V*7 has a.v.c. It is obtained from the d-c component across *R*30, and is reduced in

the required proportions by voltage divider *R*41 and *R*38, point *A* of the second i-f transformer being returned to the negative side of cathode bias resistor *R*34. Thus the a-v-c action on the grid of *V*7 is practically independent of the setting of the manual sensitivity control (*X* band). The circuit controls the gain of *V*7 twice—at intermediate frequency and at audio frequency—and results in exceptionally flat a-v-c action where the latter is employed.

The a-v-c diode *D*2 is fed through capacitor *C*54 from *D*1. Rectification of i-f signal causes direct current to appear across *R*31, provided the peak i-f voltage exceeds the "voltage-delay" bias appearing across *R*34 and *R*29. The rectified direct current is filtered by the common a-v-c line elements *R*32 and *C*46 and by individual stage filters including series elements *R*17, *R*21, and *R*25 for *V*4, *V*5, and *V*6, respectively. The voltage delay prevents action of the a.v c. until a certain antenna input signal has been attained.

The tuning meter is in the common cathode return of tubes *V*4, *V*6, and *V*7. When a.v.c. is on, a signal causes these tubes to be biased considerably more negative, so that the plate (and hence cathode) current is reduced, and this indication is given on the meter.

Manual Sensitivity Control.—At all times, the cathode bias resistor *R*23 of tube *V*5 returns to ground. However, the corresponding resistors *R*18 of *V*4 and *R*26 of *V*6 return through sensitivity control *R*53 to ground. *R*53 and *R*43 constitute a voltage divider to raise the cathode bias higher above ground as the sensitivity control is "reduced" (*i.e.*, as *R*53 is *increased*). Automatic volume control continues to be developed under these conditions (*X*-band reception or *X*-band aural-null direction finder operation), but its action is overridden by the manual control, so that the automatic action serves only to prevent overload and course reversal. For this reason, it will be referred to as "A.v.c. off." Automatic volume control switching is accomplished by switch *S*8.

Headphone Output Amplifier.—The a-f signal fed into the phone audio amplifier through *C*56 passes through the audio compensator circuit composed of reactor *L*34 and capacitor *C*81. This is tuned to boost the higher audio frequencies necessary for intelligibility (1500 to 2000 cycles) without affecting the 3-kc

adjacent channel attenuation of the direction finder system.[1] Audio then feeds into the grid of tetrode headphone output tube *V*8, the plate of which couples to balanced dual channel output transformer assembly *T*1. This hybrid coil system feeds audio from *V*8 into both headphone channels (terminals 3–4 and 5–6 on *T*1), but prevents signal fed externally into one channel from being heard in the other channel. This allows parallel operation of a number of similar receivers, each designed for two headphone circuits.

The two pairs of output terminals may be considered as conjugate terminals (*i.e.*, battery and detector) of a Wheatstone bridge, with the signal from *V*8 fed unsymmetrically into one arm. Reactor *L*40 constitutes an l-f balancer, while *R*69 and *R*70 make up two arms of the bridge.

6.10. Automatic Direction Finder Operation (Nondirectional Sense Antenna). *Loop Amplifier Channel.*—The receiver channel functions in the same manner as described in Sec. 6.09. In addition to signal from the nondirectional antenna, there is a signal from the null loop *L*1 fed through the entire loop channel to primary *L*10 of the antenna transformer. The loop connects through the shielded transmission line of the loop cable to primary *L*30 of the loop input coupling transformer. Secondary *L*31 of this unit is tuned by the first section of the gang capacitor *C*1. *C*18 is the h-f trimmer, and *L*31 is adjustable in inductance. The transformer connects to the grid of tube *V*1.

The pentode section of this tube constitutes an amplifier and r-f phase shifter. In order to cause the signal from the loop *L*1 to be *in phase* (or 180° out of phase) with the signal from the antenna at the point where these inputs mix at the grid of *V*4, a phase shift of approximately 90° must be introduced in one channel for the reasons described in Secs. 4.02 to 4.06. The shift is accomplished by the plate load *L*33 of *V*1, which is resonated by its own distributed capacity at a frequency below the tuning band, and hence constitutes approximately a pure reactive load throughout the band. The function of the diodes in *V*1 is explained in the discussion of the loop overload control circuit on page 202.

[1] The radio range transmitters of the civil airways in the United States have frequency assignments based on a 3-kc channel separation.

Tubes $V2$ and $V3$ constitute a balanced modulator of the type analyzed in Sec. 6.04. The control grids are excited in parallel by the r-f carrier from $V1$ through r-f coupling capacitors $C28$ and $C27$. Simultaneously these grids are fed in push-pull at an audio frequency of 100 cycles from the a-c vibrator supply through a filter and phase-shifting network. The plates of triodes $V2$ and $V3$ are connected in push-pull to primary $L10$ of the antenna transformer. Since this transformer will not transmit audio frequencies appreciably, the net result is that there appears from the loop channel at the grid of $V4$ a carrier-suppressed double side-band signal, the side bands corresponding to the 100-cycle modulating frequency. This is combined with the

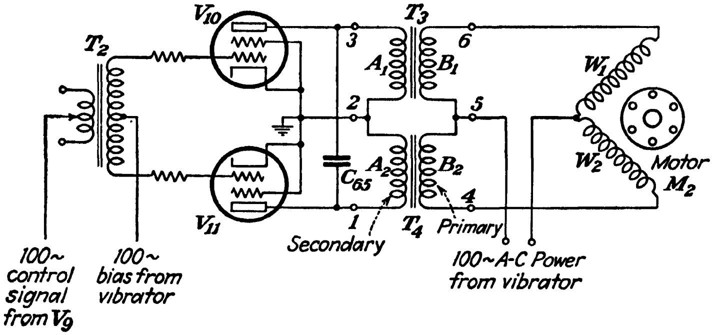


FIG. 6.22.—Simplified motor control circuit of Mark I automatic direction finder. The symbols are the same as in Fig. 6.21.

carrier from the antenna in $L11$, the phase relationship being as described in Sec. 6.06.

Motor Control Circuit.—The audio output is obtained from diode load resistor $R30$ and fed through $C70$ to the input of the motor control amplifier. It consists of the 100-cycle component introduced by the balanced modulator $V2$ and $V3$ and all speech and other audio components present on the received carrier. Filter $L35$ and $C80$, tuned to 100 cycles, attenuates the speech components and passes the 100-cycle modulating frequency. This latter is termed the *control signal.*

The control signal then feeds to the first triode section of $V9$, serving as a resistance-capacity coupled amplifier and driving the second triode section. The latter is transformer-coupled by $T2$ to the push-pull grids of $V10$ and $V11$. Resistor $R73$ is

short-circuited by switch *S8A* to permit normal bias to be applied to the cathode of the second section of *V*9 for automatic operation.

Drive motor *M*2 is a two-phase two-pole induction motor operating in the manner shown in Fig. 6.22. *W*1 and *W*2 are the two-phase motor windings, *T*3 and *T*4 are the motor control transformers, and *C*65 is the capacitor that provides the quadrature component required for motor operation. The a-c power is applied to the junction of the *primaries* of *T*3 and *T*4 at terminal 5 and to the common of the two motor windings. *T*3 and *T*4 are connected as shown so that secondary terminals 1 and 3 are of the *same* polarity. When the tubes are inoperative, *C*65 is consequently across points of no voltage difference. Under this same condition the primaries of the transformers appear as high impedances due to the open secondaries, and no power is supplied to the motor.

But if tube *V*10 is made operative and presents low impedance across secondary *A*1 of one transformer, the impedance looking into primary *B*1 is also low, and winding *W*1 is effectively connected across the a-c power supply. At the same time, if *V*11 exhibits high impedance, the load across secondary *A*2 will be due solely to the capacitor *C*65. Owing to the high impedance ratio of the transformer, the reflected impedance in *B*2 appears as a large capacity in series with winding *W*2 across the a-c supply. This capacity is the same value as would be chosen to give the approximate 90° phase displacement required for a two-phase capacitor-type motor. The conditions of 90° phase shift between voltages applied to the motor windings are those for maximum torque in one direction.

When *V*10 is made high in plate impedance while *V*11 is low, the roles of *T*3 and *T*4 are interchanged. *W*2 is connected across the a-c line while *W*1 is in series with the large capacity because of the "transfer" of *C*65 to secondary *A*1. The phase of the excitation to *W*2 is now $-90°$ instead of $+90°$, and the motor rotates in the opposite direction.

Any types of variable impedances might be considered for *V*10 and *V*11. In the actual circuit used in the Mark I direction finder, these are grid-controlled gaseous tetrodes, commonly known as "thyratrons." They are characterized by low arc drop or low internal resistance when conducting. The arc drop is of the order of 10 volts and is independent of the plate current, so

that if the plate voltage is high, the voltage drop in the tube may be neglected. The plate current is limited only by the plate load impedance. With the grid kept negative, the tube does not conduct, and the plate impedance is very high. But as the grid voltage is made less negative, the point is reached where the tube conducts or "fires." The grid then no longer has any control regardless of grid voltage, and the arc can be extinguished only by reducing the applied plate voltage below the internal arc drop voltage. With an a-c supply for the plate, this occurs in every cycle, and thus the tube can be started and stopped by making the grid less or more negative, respectively. It is to be noted that the tubes can conduct only on the positive half cycles. Owing to the inductance of the motor windings and transformers, the half-cycle pulses are smoothed into fair sine wave form. If the applied grid voltages are direct, the average plate currents may be varied continuously over a considerable range, and hence the plate impedances may be made low or high at will.

Figure 6.22 shows the actual circuit with various filter components omitted. The voltage difference across primaries *B*1 and *B*2 due to the applied a-c voltage is stepped up to 300 to 350 volts and applied to the plates of *V*10 and *V*11. To the *tubes*, each transformer is a source of a-c plate voltage. To the *motor*, each tube, when conducting, acts like a low resistance across its transformer secondary.

The reversible phase 100-cycle control signal from amplifier *V*9 is applied in push-pull to the grids of *V*10 and *V*11 by input transformer *T*2. The two plates are fed from *A*1 and *A*2 in such a manner as to be in phase with each other. Low-voltage a-c bias from the 100-cycle power source is adjusted by phase shift bridge *R*106, *R*107, *C*110, *R*108 to lag the plate voltage by nearly 180°, and is applied to the grids *in parallel* by the center tap connection to *T*2 secondary. By means of phase-shift adjuster *R*10, *R*19, *C*150, *C*151 in the a-c supply to the modulator grids, the phase of the control signal is properly adjusted so that, at the grids of *V*10 and *V*11, it is exactly in phase or 180° out of phase with the plate voltage. In other words, for the loop displaced a small amount in one direction from the null position, control signal on the grid of *V*10 will be in phase with the plate voltage on this same tube, while the grid of *V*11 is fed 180° out of phase with its plate. The grid phases are reversed if the loop

is then rotated to the other side of the null position. The control signal is added vectorially to the a-c bias voltage in $T2$ secondary to produce resultant push-pull grid voltages which will swing in phase with the plate of one tube and out of phase with the other, making one tube conduct and blocking the other. The phase of the control signal voltage determines which tube will conduct, and the various connections throughout the system are chosen so that the conducting tube will cause rotation of the loop toward the null.

The purpose of smooth phase-shift control of the thyratrons is to provide a control system in which the motor torque is substantially proportional to the control signal for very small displacements off the null. An off-on thyratron system, in which the tubes act like relays and are turned only *full off* or *full on*, cannot discriminate between large and small displacements. As a result, under conditions of slow speed following such as are demanded from the control when the airplane changes direction, the loop motion is abrupt and irregular. Contrasted with this, the phase-shift control provides smooth and uniform follow-up action at all speeds when used with an appropriate antihunt circuit as will be described on page 201.

Figure 6.23 shows the phase relations involved in phase-shift control. In *a* of this figure, E_p is the alternating voltage applied in parallel to the plates of $V10$ and $V11$. The dotted line indicates E_c, the critical grid voltage, which is the negative grid voltage that will just keep the tube from firing. E_0 represents the a-c bias applied in parallel to the grids and nearly in phase opposition to the plate voltage. It intersects E_c late in the positive half cycle, and therefore both tubes conduct over the remaining portion of the half cycle as shown by the shadowed area. This is the a-c bias stand-by condition that occurs in the absence of control signal. The amount each tube conducts is rather small, perhaps 4 to 8 ma as read on a d-c meter in each plate circuit.

In *b* of Fig. 6.23 the loop is slightly off the null. The small control signal E is in phase with the plate voltage of $V10$ and therefore is 180° out of phase with the plate of $V11$, owing to the push-pull grid connection. If E is added vectorially to E_0 for $V10$, the resultant grid voltage E_g is seen to be *advanced* in phase with respect to E_p, and $V10$ conducts over a greater portion of

each positive half cycle than it did on the stand-by a-c bias condition. Conversely, E_g for $V11$ is further *retarded* and the current reduced. It is clear that, as the loop is displaced farther from the null so that the control signal E increases in magnitude, the

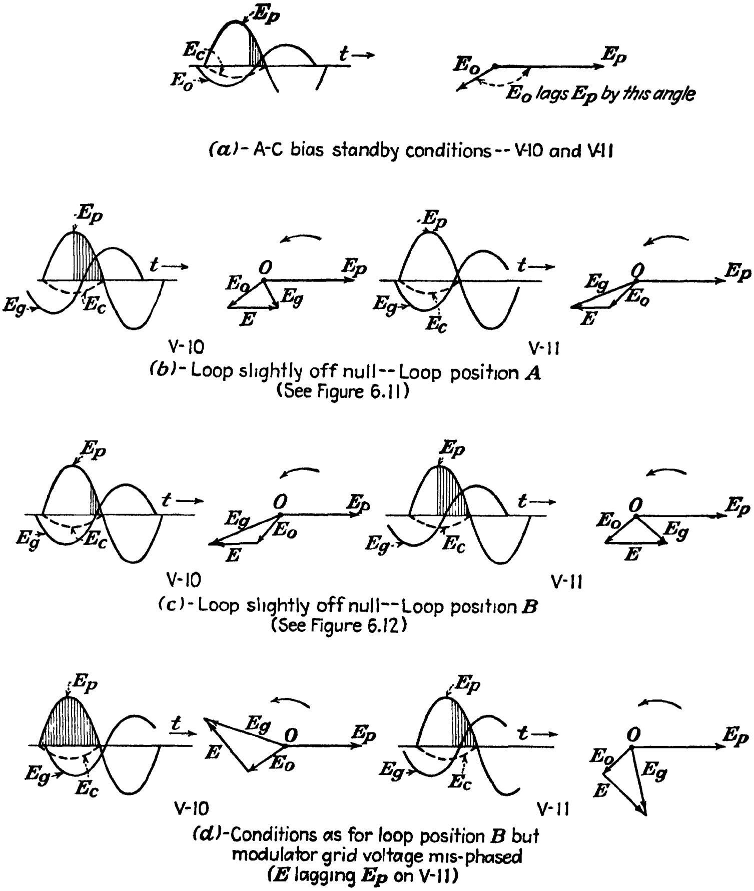


FIG. 6.23.—Phase relations of grid and plate voltages on thyratrons $V10$ and $V11$ of motor control circuit.

resultant E_g for $V10$ swings nearly in phase with the plate voltage. The plate current then increases to a maximum. The voltage E_g for $V11$ becomes nearly in phase opposition to its plate, and the corresponding plate current diminishes. Actually, automatic overload control on the loop amplifier and modulator

tubes limits the maximum value of E so that it does not increase much beyond the value required for optimum control. The signal E rises rapidly to give full motor torque near the null and then flattens off for larger displacements.

In case c of Fig. 6.23 the loop is on the other side of the null, and consequently the control signal is reversed in phase compared with b. Since in $V11$ grid and plate are in phase, $V11$ conducts over every positive half cycle an amount depending on the magnitude of the control signal, and $V10$ is cut off.

It is important that the phase of the control signal be properly adjusted nearly to coincide with the phase of the plate voltage. Diagram d shows conditions as in c, except that the control signal is badly misphased so that it lags the plate of $V11$. The only effect on $V11$ is to reduce its plate current slightly, but the resultant grid voltage on $V10$ now leads the plate voltage and, instead of being cut off, this tube is nearly full on. Such a condition results in very erratic operation, and the motor may stall.

Antihunt Circuit.—Generator $M3$ is mounted on the same shaft as motor $M2$, as will be seen in the view of the loop unit in Fig. 6.20. The generator develops a 100-cycle voltage of *reversing phase* and of *varying amplitude* depending upon *direction* and *speed* of rotation, respectively. It consists of a two-pole exciting winding $W3$, two-pole output winding $W4$, and an iron rotor that has a copper shell over it. At standstill the 100-cycle alternating flux due to $W3$ does not couple with the output winding. When rotation occurs, eddy currents in the copper shell distort the flux and couple it to $W4$, thus producing output voltage. This may be referred to as "armature reaction." The magnitude of this voltage is proportional to the speed, and it reverses in phase with reversal of rotation. This antihunt voltage is fed through $R42$ into the 100-cycle filter at the input of control amplifier $V9$, and is superimposed on the 100-cycle control signal. It is phased to be always in direct opposition to the control signal when the loop is off the null and driving toward it. The signal overrides the small bucking antihunt voltage until within about 2° of the null position, when the signal and generator voltages are about of equal magnitude at full motor speed, resulting in zero control signal input to $V9$.

At this point the reversed phase generator voltage overrides the diminishing loop signal and fires the reverse thyratron to

slow the motor. Owing to the phase-shift control of the thyratrons, the braking action is proportional to the excess of antihunt signal over loop signal. As the motor slows down, the antihunt voltage diminishes and the control signal continues to drive the motor, so that the loop comes to rest on the null. The antihunt voltage constitutes a form of dynamic braking that is far superior to a friction brake system in securing accurate follow-up operation with freedom from sustained oscillation.[1]

Loop Overload Control.—Control signal from the output of the second section of *V*9 is fed back to *V*1, where it is rectified by the diodes and used to develop direct current across resistor *R*5. This serves to bias the three tubes, *V*1, *V*2, and *V*3, of the loop amplifier to reduce their gain and hence to limit the increase in control signal from *V*9 as the loop departs from the null point. This, in turn, makes the balance between loop and antenna pickup much less critical, while allowing full motor torque near the null point of the loop. *C*21, *R*4, and *C*20 constitute a filter to prevent feeding of control signal back to the grids of the three loop channel tubes.

6.11. Automatic Direction Finder Operation (Antistatic).—Under the conditions of operation during precipitation static, the antenna coupling transformer is disconnected from *L*11 and grounded by means of relay *RE*1. At the same time, this relay introduces a compensating circuit having the correct reactance to simulate the reactance of the antenna coupling transformer and transmission line.

An auxiliary, or *sense*, loop *L*2 is connected into the circuit also by means of *RE*1, and feeds into primary *L*9 of the antenna transformer. The sense loop is mounted at right angles to the other or *null* loop and gives the reference r-f phase for the null loop. However, it has two null points, and consequently two points of r-f phase reversal in its polar response. It may be readily seen then that the operation differs from that described in Sec. 6.10 in having two null points at which the indicator may come to rest, these being 180° apart. This means that automatic direction finding under these conditions will be subject to 180°

[1] H. L. HAZEN, Theory of Servo-mechanisms, *J. Franklin Inst.*, **218**, 279 (September, 1934). Extensive bibliography.

ambiguity.[1] This mode of operation may be employed when precipitation static renders the nondirectional sense antenna inoperative.

In order to cause the signal from loops *L*1 and *L*2 to be in phase (or 180° out of phase) at the point where these inputs mix at the grid of *V*4, the phase shift of 90° previously introduced in the *V*1 stage is no longer required. Consequently, the plate load of *V*1 is made a pure resistance over the tuning range of each band. This load in the *X* band consists of a resistor *R*79 in series with which is an inductor *L*51, the latter resonating with the circuit capacity above the tuning band, so that the phase shift is practically zero throughout the band. The operation of the receiver proper and of the motor control circuit is the same as that described in Secs. 6.09 and 6.10.

6.12. Loop Reception and Aural-null Direction Finder Operation.—For reception on the loop antenna or for aural-null operation, the switching is automatically accomplished by *S*8, *S*8*A*, *S*9, and *S*9*A* in the function selector assembly. Loop *L*1 couples to *V*1 as in automatic operation and thence to tube *V*2. The bias of the latter is automatically adjusted for correct amplifier operation when the cathode of *V*3 is opened by means of switch *S*8*A*. The latter switch also serves to remove the 100-cycle modulating voltage from the grid of *V*2 so that this tube may function as an amplifier feeding into primary *L*10 of the antenna transformer.

The receiver end of the antenna coupling transformer transmission line is grounded by means of switch *S*9. In its place is interposed an identical unit, part of the loop compensator assembly, and made up of *L*43, *L*44, and associated capacitors. This unit serves to maintain alignment of the antenna transformer with the other r-f circuits.

Tube *V*9 is made inoperative by a higher positive bias applied to the cathode of the second section when *R*73 is inserted in the circuit by means of switch *S*8*A*. This prevents any external signal from affecting tubes *V*10 or *V*11. The *loop motor* drive is now available to rotate the loop in either direction rather than to require cranking the loop by hand. This electric drive is

[1] This condition is not altogether consistent with the limitation given in Sec. 6.01 in the definition of automatic direction finders.

secured by means of switch *S*15 in the control unit which short-circuits the motor winding of transformer *T*3 or *T*4, depending upon the direction of rotation desired. Operation then becomes substantially identical to that described in the simplified motor control circuit of Fig. 6.22 except that the switch has now actually been inserted across *B*1 or *B*2. This type of operation may be used whether or not tubes *V*10 and *V*11 are in the circuit, as it requires only that the a-c power supply be available. In event of failure of this latter, the loop may be driven by the manual crank provided on the control unit.

6.13. Mark I Power Supply Unit.—The d-c power supply unit for 12-volt operation includes transformer *T*102 and associated vibrator for providing *B* supply to the receiver. This unit is of conventional synchronous vibrator type and requires no detailed description.

For a-c supply, transformer *T*101 is connected to a non-synchronous constant-frequency temperature-compensated 100-cycle vibrator. The primary of this transformer from terminals 4 to 8 constitutes the supply for actually driving the loop motor itself. *C*106 and *C*107 constitute the necessary buffer circuits, and r-f filters are placed in the outgoing leads. Across terminals 2 and 3 in the secondary circuit, voltage at low power is derived to excite the balanced modulator tubes *V*2 and *V*3 and to furnish the a-c bias for *V*10 and *V*11. Reactor *L*104 and *C*115 are used to tune the secondary, and together with the resistance-condenser filters provide good wave form for the modulator and a-c bias supplies. *R*108 and *C*110 comprise the phase shifter for the a-c bias. Adjustment may be made by changing *R*108, but it ordinarily requires no resetting in the field. Phase adjustment for the a-c voltage for the modulator is obtained by variable resistors *R*10, *R*19, and fixed capacitors *C*150, *C*151 in the receiver chassis. A similar power supply unit for 28-volt d-c operation may be substituted readily.

The manner in which such a phase shifter as the *R*108 and *C*110 combination operates may be seen from the simplified circuit of Fig. 6.24. The low-impedance source is shown as a transformer with a center tap. Alternatively, the resistors *R*106 and *R*107 of Fig. 6.21 constitute such a source. A resistor *R* and a capacitor *C* are connected across the full secondary, and consequently the vector sum of the voltage drops e_r and e_c is the

voltage e_1. Points M and N have potentials referred to A or B as shown in b of Fig. 6.24, where AM is $e_1/2$ because of the center-tap connection. The output voltage on open-circuit e_2 is the vector MN of this latter figure. But e_r and e_c are in quadrature since C is a pure reactance. Thus the point N always lies on a semicircle with AB as the diameter. Thus, if R is varied, the phase angle ϕ of e_2 with respect to e_1 varies between the limits of 0 and 180°, while the *magnitude* of e_2 remains constant.

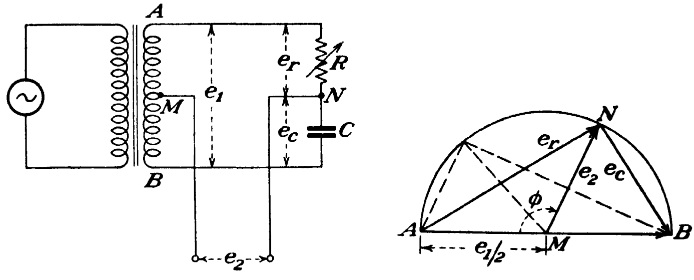


FIG. 6.24.—Method of securing adjustable phase shift.

6.14. Model MN-31 Automatic Direction Finder.—Many of the same principles of visual systems described in the foregoing sections are employed in the MN-31 aircraft automatic direction finder built by Bendix Aviation Corporation.[1] This is designed for commercial or military applications in which the following types of operation are required:

1. Reception (nondirectional) of either modulated or unmodulated signals.
2. Automatic direction finding (with nondirectional sense antenna).
3. Loop reception and aural-null direction finding with either modulated or unmodulated signals.

The system is of the self-orienting loop type like the Mark I and provides automatically a direct indication of the bearing of the radio station that has been tuned in. Various models are available differing principally in the frequency coverage. Typical is the equipment for covering the aircraft beacon, the marine

[1] W. L. WEBB and G. O. ESSEX, The Automatic Radio Compass, *Aeronautical Engineering Review*, **1**, 23 (November, 1942).

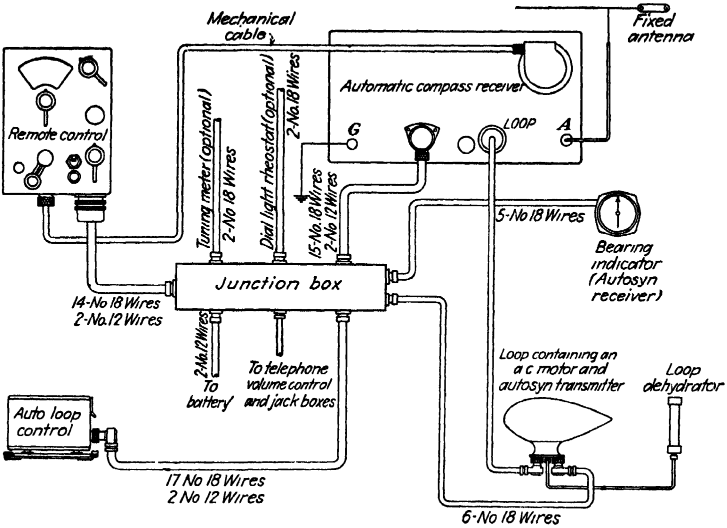


FIG. 6.25.—Equipment arrangement of Bendix MN-31 automatic direction finder.

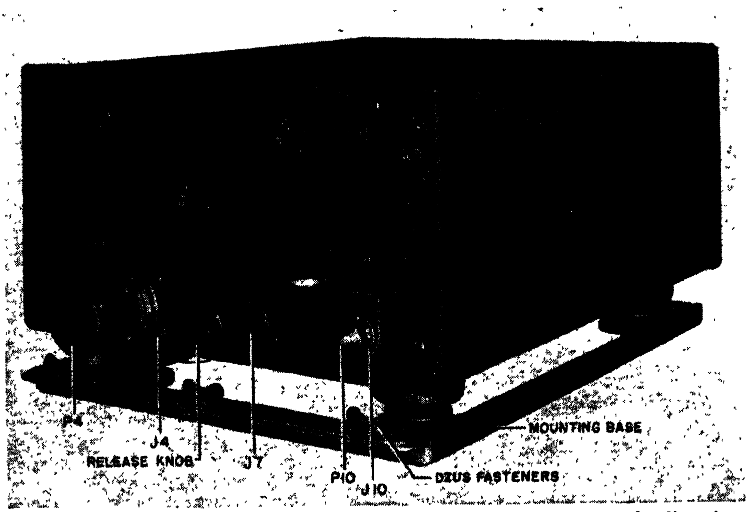
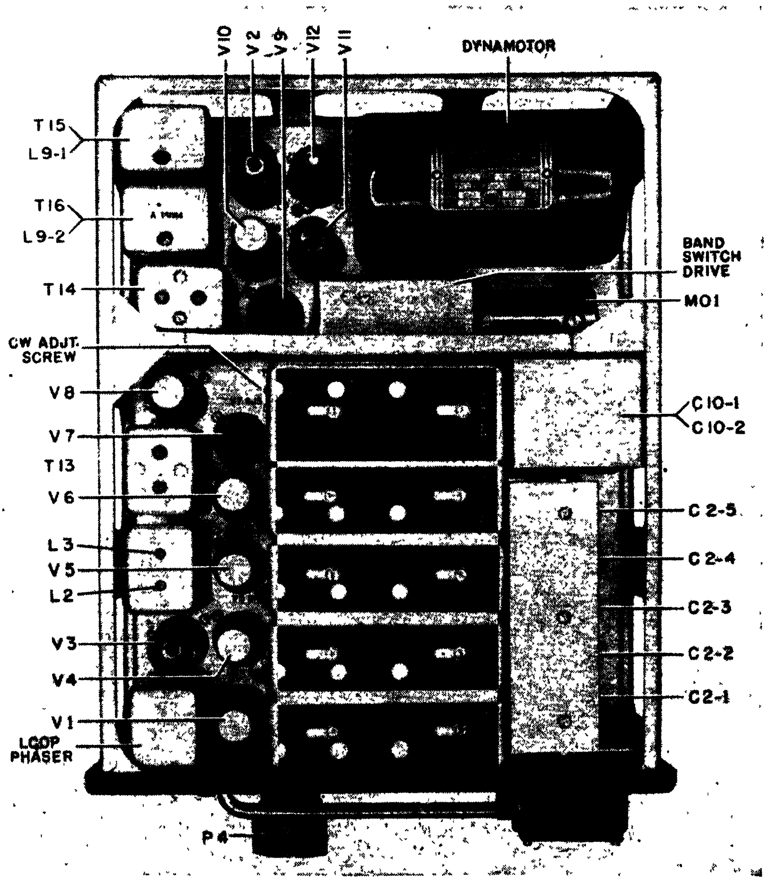


FIG. 6.26.—Receiver unit of MN-31 automatic direction

beacon and communication, and the broadcast bands in three ranges: (1) 200 to 410 kc, (2) 410 to 850 kc, and (3) 850 to 1750 kc. Other models cover frequencies down to 150 kc and may substitute communication reception in the range 2200 to 4250 kc or 2900 to 6000 kc for direction finder operation on band 3.

Some points of difference may be noted in comparison with the Mark I equipment. The bearing indicator unit is not mechanically driven from the rotating loop, but instead in the MN-31 it is electrically controlled by means of a self-synchronous repeater



finder. (*Courtesy of Bendix Aviation Corporation.*)

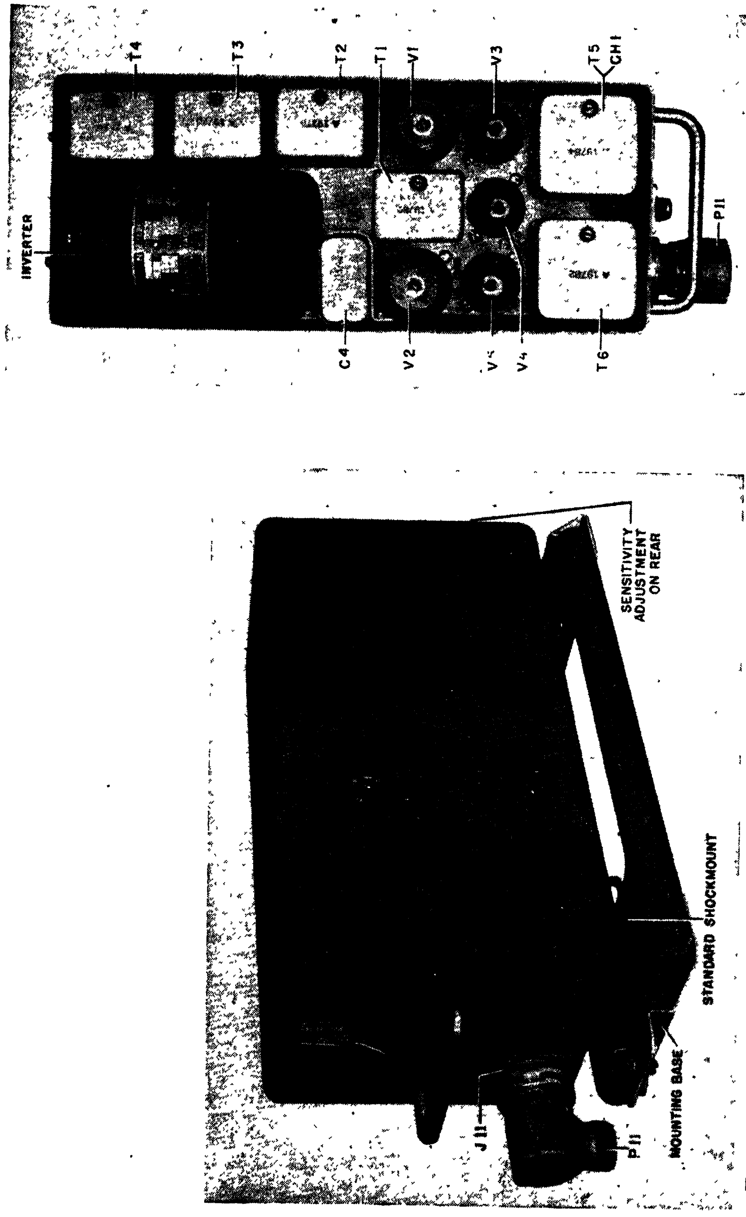
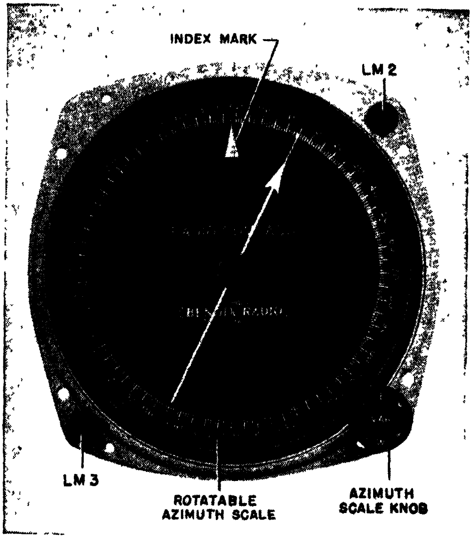


FIG. 6 27.—Automatic loop-control unit of MN-31 automatic direction finder. (*Courtesy of Bendix Aviation Corporation.*)



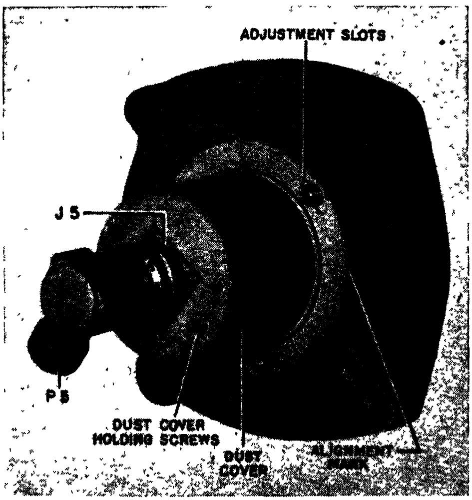


FIG. 6.28.—Bearing indicator unit of MN-31 automatic direction finder. (*Courtesy of Bendix Aviation Corporation.*)

system.[1] Several such indicators may be connected to the "transmitter" unit located in the loop assembly. The motor control circuits are located on a separate chassis rather than as

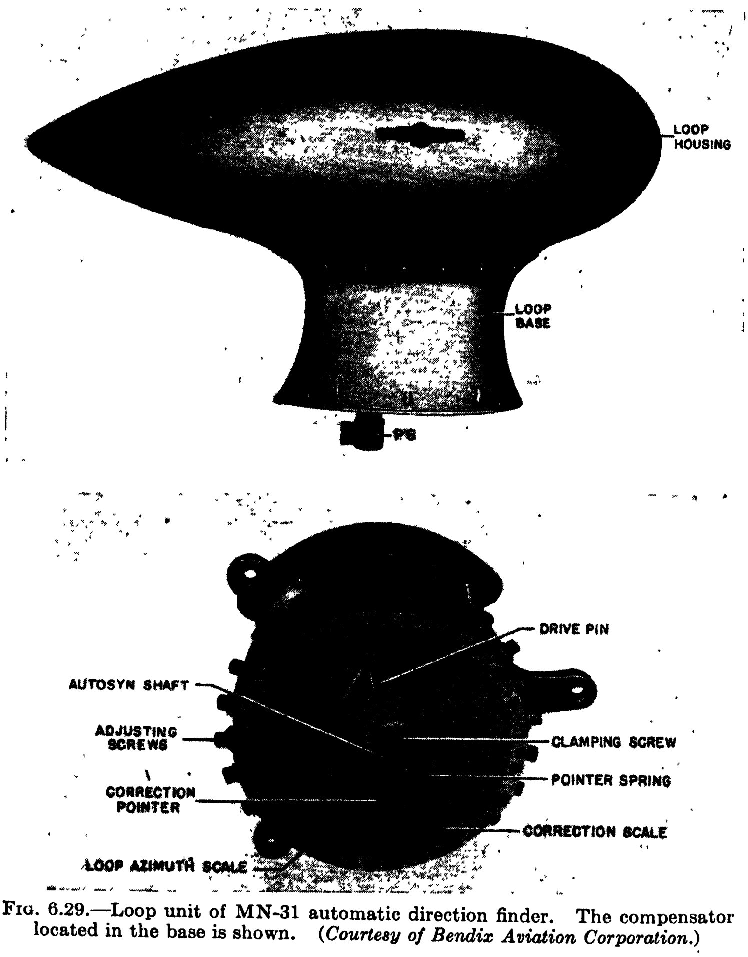


FIG. 6.29.—Loop unit of MN-31 automatic direction finder. The compensator located in the base is shown. (*Courtesy of Bendix Aviation Corporation.*)

part of the receiver. The control unit is separate from the bearing indicator. This latter arrangement is often of advantage when installation space in the cockpit of an airplane is at a

[1] These systems are known by such trade names as Autosyn or Selsyn.

premium. There is no provision in the MN-31 equipment for substitution of a "sense" loop for the nondirectional antenna under precipitation static conditions when automatic operation is required.

The interconnection diagram of the MN-31 automatic direction finder is shown in Fig. 6.25. The various major units are illus-

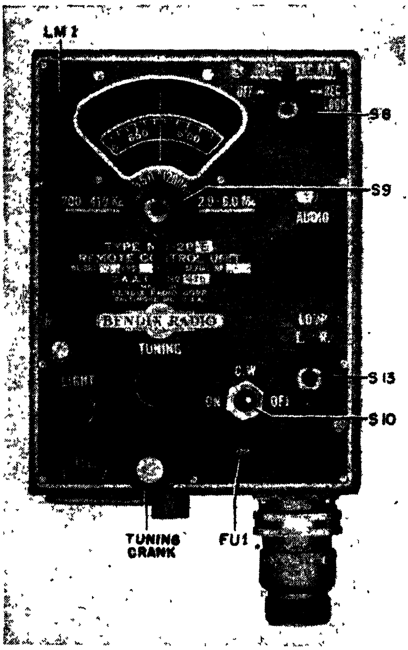


FIG. 6.30.—Remote-control unit of MN-31 automatic direction finder. Tuning, band-change, and function-selector controls are located here. (*Courtesy of Bendix Aviation Corporation.*)

trated in Figs. 6.26 to 6.30. The circuit embodies the same essential functions as are given in the block diagram of Fig. 6.01. Reference may be made to the complete circuit diagram of Fig. 6.31, for equipment serving as a direction finder on two bands (200 to 410 kc and 550 to 1200 kc) and as an airline communication receiver on the third band (2900 to 6000 kc).

6.15. Automatic Direction Finder Operation with the MN-31 Equipment. *Receiver Circuits.*—Some of the points of difference between the Bendix MN-31 direction finder and the Mark I

equipment may be seen by a study of Fig. 6.31. Operation of the circuit will be considered for the lowest band. The signal picked up by the shielded loop of the MN-36A unit is fed through a transmission cable to the loop circuit transformer *T*1 in the radio compass receiver unit. This transformer in turn couples to loop amplifier *V*1. This tube has the same sort of reactive plate load as in the apparatus previously considered. There is a resultant 90° phase shift of the signal between the grid of *V*1 and the grids of the following balanced modulator stage. This latter consists of a double triode *V*3 and performs the function of balanced modulator *A* of Fig. 6.01. The modulating frequency in this case is 48 cycles.

Because of a different type of motor control circuit, it is unnecessary to furnish power for the loop driving motor from this a-c source. Accordingly, the 48-cycle oscillator consists of *V*2 coupled to a tuned circuit consisting of transformer *T*5 and capacitor *C*7 in the MN-31A automatic loop control unit.

The carrier-suppressed double side-band output of the loop channel feeds from the plate of *V*3 in the receiver in push-pull fashion to the corresponding primary of antenna transformer *T*4. The nondirectional antenna is coupled to the other primary of *T*4, since under conditions of operation as an automatic direction finder the antenna relay *RE*1 is in the normal position shown. It will be noted that protective neon tubes, *NE*1 and *NE*2, are connected across the grid circuits of loop and antenna transformers, respectively, to prevent damage when a near-by transmitter is operated at or near receiver frequency.

The r-f amplifier system in the MN-31 contains two tubes, *V*4 and *V*5. The total number of tuned circuits is the same as in the Mark I, but the latter uses a so-called "link-coupled" circuit instead of the additional r-f amplifier tube. The converter or first detector *V*6 is driven from a separate oscillator tube *V*7. The advantage of the separation of tube functions in this stage is more evident on the h-f communication band. The intermediate frequency is 112.5 kc. Two wave traps tuned to this frequency are interposed in the cathodes of the r-f amplifier tubes to reduce the spurious response at intermediate frequency.

The i-f amplifier has tube *V*8 and two double-tuned transformers, *T*13 and *T*14, feeding into *V*10. This latter serves as detector, a.v.c., and first a-f stage. A separate CW oscillator

*V*9, work..g 1 kc above the intermediate frequency, is provided for communication reception with unmodulated waves. The tube may be turned on by means of a control on the operator's uni

T... ·sists ordinarily of *V*11 feeding into one or m... .iels. In case dual output is desired

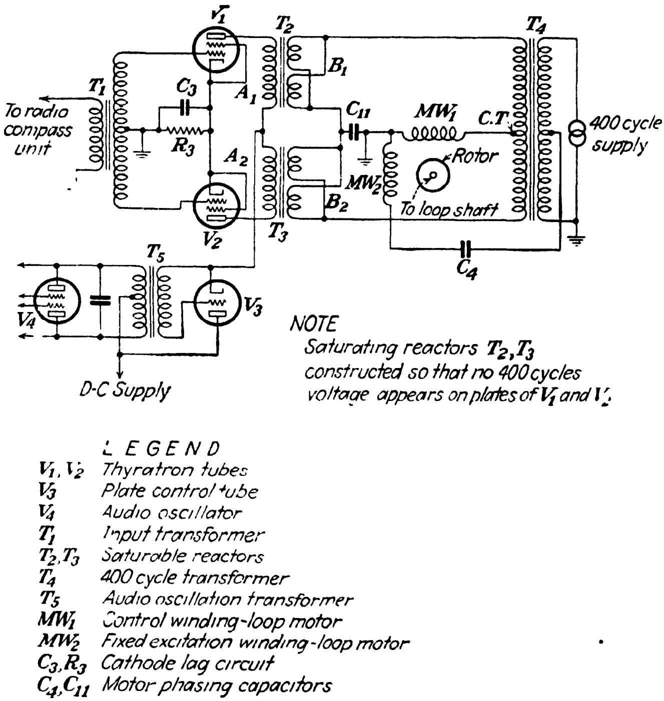


Fig. 6.32.—Simplified motor control circuit of MN-31 automatic direction finder. The symbols are the same as in Fig. 6.31.

with no interaction of one channel upon the other, a supplementary pair of output tubes may be used. These are included in the automatic loop control unit and are designated as *V*4 and *V*5. A dynamotor serves to furnish the *B* supply.

As in the Mark I system, loop overload control is secured by rectification of the control signal by the diode of *V*12 and connection of this output back to the grid return of amplifier *V*1 in the loop channel.

Loop Control Circuit.—Audio-frequency signal from the plate of $V10$ is fed to the compass output tube $V12$. It will be observed that transformer $T16$ is connected in the plate circuit of this tube and is tuned to the modulating frequency of 48 cycles. It thereby rejects the main portion of speech modulating frequencies and furnishes a 48-cycle signal of reversing phase and variable

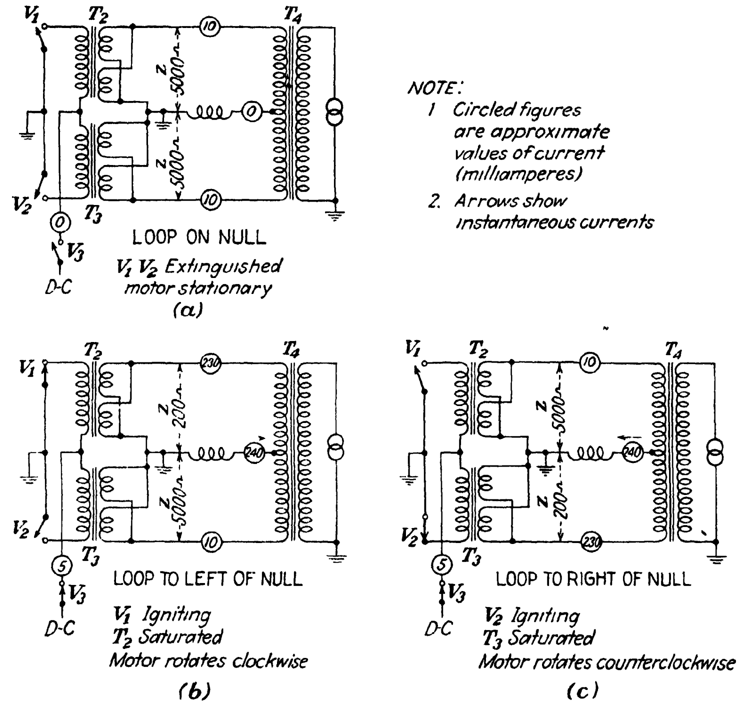


FIG. 6.33.—Typical current and impedance relations in motor control circuit using saturable reactors.

amplitude to the input of the automatic loop control unit. This voltage is applied through push-pull transformer $T1$ to the grids of thyratron tubes $V1$ and $V2$, in the same manner as in the Mark I design. The operation of the motor control circuit is rather different however. The simplified schematic diagram of Fig. 6.32 will illustrate the operation.

$T2$ and $T3$ in Fig. 6.32 are saturable reactors connected in the plate circuits of the two thyratrons. The d-c windings carry the

plate current whose magnitude determines the impedance measured across the a-c windings, *B*1 and *B*2. Motor winding *MW*1 becomes effectively connected to either terminal of transformer *T*4, dependent upon the impedance presented by *B*1 or *B*2. When the loop is at the null position, so that neither *V*1 nor *V*2 is conducting, both reactors, *T*2 and *T*3, present high impedance. As a consequence, there is then no current through *MW*1. This is illustrated in Fig. 6.33*a*. But when the loop is off the null position in one direction so that *V*1 is conducting, current flows from the appropriate half of the secondary of *T*4 through *B*1 and the phasing capacitor *C*11 to the motor winding *MW*1. This is case *b* of Fig. 6.33. On the other hand, when the phase of the 48-cycle voltage is reversed with respect to the plate supply on *V*1 and *V*2, it is *V*2 whose impedance becomes low, and a current from the 400-cycle supply of opposite phase flows through *MW*1. This is shown as case *c*.

The plates of *V*1 and *V*2 are excited in the same phase from a 48-cycle supply derived from transformer *T*5 in the loop control unit. Plate control tube *V*3 is fed from this supply, and its load is placed in the cathode circuit. On negative half cycles of the grid voltage *V*3 is cut off, but, on positive half cycles, voltage is applied to the plates of *V*1 and *V*2 through reactors *T*2 and *T*3.

At all times the second winding *MW*2 of the two-phase motor is excited continuously from a voltage obtained from the primary of *T*4 serving as a step-down autotransformer. Phasing capacitors *C*11 and *C*4 are in the circuits of *MW*1 and *MW*2, respectively. The proper conditions are thereby established for reversal of direction of rotation in accordance with the phase of the 48-cycle grid signal.

It is well to note at this point that such a circuit allows power to be supplied from a source of quite different frequency (400 cycles) from the modulating frequency (48 cycles) used in the loop circuit. As a result, the phase relationships of the two systems are entirely independent. Advantage is taken in such a circuit of the use of saturable reactors so that much lower power handling capacity of thyratrons *V*1 and *V*2 is necessitated. Each reactor is so wound that the split a-c windings which make up *B*1 or *B*2 induce very little alternating voltage in the plate winding *A*1 or *A*2. In small-size units, where the required torque is also small, it becomes feasible to keep motor winding *MW*2 con-

tinuously excited. The system of Mark I avoids this difficulty when the loop has reached the null position.

In the MN-31 direction finder antihunt operation is secured by two means. In the first place, the loop motor is designed to have extremely small moment of inertia. This becomes more practical because of the fact that it is not required to drive a tachometer type of flexible shaft connected to the bearing indicator unit. In the second place, the automatic loop control unit serves to give antihunt action by virtue of a circuit that is frequently referred to as an "anticipator." In the common cathode lead of thyratrons $V1$ and $V2$ a resistor-capacitor combination, $R3$ and $C3$, is included. When either thyratron passes plate current, the voltage across $R3$ biases off both tubes by an appropriate amount. Then, when the 48-cycle signal diminishes as the null point is being approached, a condition is reached at which the conducting tube is cut off. This will occur before the control signal reaches zero, and, as a result, the motor will coast (but with rapid damping) to the null point. The exact adjustment of $R3$ is not important because of the fact that if the loop stops short of the correct position, the d-c bias appearing across $C3$ will fall to zero in a very short interval. Then, if there is a control signal from $T1$ still present on the grids, the motor will start up again and complete its drive into the proper rest point.

Bearing Indicator System.—Indication of loop position is given by means of a self-synchronous transmission system. Mechanically connected to the loop is Autosyn transmitter $MO3$. At the indicator itself is a similar unit, receiver $MO4$. The rotor windings of these two units are connected in parallel across the 400-cycle supply. The phase windings, denoted by $\phi 1$, $\phi 2$, $\phi 3$ in Fig. 6.31 or the simplified circuit of Fig. 6.34, are interconnected. Then, if the two rotors do not occupy the same relative angular position, currents will be set up in the phase windings in a manner to develop a restoring torque and to bring the indicator unit, $MO4$, to the correct position. The angular accuracy of such a data transmission system is of the order of $\pm 1°$ since most of the fixed residual errors of a given installation may be corrected by means of the mechanical compensator described below. Power supply for the indicator unit and for the motor control circuits is derived from a rotating machine, a 400-cycle inverter, shown in Fig. 6.27.

Mechanically interposed between the loop with its motor drive and the self-synchronous transmitter, *MO3*, is a mechanical compensator. This is illustrated in Fig. 6.29. It shows the point of connection of the Autosyn shaft and the correction means. This latter consists of a series of adjusting screws spaced at 15° intervals around the periphery. These may be set to insert at each of these points as much as ±25° of angular displacement between the loop and the Autosyn unit. The correction scale indicates directly this compensation. This may be contrasted with the method used in the Mark I direction finder, where a cam, illustrated in Fig. 6.19, is cut to give the required correction. In the MN-31 unit the compensator adjustment

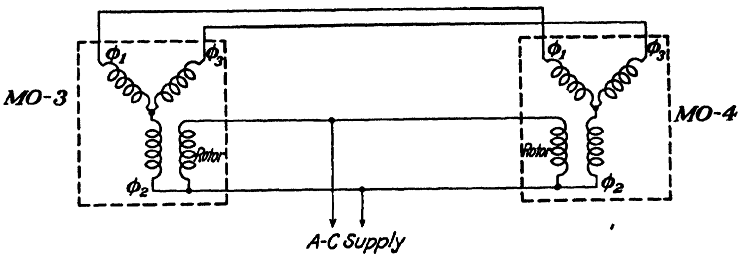


FIG. 6.34.—Autosyn bearing-indicator system of MN-31 automatic direction finder. *MO3* and *MO4* are located in loop and indicator units, respectively.

screws act to displace radially a flexible tape, against which a cam follower presses. Thus quadrantal or other types of error of a given installation may be compensated.

6.16. Right-left Direction Finders.—The second type of visual direction finders referred to on page 171 is the *right-left* or *homing* type. This system utilizes most of the same principles as have been discussed in connection with the study of self-orienting direction finders. The main differences are a sacrifice of operating convenience together with a reduction in equipment weight. Consequently, this type of apparatus finds favor on itinerant aircraft, while the fully automatic device is of greatest use on commercial airline or military airplanes.

The essential elements of a right-left visual direction finder are substantially the same as in Fig. 6.01. The main differences are that the output of balanced modulator *B* goes to a zero-center meter indicator; no loop driving motor is used; and the source of a-c supply may be of considerably lower power rating. The loop

is rotated by hand, and the pilot or navigator uses the zero-center meter to indicate whether the loop is turned to the right or to the left of the proper null direction.

In many designs the output of balanced modulator *B* is direct current, reversing in polarity as the phase of the a-c output of the a-f amplifier reverses. Then the indicator may be a d-c micro-ammeter of suitable range. Occasionally the balanced modulator and the meter functions are combined by the use of an a-c dynamometer type of meter. With such a unit, reversing phase alternating current is supplied from the amplifier to one winding of the meter, while the other is energized continuously with a fixed phase of a-c signal from the power supply. Since the power supply itself need not operate a driving motor, it is called upon to supply a much smaller amount of power than in an automatic direction finder. Consequently, it is frequently composed of a vacuum tube oscillator circuit.

Consideration of the polarity of the d-c output as a function of loop setting shows that the indicator gives a sense indication which is free from 180° ambiguity. This will be evident from Table XI, showing the direction of meter deflection as a function of the heading of the airplane with respect to the line of bearing of the station to which the equipment is tuned.

TABLE XI.—SENSE DETERMINATION WITH RIGHT-LEFT DIRECTION FINDER

Direction of flight	Meter deflection	Bearing of ship's head (referred to direction to station)
Toward station	Right	Right
	Left	Left
Away from station	Right	Left
	Left	Right

Analogous cases exist for other directions of flight. The same convention, as shown above, applies with reference to the orientation of the movable loop under such circumstances.

Balanced modulator *B* is frequently in accordance with the circuit of Fig. 6.09. In the analysis of Sec. 6.05, it was seen that there is a reversible d-c component of e_M. Thus the zero-center indicator meter is connected across the points at which e_M is measured. A large capacitor is usually shunted across the ter-

minals of the meter for damping purposes. Although such damping is not required on a strong modulated continuous carrier, extraneous bursts of noise or keying of the carrier will cause instability of the meter indication unless a suitable damping network is employed. As an alternative to the two-element modulator, one may use a balanced ring-type system like that of

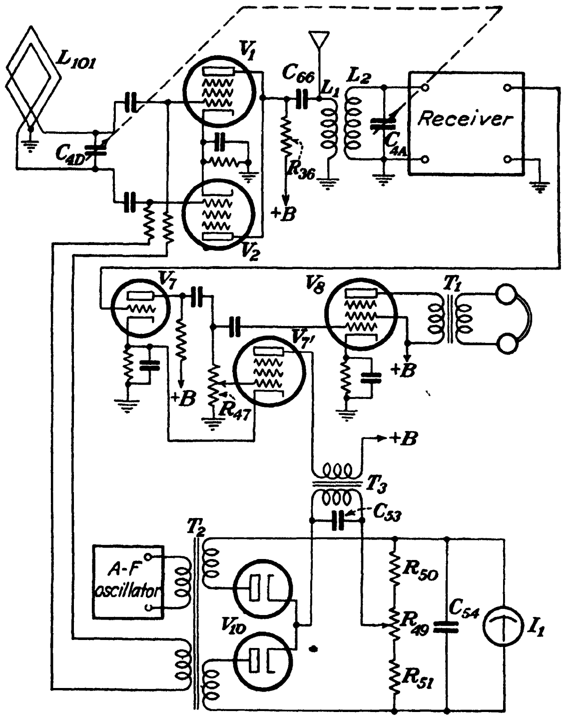


FIG. 6.35.—Simplified circuit of AVR-8F right-left direction finder. (*Courtesy of Radio Corporation of America.*)

Fig. 6.06. It is obviously necessary to use a suitable d-c load in the modulator output circuit.

A simplified circuit of a conventional right-left type of visual direction finder is shown in Fig. 6.35, with the detailed circuit shown in Fig. 6.36. This applies to the type AVR-8F equipment as manufactured by the Radio Corporation of America.[1] Signal

[1] E. D. BLODGETT and E. T. DICKEY, An Aircraft Radiocompass, *Communication and Broadcast Engineering*, **4**, No. 1, 14 (January, 1937).

from the rotatable loop $L101$ is fed in push-pull to the grids of loop modulators $V1$ and $V2$. The loop is tuned directly by means of capacitor $C4D$ ganged to the other tuning capacitors of the receiver. Tubes $V1$ and $V2$ are modulated in push-pull also at audio frequency from transformer $T2$. An analysis of such a circuit shows that the condition for carrier-suppressed double side-band output is that of *parallel* connection of the plates of $V1$ and $V2$. These are consequently coupled from the output load resistor $R36$ through $C66$ to the antenna circuit. Here the carrier is resupplied in the conventional manner, and the combined output is fed through the receiver proper.

The receiver output consists of an audio amplifier $V7$ (triode section), common to the phone and the direction finder channels, and separate amplifiers $V8$ and $V7'$ (pentode section of $V7$) for isolating one from the other. The gain of the compass channel may be varied by means of the course indicator sensitivity control $R47$. Transformer $T3$ provides the means of introducing voltage E_B, as illustrated in Fig. 6.09. The reference a-c voltage E_A of this same figure is introduced through transformer $T2$ from the a-f oscillator.

$V10$ contains the two nonlinear diode elements. The use of the split windings of $T2$ is necessitated because of the fact that the cathode connections of $V10$ are common. Direct voltage is developed across $R50$, $R49$, and $R51$. The return of $T3$ goes to the adjustment $R49$ to serve as a zero-centering adjustment of the meter $I1$. Capacitor $C54$, a low-voltage electrolytic unit of 200 μf, is the damping unit employed. Transformer $T3$ is tuned to the frequency of the a-f oscillator, 95 cycles, and serves simultaneously as a band-pass filter and as a means of setting initially the proper audio phase at balanced modulator B.

It will be observed from a study of the r-f phase relationship that the loop signal will not combine properly with the carrier if the loop circuit is tuned to resonance. This will be noted from a study of Sec. 4.02. In the case of the automatic direction finder, an additional stage was introduced to secure the necessary 90° phase shift. In the case of this right-left equipment, the loop circuit is purposely detuned by an amount sufficient to give approximately this necessary additional shift in phase. This results in some sacrifice in performance and the danger that, at some frequencies in the band, poor tracking will cause the circuit

to be detuned to the opposite side of resonance. Under the latter conditions, the phase will be shifted nearly 180° from its proper value, and a reversal of sense will result. For this reason a circuit with a detuned loop has not been used on more recent designs.

6.17. Experimental Methods of Direction Finder Testing.— The testing of the receiver circuits of a direction finder of the aural-null or the visual type may be carried out by conventional methods for receivers as outlined in Chap. I. Those properties,

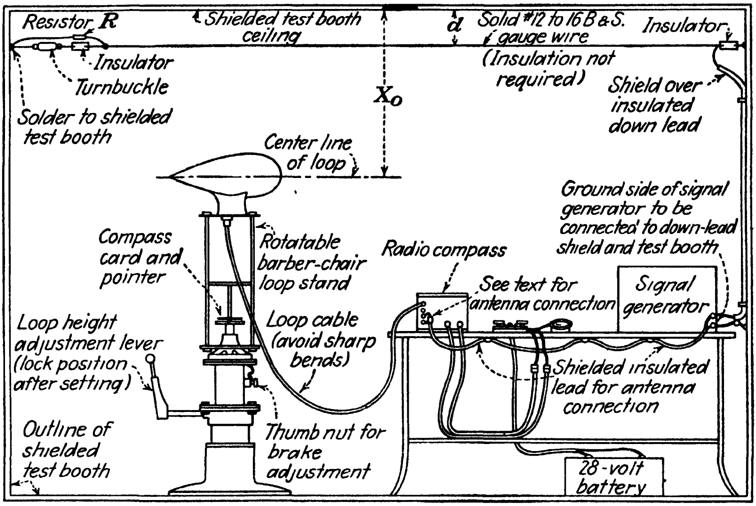


FIG. 6.37. Equipment arrangement suitable for the test of loop direction finders. A shielded test booth is required. The field due to the straight wire or test line has a known value at the loop location. A modified barber chair has been found to be a convenient rotatable support for the loop unit.

however, which depend upon the behavior of loops or other antennas in a field require a somewhat different experimental technique. It consists of generating in the vicinity of the antennas a field that simulates the actual electromagnetic radiation field encountered in normal operation. Although this is referred to in Secs. 1.07 and 1.08, details of the appropriate methods are not given there.

The magnetic field beneath a horizontal straight wire is used as the source of the field to simulate the field of a horizontally propagated, vertically polarized, plane radio wave. The experimental arrangement in a shielded test room is shown in Fig. 6.37.

The horizontal wire is fed from a signal generator at one end and is terminated with a suitable resistor R at the other end.

The loop is placed on a stand which may be rotated about a vertical axis. This is of especial value in the test of automatic direction finders, for in these, the loop itself will return to a fixed position with respect to the test line after its housing has been rotated. In any case the null of the figure-of-8 pattern of a loop occurs when the axis of the loop is parallel to the test line.

It is essential that the center of the loop be maintained at the distance from the line for which a field intensity calibration is known. The means of computing this latter is described in Secs. 6.18 and 6.19, and the corresponding experimental method is given in Sec. 6.20.

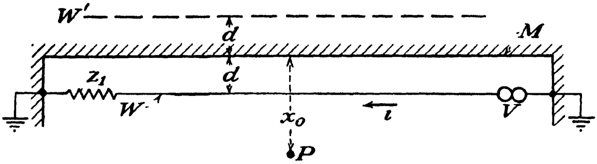


FIG. 6.38.—Transmission line located near conducting plane M. The wire W has a diameter a. Note in Eqs. (6.22) and (6.23) that the distance d is *half* the distance between W and its image W'.

When a sense antenna is required, it may consist of a wire parallel to the test line and of such length and separation as to give a pickup voltage properly related to the field intensity. Alternatively, a voltage divider may be connected across the output terminals of the signal generator and the antenna connection made to its tap. The dimensioning of a capacity voltage divider is discussed in Sec. 6.21.

6.18. Computation of Test Line Constants.—If one considers a test line adjacent to and parallel to the ceiling of a shielded room, the presence of the walls and the floor may be ignored. The field strength near the line for a given output from the signal generator used to feed the line will be computed. First of all it will be assumed that the line is terminated in its characteristic impedance to prevent standing waves. It is evident that a wire W parallel to an infinite conducting plane behaves as if there were an image wire W' on the opposite side of the plane and at a like distance as shown in Fig. 6.38. This two-wire line has a characteristic

impedance given by the well-known formula

$$Z_2 = 276 \log_{10} \frac{4d}{a} \tag{6.22}$$

where a is the diameter of W, measured in the same units as d. Z_2 is in ohms. The characteristic impedance Z_1 between W and the plane M is half this, since two equal impedances, each equal to Z_1, are in series to constitute Z_2. Hence for the impedance of a single wire of diameter a at a distance d from a conducting plane

$$Z_1 = 138 \log_{10} \frac{4d}{a} \tag{6.23}$$

The magnetic field H at a point P at a distance x_0 below the metal plane of Fig. 6.38 consists of components H_1 and H_2.

$$H_1 = \frac{2i}{x_0 - d} \tag{6.24}$$

since if the wire is long and terminated in Z_1, the position of P along the wire is not important.

Here i is the current in abamperes or e.m.u. through the wire, as may be deduced from Eq. (A.6) in Appendix A. For the image W' through which the return current may be assumed to flow

$$H_2 = -\frac{2i}{x_0 + d} \tag{6.25}$$

Consequently the field due to both is

$$H_{\text{emu}} = \frac{2i_{\text{amp}}}{10}\left(\frac{1}{x_0 - d} - \frac{1}{x_0 + d}\right) \tag{6.26}$$

Associated with this induction magnetic field is a fictitious electric field E having a magnitude in e.s.u. equal to H in e.m.u. as shown on page 263. The quantity E is defined so that, if H represented the magnetic field due to radiation in free space, then E would be the corresponding *radiation electric field*. Thus, if the appropriate value of i is inserted, it is found that

$$\begin{aligned} E &= \frac{2V}{10Z_1}\left(\frac{1}{x_0 - d} - \frac{1}{x_0 + d}\right) \\ &= \frac{0.4V}{Z_1}\left(\frac{d}{x_0^2 - d^2}\right) \end{aligned} \tag{6.27}$$

Here E is in e.s.u. or statvolts per centimeter if x_0 and d are in centimeters. V and Z_1 are in volts and ohms, respectively.

Since E (volts per meter) $= 100E$ (volts per centimeter) $= 3 \times 10^4 E$ (e.s.u.)

$$E_{\text{volts/m}} = \frac{1.2 \times 10^4 V}{Z_1}\left(\frac{d}{x_0^2 - d^2}\right) \tag{6.28}$$

If the line constant K is defined as

$$K = \frac{V}{E} \tag{6.29}$$

it is evident that K in meters is given by

$$K = 8.33 \times 10^{-5} Z_1 \left(\frac{x_0^2 - d^2}{d}\right) \tag{6.30}$$

When x_0 and d are in inches, this becomes

$$K = 2.115 \times 10^{-4} Z_1 \left(\frac{x_0^2 - d^2}{d}\right) \tag{6.31}$$

This is the desired result for an infinitesimal loop at the point P.

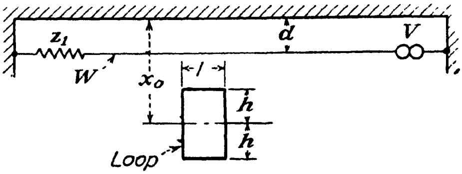


FIG. 6.39.—Rectangular loop located near transmission line and conducting plane.

When K is known, the field strength E may be determined from the signal generator output voltage V by means of Eq. (6.29).

6.19. Test Line Constants (Nonhomogeneous Fields).—A rectangular loop antenna of dimensions comparable to x_0 is illustrated in Fig. 6.39. When the loop is not near either end, the field is constant in a direction parallel to W. For convenience, then, the loop will be assumed to be of unit length in this direction. With x_0 the distance to the center of the loop of height $2h$, one may find the equivalent magnetic field H_{eq} from the total flux ϕ by the relation

$$H_{eq} = \frac{\phi}{A} = \frac{\phi}{2h} \tag{6.32}$$

where A is the loop area. The flux through the loop is

$$\phi = \int_{x_0-h}^{x_0+h} H\,dx \tag{6.33}$$

where H is given by Eq. (6.26) with x_0 replaced by x. This may be expressed in terms of an equivalent E

$$E_{eq} = \frac{1}{2h}\int_{x_0-h}^{x_0+h} \frac{1.2 \times 10^4 V}{Z_1}\left(\frac{d}{x^2 - d^2}\right) dx \tag{6.34}$$

$$= \frac{6 \times 10^3 Vd}{hZ_1}\int_{x_0-h}^{x_0+h} \frac{dx}{x^2 - d^2} \tag{6.35}$$

$$= \frac{6 \times 10^3 Vd}{hZ_1}\left(\frac{1}{2d}\log\frac{x-d}{x+d}\right)_{x_0-h}^{x_0+h} \tag{6.36}$$

$$= \frac{3 \times 10^3 V}{hZ_1}\log\frac{(x_0+h-d)(x_0-h+d)}{(x_0+h+d)(x_0-h-d)} \tag{6.37}$$

$$K_{eq} = 3.33 \times 10^{-4} Z_1 h \left[\frac{1}{\log\dfrac{x_0^2-(h-d)^2}{x_0^2-(h+d)^2}}\right] \tag{6.38}$$

Here the units are as in Eq. (6.30). For K_{eq} in meters when x_0, h, and d are in inches, the result is

$$K_{eq} = 8.45 \times 10^{-4} Z_1 h \left[\frac{1}{\log\dfrac{x_0^2-(h-d)^2}{x_0^2-(h+d)^2}}\right] \tag{6.39}$$

for a rectangular loop. Note that *natural* logarithms are used throughout.

A comparison of the line constants for the infinitesimal loop and the finite rectangular one shows how much a correction must be made for the latter case. From Eqs. (6.31) and (6.39),

$$\frac{K}{K_{eq}} = \frac{x_0^2 - d^2}{4hd}\log\frac{x_0^2-(h-d)^2}{x_0^2-(h+d)^2} \tag{6.40}$$

For simplification one may let

$$\left.\begin{aligned} \alpha &= \frac{h}{d} \\ \beta &= \frac{x_0}{d} \end{aligned}\right\} \tag{6.41}$$

Then Eq. (6.40) becomes

$$\frac{K}{K_{eq}} = \frac{\beta^2 - 1}{4\alpha} \log \frac{\beta^2 - (\alpha - 1)^2}{\beta^2 - (\alpha + 1)^2} \tag{6.42}$$

Since

$$\log x = 2\left[\frac{x-1}{x+1} + \frac{1}{3}\left(\frac{x-1}{x+1}\right)^3 + \frac{1}{5}\left(\frac{x-1}{x+1}\right)^5 + \cdots\right] \tag{6.43}$$

and this series converges for $x > 0$,

$$\log \frac{\beta^2 - (\alpha - 1)^2}{\beta^2 - (\alpha + 1)^2} = 2\left[\frac{2\alpha}{\beta^2 - \alpha^2 - 1} + \frac{1}{3}\left(\frac{2\alpha}{\beta^2 - \alpha^2 - 1}\right)^3 + \frac{1}{5}\left(\frac{2\alpha}{\beta^2 - \alpha^2 - 1}\right)^5 + \cdots\right] \tag{6.44}$$

$$\frac{K}{K_{eq}} = \frac{\beta^2 - 1}{2\alpha}\left[\frac{2\alpha}{\beta^2 - \alpha^2 - 1} + \frac{1}{3}\left(\frac{2\alpha}{\beta^2 - \alpha^2 - 1}\right)^3 + \frac{1}{5}\left(\frac{2\alpha}{\beta^2 - \alpha^2 - 1}\right)^5 + \cdots\right] \tag{6.45}$$

Because of the rapidity of convergence of this series unless α is nearly as large as β, one need retain only the first term. Hence approximately

$$\frac{K}{K_{eq}} = \frac{\beta^2 - 1}{\beta^2 - \alpha^2 - 1}$$

or

$$\frac{K_{eq}}{K} = 1 - \frac{\alpha^2}{\beta^2 - 1} \tag{6.46}$$

This is illustrated in Fig. 6.40.

Example.—Thus for the following conditions:

d = distance from ceiling to test line = 12 in.
x_0 = distance from ceiling to center of loop = 36 in.
$2h$ = height of loop = 12 in.

Then $\alpha = 0.5$ and $\beta = 3$, and thus

$$\frac{K_{eq}}{K} = 0.968$$

The line constant is thus 3.2 per cent less for the rectangular loop than for a small loop at its center. From Eq. (6.23) for a line of No. 12 Brown and Sharpe gauge wire (diameter = 0.0808 in.), properly terminated:

$$\begin{aligned} Z_1 &= 138 \log_{10} \frac{4 \times 12}{0.0808} \\ &= 138 \times 2.7731 \\ &= 382 \text{ ohms} \end{aligned}$$

Then, from Eq. (6.31),

$$K_{eq} = 0.968 \times 2.115 \times 10^{-4} \times 382 \left(\frac{36^2 - 12^2}{12}\right)$$
$$= 7.50 \text{ m}$$

Thus for a field strength of 1000 μv/m at the loop location, the signal generator serving as the source must have an output of 7500 μv.

For a circular loop, ϕ may be found by integration of H over the loop area, but the result is cumbersome. Rather an approxi-

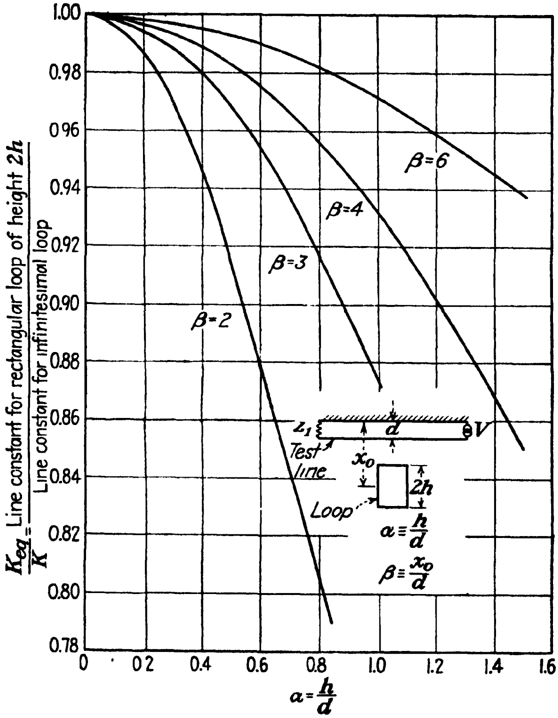


FIG. 6.40.—Correction factor to test line constant for rectangular loop of height h.

mate method may be used to bound the value of K_{eq}/K for the circular loop. If the loop is of radius r, one may circumscribe a square loop of sides $2r$ so that $h = r$. This establishes the lower bound for K_{eq}/K. If a square is inscribed in the circle it

will have sides $\sqrt{2}r$, or $h = \sqrt{2}r/2$, and K_{eq}/K has an upper bound.

$$\left(\frac{K_{eq}}{K}\right)_{h=r} < \left(\frac{K_{eq}}{K}\right)_{circ} < \left(\frac{K_{eq}}{K}\right)_{h=0.707r} \tag{6.47}$$

Example.—For a loop 12 in. in diameter, $r = 6$ in., and for d and x_0 as above

$$\left(\frac{K_{eq}}{K}\right)_{h=6} < \left(\frac{K_{eq}}{K}\right)_{circ} < \left(\frac{K_{eq}}{K}\right)_{h=4.23}$$

For the first member $\alpha = 0.5$, and for the third $\alpha = 0.353$, and $\beta = 3$ for each case.

$$0.968 < \left(\frac{K_{eq}}{K}\right)_{circ} < 0.984$$

and this establishes the correction factor with enough accuracy except for very large loops near the test line.

The exact equation for the line constant of a circular loop is

$$K_{eq\,(circ)} = 2.12 \times 10^{-4} Z_1 \frac{r^2}{\sqrt{(x_0 + d)^2 - r^2} - \sqrt{(x_0 - d)^2 - r^2} - 2d} \tag{6.48}$$

When $x_0 >> r$, the denominator is the difference between two large quantities which are nearly equal, and under these conditions this equation is not suitable for computation. But for a large loop near the line, this limitation does not exist. This is the condition, moreover, under which Eq. (6.47) would not be applicable.

6.20. Measurements of Test Line Constants.—It is evident from Eq. (6.29) that the line constant K may be determined experimentally at any frequency by a measurement of the field intensity E with the conventional field intensity meter. The signal generator output V is the indicated value, corrected for the loading effect of Z_1. For a properly terminated line, K is independent of frequency.

By an alternative method no field intensity meter is required. In this method any convenient receiver (the receiver of a direction finder, for example) is used as a high-impedance vacuum tube voltmeter tuned to signal frequency. For instance, it may be the automatic direction finder whose circuit is given in Fig. 6.21.

An auxiliary calibration loop, whose natural resonant frequency is much higher than the highest test frequency, is constructed to have the appropriate dimensions, usually approximately the same as those of the loop of the equipment to be tested. A convenient method of constructing the auxiliary calibration loop suitable for this direction finder is shown in Fig. 6.41.

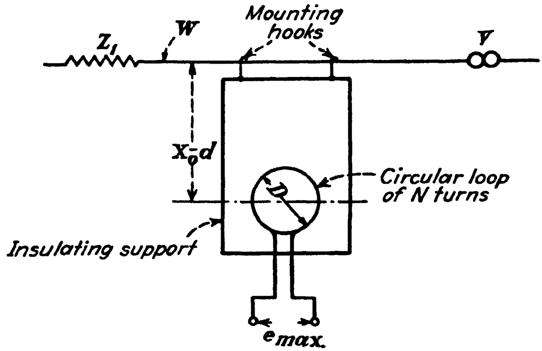


FIG. 6.41.—Experimental method of measuring test line constant. The calibration loop shown should be of the same dimensions and be located at the same position as the direction finder loop. The insulating support may be a sheet of bakelite.

The method of calibration consists of

1. Applying to the test line a signal generator voltage V at a frequency f.

2. Measuring the voltage e_{max} across the calibration loop terminals, using a high-impedance vacuum tube voltmeter (receiver).

3. Calibrating this tube voltmeter from the signal generator. From Eq. (3.29) for the maximum value of e with $\theta = 0$

$$e_{max} = \frac{2\pi NAf}{c} E \tag{6.49}$$

where $E = E_{max}$. Then

$$K = \frac{2\pi NAfV}{ce_{max}} \tag{6.50}$$

For a circular loop of diameter $D = 2r$ this becomes

$$K = 1.06 \times 10^{-8} ND^2 f_{kc} \frac{V}{e_{max}} \tag{6.51}$$

when D is in *inches* and K in *meters*.

Example.—For the loop of Fig. 6.41 at a frequency $f = 400$ kc,

$$N = 1 \quad \text{and} \quad D = 7.5$$

and, if $V = 50{,}000$ μv when $e_{max} = 2$ μv, then

$$K = 1.06 \times 10^{-8} \times 7.5^2 \times 400 \times \frac{50{,}000}{2}$$
$$= 5.96 \text{ m}$$

6.21. Dummy Sense Antenna Constants.—As is shown in Sec. 3.08, there is an optimum ratio of loop to vertical (nondirectional) antenna pickup for a cardioid pattern or for visual direction finder operation. The nondirectional antenna pickup is usually expressed in terms of the effective height h_e as dis-

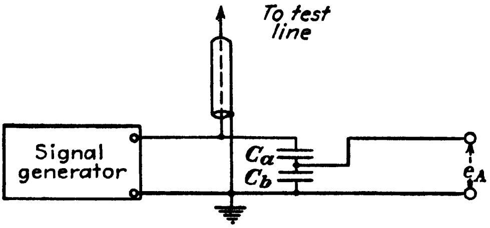


FIG. 6.42.—Voltage divider for securing proper vertical antenna pickup in a standard field from a test line.

cussed on pages 28 and 84–86. The open-circuit voltage at the base of such an antenna is

$$e_A = h_e E \tag{6.52}$$

Under the test line, E is given by Eq. (6.29), so that

$$e_A = \frac{h_e V}{K} \tag{6.53}$$

Thus an antenna input voltage e_A may be obtained from the signal generator as shown in Fig. 6.42 if a suitable voltage divider is employed to give the ratio

$$\frac{e_A}{V} = \frac{h_e}{K} \tag{6.54}$$

With a capacity divider the proper total dummy input capacity C_1 may be obtained by letting

$$C_1 = C_a + C_b \tag{6.55}$$

and

$$\frac{e_A}{V} = \frac{C_a}{C_a + C_b} \tag{6.56}$$

as was discussed in Sec. 4.05.

$$C_a = C_1 \frac{h_e}{K} \tag{6.57}$$

Example.—If $h_e = 0.2$ m, $K = 5.96$ m, and the proper dummy antenna capacity $C_1 = 100$ $\mu\mu$f; then

$$\begin{aligned} C_a &= 100 \times \frac{0.2}{5.96} \\ &= 3.35\ \mu\mu\text{f} \\ C_b &= C_1 - C_a \\ &= 96.7\ \mu\mu\text{f} \end{aligned}$$

Obviously, C_a and C_b should be located as near as possible to the antenna input terminals on the direction finder as shown in Fig. 6.37.

Bibliography

BLODGETT, E. D. and E. T. DICKEY: An Aircraft Radiocompass, *Communication and Broadcast Engineering*, **4**, 14 (January, 1937).

BUSIGNIES, H.: The Automatic Radio Compass and Its Application to Aerial Navigation, *Communication and Broadcast Engineering*, **4**, 10 (January, 1937).

———: The Automatic Radio Compass and Its Application to Aerial Navigation, *Electrical Communication*, **15**, 157 (October, 1936).

CARUTHERS, R. S.: Copper Oxide Modulators in Carrier Telephone Systems, *Bell System Tech. J.*, **18**, 315 (April, 1939).

HUCKE, H. M.: Precipitation-static Interference on Aircraft and at Ground Stations, *Proc. I.R.E.*, **27**, 301 (May, 1939).

MORGAN, H. K.: Rain Static, *Proc. I.R.E.*, **24**, 959 (July, 1936).

PETERSON, E., and L. W. HUSSEY: Equivalent Modulator Circuits, *Bell System Tech. J.*, **18**, 32 (January, 1939).

CHAPTER VII

RADIO NAVIGATION AIDS

7.01. Navigation Methods.—The term *navigation* will be used to refer to the determination of position coordinates on the earth's surface. No essential distinction will be made between the problems of sea and air navigation. The use of radio aids is important for both problems but, because the development has been so much more rapid under the impetus of flying requirements and since some of the radio equipment is peculiar to aviation only, this latter will be described in the greater detail. It becomes then only a simple matter to translate an aviation problem into one of navigation of a surface vessel.

There are four generally accepted means for solving a navigation problem:

1. *Piloting.*—This is the process of directing the airplane or other craft with respect to visible landmarks whose positions are known.

2. *Dead Reckoning.*—In this method information as to distance and direction traversed from a given known position is employed to give the new location. It is obvious that this ignores such factors as drift due to wind or current of unknown or varying characteristics.

3. *Radio Navigation.*—In such a procedure, the position of the craft is determined from radio bearings or other radio indications.

4. *Celestial Navigation.*—This is position determination by means of sextant observations of heavenly bodies at a known time.

In a discussion of radio direction finders, one obviously concentrates his attention upon the third of these methods; but certain navigation features, such as the use of maps and charts, are common to all and hence should be studied in enough detail so that intelligent utilization of bearings as obtained from a radio direction finder can be carried out. In the case of long-distance flights for aircraft, the four methods have been employed and

developed to their present status in the order named. At the present time for transcontinental flights, the first three methods are extensively employed, radio navigation being of especial importance when the ground is obscured from view. In long over-water flights, methods 2, 3, and 4 may be used to serve as checks upon each other.

7.02. Map Projections.—The necessity of knowing the location of the point of departure and the destination of a flight is so obvious as to require no comment. It is equally essential to have a knowledge of the intervening terrain, the location of intermediate radio stations and emergency facilities, and a knowledge of the most satisfactory route to follow from starting point to destination. This demands the use of maps or, more properly, *charts*. One may distinguish these two terms by defining "charts" as those maps that are especially suited for use in navigation. The choice of a chart as to scale and dimensions is determined by the navigation problem that is to be solved.

One must start with the fundamental surface to be represented, that of the earth, which will be assumed to be spherical for the order of accuracy required. The accuracy of a chart must be determined by comparison of it with the actual surface of a sphere. There is a fundamental distinction between two types of three-dimensional surfaces: *developable* and *nondevelopable* surfaces. A surface of the former class may be spread out into a plane surface without distortion or tearing. An example of this is the surface of a cylinder. This can obviously be broken along a surface element parallel to the axis, and the outer surface flattened out to form a rectangle. In this latter plane surface, directions from one point to another on the surface are retained, and likewise areas are represented in their proper proportions. Another example is a conical surface, which can be developed into a sector of a circle. It retains the same properties of correct representation of angles and of areas as did the prototype cone.

In contrast, a sphere is an example of a nondevelopable surface. It is readily seen that no finite number of breaks of the surface will allow it to be spread out into a plane without crowding, stretching, or tearing. Map making consists in choosing a developable three-dimensional surface that gives a good enough approximation to the spherical surface to represent one or more characteristics properly and within the required degree of accu-

racy, and then using the plane development of this auxiliary developable surface. There is no unique choice, and a representation or projection that may be suitable for one purpose, such as the accurate measurement of distances, may be very unsatisfactory for some other need, perhaps the true representation of areas.

Actually, map making involves the first step of choosing this developable surface and projecting on it from the sphere the series of lines representing meridians and parallels of latitude. This may be done by graphical means or by a mathematical computation. When the surface is then developed, the coordinate system of a chart projection is established. After this has been done, the details of the area to be represented may be filled in by reference to the coordinates set up on the projection.

There are a number of desirable properties that one looks for in a projection of this sort. It may be possible to secure but one of them accurately, or on the other hand a compromise may be made that represents two or more with a reasonable degree of accuracy. The larger the area to be represented, the more difficult is it to do justice to all the desirable properties at the same time.

1. It is desirable to retain the true shape of physical features, including the correct representation of angles.

2. Equal areas on a sphere should be represented by equal areas on the projection. In general, then, areas should be represented in their true relative proportions.

3. A true scale of distance values is desired, preferably one that remains unchanged at all points and in all directions on the surface of the map.

Other properties are often desired, although they may be subordinate to the three mentioned above:

4. Great circles should be represented as straight lines. A great circle on a sphere is the line of intersection of the surface with a plane passing through the center of the sphere.

5. Rhumb lines should be represented as straight lines. A rhumb line is a curve on a sphere that makes equal angles with all meridians. It is obvious that, under most conditions, 4 and 5 cannot be fulfilled simultaneously.

Of the many hundred types of projections that have been invented, there are only two that are of fundamental importance

for navigation problems. One or two others are occasionally used for planning purposes although not in flight. The two that find general application are the *Mercator* and the *Lambert conformal conic.*

7.03. Mercator Projection.—This chart projection is used almost exclusively for nautical charts. It is a developable surface of the cylindrical type. One might imagine a cylinder whose axis coincides with that of the earth being placed tangent to the latter at the equator. Then the projection of the parallels of latitude would be a series of circles spaced farther and farther apart as the latitude increases. The spacing in fact would vary as the secant of the latitude. The meridians would be projected upon the cylindrical surfaces as a series of equidistant lines all parallel to the earth's axis. When this surface is developed, there results a rectangular grid with parallel meridians crossed at right angles by straight lines representing latitude circles. These latter are spaced at greater and greater distances toward the upper and lower extremities of the map. With this type of representation, the scale increases indefinitely as the poles are approached. If such a Mercator projector is used to represent the entire earth's surface, the scale changes quite rapidly even between the northern and southern boundaries of the United States. For example, if it is 8 miles/in. in southern latitudes, it drops to 4.8 miles/in. along the Canadian border. The great advantage provided by a Mercator projection is that rhumb lines are represented by straight lines. Since a surface vessel usually steers by means of the compass, this means that a constant course angle, as indicated by the compass, may be maintained over a considerable length of time, perhaps a whole day's sailing. An actual long-distance east-west trip is then a series of successive rhumb lines. There are two very great disadvantages of such a projection however. In the first place, the area is very badly distorted. On a Mercator projection, one could easily estimate that Greenland has an area greater than that of the United States, whereas the actual area is only about one-fourth as great. In the second place, the rapidly changing scale makes the computation of distances extremely difficult. The projection from the sphere on the cylindrical surface is illustrated in Fig. 7.01 while the development to give the final Mercator projection is shown in Fig. 7.02.



FIG. 7.01.—Projection of a sphere on a cylindrical surface. [*Courtesy of Life Magazine*, **13**, *No.* 5, 57 (*Aug.* 3, 1942).]

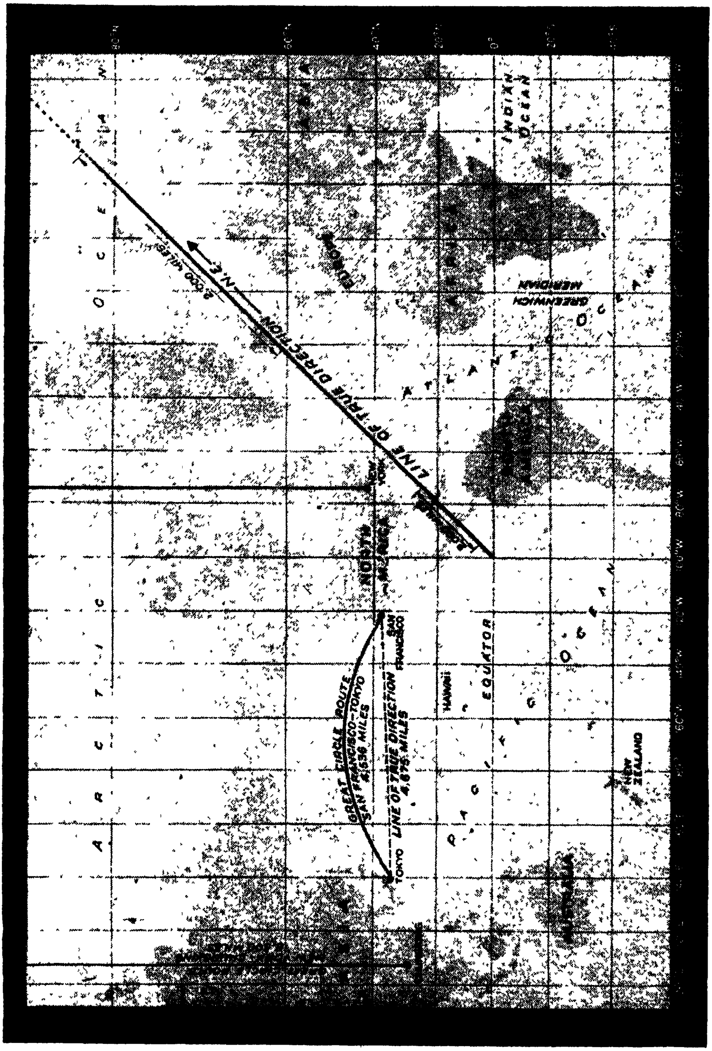


FIG. 7.02.—Plane development of cylindrical projection to form a Mercator map. [*Courtesy of Life Magazine*, 13, *No.* 5, 57 (*Aug.* 3, 1942).]

7.04. Lambert Conformal Conic Projection.—Of much greater use for air navigation in areas as large as the whole of the United States is the Lambert projection.[1] (The designation *Lambert* will be used to represent the *Lambert conformal conic* system.) In this a cone is caused to coincide with the earth's surface along two parallels of latitude, the axis of the cone coinciding with that of the earth. These two small circles of intersection are referred to as the "standard parallels." Such a projection method is illustrated in Fig. 7.03. The development for the United States is given in Fig. 7.04. It is instructive to compare the complete projection for the Northern Hemisphere in Figs. 7.05 and 7.06. This latter is not strictly a Lambert conformal conic because the two standard parallels have been permitted to coincide at 45°N.

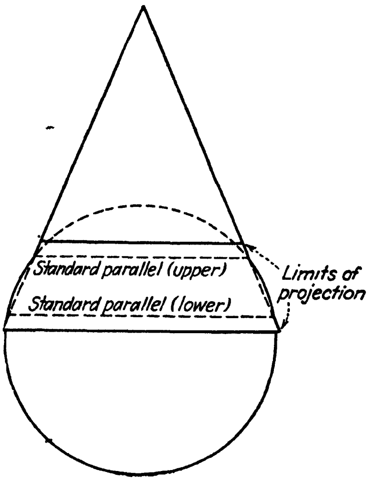


FIG. 7.03.—Method of obtaining a Lambert conformal conic projection. The two circles of intersection of the cone with the sphere are the "standard parallels."

When an area in middle latitudes is to be represented, the standard parallels are chosen near, but not at, the limits of the projection in latitude. For example, in the U.S. Coast and Geodetic Survey Lambert projection of the United States, the standard parallels are 33 and 45°N., and the limits of the projection are from 25 to 49°N.

On a Lambert the meridians are straight lines, but they converge to a point that is usually off the surface of the map. This is the developed apex of the cone. At right angles to these lines are concentric circles, these arcs representing the parallels of latitude. This system of orthogonal coordinates maintains the accuracy of angular representation.

[1] Much of the following discussion follows the presentation given by T. C. Lyon, Practical Air Navigation, *Civil Aeronautics Bull.* 24, U.S. Government Printing Office, Washington, D.C., 1940.



FIG. 7.04.—Lambert conformal conic map of the United States. The standard parallels, 33 and 45° N., are chosen to make the average scale errors over the entire projection as small as possible.

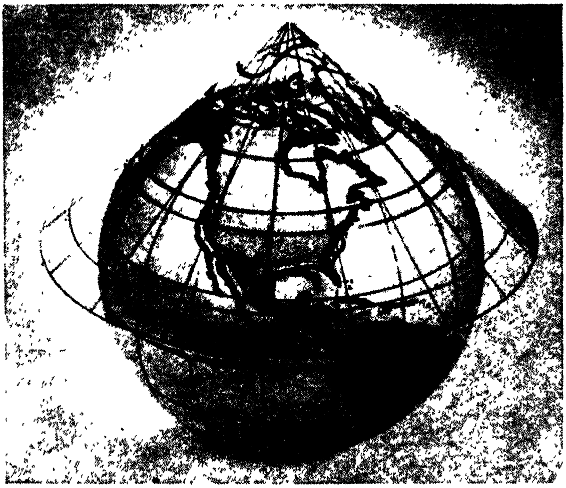


FIG. 7.05.—Projection of a sphere on a conical surface. For illustrative purposes the cone has been chosen to be tangent at one parallel only. This is the limiting case of a Lambert conformal conic projection. [*Courtesy of Life Magazine*, **13**, *No.* 5, 57 (*Aug.* 3, 1942).]

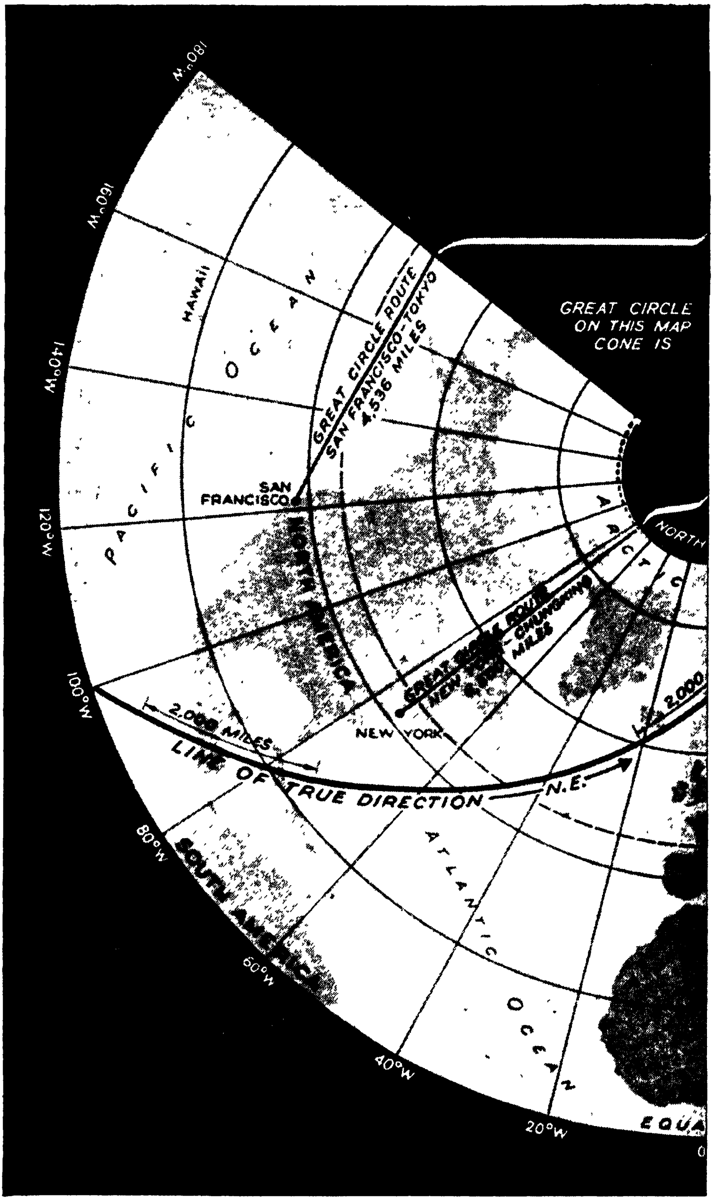


FIG. 7.06.—Plane development of the conical projection of the Northern



Hemisphere. [*Courtesy of Life Magazine*, **13**, *No.* 5, 57 (*Aug.* 3, 1942).]

There are several advantages to the Lambert that result from the fact that it is essentially a compromise system. The angular representation is accurate owing to the method of establishing the coordinate system. The scale properties are nearly enough accurate for areas as large as the United States. For example, in the Coast and Geodetic map referred to above, the scale error is less than about 0.5 per cent between the standard parallels and is still rather small at the northern and southern extremities. This may be illustrated as follows:

Latitude, °	Scale, Per Cent
25	102 34
33	100
39	99.45
45	100
49	101.04

A straight line on a Lambert projection is very close to a great circle. There is actually a slight deviation on this for an east-west line measured at either the northern or southern boundary of the United States.

The scale is such that adjacent charts of smaller sections to the same scale may be joined together without a break. The compromise of these conditions makes this projection the most suitable for rad'. navigation purposes, and it will be found that the majority of the aeronautical charts are on the Lambert projection with this in view. There is a disadvantage that straight lines do not represent great circles exactly. For flights of increasing length this means that the initial planning may be carried out with a great-circle or *gnomonic* chart if the greatest accuracy is desired.

7.05. Gnomonic Projection.—If a plane is made tangent to the sphere and the coordinates projected from the center of the sphere to this plane, there results a *gnomonic* projection. It will readily be seen that certain planes through the center of the sphere intersect this latter as great circles and also strike the tangent plane as straight lines passing through the point of tangency. Thus all straight lines passing through the center of projection of the plane map represent great circles. To this property the gnomonic projection owes its usefulness, for directions and distances *from this one point* are correctly represented. Courses may be laid out and radio bearings determined here



FIG. 7.07.—Projection of a sphere on a tangent plane. This is a gnomonic projection. [*Courtesy of Life Magazine*, **13**, *No.* 5, 57 (*Aug.* 3, 1942).]

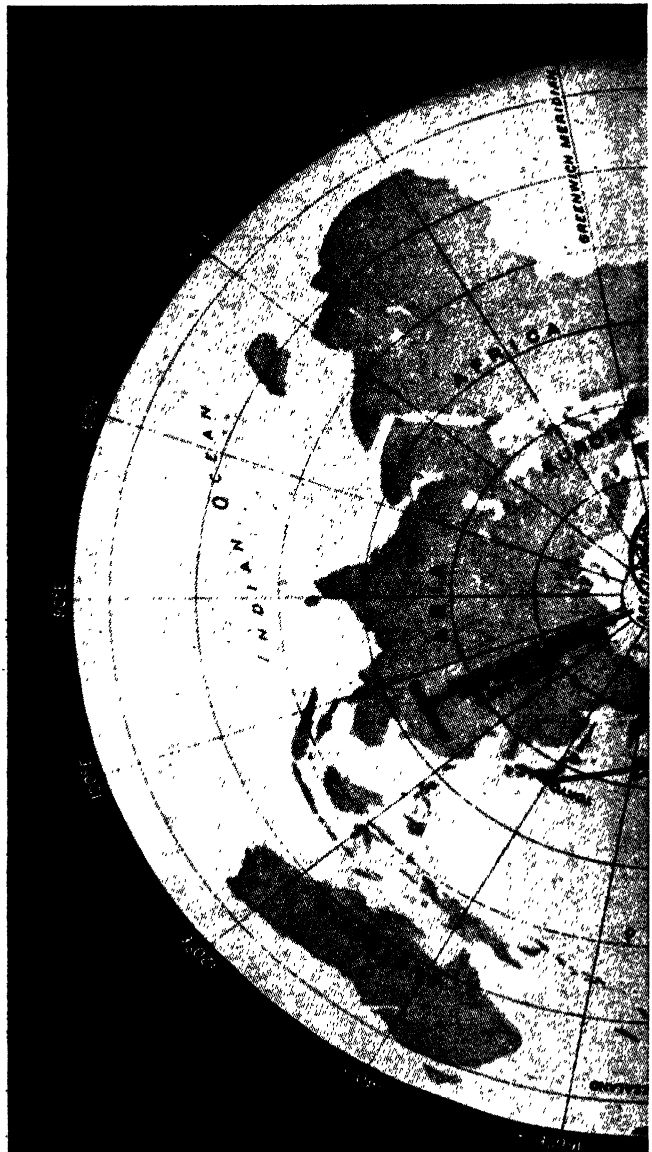
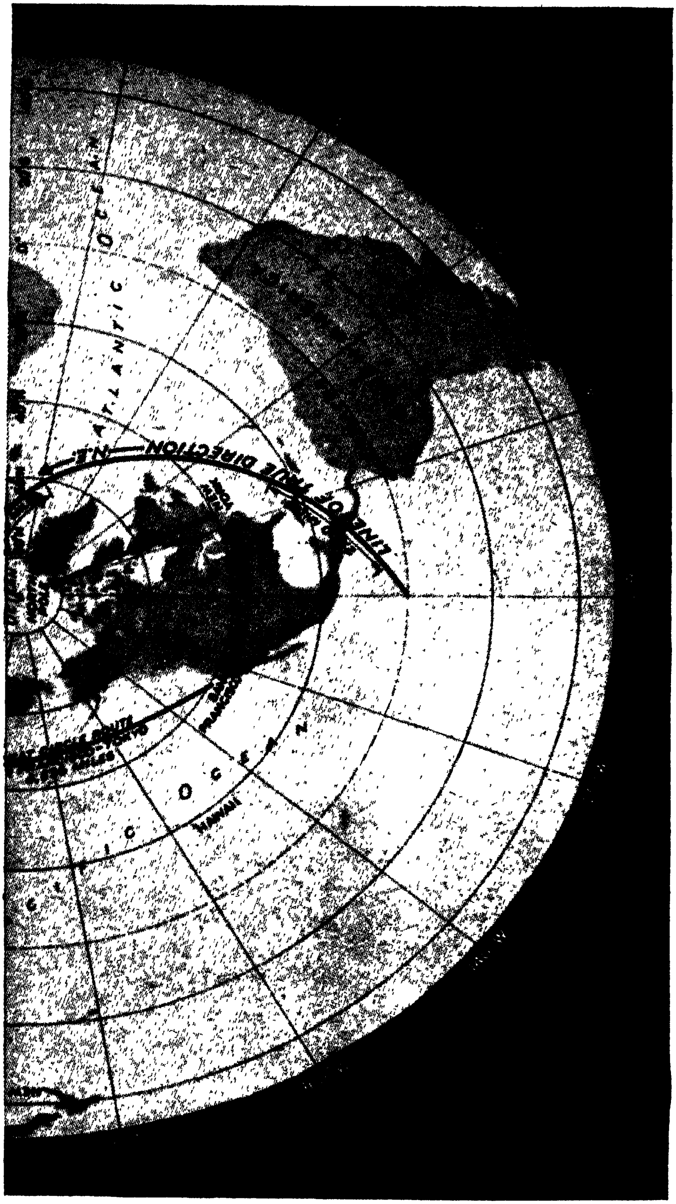


FIG. 7.08.—Gnomonic projection with North Pole as point of tangency. Straight are curved lines. [*Courtesy of Life*



lines passing through this point represent great circles. All other great circles
Magazine, **13**, *No.* 5, 57 (*Aug.* 3, 1942).]

without map error. Unfortunately many of the other desired properties are lost, including the simple representation of great circles not passing through the center of projection. A chart must be prepared for each origin (or each small region) in order to be useful.

The special type for which the point of tangency is at one of the earth's poles is called a *polar chart.* The projection method for obtaining this is shown in Fig. 7.07. It will be noted that meridians are radial lines, and parallels of latitude become concentric circles. The final chart is illustrated in Fig. 7.08.

7.06. Plotting of Direction Finder Bearings.—In discussions of wave propagation over a plane earth in earlier chapters, it was

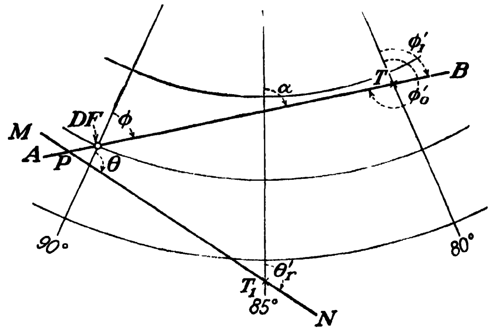


FIG. 7.09.—Measurement of direction finder bearings on a Lambert projection. The *bearing* of *T* measured at *DF* is ϕ, while the *course* to be flown from *DF* to *T* is the angle α.

assumed that the path of the radio rays lay in the vertical plane including transmitter and direction finder arrays. An exception to this of course is the phenomenon of lateral deviation described in Sec. 3.18. When the spherical shape of the earth's surface is taken into account, the vertical plane serves to define a great-circle path between the two stations. For navigation purposes it may be assumed that both ground and sky waves follow great-circle paths. A *bearing* of a transmitter at the direction finder location *DF* is the angle between the meridian and the great circle between *T* and *DF*, and *measured at DF*. This is illustrated as ϕ in Fig. 7.09 for a Lambert projection.

To the necessary degree of accuracy the great-circle path is represented as a straight line even for Lambert projections of areas as large as a considerable portion of the United States, as

was seen previously. One fact becomes obvious by an inspection of Fig. 7.09, however. The angle ϕ_r' measured between the meridian at the more easterly point T and the great-circle path is not equal to ϕ. This is due to the convergence of the meridians. Thus, if the transmitter and direction finder locations were interchanged, the *reciprocal* bearing ϕ_r' at the latter place would be greater than the original bearing ϕ measured at the more westerly location.

In the case of the Lambert charts of the United States used generally for air navigation purposes[1] and having the standard parallels and scale factors described in Sec. 7.04, the convergence of the meridians is approximately 0.6° per degree of longitude. Thus in Fig. 7.09 if the longitude values differ by 10°, the quantity $\phi_r' - \phi$ will be 6°. In this example, if the bearing ϕ at *DF* is 70° (always measured *clockwise* from the north point), the corresponding value ϕ_r' at T is 76° and the bearing toward *DF* at this same point $\phi_0' = 256°$.

The reason for plotting bearings in this manner becomes obvious. If the direction finder is aboard the craft, the location of *DF* is usually unknown. When the bearing ϕ is determined, this establishes that the aircraft lies along a line AB passing through T. If the approximate longitude difference can be estimated, then ϕ_r' can be established, and the *line of bearing AB* plotted. The correction for convergence is relatively small, so that the dead-reckoning position suffices to establish its approximate magnitude. In plotting the (reciprocal) bearing at the transmitter from the observed direction finder value, one may remember: *plane west add* (*P.W.A.*).

If a second bearing θ is determined, from signals from another transmitter T_1, the bearing θ_r' may be calculated as before, and from it the second line of bearing MN plotted as shown in Fig. 7.09. When direction finder errors are neglected, the point P is then known to be the actual direction finder location. Thus, a *fix* may be determined from two transmitters not in the same straight line to the receiver location. The point P is purposely not shown at the originally assumed location, to illustrate that

[1] U.S. Coast and Geodetic Survey, sectional aeronautical charts (1:500,000); regional aeronautical charts (1:1,000,000); aeronautical radio direction finding charts (1:2,000,000); and No. 3060*b*, aeronautical planning chart, United States (1:5,000,000), all on the Lambert projection.

the meridian convergence error for 1 or 2° error in longitude estimate is small. This is especially true in aircraft navigation. For precise navigation of surface vessels, a second application of these principles on the basis of a preliminary fix becomes adequate.

Whenever a third transmitter is conveniently available, a bearing should be taken on it as well as on T and T_1. Ideally, all three lines intersect in a point, but practically they form a small triangle, the lengths of whose sides give a measure of the errors of observation. One of the errors results when the bearings on all three stations are not taken simultaneously. An outstanding merit of automatic direction finders of the types described in Chap. VI is that bearings may be taken almost as rapidly as the stations can be tuned in successively and identified.

A careful distinction should be made between the *bearing* of T measured at DF and the *course* to be flown from the latter point to reach T. A constant direction, established from compass readings, determines a rhumb line, making a constant angle with successive meridians. On a Lambert, the direction of the rhumb line (the *course*) is approximately parallel to the great circle (the *bearing*) at the meridian of mean longitude between DF and T. Hence, in Fig. 7.09, the course between these two points is the angle α. When a long east-west flight is to be made, the great circle is usually broken up into intervals of 3 to 4° in longitude, and the course for each determined for the mid-point. Thus the succession of rhumb lines approximates the great-circle path.

7.07. Relative, Magnetic, and True Bearings.—In Sec. 7.06 it was assumed that the bearing ϕ referred to true north was known. There are actually three measurements of bearing frequently used:

1. The *relative bearing* referred to the nose of the airplane or the bow of the ship. This is ϕ_h in Fig. 7.10.

2. The *magnetic bearing* ϕ_m referred to magnetic north N' as indicated by the magnetic compass. The angle ϕ_m may be computed as

$$\phi_m = \phi_h + \alpha_m \tag{7.01}$$

if the corrected magnetic heading of the craft is α_m.

3. The *true bearing* ϕ referred to true north N and differing from ϕ_m by the *magnetic variation* β. From the figure

$$\beta = \alpha_m - \alpha \tag{7.02}$$

and hence, in terms of magnetic heading and relative bearing, the true bearing is

$$\phi = \phi_h + \alpha_m - \beta \tag{7.03}$$

For westerly variation, β has the positive sign in accordance with Fig. 7.10. Hence, to compute true bearing from magnetic value, one must *subtract westerly variation.*

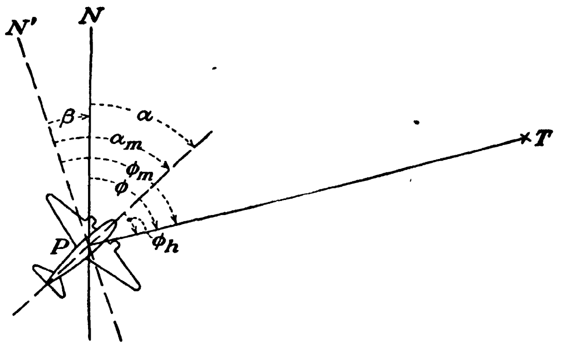


FIG. 7.10.—Relative, magnetic, and true bearings. The various angles are as follows: ϕ_h is the relative bearing of T, ϕ_m is the magnetic bearing of T, ϕ is the true bearing of T, β is the magnetic variation.

7.08. Direct Reading of Bearings with Automatic Direction Finders.—The three indicator scales of the Mark I automatic direction finder shown in Fig. 6.19 are used to give direct reading of relative, magnetic, or true bearings. It is readily evident that care should be taken in choosing the proper algebraic sign for each of the terms in Eq. (7.03) and in subtracting 360° in certain cases. Under conditions of stress and at just those times when radio navigation is most necessary, the pilot who is also navigator of an aircraft is apt to become confused in this matter. Therefore direct and continuous indications of the proper bearings are very much to be desired.

The computing scales are shown in Figs. 7.11 and 7.12. The outermost scale is fixed, 0° being in the direction of the nose of the ship. Thus this scale gives directly *relative bearings* by the indication of the head of the pointer. The silhouette of the airplane serves to make this point more evident. The inner complete (360°) scale may be rotated manually by means of the

Set Scale knob and may be used to give magnetic or true bearings. For the former this scale is set to the magnetic heading of the airplane, with the 0° point of the fixed scales as a reference. In the example of Fig. 7.11 the magnetic heading is 20°, as determined from the corrected compass value. Then the magnetic bearing of the radio station is read under the pointer on the movable scale. In the example it is 80°.

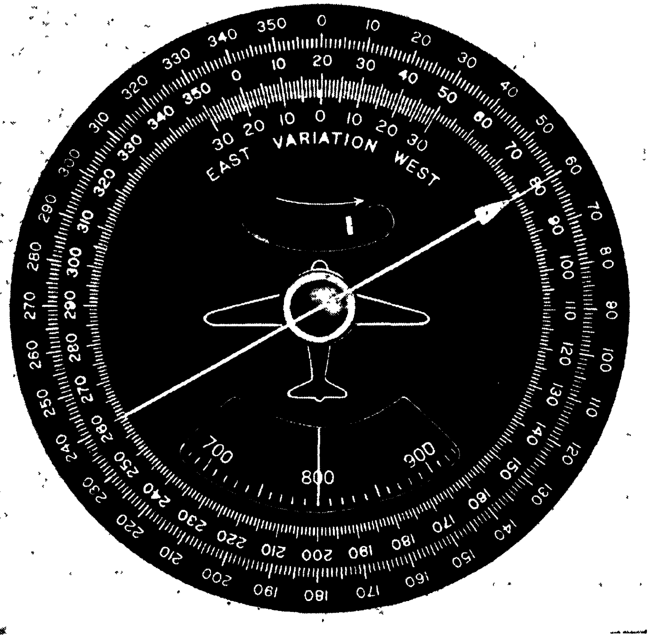


FIG. 7.11.—Scales on indicator unit of RCA-Sperry Mark I automatic direction finder. The outer scale gives relative bearings (referred to the nose of the aircraft). In this example the inner scale is set for a magnetic heading of 20°. Consequently this scale reads the bearing of the transmitter as 80° referred to magnetic north. (*Courtesy of Sperry Gyroscope Company.*)

The final case is that of determining *true* bearings. The movable scale is set so that the magnetic heading coincides not with 0°, but with the appropriate value on the innermost or *variation* scale corresponding to the actual magnetic variation at the plane's location. The movable scale then becomes a scale of true bearings. The head of the pointer then gives such readings directly. This is illustrated in Fig. 7.12 for a magnetic

heading of 30° in a region of 10°W. compass variation. Of course it must be remembered that if the heading of the craft is changed, the new value must be set by hand on the movable scale. The tail of the pointer, purposely made short so that it will read only on the movable scale, is often of convenience in indicating the reciprocal bearing that must be plotted from the transmitter

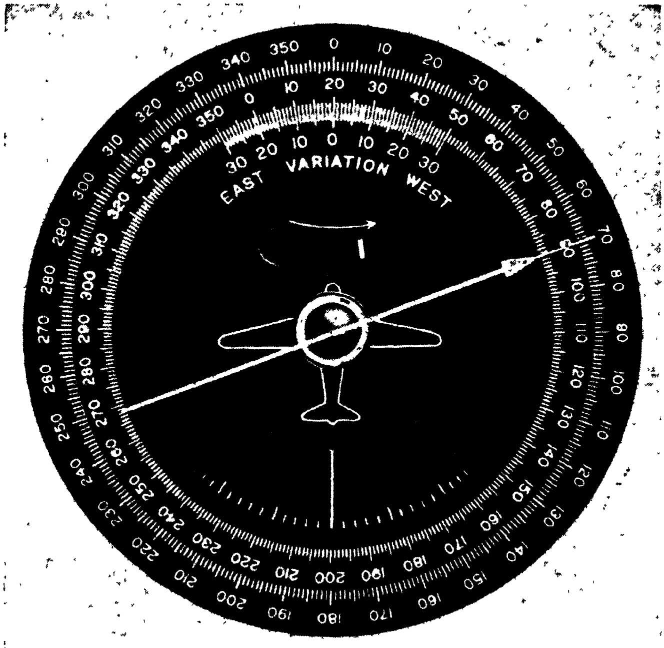


FIG. 7.12.—Indicator unit of Mark I automatic direction finder. The relative bearing of the transmitter, as read on the outer scale, is 70°. The inner scale is set for a magnetic heading of 30° in a region of 10°W. compass variation. The pointer therefore reads a true bearing of 90°. (*Courtesy of Sperry Gyroscope Company.*)

location. This will be seen from Fig. 7.09. Correction for meridian convergence must of course still be made.

An inspection of Fig. 6.28 shows that the same general principle of a movable scale to allow direct indication of magnetic or true bearings is used in the MN-31 automatic direction finder. In this case the three scales are not provided separately, however. Instead there is a fixed index mark, corresponding to the direction

of the nose of the aircraft, and a movable scale which may be set opposite this index to the magnetic heading. Magnetic bearings may then be read directly. The azimuth scale knob is appropriately marked as to direction of rotation in order to correct for *east* or *west* variation and thus to give a scale of true bearings. The magnitude of the variation is added mentally by the operator in this last step.

7.09. Calibration of Automatic Direction Finders.—The Mark I and the MN-31 direction finders are provided with compensators for correcting automatically for quadrantal and other types of deviation errors. Initial calibration must be carried out in a given aircraft installation in order to determine the amount of this correction. In either of the types described this is carried out at one frequency, often near the middle of the beacon band, because this latter frequency range is of greater importance to the airline user than the broadcast band. The same precautions as to location of other antennas and as to the securing of such rigging in its permanent position must be observed as for shipboard equipment described in Secs. 4.11 to 4.13. Fortunately, it is found that for airplanes that are substantially identical in structure and rigging, as is the case on an airline, a calibration on one airplane will be close enough for all of this same type.

Ground calibration is occasionally carried out. For loops mounted above the fuselage, as in seaplane installations, the accuracy is usually satisfactory if the craft is near enough to its flying attitude. Serious errors may result in installations where the loop is beneath the fuselage, as it normally is for land-based planes. This may be true even if the correct flight attitude is maintained. Nevertheless, if such a calibration is to be made, a suitable transmitter 5 to 50 miles away is chosen. Care should be taken to avoid a near-by radio range transmitter because the combination of radiation and induction fields due to an extended array produces an effect analogous to parallax. The airplane should be well away from hangars or other metallic structures.

The airplane is headed directly toward the transmitter and the direction finder bearing observed. The proper heading involves checking with magnetic compass or with a pelorus on a known landmark. Then the craft is swung around in equal increments of about 10 to 15° each and the direction finder bearing indicator observed. The data of *true relative bearing* of the transmitter and

observed direction finder bearing then form the basis of a calibration curve. This is plotted as *deviation* against *observed* bearing. The deviation has the proper algebraic sign so that it is to be *added* to the observed value to give true or correct bearing, as was given in Eq. (4.43).

From the smoothed calibration curve the compensator cam of the Mark I direction finder indicator may be cut to provide this correction. Similarly the adjustment screws of the MN-31 compensator may be set to give the desired correction at each 15° interval. It may be remarked that a symmetrical loop location on the fore-and-aft axis of the airplane usually gives no deviation at the 0 and 180° points, and very little at 90 and 270° (off the wings). The maximum correction (perhaps 10 to 20°) occurs near the odd multiples of 45° of such sign that the apparent station location is always nearer the longitudinal axis. Thus for a true bearing of 45° the observed bearing without compensation might be 32°. A true bearing of 225° would give a corresponding observed value of 212°. In other words, deviation is positive in the first and third quadrants.

Numerous methods of calibration in flight have been proposed.[1] They differ in convenience and required time for calibration and in some cases in accuracy. The air should be smooth, visibility good, and the wind velocity below about 10 m.p.h. A directional gyro should be used in preference to a magnetic compass. Flight should be at a low altitude, perhaps 1000 ft., in order to allow accurate observation of landmark fixes.

Figure-of-eight Method.—A suitable landmark, such as a straight road, a section line, a railroad, or a power line, is chosen at a distance of 75 to 100 miles from the desired transmitter. An easily identified point P on this base line is also chosen. Then from a chart it is determined that the bearing of the transmitter with respect to the base line at the point P is a certain angle α of Fig. 7.13. The procedure is to fly along the base line long enough

[1] The U.S. Navy carried out pioneer work in this investigation. The U.S airlines, the Civil Aeronautics Administration, and other organizations have contributed extensively to practical methods of calibration. The particular procedures to which reference is made here have made use of this background and have been put in specific form by the staffs of Sperry Gyroscope Company and Bendix Aviation Corporation. See WEBB and ESSEX, *loc. cit.*

to steady down on a fixed heading. The cross wind must be very small so that the ship will not be crabbing under these conditions. The directional gyro is set to 0° and uncaged. The heading of the airplane with respect to MN may then be read from the gyro as the angle β.

At the instant of passing directly over P with a relative heading of 0° ($\beta = 0$), the bearing of the transmitter is observed on the

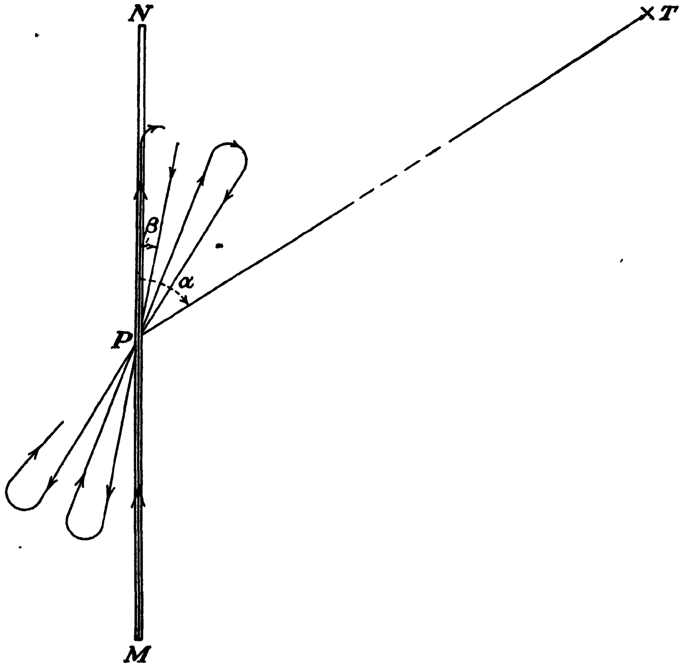


FIG. 7.13.—Calibration of aircraft direction finder by figure-of-8 method.

automatic direction finder. The pilot then flies far enough out in the direction N to make a normal turn of about 190°, in such a manner as to maintain this new heading at the instant of passing over the point P in nearly the opposite direction. Directional gyro reading and direction finder bearing are obtained simultaneously at the point P. The pilot then flies out in the general direction of M as shown in Fig. 7.13, executes a similar 190° turn, and returns with a heading of 20° referred to the line MN. This procedure is repeated at appropriate intervals

until the full 360° calibration has been carried out. It becomes obvious from the geometry of Fig. 7.13 how to compute the true relative bearing with respect to the line PT. From this a plot of deviation against observed direction finder bearings can be made, and the compensation carried out in just the same way as for the calibration on the ground discussed previously.

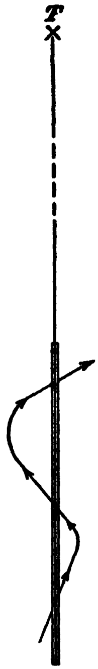


FIG. 7.14. Calibration of aircraft direction finder by ground-reference-line method.

Ground-reference-line Method.—If it is possible to find a base line that may be readily identified from the air and that points directly toward the desired station, the previous procedure may be considerably simplified. It no longer becomes necessary to establish the correct heading at the same time as the craft passes over a fixed *point*. In this method the pilot executes a series of alternate left and right turns so that he pursues a zigzag path toward the transmitter and later away from it, but always remaining at a considerable distance on the same side of it. This is illustrated in Fig. 7.14, and in greater detail in Fig. 7.15. Radio bearings are taken each time the reference line is crossed. It will be observed that this procedure allows more frequent returns to a known heading, either directly toward or directly away from the transmitter, so that the directional gyro may be checked at each occasion. This is of especial importance because of the precession or "drift" of the standard directional gyro. It will be seen from Fig. 7.15 that the flying time is held to a minimum because of the small number of 180° turns which are required. The method is accurate as long as the aircraft stays at a considerable distance (25 to 100 miles) from the station at all times during the flight check.

Two-circle Method.—A less accurate system, but one that requires considerably less flying time, is occasionally used. The general procedure will be noted by reference to Fig. 7.16. A check point 75 to 100 miles from the chosen transmitter is established and the true bearing of the transmitter determined at this point from a chart. The direction toward the transmitter is found in the air at this point by means of the magnetic compass.

(Actually the radio direction finder itself is frequently used to check the zero heading by the assumption that there is no deviation in that direction.) The directional gyro is then set to zero for this heading. A right turn is made in the form of a series of successive chords of equal flying time and with the heading

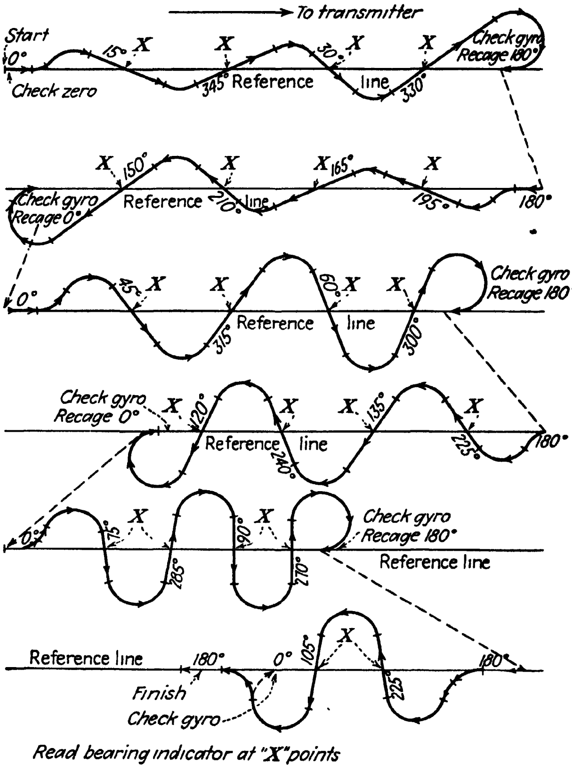


FIG. 7.15.—Details of method of calibration of aircraft direction finder shown in FIG. 7.14. (*Courtesy of Bendix Aviation Corporation.*)

established in equal increments as shown in Fig. 7.16. If this procedure is carefully carried out, the circle should be completed at the original check point, and there the gyro heading may be rechecked. Then a turn in the opposite direction is made in a similar manner starting from this original point. Two curves of deviation against airplane heading are plotted from these data,

one for the right-turn run and the other for the left-turn series of readings. An average curve that is the mean of these two smoothed curves is plotted, and this is the desired calibration characteristic. The inaccuracy in the method is due to the fact that at the 180° heading points the bearing of the transmitter has changed appreciably. Since this error is in opposite directions for the two circles, only a second-order inaccuracy remains

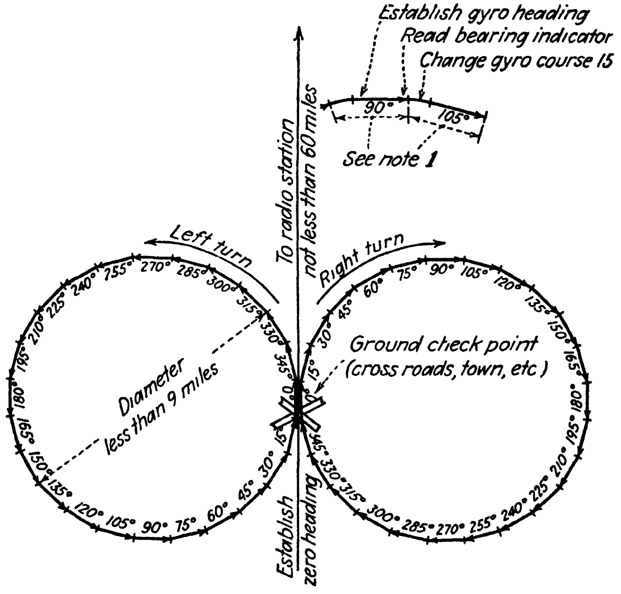


FIG. 7.16.—Calibration of aircraft direction finder by two-circle method. The following precautions should be observed: (1) Allow equal times for each heading, 25 sec. or less if possible; (2) execute turn to finish over check point; (3) wind velocity should not exceed 10 m.p.h. (*Courtesy of Bendix Aviation Corporation.*)

if a proper average is taken. For example, it can be shown that at a distance of 60 miles, for a circle diameter of 9 miles, the maximum resultant error is of the order of 1° for each of these points. If appropriate precautions about cross winds and accuracy in flying the circular courses are observed, this method is found to be reasonably accurate.

Bibliography

DAY, K. S.: *Instruments and Radio Flying*, distributed by Air Associates, Inc., Garden City, N. Y., 1938.

DUTTON, B.: *Navigation and Nautical Astronomy*, 7th ed., United States Naval Institute, Annapolis, Md., 1942.

JORDANOFF, A.: *Through the Overcast*, 1st ed., Funk and Wagnalls Co., New York, 1938.

KEEN, R.: *Wireless Direction Finding*, 3d rev. ed., especially Chaps. 14 and 17, Iliffe & Sons, Ltd., London, 1938.

U. S. NAVY: Aircraft Navigation Manual, *Hydrographic Office Publication H. O.* 216, 1st ed., rev., Government Printing Office, Washington, 1941.

APPENDIX A

RADIATION DUE TO AN INFINITESIMAL DIPOLE

Potential Functions.—A brief résumé will be made of the notion of *potential* as an aid to the solution of the problem of the fields associated with an elementary conductor carrying an electric current. One may consider first of all the potential function associated with an electrostatic field. The force at a point P on unit positive charge due to a point charge q in free space is the electric field intensity E at that point. E is a vector and is directed outward from q.

$$E = -\frac{q}{r^2} \tag{A.1}$$

The *potential difference* $\Phi - \Phi'$ between two points P and P' in the field of q is defined as the work required to move unit positive charge from P' to P. When P' is removed to an infinitely large distance, one lets $\Phi' = 0$ and calls Φ the *potential* of the point P. The work required to bring unit charge to P from infinity is

$$\Phi = \int_{\infty}^{R} E(r)\,dr \tag{A.2}$$

where $E(r)$ indicates that E is a function of the distance r from q. R is the value of r at P.

Then with the value of E from Eq. (A.1),

$$\Phi = \int_{\infty}^{R} -\frac{q}{r^2}\,dr$$
$$= \frac{q}{R} \tag{A.3}$$

The quantity Φ is a scalar and has a value that may be calculated for every point in space. When there are a number of charges q_1, q_2, q_3, . . . , the total work required to bring the unit reference charge to P is the sum of the work done against

each field alone, no matter what the path chosen may be. Hence the total potential

$$\left.\begin{aligned}\Phi &= \frac{q_1}{R_1} + \frac{q_2}{R_2} + \frac{q_3}{R_3} + \cdots \\ &= \sum_{n=1}^{n} \frac{q_n}{R_n}\end{aligned}\right\} \tag{A.4}$$

The components of E along the x, y, and z axes are the rates of change of Φ in each of these directions, respectively.

$$\left.\begin{aligned}E_x &= -\frac{\partial\Phi}{\partial x} \\ E_y &= -\frac{\partial\Phi}{\partial y} \\ E_z &= -\frac{\partial\Phi}{\partial z}\end{aligned}\right\} \tag{A.5}$$

It will thus be noted that when any complex distribution of charge as in Eq. (A.4) is considered, the potential may be calculated as an algebraic sum. By comparison, the direct evaluation of E is much more complicated if carried out from Eq. (A.1) in that the *vector* sum of all the components must be determined. The components may be determined from Eq. (A.5) with much greater ease.

The quantity Φ in this case is referred to as a *scalar potential* to distinguish it from a different type having a direction as well as a magnitude at every point in space and known as a *vector potential* function.

From Ampère's theorem it is found that the magnetic field due to an elementary length of conductor or infinitesimal dipole Δl is

$$H = \frac{i\,\Delta l \sin\theta}{r^2} \tag{A.6}$$

This is illustrated in Fig. A.1 for a current i. It will be noted that for a given *dipole moment* $i\,\Delta l$ there is dependence on the direction to the point P. This difference, introducing the factor $\sin\theta$, distinguishes the magnetic case from the electrostatic case of Eq. (A.1).

When a fictitious unit magnetic pole is moved from an infinite distance to the point P along the line MP (so that $\sin\theta$ is con-

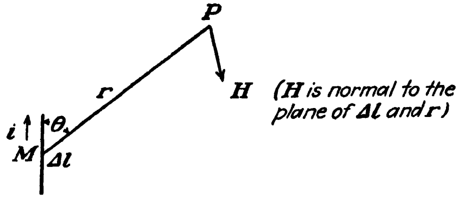


FIG. A.1.—Magnetic field due to dipole of length Δl in which a current i flows

stant), work is done, as in the electrostatic case, and a potential function may be defined as

$$\Psi = -\int_{\infty \text{ along } r}^{R} H(r)\,dr \tag{A.7}$$

and from Eq. (A.6)

$$\Psi = \frac{i\,\Delta l \sin\theta}{R} \tag{A.8}$$

and of course

$$H = -\frac{\partial\Psi}{\partial r} \tag{A.9}$$

Equations (A.7) to (A.9) apply at every point in space for steady current i. The phenomena that occur if i varies with time may be analyzed in semiquantitative fashion.

Magnetic Field Due to Varying Current.—The effect of a current change will be a wave disturbance, as Maxwell showed, and the time required for a change to be felt at a distance will be a finite quantity. In fact the wave disturbance will be propagated in free space with a velocity c, the velocity of light. Thus, if

$$i = I_{max} \cos \omega t \tag{A.10}$$

the field H at a distance r will not vary as $\cos \omega t$ but will lag by a time r/c. Consequently the potential at P will be

$$\Psi = \frac{I_{max}\,\Delta l \sin\theta}{r} \cos \omega\left(t - \frac{r}{c}\right) \tag{A.11}$$

This is called a *retarded vector potential* function. The rigorous derivation of Eq. (A.11) is beyond the scope of this work.

The field H at the distance r is given by Eqs. (A.9) and (A.11) but not by an extension of Eq. (A.6) directly. Thus

$$H = I_{max}\,\Delta l \sin\theta \left[-\frac{\cos\omega\left(t - \frac{r}{c}\right)}{r^2} + \frac{\omega \sin\omega\left(t - \frac{r}{c}\right)}{rc} \right] \qquad (A.12)$$

Equation (A.12) shows that the total magnetic field is made up of two parts. One, namely,

$$H_i = \frac{I_{max}\,\Delta l \sin\theta}{r^2} \cos\omega\left(t - \frac{r}{c}\right) \qquad (A.13)$$

varies inversely as the square of the distance and is independent of the frequency of the alternating current in Δl. Except for the propagation time term r/c in the sinusoidal function, it is the same as Eq. (A.6). It is referred to as the *induction magnetic field.* It has a maximum numerical value of

$$H_{i(max)} = \frac{I_{max}\,\Delta l \sin\theta}{r^2} \qquad (A.14)$$

The other part (neglecting the negative sign)

$$H_m = \frac{I_{max}\,\Delta l \sin\theta}{rc}\,\omega \sin\omega\left(t - \frac{r}{c}\right) \qquad (A.15)$$

varies inversely as the first power of the distance and directly with the frequency $\omega/2\pi$. Because of the slower rate of diminution as r is made large, H_m is the predominating component at large distances, and H_i may be neglected. H_m is called the *radiation magnetic field.* It has a maximum value of

$$H_{m(max)} = \frac{\omega I_{max}\,\Delta l \sin\theta}{rc} \qquad (A.16)$$

or since $\omega = 2\pi f$ and $f = c/\lambda$ where λ is the wave length,

$$\omega = \frac{2\pi c}{\lambda} \qquad (A.17)$$

and

$$H_{m(max)} = \frac{2\pi I_{max}\,\Delta l \sin\theta}{\lambda r} \qquad (A.18)$$

Here the magnetic fields and I_{max} are in e.m.u. and r is in centimeters.

It will be seen from Eqs. (A.14) and (A.18) that

$$H_{i(\max)} = H_{m(\max)}$$

when $r = \lambda/2\pi$, or the induction and radiation fields have equal magnitudes at 0.159 of one wave length.

Equations (A.13) and (A.15) show that the two fields differ in time phase by 90°. A consequence of this is the anomalous behavior of a direction finder close to a directive transmitting antenna. This is frequently observed with an automatic aircraft direction finder as the airplane passes over a so-called radio range transmitter.

Magnetic and Electric Fields.—It can be demonstrated that in free space there is associated with the magnetic field an electric field in phase in time and having the same energy density. The magnetic energy density is

$$\rho_H = \frac{H^2}{8\pi}$$

and the electric energy density

$$\rho_E = \frac{E^2}{8\pi} \qquad \text{(A.19)}$$

$$\rho_H = \rho_E \qquad \text{(A.20)}$$

and the total energy density ρ_w is

$$\rho_w = \frac{H^2}{4\pi} = \frac{E^2}{4\pi} \qquad \text{(A.21)}$$

provided H is in e.m.u. and E in e.s.u.

Thus, there is an electric field due to the varying current given by the analogue of Eq. (A.12).

$$E = I_{\max}\,\Delta l \sin\theta \left[-\frac{\sin\omega\left(t - \frac{r}{c}\right)}{r^2} + \left(1 - \frac{\lambda^2}{4\pi^2 r^2}\right)\frac{\omega \sin\omega\left(t - \frac{r}{c}\right)}{rc} \right] \qquad \text{(A.22)}$$

It will be noted that there is actually a more complicated coefficient of the second term, as rigorous analysis would show. This vector E is at right angles to H and to the line MP of Fig. A.1 and hence lies in the plane of Δl and r. For most practical applications consideration will be given to the electric field

component, although E and H always are present simultaneously in the radiation case.

The directions of H and E are shown in Fig. 2.09. There is also a radial electric field E_r that has a magnitude[1] of $2I_{max}\,\Delta l \cos\theta/r^2$, and hence becomes negligible at large distances, as does the induction electric field component of E.

E has two components similar to H_i and H_m, respectively. The *induction electric field* is

$$E_i = -\frac{I_{max}\,\Delta l \sin\theta}{r^2} \sin\omega\left(t - \frac{r}{c}\right) \qquad \text{(A.23)}$$

with a maximum numerical value of

$$E_{i(max)} = \frac{I_{max}\,\Delta l \sin\theta}{r^2} \qquad \text{(A.24)}$$

The *radiation electric field* is approximately

$$E_m = \frac{I_{max}\,\Delta l \sin\theta}{rc}\,\omega \sin\omega\left(t - \frac{r}{c}\right) \qquad \text{(A.25)}$$

if $\lambda^2/4\pi^2r^2 << 1$ in Eq. (A.22). This is the result given in Eq. (2.02). This derivation follows a method used by Everitt.[2]

[1] G. W. PIERCE, *Electric Oscillations and Electric Waves*, 1st ed., pp. 428–429, McGraw-Hill Book Company, Inc., New York, 1920. Also F. R. STANSEL, A Study of the Electromagnetic Field in the Vicinity of a Radiator, *Proc. I.R.E.*, **24**, 802 (May, 1936).

[2] W. L. EVERITT, *Communication Engineering*, 2d ed., Chap. XIX, McGraw-Hill Book Company, Inc., New York, 1937.

APPENDIX B

CALCULATION OF FIELD STRENGTH FOR PROPAGATION OVER PLANE EARTH OF FINITE CONDUCTIVITY

Reflection Coefficients near Grazing Incidence.—Fresnel's laws of reflection permit a computation of the field strength that results when the direct and reflected waves are considered at ultra-high frequency. The result was employed in Sec. 2.20, For vertical polarization, as was seen in Eq. (2.68),

$$K_V = \frac{\epsilon_0 \sin \phi - \sqrt{\epsilon_0 - 1 + \sin^2 \phi}}{\epsilon_0 \sin \phi + \sqrt{\epsilon_0 - 1 + \sin^2 \phi}} \tag{B.1}$$

When r, the distance between elevated transmitting and receiving antennas, is much larger than h_1 or h_2, their respective heights, the approximation may be made that

$$\sin \phi = \phi = \frac{h_1 + h_2}{r} \tag{B.2}$$

Then Eq. (B.1) becomes, since $\epsilon_0 - 1 >> \phi^2$,

$$K_V = \frac{\epsilon_0\phi - \sqrt{\epsilon_0 - 1}}{\epsilon_0\phi + \sqrt{\epsilon_0 - 1}} \tag{B.3}$$

$$= -\left(\frac{1 - \dfrac{\epsilon_0\phi}{\sqrt{\epsilon_0 - 1}}}{1 + \dfrac{\epsilon_0\phi}{\sqrt{\epsilon_0 - 1}}}\right)$$

$$= -\left(1 - \frac{2\epsilon_0\phi}{\sqrt{\epsilon_0 - 1}} + \frac{2\epsilon_0{}^2\phi^2}{\epsilon_0 - 1} - \cdots\right) \tag{B.4}$$

If only the first two terms of the series are taken,

$$K_V = -\left[1 - \frac{2\epsilon_0(h_1 + h_2)}{r\sqrt{\epsilon_0 - 1}}\right] \tag{B.5}$$

Here the negative sign shows that there is a phase reversal upon reflection, as was assumed in Sec. 2.16 for σ large.

The corresponding result for K_H is the approximation

$$K_H = \frac{\phi - \sqrt{\epsilon_0 - 1}}{\phi + \sqrt{\epsilon_0 - 1}} \tag{B.6}$$

$$= -\left[1 - \frac{2\phi}{\sqrt{\epsilon_0 - 1}} + \frac{2\phi^2}{\epsilon_0 - 1} - \cdots\right] \tag{B.7}$$

$$= -\left[1 - \frac{2(h_1 + h_2)}{r\sqrt{\epsilon_0 - 1}}\right] \tag{B.8}$$

Field Strength Due to Direct and Reflected Components.— For the case of an earth's surface of finite conductivity, the resultant field E_V of the vertical component is given as the vector sum of the vectors E_1 and E_2 of Fig. 2.23. However, now they are not equal in magnitude, but E_2 has a value $A_V E_1$. Furthermore, the phase difference is now due to both ψ, representing the path difference, and ϕ_V, the phase shift at reflection.

$$E_V = E_1 + E_1 K_V e^{j\psi} \tag{B.9}$$

$$= E_1(1 + K_V e^{j\psi}) \tag{B.10}$$

or

$$E_V = E_1(1 + A_V e^{j(\psi + \theta_V)}) \tag{B.11}$$

If ϕ is small, $(\psi + \theta_V - \pi)$ is also small. If this phase departure from a 180° reversal be denoted by ψ_0, then

$$E_V = E_1(1 - A_V e^{j\psi_0}) \tag{B.12}$$

The series expansion for the exponential is

$$e^{j\psi_0} = 1 + j\psi_0 - \frac{\psi_0^2}{2!} - \frac{j\psi_0^3}{3!} + \cdots \tag{B.13}$$

and approximately

$$e^{j\psi_0} = 1 + j\psi_0 \tag{B.14}$$

$$E_V = E_1(1 - A_V - jA_V\psi_0) \tag{B.15}$$

Thus the magnitude of E_V is

$$|E_V| = |E_1| \sqrt{(1 - A_V)^2 + A_V^2\psi_0^2} \tag{B.16}$$

The result can be somewhat modified for ϕ small enough so that θ_V is approximately π. Then $K_V = A_V$, and Eq. (B.15) becomes

$$E_V = E_1 \left\{1 - \left[1 - \frac{2\epsilon_0(h_1 + h_2)}{r\sqrt{\epsilon_0 - 1}}\right](1 + j\psi)\right\} \tag{B.17}$$

$$= \frac{E_1}{r}\left\{\frac{2\epsilon_0(h_1 + h_2)}{\sqrt{\epsilon_0 - 1}} - j\left(\frac{4\pi h_1 h_2}{\lambda}\right)\left[1 - \frac{2\epsilon_0(h_1 + h_2)}{r\sqrt{\epsilon_0 - 1}}\right]\right\} \tag{B.18}$$

For ϕ small, $(h_1 + h_2) << r$, so that the last term is negligible compared to unity. Then

$$E_V = \frac{E_1}{r}\left[\frac{2\epsilon_0(h_1 + h_2)}{\sqrt{\epsilon_0 - 1}} - j\,\frac{4\pi h_1 h_2}{\lambda}\right] \tag{B.19}$$

The magnitude of E_V is

$$|E_V| = \frac{|E_1|}{r}\sqrt{\frac{4\epsilon_0^2(h_1 + h_2)^2}{\epsilon_0 - 1} + \left(\frac{4\pi h_1 h_2}{\lambda}\right)^2} \tag{B.20}$$

This is the result used in Sec. 2.20.

For horizontal polarization, a result similar to Eq. (B.16) may be obtained, namely,

$$|E_H| = |E_1|\sqrt{(1 - A_H)^2 + A_H^2\psi_0^2} \tag{B.21}$$

The following equation holds over a wider range of ϕ (if the approximation $K_V = A_V$ is made) than in the case of vertical polarization:

$$E_H = E_1\left\{1 - \left[1 - \frac{2(h_1 + h_2)}{r\sqrt{\epsilon_0 - 1}}\right](1 + j\psi)\right\} \tag{B.22}$$

$$= \frac{E_1}{r}\left[\frac{2(h_1 + h_2)}{\sqrt{\epsilon_0 - 1}} - j\,\frac{4\pi h_1 h_2}{\lambda}\right] \tag{B.23}$$

And, finally,

$$|E_H| = \frac{|E_1|}{r}\sqrt{\frac{4(h_1 + h_2)^2}{\epsilon_0 - 1} + \left(\frac{4\pi h_1 h_2}{\lambda}\right)^2} \tag{B.24}$$

For propagation very near to grazing incidence, it was shown by Burrows[1] that Eqs. (B.19) and (B.23) should be modified to include a term of importance only for low frequencies and small h_1 and h_2.

$$E_V = \frac{E_1}{r}\left[\frac{2\epsilon_0(h_1 + h_2)}{\sqrt{\epsilon_0 - 1}} - j\,\frac{4\pi h_1 h_2}{\lambda} + j\,\frac{\epsilon_0^2\lambda}{\pi(\epsilon_0 - 1)}\right] \tag{B.25}$$

$$E_H = \frac{E_1}{r}\left[\frac{2(h_1 + h_2)}{\sqrt{\epsilon_0 - 1}} - j\,\frac{4\pi h_1 h_2}{\lambda} + j\,\frac{\lambda}{\pi(\epsilon_0 - 1)}\right] \tag{B.26}$$

This results from the inclusion of the effect of the Sommerfeld surface wave.

[1] C. R. Burrows, Radio Propagation over Plane Earth: Field Strength Curves, *Bell System Tech. J.*, **16**, 45 (January, 1937).

APPENDIX C

EXTENDED DIPOLE ANTENNA

Directive Pattern of Long Wire Antenna.—Under the conditions specified in Sec. 3.02 for a long straight wire, Eq. (3.05) may be derived in the following manner. The *instantaneous* electric field due to dx of Fig. 3.01 is

$$dE = dE_{\max} \sin \omega \left(t - \frac{r - x \cos \theta}{c} \right) \tag{C.1}$$

when

$$I(x) = I_{\max}(x) \cos \omega t \tag{C.2}$$

because the time of propagation from dx to P is given by

$$\frac{r - x \cos \theta}{c}$$

It is this phase factor which is of importance in determining the directive pattern rather than the attenuation along r_x compared to r.

Then from Eqs. (3.03), (C.1), (C.2):

$$dE = \frac{60\pi I_{\max}(x) \sin \theta}{\lambda r} \sin \left[\omega t - \frac{2\pi}{\lambda} (r - x \cos \theta) \right] dx \tag{C.3}$$

$$= \frac{60\pi I_{0(\max)} \sin \theta}{\lambda r} \left(\cos \frac{2\pi}{\lambda} x \right) \sin \left[\omega t - \frac{2\pi}{\lambda} (r - x \cos \theta) \right] dx \tag{C.4}$$

For convenience one may set

$$K = \frac{60\pi I_{0(\max)} \sin \theta}{\lambda r} \tag{C.5}$$

and

$$\alpha = \frac{2\pi}{\lambda} \tag{C.6}$$

Equation (C.4) then becomes

$$dE = K \cos \alpha x \sin \left[(\omega t - \alpha r) + \alpha x \cos \theta \right] dx \tag{C.7}$$

The total field at P is then the integral of Eq. (C.7) between the limits $x = L/2$ and $x = -L/2$.

$$E = K \int_{-L/2}^{L/2} \cos \alpha x \sin [(\omega t - \alpha r) + \alpha x \cos \theta]\, dx \quad (C.8)$$

The indefinite integral of Eq. (C.8) is given in tables[1] and so the result for E is

$$E = -K \left\{ \frac{\cos [\alpha(\cos \theta + 1)x + (\omega t - \alpha r)]}{2\alpha(\cos \theta + 1)} + \frac{\cos [\alpha(\cos \theta - 1)x + (\omega t - \alpha r)]}{2\alpha(\cos \theta - 1)} \right\}_{-L/2}^{L/2} \quad (C.9)$$

For the present case of an odd number of half wave lengths,

$$L = \frac{m\lambda}{2} \quad (C.10)$$

so that the limits of integration are $x = \frac{m\lambda}{4}$ and $-\frac{m\lambda}{4}$; and $\frac{\alpha m\lambda}{4} = \frac{m\pi}{2}$.

Then

$$E = -K \left\{ \frac{\cos \left[\frac{m\pi}{2} (\cos \theta + 1) + (\omega t - \alpha r)\right]}{2\alpha(\cos \theta + 1)} + \frac{\cos \left[\frac{m\pi}{2} (\cos \theta - 1) + (\omega t - \alpha r)\right]}{2\alpha(\cos \theta - 1)} - \frac{\cos \left[-\frac{m\pi}{2} (\cos \theta + 1) + (\omega t - \alpha r)\right]}{2\alpha(\cos \theta + 1)} - \frac{\cos \left[-\frac{m\pi}{2} (\cos \theta - 1) + (\omega t - \alpha r)\right]}{2\alpha(\cos \theta - 1)} \right\} \quad (C.11)$$

[1] For example, see B. O. PEIRCE, *A Short Table of Integrals*, 3d rev. ed., Ginn and Company, Boston, 1929, p. 61, where the integral is given in the form

$$\int \sin (mx + a) \cos (nx + b)\, dx = -\frac{\cos (mx + nx + a + b)}{2(m + n)} - \frac{\cos (mx - nx + a - b)}{2(m - n)}$$

$$E = K \frac{1}{2\alpha(\cos\theta + 1)} \left\{ \cos\left[\frac{m\pi}{2}(\cos\theta + 1) - (\omega t - \alpha r)\right] - \cos\left[\frac{m\pi}{2}(\cos\theta + 1) + (\omega t - \alpha r)\right]\right\} + K \frac{1}{2\alpha(\cos\theta - 1)} \left\{ \cos\left[\frac{m\pi}{2}(\cos\theta - 1) - (\omega t - \alpha r)\right] - \cos\left[\frac{m\pi}{2}(\cos\theta - 1) + (\omega t - \alpha r)\right]\right\} \quad \text{(C.12)}$$

$$E = \frac{K}{\alpha}\left[\frac{1}{\cos\theta + 1} \sin\frac{m\pi}{2}(\cos\theta + 1) \cdot \sin(\omega t - \alpha r) + \frac{1}{\cos\theta - 1} \sin\frac{m\pi}{2}(\cos\theta - 1) \cdot \sin(\omega t - \alpha r)\right] \quad \text{(C.13)}$$

$$= \frac{K \sin(\omega t - \alpha r)}{\alpha} \left[\frac{(\cos\theta - 1)\sin\frac{m\pi}{2}(\cos\theta + 1) + (\cos\theta + 1)\sin\frac{m\pi}{2}(\cos\theta - 1)}{\cos^2\theta - 1}\right] \quad \text{(C.14)}$$

The last factor has a value of

$$\frac{2}{\sin^2\theta} \cos\left(\frac{m\pi}{2}\cos\theta\right)$$

for m odd (disregarding a factor $(-1)^{\frac{m+1}{2}}$ which gives alternate algebraic signs), E has an amplitude E_{max} obtained by setting $\sin(\omega t - \alpha r)$ equal to unity, with the result that

$$E_{max} = \frac{2K}{\alpha} \frac{1}{\sin^2\theta} \cos\left(\frac{m\pi}{2}\cos\theta\right) \quad \text{(C.15)}$$

giving finally,

$$E_{max} = \frac{60 I_{0(max)}}{r} \frac{1}{\sin\theta} \cos\left(\frac{m\pi}{2}\cos\theta\right) \quad \text{(C.16)}$$

Effective Height of Vertical Antenna.—The effective height as considered in Sec. 3.04 may be defined[1] as

[1] K. A. Norton, The Propagation of Radio Waves over the Surface of the Earth and in the Upper Atmosphere, *Proc. I.R.E.*, **24**, 1367 (October, 1936). See also H. E. Gihring and G. H. Brown, General Considerations of Tower Antennas for Broadcast Use, *Proc. I.R.E.*, **23**, 311 (April, 1935).

$$h_e = \frac{\sin\theta}{I_0}\int_0^h I(x)\cos\left(\frac{2\pi}{\lambda}x\cos\theta\right)dx \qquad \text{(C.17)}$$

This takes into account the phase factor for the difference in path between the point x and the image at $-x$.

As was done in the case of the long wire in Sec. 3.02, a sinusoidal standing wave distribution will be assumed. In Fig. 3.11 or 3.12 this will be

$$I(x) = I_{max}\sin\frac{2\pi(h-x)}{\lambda} \qquad \text{(C.18)}$$

Consequently, along the ground plane for $h \lesseqgtr \lambda/4$

$$h_e = \int_0^h \sin\frac{2\pi(h-x)}{\lambda}\,dx \qquad \text{(C.19)}$$

$$= \frac{\lambda}{2\pi}\left(1-\cos\frac{2\pi h}{\lambda}\right) \qquad \text{(C.20)}$$

$$= \frac{\lambda}{\pi}\sin^2\left(\frac{\pi h}{\lambda}\right) \qquad \text{(C.21)}$$

This is the result of Eq. (3.11).

If $h \gtreqless \lambda/4$, the first definition of I_0 in Eq. (3.10) may be adopted, and it is found that

$$I_0 = I_{max}\sin\frac{2\pi h}{\lambda} \qquad \text{(C.22)}$$

so that

$$h_e = \frac{1}{\sin\frac{2\pi h}{\lambda}}\int_0^h \sin\frac{2\pi(h-x)}{\lambda}\,dx \qquad \text{(C.23)}$$

$$= \frac{\lambda}{\pi\sin\frac{2\pi h}{\lambda}}\sin^2\left(\frac{\pi h}{\lambda}\right) \qquad \text{(C.24)}$$

This is Eq. (3.12).

APPENDIX D

PHASE RELATIONS IN COUPLED CIRCUITS

Two Coupled Resonant Circuits.—The double-tuned circuit fed from a high-impedance source shown in Fig. 4.04 may be examined for the case when primary and secondary circuits are resonant at the same frequency f_0.

For the circuit $L_1C_1r_1$:

$$i_1\left(r_1 + j\omega L_1 + \frac{1}{j\omega C_1}\right) + i_2 j\omega M = i_p \frac{1}{j\omega C_1} \qquad \text{(D.1)}$$

For the circuit $L_2C_2r_2$:

$$i_1 j\omega M + i_2\left(r_2 + j\omega L_2 + \frac{1}{j\omega C_2}\right) = 0 \qquad \text{(D.2)}$$

The solution for i_2 in terms of i_p and the circuit constants may be expressed by the determinant relation:

$$i_2 = \frac{\begin{vmatrix} r_1 + j\omega L_1 + \dfrac{1}{j\omega C_1} & i_p \dfrac{1}{j\omega C_1} \\ j\omega M & 0 \end{vmatrix}}{\begin{vmatrix} r_1 + j\omega L_1 + \dfrac{1}{j\omega C_1} & j\omega M \\ j\omega M & r_2 + j\omega L_2 + \dfrac{1}{j\omega C_2} \end{vmatrix}} \qquad \text{(D.3)}$$

$$= \frac{-i_p \dfrac{M}{C_1}}{\left(r_1 + j\omega L_1 + \dfrac{1}{j\omega C_1}\right)\left(r_2 + j\omega L_2 + \dfrac{1}{j\omega C_2}\right) + \omega^2 M^2} \qquad \text{(D.4)}$$

$$= \frac{-i_p \dfrac{M}{C_1} \cdot \dfrac{1}{j\omega L_1} \cdot \dfrac{1}{j\omega L_2}}{\left(\dfrac{r_1}{j\omega L_1} + 1 - \dfrac{1}{\omega^2 L_1 C_1}\right)\left(\dfrac{r_2}{j\omega L_2} + 1 - \dfrac{1}{\omega^2 L_2 C_2}\right) - \dfrac{M^2}{L_1 L_2}} \qquad \text{(D.5)}$$

When the two circuits are tuned to the same frequency $f_0 = \omega_0/2\pi$

$$\omega_0^2 = \frac{1}{L_1C_1} = \frac{1}{L_2C_2} \tag{D.6}$$

The figures of merit of the circuits may be written

$$Q_1 = \frac{\omega L_1}{r_1} \qquad \text{and} \qquad Q_2 = \frac{\omega L_2}{r_2} \tag{D.7}$$

Then Eq. (D.5) becomes

$$\frac{i_2}{i_p} = \frac{\dfrac{\omega_0^2}{\omega^2}\dfrac{M}{L_2}}{\left(-\dfrac{j}{Q_1} + 1 - \dfrac{\omega_0^2}{\omega^2}\right)\left(-\dfrac{j}{Q_2} + 1 - \dfrac{\omega_0^2}{\omega^2}\right) - \dfrac{M^2}{L_1L_2}} \tag{D.8}$$

$$= \frac{\dfrac{\omega_0^2}{\omega^2}\dfrac{M}{L_2}}{\left(\dfrac{\omega^2 - \omega_0^2}{\omega^2} - \dfrac{j}{Q_1}\right)\left(\dfrac{\omega^2 - \omega_0^2}{\omega^2} - \dfrac{j}{Q_2}\right) - \dfrac{M^2}{L_1L_2}} \tag{D.9}$$

By the use of the same definition of the detuning factor β as in Eq. (4.10), it is found that

$$\frac{i_2}{i_p} = \frac{\dfrac{\omega_0^2}{\omega^2}\dfrac{M}{L_2}}{\left(\beta + \dfrac{j}{Q_1}\right)\left(\beta + \dfrac{j}{Q_2}\right) - \dfrac{M^2}{L_1L_2}} \tag{D.10}$$

If the coefficient of coupling is defined as in Eq. (4.23), then Eq. (D.10) becomes

$$\frac{i_2}{i_p} = \frac{\dfrac{\omega_0^2}{\omega^2} k \sqrt{\dfrac{L_1}{L_2}}}{\left(\beta + \dfrac{j}{Q_1}\right)\left(\beta + \dfrac{j}{Q_2}\right) - k^2} \tag{D.11}$$

The voltage

$$e_2 = \frac{i_2}{j\omega C_2} \tag{D.12}$$

$$\frac{e_2}{i_p} = \frac{-j\dfrac{\omega_0^4}{\omega^3} k \sqrt{L_1L_2}}{\left(\beta + \dfrac{j}{Q_1}\right)\left(\beta + \dfrac{j}{Q_2}\right) - k^2} \tag{D.13}$$

$$\frac{i_p}{e_2} = \frac{j\left(\beta^2 - \dfrac{1}{Q_1Q_2} - k^2\right) - \beta\left(\dfrac{1}{Q_1} + \dfrac{1}{Q_2}\right)}{\dfrac{\omega_0^4}{\omega^3} k \sqrt{L_1L_2}} \tag{D.14}$$

The phase angle is obtained as in Sec. 4.02, giving the result

$$\tan \phi = \frac{\beta^2 - \dfrac{1}{Q_1 Q_2} - k^2}{-\beta\left(\dfrac{1}{Q_1} + \dfrac{1}{Q_2}\right)} \tag{D.15}$$

$$= \frac{1 + k^2 Q_1 Q_2 - Q_1 Q_2 \beta^2}{\beta(Q_1 + Q_2)} \tag{D.16}$$

If the *geometric mean* of the primary and secondary circuit Q factors is denoted by $\bar{Q}$ and the *arithmetic mean* by Q_m and if these quantities are defined as in Eqs. (4.21) and (4.22), then

$$\tan \phi = \frac{1 + \bar{Q}^2(k^2 - \beta^2)}{2Q_m\beta} \tag{D.17}$$

The result was given in Eq. (4.24).

NAME INDEX

SUBJECT INDEX

B

S